UNIVERSIDAD NACIONAL AUTÓNOMA DE MÉXICO

PROGRAMA DE MAESTRÍA Y DOCTORADO EN CIENCIAS QUÍMICAS

Modificación de matrices poliméricas mediante rayos γ para la inmovilización de agentes antimicrobianos

TESIS

PARA OPTAR POR EL GRADO DE

DOCTORA EN CIENCIAS

PRESENTA

M. en C. MARLENE ALEJANDRA VELAZCO MEDEL

ASESOR:
DR. EMILIO BUCIO CARRILLO
DPTO. DE QUÍMICA DE RADIACIONES Y RADIOQUÍMICA
INSTITUTO DE CIENCIAS NUCLEARES

CIUDAD UNIVERSITARIA, CD. MX., AGOSTO 2021

UNIVERSIDAD NACIONAL AUTÓNOMA DE MÉXICO

PROGRAMA DE MAESTRÍA Y DOCTORADO EN CIENCIAS QUÍMICAS

Modificación de matrices poliméricas mediante rayos γ para la inmovilización de agentes antimicrobianos

T E S I S

PARA OPTAR POR EL GRADO DE

DOCTORA EN CIENCIAS

P R E S E N T A

M. en C. MARLENE ALEJANDRA VELAZCO MEDEL

Ciudad de México, agosto 2021

MIEMBROS DEL COMITÉ TUTOR

Dra. Selena Gutiérrez Flores
Dr. Braulio Víctor Rodríguez Molina

JURADO

Dra. Sofía Guillermina Burillo Amezcua
Dr. Ricardo Vera Graziano
Dr. Héctor García Ortega
Dr. Roberto Sato Berrú
Dra. Selena Gutiérrez Flores

ADSCRIPCIÓN, CONGRESOS Y PUBLICACIÓN

Este trabajo se realizó en el laboratorio de Química de Radiaciones en Macromoléculas del Instituto de Ciencias Nucleares de la Universidad Nacional Autónoma de México bajo la asesoría del Dr. Emilio Bucio Carrillo con recursos financieros de CONACyT (583700/696062) y de la Dirección General de Asuntos del Personal Académico de la UNAM (IN202320).

De este trabajo se derivan las siguientes publicaciones:

Velazco-Medel, M. A.; Camacho-Cruz, L. A.; Magaña, H.; Palomino, K.; Bucio, E. Simultaneous Grafting Polymerization of Acrylic Acid and Silver Aggregates Formation by Direct Reduction Using γ Radiation onto Silicone Surface and Their Antimicrobial Activity and Biocompatibility. *Molecules* **2021**, *26*, 2859. https://doi.org/10.3390/ molecules26102859.

Velazco-Medel, M. A.; Camacho-Cruz, L. A.; Bucio, E. Modification of PDMS with Acrylic Acid and Acrylic Acid/Ethylene Glycol Dimethacrylate by Simultaneous Polymerization Assisted by Gamma Radiation. *Radiat. Phys. Chem.* **2020**, *171* (December 2019), 108754. https://doi.org/10.1016/j.radphyschem.2020.108754.

Velazco-Medel, M. A.; Camacho-Cruz, L. A.; Lugo-González, J. C.; Bucio, E. Antifungal Polymers for Medical Applications. *Med. DEVICES SENSORS* **2021**, *4* (1). https://doi.org/10.1002/mds3.10134.

Velazco-Medel, M. A.; Camacho-Cruz, L. A.; Bucio, E. Modification of Relevant Polymeric Materials for Medical Applications and Devices. *Med. DEVICES SENSORS* **2020**, *3* (6), 1–17. https://doi.org/10.1002/mds3.10073.

Este trabajo se presentó en:

- Presentación oral "Modification of PDMS with acrylic acid/ethylene glycol dimethacrylate mixtures by simultaneous polymerization assisted by gamma radiation for biomedical applications", Advanced POLYMERS **2021**. Mayo 2021.
- Presentación oral "Uso del mecanismo irradiación-reducción para la síntesis de AgNPs y reacción de injerto sobre PDMS para obtener una superficie antimicrobiana/biocompatible", XXX Congreso Técnico Científico ININ-SUTIN. Mayo **2021**.
- Presentación oral "Modificación de membranas de silicona con fragmentos acrílicos mediante radiación gamma para aplicaciones biomédicas" en el IX Congreso Anual de la Sociedad Mexicana de Ciencia y Tecnología de Membranas. Octubre **2020**.
- Póster "PDMS modification with AAc and AAc/EGDMA through simultaneous polymerization assisted by γ radiation", Latin Chemistry Twitter Conference, September **2020**. Póster con mención honorífica en el área de Química de Nanomateriales.

AGRADECIMIENTOS

Principalmente quiero agradecer al Consejo Nacional de Ciencia y Tecnología por otorgarme la beca para efectuar mis estudios de doctorado (583700/696062) así como a la Dirección General de Asuntos del Personal Académico de la UNAM proyecto IN202320, por el apoyo económico para realizar la sección experimental de este proyecto.

Agradezco al Posgrado en Ciencias Químicas de la UNAM, a su planta administrativa, al Dr. Emilio Orgaz y la Q.F.B. Josefina Tenopala. A las secretarias: Ana María, Valeria y Mary Cruz, y al maestro Gumaro Viacobo, en el proceso de beca. A la sección administrativa de la que recibí apoyo, a Elsa Mora del ICN, Adriana Martínez y Marcos Ordaz de la Facultad de Química.

Agradezco al **Dr. Emilio Bucio Carrillo**, quien siempre se mostró amable y dispuesto a escucharme, le doy las gracias por confiar en mí y en mis ideas, por su apoyo en lo personal y en lo académico, por siempre tenderme la mano y estar presente.

Todo mi agradecimiento y admiración a la Dra. Guillermina Burillo, quien siempre me resolvió dudas y apoyó, también por su confianza y por enseñarme que todo lo que uno se propone se puede lograr.

Agradezco a los miembros de mi comité tutor, la Dra. Selena Gutiérrez y el Dr. Braulio Rodríguez, quienes me vieron crecer, siempre me brindaron su apoyo, me guiaron y aconsejaron para que todo saliera bien. A los miembros del comité tutor ampliado, la Dra. Alicia Negrón y el Dr. Roberto Olayo, por sus aportaciones a mi proyecto. De la misma manera agradezco al Dr. Ricardo Vera, Dr. Roberto Sato y Dr. Héctor García por sus aportaciones a mi tesis como jurado.

A la parte técnica del proyecto: a la sección de radiación del ICN, Mtro. Benjamín Leal y al Sr. Francisco García. También gracias al Mtro. Gerardo Cedillo por los espectros de RMN, al Dr. Roberto Sato (ICAT) por la asesoría en la manipulación de las nanopartículas, al Dr. Héctor Magaña y Dra. Kenia Palomino (UABC) por las pruebas de biocompatibilidad y de microbiología, así como al Q.F.B. Alejandro Camacho (FQ) por las pruebas preliminares de microbiología. Al I.Q. Iván Puente Lee (USAII) por la microscopía. Gracias a Lic. en Diseño Gráfico César Eduardo Velazco Medel por el diseño de las ilustraciones.

Al **M. en C. Luis Alberto Camacho Cruz**, porque sin su apoyo personal y académico, esto no sería posible. Juntos somos el mejor equipo.

Con mucho cariño, a mis compañeros del Lab. de Química de Radiaciones en Macromoléculas del ICN: Lorena Duarte, Felipe López, Ema Valencia, Aylin Esquivel, Mitzi Pérez, Angélica Cruz, Daniel Espinosa, Jessica Audifreud, Víctor Pino, Gabriel Flores, Eduardo Barriguete, Omar Reyes y Frida Ruíz. Del mismo laboratorio agradezco a la Dra. Alejandra Ortega y a Saúl por su ayuda durante la realización del proyecto y por las pláticas en el laboratorio.

Agradezco a mis compañeros del Lab. 110 del Departamento de Química Analítica de la FQ-UNAM: Daniel Zárate, Diego Serralde, Miguel Peñaloza y Rocío, ustedes fueron un gran soporte durante mi doctorado, gracias por la ayuda. Igualmente, gracias a mis grandes amigos: Arturo Rodríguez, María Cano, Itzia Cardoso, Eliud Badillo y Ana Cuéllar.

Gracias a mis amigos del Lab. 201 del Departamento de Química Orgánica de la FQ-UNAM: Nancy Aguilar, Óscar González Antonio, Geraldyne Castro, Alejandro Enríquez, y una mención muy especial a la Mtra. Margarita Romero Ávila, ejemplo de mujer, de científica y de ser humano.

A mis amigos y colegas del 1-1 del IQ: Al Dr. Gabriel Cuevas, Tania Rojo, Eduardo Hernández, Fátima Soto, Elizabeth Reyes y Lydia Ledesma. Especialmente a mi amigo el Dr. Fabian Cuetara.

De manera personal agradezco Dr. Rodrigo Razo de la UAEM y a la Dra. Hortensia Parra de la UCOL quienes siempre me apoyaron en todos los aspectos, me alentaron y siempre me han aconsejado desde que decidí entrar en este camino en 2010.

Agradecimiento a la Asociación DGYSP por su apoyo en mi desarrollo personal, por su amistad siempre, los quiero.

A mi gran amiga, quien siempre estuvo ahí, para todo: Aranzazú Gómez Figueroa, hermosa experiencia tenerte a mi lado.

Especial agradecimiento a Carlos Jiménez, pláticas eternas, mucha amistad.

Para mi amigo Luis Ramón Ortega Valdovinos, gracias.

A mis rommies de seis años, a quienes quiero con todo el corazón: Mauro Velasco, Carlos Ponce, Alejandra Jiménez, Maria Clara Avendaño y Amaury Aguilar. A Karla Trejo y Caterine Daza, por su amistad este tiempo, su apoyo y complicidad.

Gracias a Ana Virgen Solano y Adriana Carolina González, compañeras de licenciatura, quienes juntas decidimos amar la ciencia y pasar los veranos de investigación científica, las quiero mucho.

Al Mtro. Joel Nino por su invaluable apoyo durante este camino de la ciencia.

Gracias a Gabriela Hernández quien siempre me animó en el proceso de inscripción al posrgado, y estuvo conmigo, al igual que la Dra. Vianney Curiel, de quien recibí mucho apoyo.

A mis amigas de toda la vida: Ameyali y Rocío Cruz López, por siempre estar al pendiente de mí, y a Luis Cabral.

A quienes me tendieron la mano cuando llegué a la CDMX ahora mis grandes amigos Adriana García, Pilar Marroquín, Rafael Pérez Cervantes, Mónica Portillo y Arturo Campillo. No habría aguantado la Ciudad sin ustedes. Igualmente, gracias a Ana Zapien y Jatsiri Jaimes, por alegrarme los días en la alberca y los entrenos.

José Carlos Lugo González, gracias por TODO lo que tenemos y TODO lo que somos.

A mi familia, en especial a mi mamá **Alejandra Medel Valtierra**, por confiar en mí, por quererme, y apoyarme en cada una de mis decisiones. A mis hermanos Lucero y Eduardo Velazco Medel. Mi papá Gerardo Velazco Ruíz. Mi sobrino, el dueño de mi corazón, Carlos Santiago Vargas Velazco. Mis abuelos: Guillermina Valtierra, Socorro Ruíz, José Velazco y Martín Medel. A Miriam Medel Valtierra, Julia Felipe Medel, María Ruiz Ramos y a todos mis familiares.

ÍNDICE

ÍNDICE DE FIGURAS

SIGLAS Y ABREVIATURAS

AAc	Ácido Acrílico
ADN	Ácido Desoxirribonucleico
AgNP's	Nanopartículas de plata
AmB	Anfotericina B
Bq	Becquerel
CP/MAS	Cross Polarization/Magic Angle Spinning
DSC	Calorimetría Diferencial de Barrido
EGDMA	Etilénglicol dimetacrilato
ENH	Electrodo Normal de Hidrógeno
eV	Electronvoltio
FTIR-ATR	Infrarrojo con reflectancia total atenuada y transformada de Fourier
GY	Grado de injerto
I	Intensidad de radiación
kGy	Kilogray
LET	Transferencia Lineal de Energía
MeOH	Metanol
MIC	Concentración Mínima Inhibitoria
MPE	Matriz Polimérica Extracelular
NP	Nanopartícula
PBS	Solución salina de fosfatos
PDMS	Polidimetilsiloxano
PTFE	Politetrafluoroetileno
PLA	Poli(ácido láctico)
PP	Polipropileno
PE	Polietileno
PDEMAEMA	Dimethylaminoethyl methacrylate
PET	Poli(etilén tereftalato)
SD	Grado de hinchamiento
SEM/EDX	Microscopia Electrónica de Barrido/Espectroscopia Dispersiva de Energía de Rayos X
SS ^{13}C NMR	Resonancia Magnética Nuclear de carbono-13 en estado sólido
TGA	Análisis Termogravimétrico
UV-Vis	Ultravioleta-Visible
XPS	Espectroscopía de fotoelectrones por rayos X

RESUMEN

La formación de la película bacteriana en los dispositivos médicos es uno de los principales causantes de enfermedades infecciosas en el ambiente hospitalario. De este problema surge la necesidad de mejorar los materiales con que estos son diseñados para evitar ese anclaje de bacterias. El polidimetilsiloxano (PDMS) o silicona es un polímero que se ha utilizado para la elaboración de válvulas, catéteres, *stens*, tubos, implantes, entre otros debido a su alta biocompatibildad, baja reactividad, estabilidad térmica y flexibilidad. Se ha modificado su superficie mediante diversas técnicas para crear superficies antimicrobianas, esa modificación ha permitido la inmovilización de distintos agentes antimicrobianos de naturaleza orgánica e inorgánica. Los polímeros de injerto sobre la superficie y dentro de la matriz polimérica favorecen la adición de fármacos y, además, dependiendo de la naturaleza del injerto, se puede controlar la forma en que el fármaco es liberado en un ambiente biológico. Con este fin los polímeros sensibles a estímulos has sido ampliamente utilizados, aprovechando aquellos que responden a los cambios de pH y a la temperatura, por mencionar algunos.

En el presente trabajo se presenta la modificación del PDMS con un injerto binario constituido por ácido acrílico y etilénglicol dimetacrilato (AAc:EGDMA) utilizando radiación gamma para inmovilizar agentes antimicrobianos. Como estudio preliminar se hizo el estudio del efecto de la dosis de radiación, disolvente y concentración de monómeros para la obtención de PDMS injertado con AAc:EGDMA (PDMS-*g*-(AAc/EGDMA)). Se logró injertar el AAc y la mezcla de los monómeros utilizando el método simultáneo de polimerización en medio no polar (tolueno) y en medio hidroalcohólico. La caracterización de las películas modificadas se realizó utilizando Espectroscopía Infrarrojo (IR), Resonancia Magnética Nuclear de ^{13}C en estado sólido (SS ^{13}C NMR), y análisis térmico. Debido a las características químicas del injerto de AAc, se evaluó la respuesta a pH de las películas y la hidrofilicidad de su superficie. El pH crítico se obtuvo con estudios de hinchamiento en función del pH. Con respecto a la hidrofilicidad se utilizó el estudio del ángulo de contacto para evaluar la absorción de agua en la superficie, mostrando una disminución en el ángulo de contacto con respecto a la silicona que es un polímero altamente hidrofóbico, de 105° a ~90°. Las mismas películas fueron sometidas a pruebas de biocompatibilidad con fibroblastos de ratón (BALB/3T3) mostrando muerte celular en aquellas que fueron modificadas con mayor concentración de ácido acrílico.

En la primera sección, conociendo las condiciones necesarias para modificar las películas, se logró reducir de manera simultánea el ión plata (Ag^{+1}) a plata reducida (Ag^{0}) utilizando la radiación en un medio hidroalcohólico. La presencia de las partículas y agregados de plata se comprobó mediante espectrofotometría Ultravioleta-Visible y Microscopia Electrónica de Barrido/Espectroscopia Dispersiva de Energía de Rayos X (SEM/EDX). Las pruebas antimicrobianas y de biocompatilibidad de las películas con plata mostraron que los materiales poseen capacidad antimicrobiana contra *S. aureus* y no afecta la viabilidad de fibroblastos.

En la segunda sección, se utilizaron las películas modificadas con el injerto binario AAc:EGDMA en medio no polar para la carga de ciprofloxacino. Se logró una liberación del 60% del antibiótico, durante 48 h, en un medio biológico simulado. Las películas cargadas con el antibiótico mostraron alta eficiencia contra *E. coli*, después de 48 h de cultivo.

Resumen gráfico

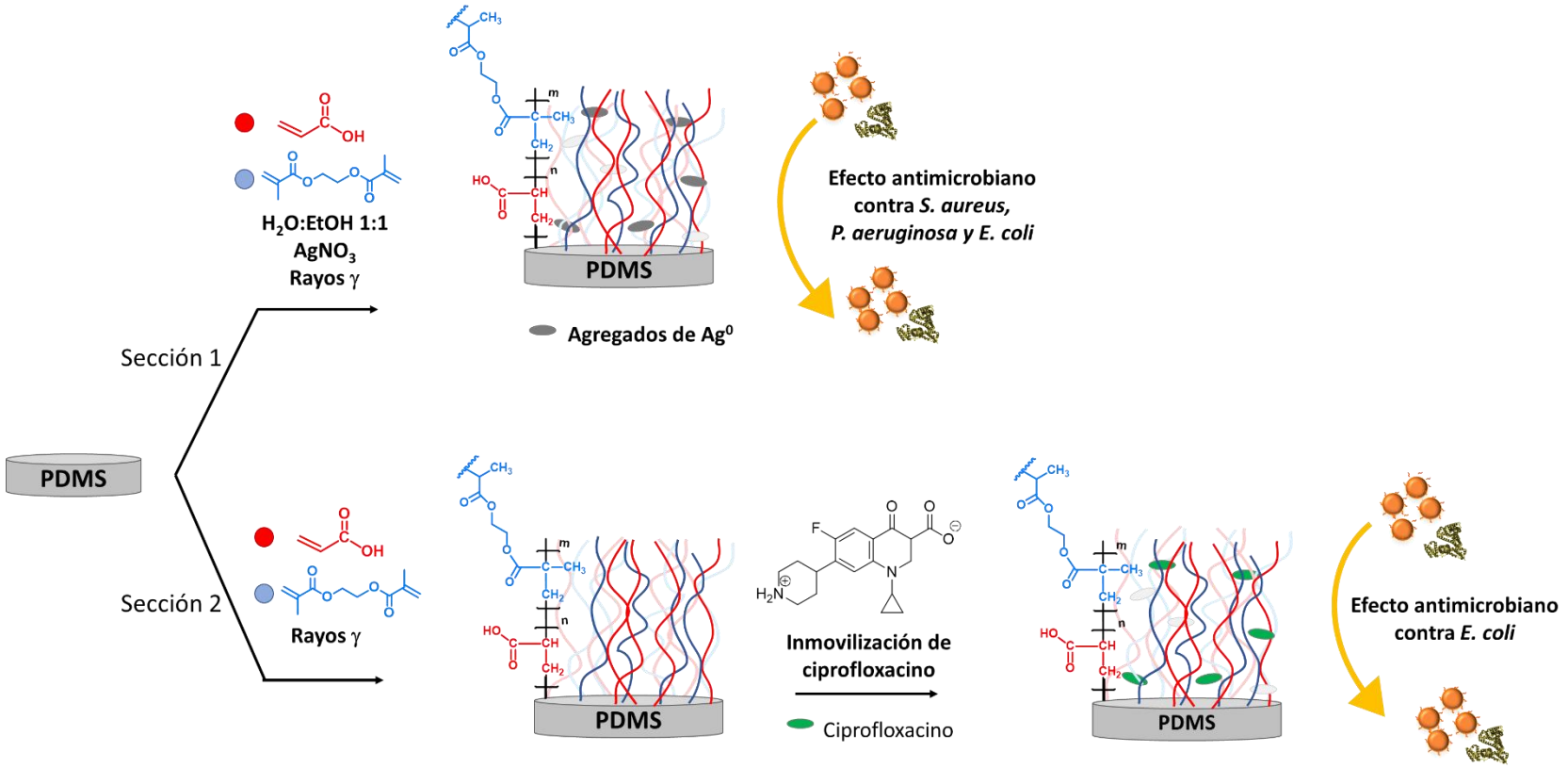

ABSTRACT

The formation of biofilm on medical devices is one of the main causes of infectious diseases in hospitalized patients. This problem arises the need to improve the materials with which they are made of to avoid the primary anchoring of bacteria onto the polymeric surface. Polydimethylsiloxane (PDMS) or silicone is a polymer that has been used to make valves, catheters, stens, tubes, implants, among others due to its high biocompatibility, low reactivity, thermal stability, and flexibility. Its surface has been modified by various techniques to create antifouling surfaces, this modification has allowed the immobilization of different inorganic or organic antimicrobial agents. The graft polymers on the surface or in bulk favor the addition of drugs and depending on the nature of the graft, the delivery mechanism of the drug can be controlled. In this line, stimuli-responsive polymers have been widely used, especially those that respond to changes in pH and temperature.

In this work, we present the modification of PDMS with a binary graft made of acrylic acid and ethylene glycol dimethacrylate (AAc:EGDMA) using gamma radiation to immobilize antimicrobial agents. As a preliminary study, the effect of radiation dose, solvent and monomer concentration was carried out to obtain grafted PDMS with the mixture AAc:EGDMA (PDMS-*g*-(AAc/EGDMA)), it was possible to modify the films with AAc and the monomer mixture using the simultaneous polymerization method in a non-polar solvent (toluene) and in a hydroalcoholic medium. The characterization of the modified films was carried out using Infrared Spectroscopy (IR), Solid State ^{13}C Nuclear Magnetic Resonance (SS ^{13}C NMR), and thermal analysis. Due to the chemical structure of the AAc, the pH-sensitivity of the films and the hydrophilicity of their surface were evaluated. The critical pH was obtained by swelling studies as a function of pH. Respect to the hydrophilicity, the study of the contact angle was used to evaluate the absorption of water on the surface, showing a decrease in the angle regarding to silicone, which is a highly hydrophobic polymer, de angle passed from 105 to ~90°. The biocompatibility tests of all the films were performed using mouse fibroblasts (BALB/3T3) showing cell death in those that were modified with a higher concentration of acrylic acid.

In the first section, knowing the necessary conditions to modify the films, it was possible to simultaneously reduce the silver ion (Ag^{+1}) to reduced silver (Ag^{0}) using radiation in a hydroalcoholic medium. The presence of silver particles and aggregates was verified by Visible Ultraviolet spectrophotometry and Scanning Electron Microscopy/Energy Dispersive X-ray Spectroscopy (SEM/EDX). The antimicrobial and biocompatibility tests of the silver films showed that the materials possess antimicrobial capacity against *S. aureus* and does not affect fibroblast viability.

In the second section, the modified films with the AAc:EGDMA binary graft were used in a non-polar medium for the loading of ciprofloxacin, a 60% release of the antibiotic was achieved during 48 h in a simulated biological medium. Films loaded with the antibiotic showed high efficiency against *E. coli* after 48 h.

1. MARCO TEÓRICO

1.1. Polímeros con aplicaciones biomédicas

Actualmente, el uso de polímeros y plásticos en el área de la salud es inevitable, día con día se fabrican diversos materiales para uso en hospitales, farmacias y distintos dispositivos médicos [1]. La búsqueda en la mejora de los polímeros de uso médico es un tema de interés en los últimos años, se busca mejorar los métodos de producción para aminorar costos, así como la mejora de éstos dándoles mayor versatilidad y aplicaciones.

Una gran variedad de polímeros de distinta naturaleza (sintéticos y naturales) son utilizados en la fabricación de material quirúrgico como catéteres, *stens*, válvulas, cubiertas de heridas, tubos, implantes, etc. [2]. La Tabla 1 muestra un listado de algunos materiales de uso biomédico y el polímero con el que han sido fabricados. Estos polímeros pueden poseer distintas características físicas y químicas, así como pueden ser clasificados de acuerdo con su origen, composición, estructura y propiedades.

Una de la clasificación de estos polímeros es su comportamiento en sistemas acuosos, aquellos que tienen afinidad con el agua son polímeros hidrofílicos, por el contrario, aquellos que repelen el agua son polímeros hidrofóbicos. Esta característica es muy importante para la utilización de los polímeros en el área de la salud, por ejemplo, la biocompatibilidad de un sistema polimérico depende de qué tan hidrofílico es este, está reportado que las superficies poliméricas ricas de grupos funcionales químicos como ácidos carboxílicos (-COOH), hidroxilos (-OH) y aminas ($-NH_2$), por mencionar algunos, favorecen la adhesión de células humanas sin generar muerte celular [3].

Sin embargo, muchos de esos dispositivos médicos son susceptibles a ser atacados por bacterias y hongos, siendo esta una de las principales problemáticas en el uso de estos materiales en el área de la salud [4]. Por ejemplo, al ser instalados los catéteres venosos, tienden a contaminarse de microrganismos oportunistas comunes del ambiente hospitalario, lo cual lleva al paciente hospitalizado a un estado de infección sistémica o en el torrente sanguíneo, que en lamentables ocasiones desencadena en la muerte [5].

Las infecciones causadas por microrganismos pueden ser por bacterias y por hongos, entre las bacterias más comunes se encuentran: el *Staphylococcus aureus*, *Staphylococcus epidermidis*, *Enterococcus faecalis*, *Klebsiella pneumoniae*, *Pseudomona aeruginosa*, *Escherichia coli* y algunas especies de *Enterobacter*. En cuanto a hongos y levaduras se encuentran: la *Candida*, *Aspergillus*, *Trichophyton rubrum*, *Blastomyces*, *Saccharomyces*, *Histoplasma*, y *Cryptococcus* spp. [6-7].

Parte de la investigación actual en polímeros de uso biomédico se encuentra dirigida a la modificación de los polímeros actuales para evitar la adhesión de microrganismos sobre la superficie del dispositivo médico [8].

Tabla 1. Listado de algunos dispositivos poliméricos de uso biomédico y quirúrgico.

Polímero	Aplicación médica
Sintéticos	
Polietileno	• Implantes ortopédicos • Catéteres
Politetrafluoroetileno expandido	• Hilos de sutura • Catéteres
Poliamidas	• Piel artificial • Hilos de sutura • Implantes ortopédicos • Ingeniería de tejidos • Sistemas de liberación de fármacos
Polipropileno	• Fibras quirúrgicas • Hilos de sutura
Poli(etilén tereftalato)	• Catéteres • Injertos vasculares • Hilos de sutura
Derivados de polidimetilsiloxano	• Catéteres • Dispositivos intrauterinos • Bolsa gástrica • Tubos • Válvulas
Poli(metil metacrilato)	• Implantes dentales • Lentes de contacto
Poliuretano	• Implantes • Catéteres
Poli(cloruro de vinilo)	• Catéteres • Válvulas
Poli(alquil tiofenos)	• Prótesis de retina
Poli(etilén glicol)	• Sistemas de liberación de fármacos • Sistemas biocompatibles
Naturales	
Derivados de proteínas (Colágeno, gelatina, agar, etc.)	• Sistemas biocompatibles
Derivados de polisacáridos (Celulosa, poli(ácido láctico), etc.)	• Sistemas de liberación de fármacos • Gasas y cubiertas de heridas • Hilos de sutura

**Tabla extraída de Velazco-Medel, et al., Med Devices Sensors. 2020; 1–17.*

1.2. Formación del *biofilm* en dispositivos médicos y superficies

El término *biofilm* fue introducido por Costeron en 1978, y lo definió como un conjunto de bacterias, bien organizadas y resistentes recubiertas por un polímero producido por ellas mismas adheridas a una superficie. En español es conocida como biopelícula (de bacterias o de hongos). Los *biofilms* tienen morfologías variadas, según los microrganismos constituyentes y las condiciones en las que se formó. La estabilidad que adquieren las bacterias y hongos en esta biopelícula favorece la proliferación de más microrganismos, formando un recubrimiento de la superficie [9]. Es importante señalar que las bacterias ordenadas dentro de una película se encuentran recubiertas por una mezcla de polisacáridos, ADN y proteínas, conocida como Matriz Polimérica Extracelular (MPE). Este recubrimiento provoca que las bacterias sean más resistentes al efecto de antibióticos o bactericidas que las bacterias planctónicas[*], esto porque se limita la difusión de estos agentes a través de ella. Además, esta resistencia a los agentes antimicrobianos se atribuye a que las bacterias están en interconectadas entre ellas a través de procesos bioquímicos y de expresión génica, lo cual las hace más fuertes. Algunas biopelículas están formadas por más de una microespecie y puede ser mixta, de hongos y bacterias. Están demostradas las *biofilms* mixtas de *C. albicans* y *S. epidermidis* [4].

El *biofilm* tiende a formase sobre superficies hidrofóbicas y rugosas dónde los microrganismos se adhieren y ordenan por efecto de las interacciones no covalentes entre los polisacáridos de la pared celular y la superficie donde se adhieren [10]. Se han propuesto diversos modelos sobre cómo se forma el *biofilm* [11–13], y todos coinciden en que el primer requisito para que comience la formación de la biopelícula es que las bacterias se encuentren lo suficientemente cercanas a una superficie afín, alrededor de 10 a 20 nm. De manera general, el mecanismo de formación del *biofilm* procede en tres etapas: 1) adhesión o anclaje primario, 2) acumulación de bacterias y maduración, y 3) dispersión.

La primera etapa depende de la naturaleza química de los microrganismos y de la superficie objetivo. Las bacterias poseen cargas negativas en su superficie lo cual es incompatibles con superficies igualmente con carga negativa. Sin embargo, interacciones no covalentes logran vencer la repulsión electrostática y favorecer el anclaje. Por otro lado, las bacterias con flagelos son más afines a la adhesión, ya estos se unen de manera mecánica. Algunas especies de *Staphylococcus* inician la formación de la biopelícula por interacción con las proteínas del plasma humano como la fibronectina, fibrinógeno o albúmina. El peptidoglicano de la pared celular bacteriana se une de manera covalente con estas proteínas.

En la etapa de maduración, se comienza a formar la MPE, y una vez que se produce el proceso de anclaje a la superficie se vuelve irreversible. Se comienzan a generar proteínas, ADN, polisacáridos, etc. en grandes proporciones para proteger al conjunto de bacterias, por ejemplo, la *P. aeruginosa* comienza a secretar el polisacárido alginato. En la última etapa, la difusión, se da el desprendimiento de células planctónicas de la biopelícula, estas bacterias posteriormente pueden iniciar un nuevo ciclo de formación de biopelículas en otros sitios [14]. El diagrama del proceso puede observarse en la Figura 1.

[*] Bacterias planctónicas: Bacterias aisladas o dispersas en un medio, de libre flotación.

Figura 1. Proceso de formación del *biofilm* microbiano sobre una superficie polimérica.

Estrategias para evitar o eliminar el *biofilm* en superficies poliméricas

El *biofilm* representa un papel importante en las infecciones hospitalarias asociadas al uso de dispositivos médicos, especialmente en implantes, catéteres y válvulas. Debido a la naturaleza resistente a los antibióticos de las biopelículas, el uso de antibióticos por sí solos es ineficaz para tratar las infecciones relacionadas con el *biofilm*.

De acuerdo con el proceso de formación del *biofilm*, se han diseñado distintas estrategias para evitarlo o para derrotarlo. La primera estrategia es evitar la adhesión primaria de las bacterias, la segunda se basa en la interferencia con las moléculas que modulan el desarrollo de la MPE y, finalmente, evitar la re-difusión de bacterias planctónicas.

La estrategia más común y utilizada es la primera, que se logra de diversas maneras: 1) modificando las superficies poliméricas de tal manera que se conviertan incompatibles a estos microrganismos y 2) generando superficies que puedan atacar a la bacteria en su estado planctónico, cuando es susceptible a antibióticos de uso común [15-16].

Las propiedades de la superficie de los dispositivos médicos poliméricos como la rugosidad, la energía, la carga electrostática y la hidrofilicidad pueden ser moduladas para reducir la adhesión primaria de las bacterias. Esto también se puede lograr reduciendo la adsorción de proteínas dado que como estos dispositivos se encuentran en contacto con fluidos biológicos estos tienden también a ser blanco de la adhesión de proteínas humanas como el fibrinógeno y la albúmina; como fue mencionado en la sección anterior, algunas especies de *Staphylococcus* se anclan a las superficies por interacción entre los polisacáridos de la pared bacteriana y las proteínas.

Para modificar la superficie polimérica se pueden utilizar diferentes técnicas o aproximaciones, por ejemplo, el recubrimiento de la superficie con agentes antimicrobianos que puede inhibir la unión inicial de las células planctónicas en la superficie del dispositivo médico. También, se pueden añadir o injertar pequeñas moléculas o polímeros antimicrobianos intrínsecamente, los cuales pueden ser adicionados a la superficie del polímero utilizando reacciones químicas convencionales.

1.3. Modificación de superficies poliméricas para evitar el *biofilm*

Considerando que la adhesión bacteriana y el *biofilm* en las superficies poliméricas son de los principales problemas de salud asociados al uso de dispositivos médicos, se han creado estrategias para modificar dichas superficies y evitar o atacar el problema de la biopelícula. Sin embargo, las modificaciones de los polímeros también pueden ser utilizadas con otros fines como adicionarle propiedades que los convierta en materiales más versátiles y sofisticados. Entre las propiedades que se adicionan o mejoran en los polímeros de uso biomédico se encuentran a) propiedades mecánicas, b) biocompatibilidad, y c) prolongar la vida útil del material.

Dada la problemática que existe con el *biofilm* y la contaminación microbiana, las superficies se modifican principalmente para evitar adhesión bacteriana; lo cual puede lograrse de varias maneras. Para fines prácticos éstas se dividirán en dos: 1) Adición de agentes antimicrobianos en la superficie y 2) incorporación de sistemas de liberación controlada de fármacos.

La adición de agentes antimicrobianos a un polímero puede alcanzarse con el simple recubrimiento de la superficie con el antibiótico, el cuál puede ser de origen polimérico, un péptido, una molécula orgánica o una partícula metálica. Esta técnica se logra con la síntesis y creación de materiales compuestos[†], dónde únicamente hay proceso físico por mezclado (en sólido o en solución) para llegar al material final, el cual cuenta con propiedades antimicrobianas conferidas por los agentes antimicrobianos añadidos. La desventaja de esta técnica, en algunas ocasiones es la baja estabilidad de los materiales, ya que los agentes antimicrobianos se desanclan de la superficie cuando entran en contacto con un ambiente húmedo [17].

Por otro lado, cuando se modifican las superficies poliméricas de manera covalente con sistemas poliméricos que permiten la retención de agentes antimicrobianos o con polímeros intrínsecamente antimicrobianos, hay una mayor eficiencia *antifouling*[‡] del material. A esos fragmentos añadidos a la superficie se les conoce como polímeros de injerto o *graft* (en inglés).

Las modificaciones tipo *grafting* pueden ser de dos tipos: 1) aquellas donde se injerta un polímero sobre una superficie, conocido como *grafting to* (Figura 2a); ó 2) aquellas donde el injerto polimérico se logra mediante la polimerización de un monómero sobre la superficie, conocido como *grafting from* (Figura 2b). Ambos procesos de modificación pueden lograrse mediante diversas maneras físicas y químicas [18].

Las reacciones de injerto se han utilizado para dotar de propiedades a distintas superficies, no sólo poliméricas, sino también a superficies de origen inorgánico o nanomateriales de carbono, como el grafeno. En el caso de los materiales poliméricos de uso biomédico, se han utilizado estas reacciones para crear superficies biocompatibles, antimicrobianas o con propiedades mecánicas mejoradas [19]. Cualquiera de las dos metodologías logra superficies con propiedades antimicrobianas, o que repelan las bacterias y hongos, dependiendo de la naturaleza del polímero o monómero injertado.

[†] Material compuesto: aquellos materiales que se generan por la mezcla de dos compuestos con distintas propiedades para generar un material con ambas propiedades.
[‡] *Antifouling*: anti-adherencia microbiana.

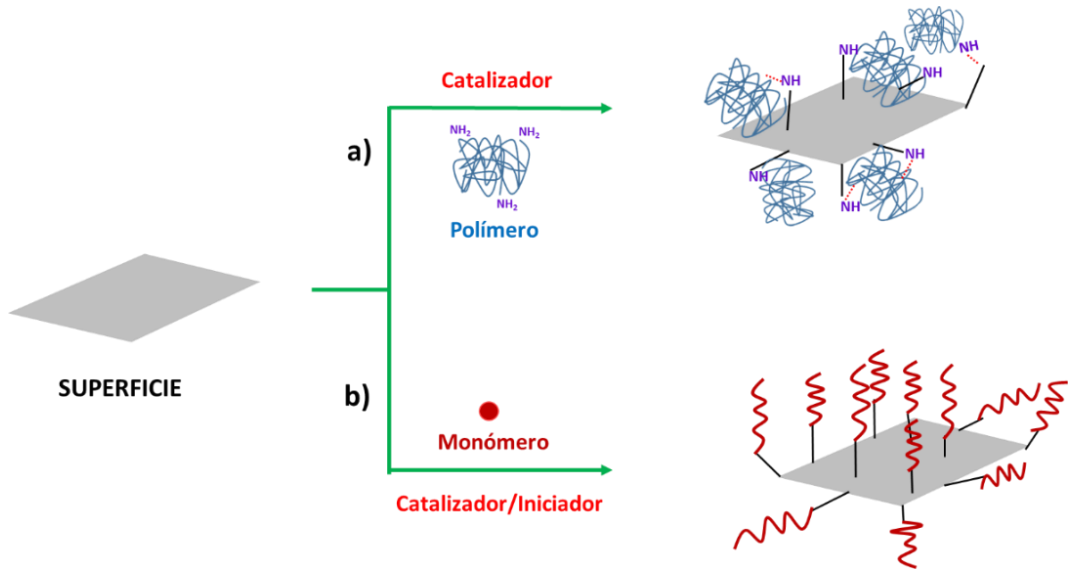

Figura 2. Proceso de injerto o *grafting:* a) *grafting to* injerto de un polímero y b) *grafting from* injerto de un monómero que polimeriza sobre la superficie.

La ventaja de los polímeros de injerto sobre las otras superficies es que se pueden aprovechar las propiedades de los polímeros funcionales que permitan incorporar e inmovilizar pequeñas moléculas que funcionen para liberación controlada de fármacos, específicamente, antibióticos y antiinflamatorios. Siguiendo esta línea, se ha implementado el uso de los polímeros inteligentes o **polímeros sensibles a estímulos** para la liberación prolongada de fármacos o para facilitar la inmovilización de otros agentes antimicrobianos, como partículas metálicas [20].

1.4. Polímeros sensibles a estímulos

Los polímeros sensibles a estímulos son aquellos que, al ser sometidos a un estímulo de cualquier naturaleza, desencadenan una respuesta. Estos polímeros responden a su entorno cambiando sus propiedades físicas o químicas, estas respuestas inducen efectos macroscópicos en el material, como colapso de las cadenas del polímero, hinchamiento, cambios de color, solubilidad o transiciones de solución a gel. Todas estas respuestas dependen de la composición química, estado físico y conformacional de las cadenas de polímero. Se han diseñado y sintetizado gran variedad de este tipo de polímeros, que sean capaces de responder a una amplia lista de estímulos, por ejemplo, pH, temperatura, fuerza mecánica, la presencia de varias moléculas pequeñas y biomoléculas, y campos eléctrico y/o magnético [21].

De los polímeros estímulo sensibles más utilizados para el diseño de sistemas de liberación de fármacos son los termosensibles y los pH-sensibles, en combinación con polímeros biocompatibles [22-23]. Por una parte, los polímeros termosensibles útiles han sido diseñados para tener su respuesta a temperatura corporal (alrededor de 37°C) y, por otra parte, los polímeros pH-sensibles pueden diseñarse para responder a valores de pH fisiológico, para controlar el sitio de liberación de los fármacos, así como su absorción, solubilidad y biodisponibilidad.

Los **polímeros pH-sensibles** también son conocidos como polielectrolitos. Éstos incluyen en su estructura grupos ácidos o básicos de Brønsted-Lowry, principalmente débiles, los cuales son

susceptibles a reacciones ácido-base y dan una respuesta ante un cambio en el pH del ambiente. Su diagrama de transición de fase se muestra en la Figura 3.

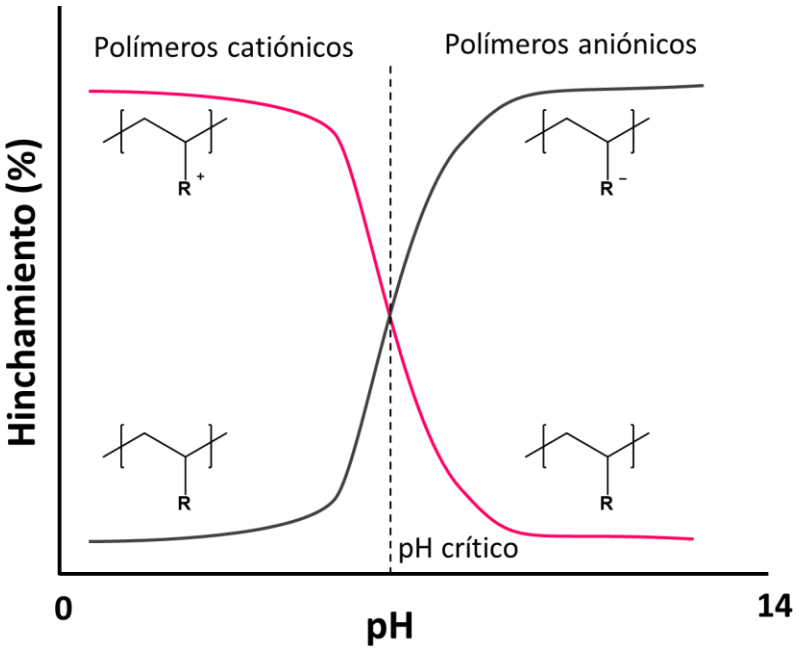

Figura 3. Representación esquemática en una transición de fase que experimenta un polímero sensible a cambios de pH.

Dichas reacciones provocan la ionización de estos grupos debido a la protonación/deprotonación, lo que genera efectos electrostáticos entre las cadenas cargadas provocando repulsión electrostática entre los grupos cargados, de tal manera que se da un aumento en el espacio entre cadenas, provocando un **hinchamiento** o una **disolución** (Figura 4a). Esta característica permite que los polímeros con grupos ionizados (forma sal) sean capaces de absorber líquidos, principalmente agua por la afinidad con los polielectrolitos, lo cual es aprovechado en la síntesis de hidrogeles y sistemas absorbentes. Por ejemplo, el poli(ácido acrílico) (PAAc) tiene una constante de disociación ($pK_a = 4.25$) y, por encima de pH 4, el grupo carboxílico se ioniza (Figura 4b). Esto conduce a la repulsión electrostática entre las cadenas que luego pueden asociarse con el agua para causar el hinchamiento. A pH bajo, los grupos carboxilo se protonan y dominan las interacciones hidrófobas, lo que lleva a la extracción de volumen del polímero que contiene los grupos carboxilo. Sin embargo, a pH alto, los grupos carboxilo se disocian en iones carboxilato, lo que da como resultado una alta densidad de carga en el polímero, lo que hace que se hinche. La configuración de la cadena del poliácido débil es función del pK_a aparente (macroscópico) de la estructura polimérica.

Un aspecto importante de los polímeros pH-sensibles es que la respuesta es dirigida por un cambio en la solubilidad del polímero, lo cual se logra al pasar de una especie neutra insoluble en agua a una sal soluble en agua, lo cual se ve reflejado como un colapso de las cadenas poliméricas, ver Figura 4a. Esta transición entre cadenas expandidas y colapsadas está influenciada por cualquier condición que modifique la repulsión electrostática, como son la fuerza iónica y el tipo de contraión. La transición del estado colapsado al estado expandido se explica por cambios en la presión osmótica ejercida los por contraiones móviles que neutralizan las cargas de la red

polimérica [24]. Cuando aumenta la fuerza iónica de la solución, el hidrogel puede intercambiar iones con la solución. De esa manera, el hidrogel mantiene la carga neutral y aumenta la concentración de contraiones libres dentro del hidrogel. Así, aparece una diferencia de presión osmótica entre el hidrogel y la solución y hace que el gel se hinche. Si la fuerza iónica es igual o superior a 1-10 M, el hidrogel se encogerá. Esto se debe a la diferencia de presión osmótica decreciente entre el gel y la solución. La solución ahora tiene una presión osmótica en el intervalo de la presión osmótica dentro del gel [25-26].

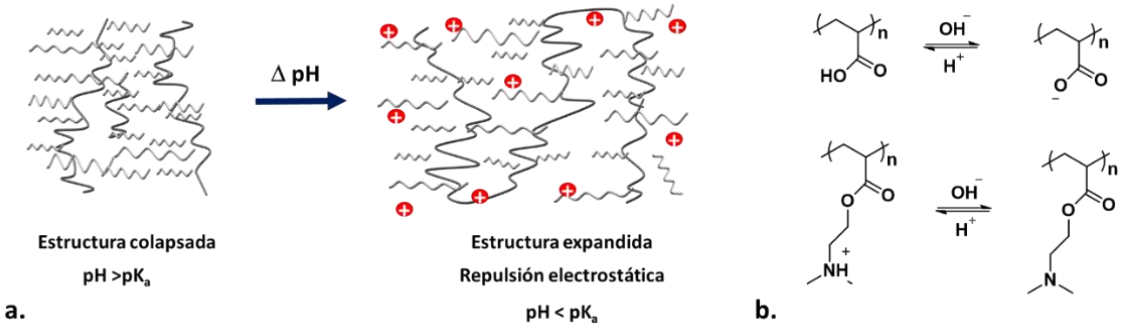

Figura 4. Polímeros pH-sensibles. a) Estado expandido y colapsado y b) Estructura del PAAc y del PDMAEMA.

La ventaja de los polímeros sensibles a pH es que las reacciones ácido-base son reversibles, lo cual permite pasar de un estado a otro modificando el pH, dependiendo de la constante de acidez (K_a) de los grupos funcionales del propio material. Este comportamiento se aprovecha para el diseño de sistemas de liberación de fármacos aprovechando los diferentes valores de pH en el sistema gastrointestinal, por ejemplo, se han diseñado micelas y acarreadores en escala nanométrica [27-28], y también han funcionado para la inmovilización de otros fármacos orgánicos e inorgánicos. Incluso, varios de estos polímeros se han injertado en otras matrices metálicas y poliméricas para aportar propiedades adicionales a otros sistemas, asimismo se han sintetizado algunos polímeros con doble respuesta, con el uso de monómeros de diferente naturaleza y sensibles a distintos estímulos.

1.5. Adición de agentes antimicrobianos a polímeros para evitar el *biofilm*

Una de las estrategias utilizadas para evitar la formación de la biopelícula bacteriana es la adición de agentes antimicrobianos a los polímeros. La incorporación de estos agentes dentro de las cadenas conduce a un polímero con alta repelencia bacteriana o provoca la inhibición del crecimiento. Ya sean, antibióticos, bactericidas o bacteriostáticos, los agentes antimicrobianos se pueden utilizar para recubrir superficies poliméricas con diferentes aplicaciones, como dispositivos médicos, aditivos para pinturas, tratamiento de agua, envasado de alimentos, entre otros [29-30]. La adición de los compuestos activos puede lograrse mediante: i) el recubrimiento de la superficie, o ii) a través de la inmovilización de dichos agentes entre las cadenas del polímero (covalente o no covalente).

En la segunda aproximación se aprovechan los polímeros de injerto y los polímeros estímulo sensibles para lograr la captura de agentes antimicrobianos de diversa naturaleza, ya sean de origen inorgánico y orgánico; por ejemplo, se ha utilizado la incorporación de péptidos o proteínas

para el mismo propósito [31]. La adición de estos compuestos se puede lograr de dos maneras: por un lado, usando métodos de síntesis química convencional para unir de forma covalente la molécula activa a la matriz polimérica; y, por otro lado, la incorporación se puede realizar mezclando el compuesto y el polímero, para obtener una inmovilización no covalente.

1.5.1. Adición de partículas metálicas

Existen gran cantidad de estudios que aplican la incorporación de compuestos inorgánicos a matrices poliméricas para dotar de capacidad antimicrobiana a los polímeros [32–34]. El enfoque más común es utilizar metales elementales que se organizan en *nanoclusters* o nanopartículas (NP) ya que estos sistemas son tóxicos para las bacterias. Las NP de plata son las partículas metálicas más utilizadas como agente antimicrobiano en compuestos poliméricos. Si bien muchos metales han mostrado buenas actividades antibacterianas, la plata es el metal más utilizado y estudiado por su actividad antimicrobiana de amplio espectro, ya que presenta alta estabilidad, bajo costo y facilidad de preparación. Las nanopartículas de plata (AgNP's) se han incorporado e inmovilizado en diferentes polímeros relevantes utilizados en la industria alimentaria y aplicaciones biomédicas [35,36]. Algunos de los polímeros que se han modificado con AgNP's son: PTFE, PLA, PE, PP; entre otros [37–40].

Una ventaja de estos metales es que su Concentración Mínima Inhibitoria (MIC por sus siglas en inglés) suele ser extremadamente baja, ya que intervienen en reacciones redox y pueden actuar como catalizadores de algunas reacciones enzimáticas. También, pueden incrementar las reacciones internas produciendo un exceso de derivados de especies reactivas de oxígeno (ROS) que producen estrés oxidativo en la célula [41]. Aunque el mecanismo de acción de estos compuestos inorgánicos no está completamente descrito, se sabe que los compuestos de plata (Ag^{+1} y Ag^{0}) tienden a unirse a las proteínas de la pared bacteriana, alterando las células patógenas. Las AgNP's también interfieren con el crecimiento de los microorganismos debido a la formación de complejos con bases nitrogenadas en el ADN y el ARN. Para este metal se ha reportado actividad antibacteriana contra bacterias Gram positivas y Gram negativas como: *E. coli*, *P. aeruginosa*, *S. aureus*, *S. epidermis*; y actividad antifúngica contra *Candida*, *Aspergillus*, *Trichophyton rubrum*, *Blastomyces*, *Saccharomyces*, *Histoplasma* y *Cryptococcus* spp [42–45].

La inmovilización de estas partículas e iones metálicos se ve favorecida por la coordinación de grupos funcionales en la estructura polimérica [46]. Por ejemplo, las AgNP's y la plata oxidada pueden coordinarse con los grupos carboxilato de las cadenas poliméricas, mediante interacciones electrostáticas, como se ve en la Figura 5a. Además, pueden interactuar con grupos con carga positiva como las sales de amonio cuando las nanopartículas metálicas se suspenden en un tensioactivo, formando una estructura tipo micela como se representa en la Figura 5b.

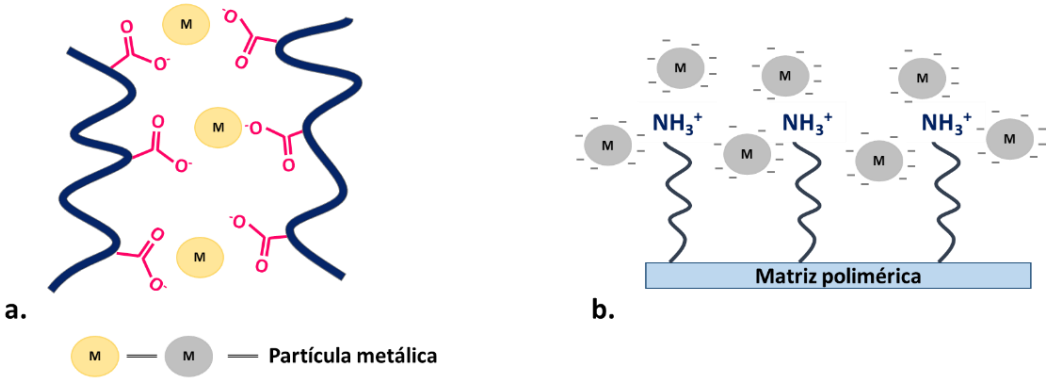

Figura 5. Inmovilización de partículas metálicas mediante interacción electrostática con: a. grupos carboxilato y b. sales de amonio.

El depósito e inmovilización de AgNP's se puede lograr por dos vías, la primera alternativa es mezclar ambos componentes (polímero y AgNP's previamente sintetizados) para formar un compuesto de polímero/metal. La segunda opción es la formación *in situ* de las AgNP's usando cualquier método de reducción química. Ambas técnicas dan como resultan en materiales con alta capacidad para inhibir el crecimiento bacteriano y fúngico.

La mayoría de los informes emplean la segunda forma de obtener AgNP's dentro de un polímero o hidrogel, principalmente por reducción química de $AgNO_3$ utilizando agentes reductores convencionales (borohidruro de sodio ($NaBH_4$), monosacáridos, citratos, polioles, etc.) [47]. También, se han logrado formar AgNP's mediante la reducción de sales de plata en solución acuosa utilizando la radiación γ [48–50].

Para la inmovilización en la superficie de las NP's metálicas, se utilizan injertos de polímero tipo peine o entrecruzados (reticulados), lo que permite la retención de las NP's entre las cadenas de polímero (Figura 6). Como una mejora a esta técnica, se emplean polímeros que responden a estímulos, los cuales proporcionan una retención y liberación controladas de la nanopartícula metálica [51].

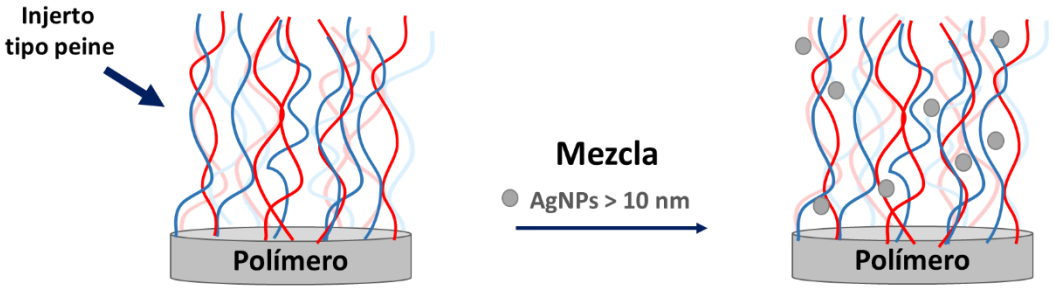

Figura 6. Retención de las AgNP's entre las cadenas del polímero de injerto tipo peine.

1.5.2. Adición de antimicrobianos orgánicos

El contenido principal de esta sección es la adición de compuestos orgánicos a matrices poliméricas para propiedades antimicrobianas y *antifouling*. Estos compuestos pueden ser biocidas, antibióticos o cualquier molécula activa contra microorganismos patógenos, como

hongos, virus o bacterias. Se han introducido varios fármacos en polímeros e hidrogeles, especialmente, aquellos con actividad antimicrobiana de amplio espectro y mecanismos de acción conocidos.

El método de injerto se ha empleado para modificar superficies, con polímeros sensibles a estímulos, con estructura tipo peine, que permita la carga y liberación de algún agente antimicrobiano. La retención del fármaco dentro de la estructura polimérica puede alcanzarse mediante un estímulo e interacciones no covalentes, y de la misma manera se puede controlar su liberación. La vancomicina se ha cargado en hidrogeles y matrices poliméricas, al igual que el ciprofloxacino, debido a que sus estructuras químicas favorecen su interacción con las cadenas poliméricas a través de enlaces de hidrógeno y otras interacciones no covalentes. Estos antibióticos se han utilizado por su actividad antimicrobiana de amplio espectro. Por otro lado, compuestos antifúngicos como la Anfotericina B (AmB) y el itraconazol, se han utilizado para combatir la película de hongos y levaduras en dispositivos médicos.

El proceso de liberación controlada de los fármacos inmovilizados puede ser controlado por distintos procesos que dependen de las características fisicoquímicas del fármaco y del polímero, así como su respuesta a factores externos como el pH, la temperatura o la fuerza iónica. Existen tres mecanismos de liberación de fármacos para una matriz polimérica: 1) sistemas controlados por difusión, 2) sistemas controlados por contacto con el disolvente y; 3) sistemas de control químico. Los mecanismos 1 y 2 son procesos controlados por difusión, sin embargo, dependen de distintos factores para llevarse a cabo.

El mecanismo de liberación para los sistemas controlados por difusión ocurre por permeación del fármaco desde el interior de la matriz polimérica, y la velocidad de liberación es controlada por la velocidad de difusión, la cual está relacionada con el coeficiente de difusión del fármaco a través de las cadenas del polímero, el cual depende de la estructura química y la concentración del fármaco [52].

1.6. Radiación ionizante

El término “radiación ionizante” involucra distintos tipos de radiación que permitan la ionización de un compuesto químico. Esto puede lograrse mediante el bombardeo de electrones u otras partículas cargadas, así como por la irradiación de un haz de luz. Transportando esto al espectro electromagnético se estaría hablando de aquella radiación con longitudes de onda muy bajas.

La radiación ionizante es aquella que acarrea mayor energía, tanta como para expulsar electrones de la materia con la que interactúe. De la radiación electromagnética se distinguen tres tipos de radiación ionizante: 1) la radiación UV, 2) los rayos X y; 3) la radiación γ (Figura 7).

Figura 7. Espectro electromagnético.

Cada una de estas radiaciones interactúa de distinta manera con la materia, lo cual depende de la cantidad de energía que se suministra al irradiar. Para cuantificar la radiación y la intensidad se han utilizado distintas unidades de medición, las cuales se representan en la Tabla 2.

Tabla 2. Formas de cuantificar la radiación y sus unidades.

Formas de cuantificar radiación	Definición	Unidad del Sistema Internacional
Actividad de radiación.	Cantidad de material inestable (átomos) que sufren decaimiento radioactivo por segundo.	Bq [=] s^{-1}
Dosis de Radiación.	Cantidad de energía que absorbe algún material por unidad de masa debido a la interacción con la radiación ionizante.	Gy [=] J/kg
Intensidad de una fuente de radiación.	Dosis de radiación emitida por una fuente por unidad de tiempo.	Gy/s

1.6.1. Radiactividad y radiación γ

La radiactividad fue descubierta a principios del siglo XX gracias a la contribución de distintos científicos de esa época, los cuales fueron acreedores al premio nobel años más tarde. Estos científicos fueron Antoine Henri Becquerel quien descubrió que el uranio emitía espontáneamente una radiación desconocida. Posteriormente, su pupila Marie Curie junto con su pareja, lograron caracterizar otras dos sustancias radiactivas, el polonio y el radio. Estos elementos tenían la capacidad de emitir radiación y partículas de manera espontánea sin previa excitación, ahí surgió el término de radiactividad. Actualmente, la radiactividad es una herramienta importante en el desarrollo de distintas tecnologías como: en la producción de energía, en tratamientos médicos y en la industria cosmética y alimentaria.

La radiactividad es un fenómeno que se produce de manera espontánea en núcleos de átomos inestables que al decaer a su forma más estable, emiten gran cantidad de energía en forma de radiación electromagnética o partículas del núcleo. La capacidad de emisión, el tipo y energía de la radiación emitida son característicos de cada elemento radiactivo. Cuando este fenómeno sucede pueden liberarse distintas partículas del núcleo atómico para alcanzar un estado energético más estable, estas partículas se dividen en radiación α, β, γ y X.

Al emitirse estas partículas pueden interactuar de distinta manera con la materia, ya que cada una posee distinta masa y energía, lo cual influye directamente en el alcance de la radiación emitida. Las partículas α ($^{2}_{4}He^{2+}$) tienen mayor masa que las β (electrones e^{-} y positrones e^{+}), mientras que los fotones de los rayos X y γ no tienen masa.

Masa $\alpha > \beta > \gamma$ o X

Cuando estas partículas chocan con la materia, le transfieren parte de su energía, de esta manera pierden energía y su alcance de penetración es menor, entonces, mientras mayor es la masa de la partícula es más fácil que choque con átomos o moléculas, lo que provoca que ésta pierda energía y tenga menor penetración. A esto se le conoce como Transferencia Lineal de Energía (LET por sus siglas en inglés) y puede cuantificarse midiendo cuánta energía pierde una partícula emitida

cuando atraviesa linealmente una muestra de materia. Mientras mayor sea el valor de LET de una partícula más energía perderá por unidad de distancia en su recorrido. Entonces, las partículas con mayor masa tienen un valor de LET más alto, es decir, pierden su energía en menos distancia. Esto permite entender el alcance de las partículas emitidas durante el decaimiento de un núcleo atómico. Cada una tiene un alcance de penetración distinto como se muestra en la Figura 8.

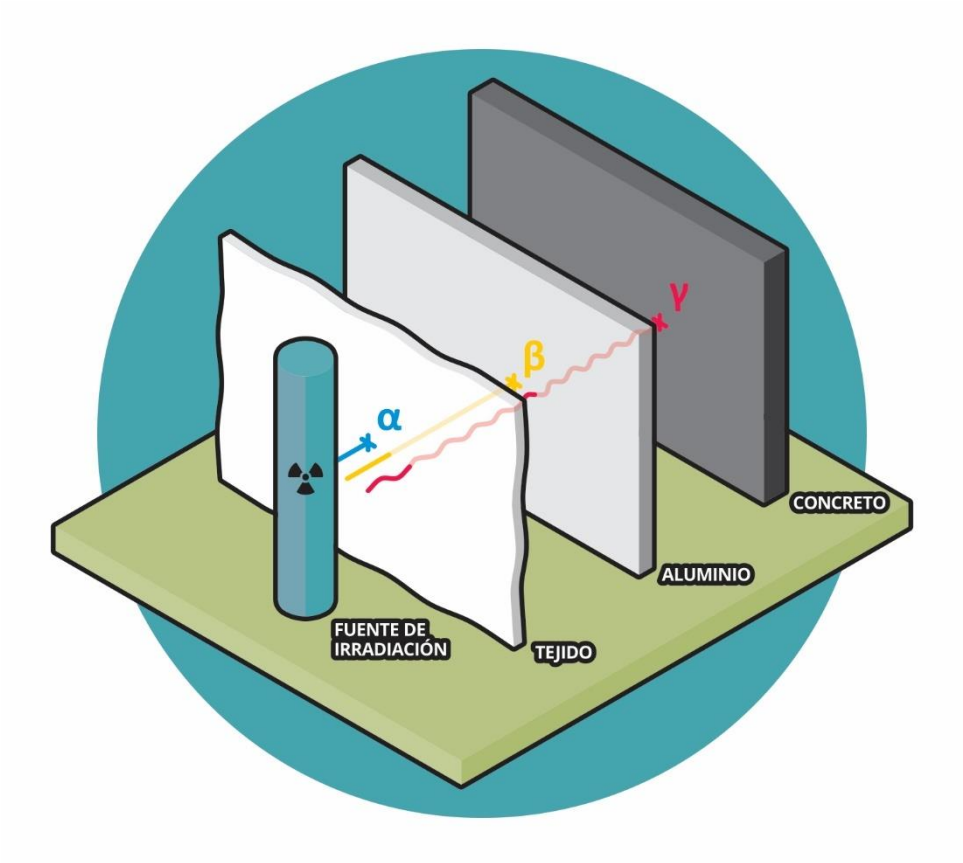

Figura 8. Alcance de penetración de las partículas emitidas durante el decaimiento de un núcleo atómico.

En la naturaleza existen diversos núcleos inestables, que al decaer a su estado más estable liberan su energía en estas formas de radiación. Algunos de ellos son de origen natural como el uranio-238 (^{238}U), siendo más pesado que el cesio-137 (^{137}Cs) y el yodo-131 (^{131}I). La radiactividad también puede inducirse, se pueden crear núcleos inestables de manera artificial mediante el bombardeo con neutrones a un átomo estable, para formar isótopos y núcleos altamente energéticos, este es el caso del cobalto-60 (Co^{60}).

El ^{60}Co es un radioisótopo artificial que emite partículas β y radiación γ. Se produce a través del bombardeo de neutrones al isótopo estable ^{59}Co, y tiene una vida media de 5.2 años, lo cual le permite ser usado por una cantidad considerable de tiempo como elemento radiactivo. El ^{60}Co siendo un isótopo inestable decae hacia el isótopo ^{60}Ni. Al suceder este fenómeno se emiten partículas β y rayos γ altamente energéticos, como se muestra en la Figura 9.

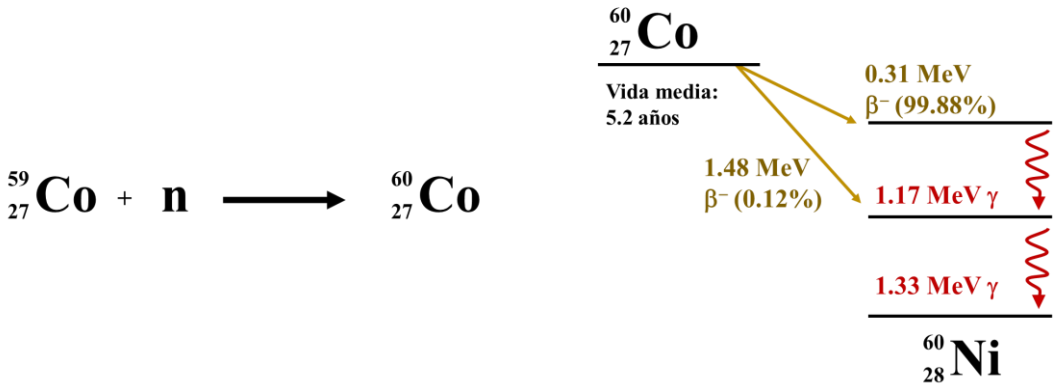

Figura 9. Formación del ^{60}Co y diagrama de decaimiento β hacia ^{60}Ni.

1.7. Radiación ionizante en la química de materiales y como estrategia en la modificación de polímeros

Debido a que la radiación ionizante tiene distintos efectos sobre la materia en la que interactúa, esta ha sido empleada dentro de la química de materiales, como fuente de energía, y para las modificaciones estructurales de éstos. En el área de la química de polímeros se ha empleado como método de iniciación de la reacción de polimerización. El uso de la radiación como iniciador de polimerización con respecto a los iniciadores químicos tiene como ventaja que no se generan subproductos indeseables que provocan contaminación del material final. Adicionalmente, la radiación γ se ha utilizado en la industria como método de esterilización de material quirúrgico y cosmético, sin provocar afectaciones estructurales en ellos.

De una manera detallada, cuando la radiación γ interactúa con la materia ocurre una reacción química que genera productos inestables que, posteriormente, forman especies más estables. Debido a que la fuente de irradiación genera radiación altamente energética, en un primer paso conduce a la formación excitación de las moléculas que forman radicales que se recombinan entre sí y forman especies radicalarias, más estables. Estas especies son clave en la química de radiaciones ya que los radicales formados, posteriormente, pueden reaccionar entré sí, o con otros compuestos aceptores (como monómeros vinílicos) para llevar a cabo reacciones convencionales de la química de radicales libres.

Considerando que una reacción de radiación se lleva a cabo en disolvente, pueden suceder distintas reacciones, dónde se forman las distintas especies excitadas, iónicas y radicalarias. Estas reacciones se clasifican en primarias y secundarias. Las primarias son aquellas que involucran la formación de especies por interacción directa con la radiación, mientras que las secundarias involucran la recombinación de las especies primarias. En la siguiente figura se muestran las reacciones típicas para la radiólisis del agua.

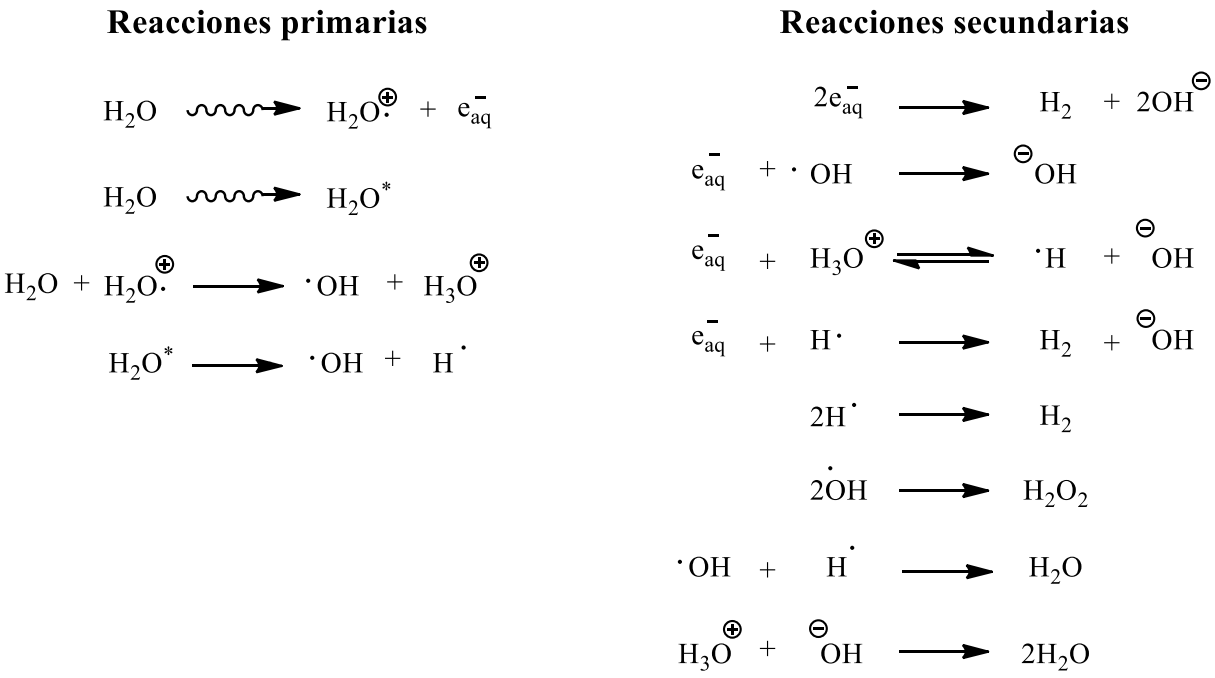

Figura 10. Reacciones primarias y secundarias para la radiólisis del agua producidas por radiación γ.

Este comportamiento de formación de radicales por la interacción de la radiación γ con el agua es muy similar para los disolventes de la misma naturaleza, es decir, aquellos con carácter polar. Para estos disolventes los electrones que se desprenden tienen suficiente energía y se encuentran libres, solvatados por moléculas del disolvente, de ahí el nombre "electrón solvatado". En el caso de que el disolvente sea agua se le conoce "electrón acuoso". Sin embargo, cuando la reacción se lleva a cabo en disolventes no polares, los electrones desprendidos poseen baja energía, y de inmediato se forma el radical-catión correspondiente, y no hay electrones en la solución.

Este electrón solvatado junto con otras especies formadas (·H y ·OH) pueden llevar a cabo diversos tipos de reacciones, incluyendo reacciones óxido-reducción. Estas especies son agentes reductores muy fuertes, por ejemplo, el potencial de reducción para el electrón acuoso es de e^-_{aq}= -2.87 *vs* ENH, similar al del radical hidroxilo. Con respecto a los radicales ·H y ·OH su efecto depende completamente del pH del medio, de esta manera también se ha empleado la radiación γ en disolución para llevar a cabo reacciones de reducción para la formación de partículas metálicas [53].

Por ejemplo, se ha reportado la síntesis de nanopartículas de plata en medio acuoso mediante un mecanismo de irradiación-reducción, el cuál comienza con la formación de las especies de la radiólisis del agua, que posteriormente reducen la Ag^{+1} a Ag^0; las reacciones se representan en la Figura 11. Con esta metodología se han logrado obtener partículas y cúmulos de plata en distintos tamaños y morfologías, esto modulando el suministro de energía a la muestra, es decir, la dosis de radiación [54–57].

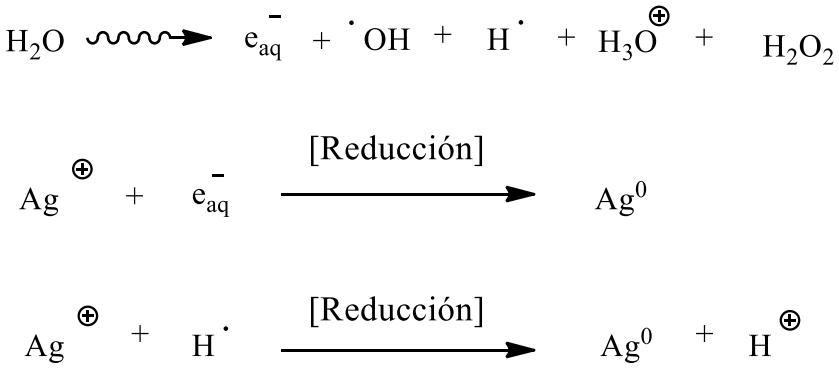

Figura 11. Mecanismo de irradiación-reducción para la formación de Ag^0 en medio acuoso.

Por otro lado, aprovechando la formación de radicales, la radiación γ también se han utilizado para llevar a cabo reacciones de polimerización sobre superficies, es decir, reacciones de injerto. Las generalidades de este tipo de modificación se abordaron en la sección 2.3, donde se habla que tal modificación se puede realizar sobre superficies de derivados orgánicos, como polímeros, para adicionarle propiedades al material.

La radiación γ al interactuar con la materia da lugar a la ruptura homolítica en los enlaces de un compuesto debido a su alta energía, lo cual forma radicales que pueden reaccionar entre ellos, con otro compuesto en el medio o con los radicales del disolvente [58]. Para generar especies reactivas e iniciar una reacción de polimerización sobre una superficie pueden utilizarse dos estrategias: i) Radiación por método directo/simultáneo o ii) Método de pre-irradiación oxidativa (ver Figura 12). En el método directo se irradia la matriz polimérica y por efecto de la energía que acarrea la radiación se conduce a la ruptura de enlaces, formando radicales para iniciar la reacción. Sin embargo, en el método de pre-irradiación oxidativa, la matriz polimérica se expone a la radiación en presencia de oxígeno para formar grupos peróxido e hidroperóxido, que al ser sometidos a un aumento de temperatura sufren una ruptura homolítica en su enlace oxígeno-oxígeno formando radicales que funcionan como iniciadores en una reacción de polimerización; de la misma manera cómo funcionan los iniciadores convencionales como el peróxido de benzoilo.

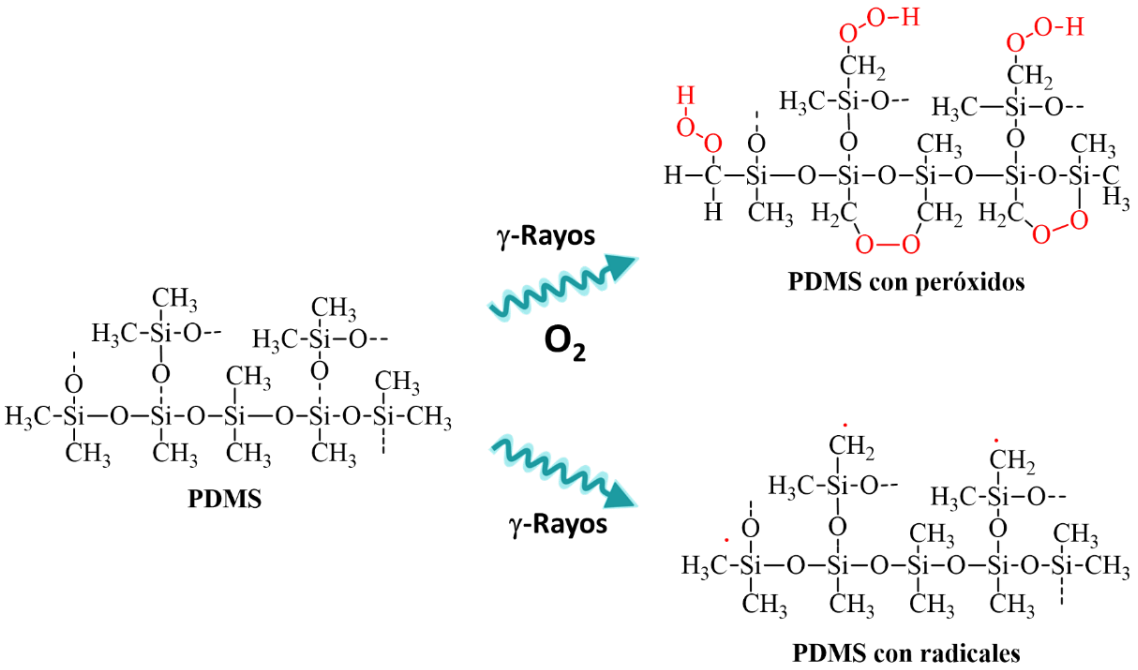

Figura 12. Generación de radicales en una matriz polimérica mediante radiación γ.

Las dos estrategias señaladas se han utilizado para modificar superficies poliméricas utilizando como fuente de radiación ^{60}Co, y su desempeño depende de la naturaleza química de la matriz polimérica a modificar, de los monómeros utilizados, y del medio de reacción (catalizadores y disolvente). Existen diversos reportes sobre la modificación de polímeros con aplicación biomédica utilizando radiación γ [20,58], debido a que tal radiación es un recurso en el proceso de esterilización de este tipo de materiales.

Además de controlar estos factores para obtener la reacción de injerto, también es necesario conocer la dosis con la cual pueden pasar otros efectos, ya que cuando se irradia una estructura polimérica se pueden observar: i) un aumento en el grado de reticulación o entrecruzamiento; o ii) la degradación del material polimérico.

La reticulación de polímeros ocurre en aquellos que tienen carbonos secundarios o terciarios en su cadena principal. Esto es debido a que en estos compuestos el enlace más lábil es el enlace C-H, el cual se rompe para formar dobles enlaces que luego pueden funcionar como centros reactivos para polimerizaciones radicalarias. Por otro lado, la degradación es común en polímeros que tienen carbonos cuaternarios o heteroátomos en la cadena principal del polímero. El proceso de degradación se da por la ruptura de los enlaces de la cadena principal del polímero, lo cual genera macromoléculas de bajo peso molecular que pueden seguir teniendo rupturas hasta descomponerse por completo.

1.8. Polidimetilsiloxano

El polidimetilsiloxano (PDMS), en su forma elastomérica, es uno de los principales polímeros utilizados para la manufactura de catéteres, tubos y válvulas [59] y, al igual que todos los polímeros, es susceptible a la contaminación bacteriana y por hongos; principalmente, por aquellos microorganismos oportunistas y comunes en el ambiente hospitalario.

El PDMS posee una estructura química intercalada de silicio, carbono y oxígeno (ver Figura 13), tiene un carácter muy hidrofóbico, altamente biocompatible e inerte. Además, sus propiedades elásticas (elongación 400%) y térmicas (descomposición a 400°C) permiten que sea útil para la fabricación de materiales flexibles. Sin embargo, se ha demostrado la formación de *biofilm* sobre la superficie de dispositivos de PDMS [60].

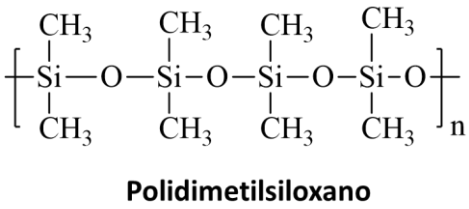

Figura 13. Estructura química del PDMS.

El PDMS se ha modificado empleando diversas técnicas físicas y químicas, dentro de éstas se encuentra el uso de la radiación ionizante, que ha permitido modificar su superficie con el objetivo de adicionar o modular sus propiedades [61–64]. La radiación γ se ha utilizado como recurso en la modificación de PDMS o silicona, ya que presenta estabilidad frente a ella, incluso a dosis mayores a 100 kGy. Este polímero no sufre degradación a dosis menores a 120 kGy debido a que el enlace Si-O es altamente estable, a comparación del enlace C-C de la cadena principal en otros polímeros, (~110 y 80 kcal mol^{-1}; respectivamente) [65-66].

Cuando se expone el PDMS a la radiación, los enlaces que se rompen son el enlace C-Si y el C-H, ya que son los que tienen energías de disociación de enlace menores. La formación de radicales en estos átomos conduce principalmente a la reticulación, lo que disminuye la movilidad de las cadenas poliméricas, y por consecuencia sus propiedades mecánicas. Esto se puede disminuir realizando la exposición a la radiación en una atmósfera con oxígeno, ya que las especies reactivas de oxígeno interfieren en con los radicales formados en la matriz, evitando que se encuentren entre ellos. La formación de radicales puede modularse mediante el suministro de la energía, a menores dosis el grado de reticulación disminuye [65].

Para evitar la formación de la biopelícula bacteriana se ha recurrido a la modificación de su superficie mediante diversos métodos, uno de ellos es el uso de radiación γ. Se han logrado llevar a cabo reacciones de injerto sobre la superficie, incorporando distintos polímeros que le confieran propiedades *antifouling*. Como primera aproximación, se han injertado monómeros con propiedades antimicrobianas intrínsecas que le confieran propiedades bactericidas o fungicidas a la superficie, como derivados del imidazol [67]. Sin embargo, también se han injertado polímeros sensibles a estímulos que permitan la inmovilización y liberación controlada de agentes antimicrobianos [20,37,68]. Adicionalmente, la funcionalización de la superficie de este polímero también ha permitido adicionar otros agentes antibacterianos, como proteínas. Por ejemplo, el anclaje covalente de proteínas como la lisozima que funge como agente antimicrobiano [69–71] o antibióticos convencionales [72].

Como se revisó en la sección 2.2, el carácter hidrofóbico de una superficie puede ser un factor que contribuya a la formación del *biofilm*, siguiendo esta línea se han injertado diversos polímeros hidrofílicos sobre el PDMS, estos polímeros tienden a absorber agua y son afines a medio acuoso, como es el caso de los derivados de acrilatos, en su forma ácida o sal.

El ácido acrílico (AAc) se ha logrado injertar a la superficie del PDMS mediante diversas técnicas, como la radiación UV, láser, química convencional, polimerización por emulsión, tratamiento con ozono y radiación γ [63,73, 79]. Pese a que es un monómero muy reactivo se han alcanzado grados de injerto sobre PDMS elastomérico cercano al 400% en masa utilizando el método de reacción de injerto por pre-irradiación oxidativa, cuando se aumenta la dosis de irradiación y la temperatura para iniciar la ruptura de peróxidos e hidroperóxidos [80].

Además de agregar hidrofilicidad a la superficie del PDMS, el AAc ha permitido la inmovilización de enzimas, fármacos y partículas metálicas, debido a la característica de los grupos carboxílicos pendantes, estos pueden fungir como donadores o aceptores de enlace de hidrógeno, o a través de fuerzas electrostáticas, en el caso de la forma desprotonada (COO^-). Incluso se han diseñado hidrogeles basados en acrilatos dónde se han logrado retener AgNP's [81] y matrices poliméricas injertadas. Ping y colaboradores (2010), lograron preparan e inmovilizar AgNP's en PET injertado con AAc (PET-*g*-AAc). La síntesis de las nanopartículas se logró utilizando un método de reducción químico [82].

El ciprofloxacino (CFX) representado en la Figura 14 se ha retenido en diversas matrices poliméricas incluyendo hidrogeles, con el objetivo de inhibir el crecimiento bacteriano [83–86].

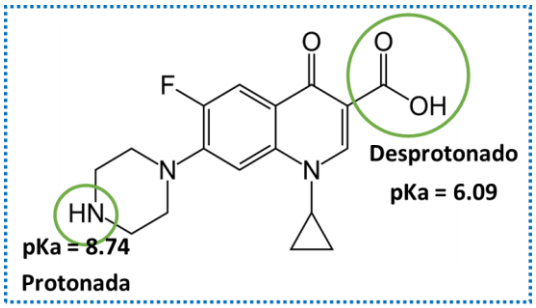

Figura 14. Estructura química del ciprofloxacino.

El ciprofloxacino es un antibiótico de la familia de las fluoroquinolonas, tiene una actividad de amplio espectro y combate a bacterias Gram positivas y negativas inhibiendo a las enzimas topoisomerasa II (girasa ADN) y topoisomerasa IV, así bloqueando los procesos de replicación, transcripción, reparación y recombinación del ADN bacteriano. Su efectividad ante diversas bacterias se presenta en la Tabla 3 [87].

Tabla 3. Concentración Mínima Inhibitoria (MIC) del ciprofloxacino ante diversas bacterias.

Organismo	MIC (µg/mL)
Escherichia coli	0.004 – 0.015
Enterococcus faecalis	0.250 – 2.000
Haemophilus influenzae	0.004 – 0.030
Neisseria gonorrhoeae	0.001 – 0.008
Pseudomonas aeruginosa	0.250 – 1.000
Staphylococcus aureus	0.120 – 0.500

2. PLANTEAMIENTO DEL PROBLEMA

2.1. Justificación

Dentro del grupo de investigación de Química de Radiación en Macromoléculas (ICN-UNAM) se ha hecho la modificación de diversas matrices poliméricas utilizando como recurso de polimerización la radiación γ. El uso de la radiación ha permitido injertar diversos monómeros sobre la silicona o PDMS, lo cual ha permitido retener fármacos en la superficie de la matriz injertada. La modificación de películas de PDMS con AAc se ha logrado mediante el método de pre-irradiación oxidativa, sin embargo, el uso del método simultáneo no ha sido del todo satisfactorio. La adición de un agente entrecruzante metacrílico (EGDMA) ayudará a la generación de injertos en 3D que dotarán de hidrofilicidad a la matriz de PDMS, y a retener ciprofloxacino (CFX). Las características fisicoquímicas de los dos monómeros permitirán llevar a cabo la reacción de injerto en medios órgano-acuosos y probar la reacción de injerto utilizando la radiación γ, síntesis e inmovilización de AgNP's en un solo paso. Lo que no ha sido reportado con anterioridad, además se buscarán condiciones para obtener AgNP's de un mismo tamaño y morfología. Finalmente, las películas modificadas PDMS-*g*-(AAc/EGDMA)/CFX y PDMS-*g*-(AAc/EGDMA)+Ag tendrán propiedades antimicrobianas debido a las características antibióticas de los agentes antimicrobianos cargados. La biocompatibilidad del PDMS de partida permitirá que la adición del injerto, las partículas de plata o el ciprofloxacino no afecten su interacción con el ambiente extracelular.

2.2. Hipótesis

Será posible cambiar las propiedades fisicoquímicas de las películas de polidimetilsiloxano (PDMS) realizando un injerto binario de ácido acrílico (AAc) y etilenglicol dimetacrilato (EGDMA), para obtener un material con respuesta a pH, que presente las características químicas e hidrofílicas provenientes del PAAc, para permitir la inmovilización de agentes antimicrobianos

Primera sección: Está demostrada la formación de AgNP's en medio acuoso utilizando radiación γ. Las AgNP's se inmovilizarán en las cadenas pendantes de PAAc a través de interacción metal-carboxilato, y se llevará a cabo la reacción de injerto y la reducción de la Ag^{+1} en la misma reacción. Además, el efecto citotóxico de las AgNP's proveerá de actividad antimicrobiana a la superficie de la película de PDMS, manteniendo su compatibilidad con células de tejido, como los fibroblastos.

Segunda sección: Los grupos funcionales favorecerán, a través de enlace de hidrógeno, la retención de ciprofloxacino con grupos funcionales similares. La difusión del agua al interior permitirá que difundan moléculas pequeñas a la matriz de PDMS. El comportamiento de hinchamiento de la matriz polimérica favorecerá la liberación lenta de ciprofloxacino.

2.3. Objetivos

Objetivo general

Modificar matrices poliméricas de polidimetilsiloxano mediante radiación ionizante con fragmentos acrílicos para la inmovilización y albergue de compuestos con actividad antimicrobiana.

Objetivos específicos

Los objetivos específicos de la tesis se enlistarán de acuerdo a la división en secciones de ésta.

Estudios preliminares:

1. Modificar películas de PDMS con AAc y EGDMA, empleando radiación γ por el método directo de polimerización.
2. Caracterizar las películas modificadas mediante técnicas espectroscópicas convencionales: FTIR-IR, RMN-SS, TGA y DSC.
3. Estudiar el comportamiento de las películas modificadas en medio acuoso mediante pruebas de hinchamiento, y la humectabilidad de la superficie haciendo uso del análisis por ángulo de contacto.
4. Evaluar la respuesta de las películas al ser expuestas a distintos valores de pH con el fin de encontrar el pH crítico, así como, evaluar la acidez de la superficie mediante titulaciones potenciométricas.

Primera Sección:

1. Llevar a cabo la reacción de injerto de AAc/EGDMA e inmovilizar AgNP's en un solo paso utilizando radiación γ.
2. Caracterizar las películas con AgNP's utilizando espectrofotometría de UV-Vis de películas y SEM/EDX.
3. Realizar pruebas de inhibición de crecimiento bacteriano y de citocompatibilidad.

Segunda Sección:

4. Realizar las pruebas de carga y liberación de ciprofloxacino en las películas modificadas en tolueno.
5. Realizar pruebas de inhibición de crecimiento bacteriano y de citocompatibilidad.

3. SECCIÓN EXPERIMENTAL

3.1. Generalidades

Materiales y reactivos

Las películas de PDMS con densidad de 1.1 a 1.5 g cm^{-3} y 1 mm de espesor se adquirieron a través de Good-Fellow (Hunting, Reino Unido). Los monómeros etilénglicol dimetacrilato (EGDMA) y ácido acrílico (AAc) se compraron en Sigma-Aldrich Co. (St Louis MO, USA). Estos los monómeros fueron purificados mediante destilación al vacío. De igual manera, el nitrato de plata ($AgNO_3$) (99.9 %) se adquirió mediante la compañía Sigma-Aldrich Co. (St Louis MO, USA). Los disolventes grado analítico (tolueno, etanol, metanol y acetona) fueron obtenidos a través de la casa comercial Baker-México. Las soluciones amortiguadoras se fabricaron utilizando fosfato de sodio, ácido bórico, carbonato de sodio y ácido cítrico, adquiridos en Sigma-Aldrich Co. (St Louis MO, USA) y como disolvente agua Milli-Q.

Recursos técnicos

La exposición a radiación-γ se hizo en el equipo Gammabeam 651PT disponible en el Unidad de Irradiación y Seguridad Radiológica del Instituto de Ciencias Nucleares de la Universidad Nacional Autónoma de México, empleando ^{60}Co con una vida media de 5.2 años y con intensidades de dosis de radiación promedio de 8 kGy h^{-1} y una actividad de 2338.4 TBq.

Infrarrojo con reflectancia total atenuada y transformada de Fourier (FTIR-ATR), modelo: Perkin-Elmer Spectrum 100 y marca: Perkin Elmer Cetus equipado con un accesorio universal ATR (DiCompTM cristal) y punta de diamante. Para la obtención de los espectros se hizo corrección de línea base y se colectaron con 16 scans.

Resonancia Magnética Nuclear en Estado Sólido (SS ^{13}C NMR): El estudio de SS ^{13}C NMR se llevó a cabo mediante la técnica de Cross Polarization/Magic Angle Spinning (CP/MAS), en un equipo marca Jeol, modelo Jeol 300 MHz, con 200 mg de muestra.

El análisis UV de las películas fue realizado en un equipo Ocean Optics HR4000CG-UV-NIR.

Los estudios de microscopía electrónica de barrido fueron realizados utilizando un microscopio JEOL JSM-5900-LV, en la Unidad de Servicios de Apoyo a la Investigación y la Industria (USAII) de la UNAM. Los estudios fueron realizados con un voltaje de aceleración de 15 kV después de cubrir las muestras por *sputtering* con grafito. Para comprobar el contenido elemental se realizó el experimento de Espectroscopia Dispersiva de Energía de Rayos X (EDX).

Comportamiento térmico. Los estudios de Calorimetría diferencial de barrido (DSC) se realizaron en un calorímetro modelo: 2010 DSC, marca: TA Instruments. El historial térmico y el disolvente ocluido de las muestras se hizo mediante un calentamiento previo desde 25 hasta 100 °C, con una velocidad de calentamiento de 10 °C min^{-1}, en atmósfera de nitrógeno. Posteriormente, se obtuvo el termograma final, en un segundo calentamiento, desde 25 hasta 350 °C, a la misma velocidad de calentamiento. El análisis termogravimétrico se realizó en un equipo TA Instruments TGA Q50, desde 25 a 800 °C, con una velocidad de calentamiento de 10 °C min^{-1}, en atmósfera de nitrógeno.

El ángulo de contacto se realizó por triplicado, a temperatura ambiente (25 °C), en un equipo KRÜSS DSA 100 (Matthews NC, EE. UU.) depositando una gota de agua bidestilada sobre la película. El ángulo de contacto fue calculado a distintos tiempos dependiendo la muestra.

Las titulaciones ácido base fueron monitoreadas con un potenciómetro HANNA HI4212, utilizando un electrodo combinado de vidrio (HANNA HI 1331B), realizando una calibración estándar de tres puntos, utilizando tampones de pH de referencia de Fisher Scientific (pH = 4.0, 7.0, 10.0). Para las pruebas, se pesó una masa constante de PDMS modificado (~ 0.2 g) y se colocó en agua desionizada con agitación constante. Se añadió lentamente KOH 0.01 mol L^{-1} hasta alcanzar un volumen base añadido del doble del volumen necesario para alcanzar el punto de equivalencia, mientras se monitoreaba el pH con el potenciómetro. El pH inicial de la titulación se estableció manualmente en un valor de dos para todas las muestras.

Los ensayos de citocompatibilidad se probaron en la línea celular de fibroblastos embrionarios murinos BALB / 3T3 (ATCC CCL-163, Manassas, VA, EE.UU.). El porcentaje de viabilidad celular se cuantificó después de la exposición al material modificado. Los ensayos se llevaron a cabo en placas de 96 pocillos sembradas con 50,000 células mL^{-1}, utilizando medio de Eagle modificado de Dulbecco (DMEM) con FBS (suero fetal bovino, 10% v/v), penicilina-estreptomicina (1% *p/v*) y gentamicina (10 µg/mL), durante 12 h, en condiciones estándar de cultivo. Las películas de PDMS, PDMS-*g*-(AAc/EGDMA), PDMS-*g*-(AAc/EGDMA)+Ag, (0.25 × 0.20 cm) se sumergieron en el medio celular y se incubaron en una atmósfera humidificada de CO_2, al 5%, a 37 °C, durante 24 h. Después de este tiempo, la temperatura de la incubadora se fijó a 30 °C para un cambio suave de temperatura durante la noche, y se analizó la viabilidad celular a las 24 h. Se retiraron las películas y se utilizó un kit MTT para cuantificar la viabilidad celular. Se utilizaron células sin películas como control negativo. Todos los experimentos se realizaron por triplicado. Por último, las absorbancias se midieron mediante espectrofotometría a 620 nm (Multiskan FC, Thermo Scientific). La evaluación de los datos estadísticos se realizó mediante ANOVA de una vía utilizando GraphPad Prism 7 (San Diego, CA, EE. UU.).

Las pruebas de inhibición de crecimiento bacteriano se realizaron en la Facultad de Química UNAM (preliminares) utilizando las bacterias *Escherichia coli (ATCC 25922), Pseudomonas aeruginosa (ATCC 27583)* y *Staphylococcus aureus (ATC 25923)* a una concentración de $1.5x10^8$ UFC mL^{-1}, 0.5 en escala McFarland. Las mediciones por UV-Vis se realizaron en un espectrofotómetro de doble haz SPECORD 200 PLUS, marca: analytikjena. Las pruebas se realizaron tomando 100 mg de la muestra PDMS-*g*-(AAc/EGDMA)+Ag (10 mM) (*I*= 10 kGy h^{-1}) (naranja) (**d**), GY ~10%, que se depositó en tubos de ensayo con los medios de cultivo con 0.5 escala McFarland. Para las pruebas preliminares, las muestras se incubaron durante 24 h a 37 °C, y se hizo la medición de la carga bacteriana utilizando el espectrofotómetro UV-Vis realizando la lectura a 600 nm. Los estudios de cinética de crecimiento bacteriano contra *Staphylococcus aureus (ATC 25923)*, se llevaron a cabo en la Facultad de Ciencias Químicas UABC, se realizó el mismo procedimiento que en los estudios preliminares, se incubaron a 37 °C y se realizó la lectura de la absorbancia en 600 nm a las 3, 6, 12, 24 y 48 h. Todos los experimentos se realizaron por triplicado y se calculó el error estándar de la media.

Carga y liberación de ciprofloxacino: Para la carga, las muestras de ~100 mg de las películas modificadas en tolueno se colocaron en frascos ámbar con 2 mL de solución salina de fosfatos

(PBS) (pH = 7.4) con ciprofloxacino (CFX) a una concentración de 0.012 mg mL^{-1}. Las muestras se mantuvieron en agitación constante, a 25 °C, durante 48 h. La cuantificación del fármaco se realizó mediante espectroscopía UV-Vis a una λ = 277 nm. Después de que ya no hubo más difusión del CFX al interior de la película, éstas se extrajeron y se secaron en una estufa de vacío a 25 °C, por 24 h, para dejar las películas cargadas. Para la liberación, las muestras previamente secadas con el CFX se depositaron en frascos ámbar con 5 mL de PBS (pH= 7.4), a 37 °C, en agitación constante, se realizó el seguimiento de la liberación acumulativa del fármaco utilizando un equipo de UV-Vis a λ = 277 nm después de 1, 3, 6, 24 y 48 h. La cuantificación para ambos experimentos se realizó utilizando la Ley de Lambert-Beer, considerando la curva de calibración previamente hecha para el ciprofloxacino, la calibración se encuentra en la sección de Anexos.

3.2. Procedimiento general para la polimerización por radiación

Para la modificación de las películas de PDMS se cortaron piezas de 1 x 4 cm que fueron lavadas dos veces con metanol (grado analítico), durante 90 minutos, para eliminar posibles impurezas. Posteriormente, las películas se secaron utilizando una estufa de alto vacío, a 50 °C, y -80 kPa; hasta obtener una masa constante. Las películas se pesaron y se registró la masa de cada una de ellas antes de introducirlas a una ampolleta de vidrio.

A la ampolleta de vidrio con la matriz polimérica en el interior, se le introduce una disolución del monómero de concentración conocida, y la película de PDMS. Posteriormente, se deja reposar hasta el hinchamiento límite, y se degasifica o se elimina el oxígeno utilizando burbujeo de argón o ciclos de *freeze-thaw* (congelar-descongelar), dependiendo el disolvente. Al terminar, se sella la ampolleta y se expone a radiación-γ. Finalmente, se saca el polímero modificado y se lava con disolvente para eliminar residuos e impurezas. Se seca al vacío y se registra su masa.

Dependiendo el objetivo del estudio, se hacen diversos experimentos variando la dosis de radiación, la concentración del monómero y el tipo de disolvente. Los experimentos se realizaron por triplicado y el error estándar de la media (Err) se reporta en los gráficos de resultados.

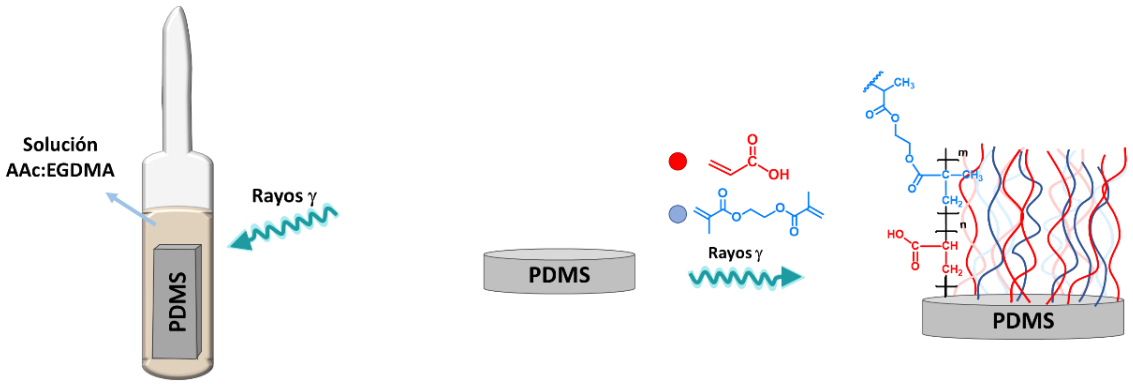

Figura 15. Representación experimental de la modificación del PDMS.

3.2.1. Injerto de AAc y AAc:EGDMA por método simultáneo

A una ampolleta de vidrio, con la película de PDMS en el interior, se le agregó una mezcla AAc:EGDMA en diferentes disolventes. La concentración de la solución se varió desde 5 hasta 50 *% v/v* con el objetivo de analizar el efecto de la concentración en el grado de injerto de los

materiales. También, la relación de monómeros AAc:EGDMA fue variada en las siguientes proporciones molares 1:0, 1:1, 2:1, 3:1, 4:1 y 5:1; para evaluar el comportamiento en solución y la estabilidad de las películas injertadas. Previo a la irradiación, la ampolleta con el PDMS y la disolución de AAc:EGDMA fue degasificada por el método de *freeze-thaw* repitiendo el proceso 4 veces, de 10 minutos cada una antes del sellado. Posteriormente, se expusieron a distintas dosis de radiación-γ producida por el decaimiento de ^{60}Co.

Después de la exposición del PDMS con la mezcla AAc:EGDMA a la radiación, las películas modificadas, PDMS-*g*-(AAc/EGDMA), se lavaron con mezcla MeOH:H_2O (2:1) por 5 ocasiones, de 2 horas cada una; para remover residuos de disolvente e impurezas de monómeros y copolímero. Finalmente, las muestras fueron introducidas en una estufa de alto vacío, a 50 °C, y -80 kPa, durante 6 horas. La masa fue obtenida en una balanza analítica.

El grado de injerto (GY) de las películas fue calculado por diferencia de masa, comparado con la masa inicial (W_0) de la película y la masa de la película modificada (W_g). La fórmula general está representada en la Ecuación 1:

$$GY\ (\%) = [(W_g - W_0)/ W_0]100 \qquad \text{(Ecuación 1)}$$

Este procedimiento general se utilizó para modificar todas las películas mediante el método simultáneo.

3.3. Modificación de las películas con acrilatos y síntesis *in situ* de AgNP's

Para la modificación de las películas con AAc:EGDMA, e inmovilización de AgNP's, se realizó la reacción variando dos parámetros: 1) la dosis y 2) la concentración de $AgNO_3$. Con base en los experimentos previos de variación de disolvente, la reacción se hizo en mezcla Agua:EtOH 1:1 (véase sección 6.1).

Inicialmente, se realizaron experimentos exploratorios variando la relación molar AAc:EGDMA hasta encontrar la proporción que permitió obtener injertos superficiales alrededor de 10%. La proporción AAc:EGDMA 1:3 fue la que generó materiales con buenas propiedades de absorción de agua y películas con propiedades mecánicas deseables. Además, esta concentración fue la ideal para obtener películas con plata inmovilizada en la superficie. El grado de injerto se calculó de la misma manera que para las películas sin plata, utilizando la Ecuación 1.

4. RESULTADOS Y DISCUSIÓN:

4. 1. Estudios Preliminares: Modificación de las películas utilizando radiación

Las diferentes películas PDMS-*g*-(AAc/EGDMA) y PDMS-*g*-AAc fueron preparadas por el método simultáneo de polimerización (Figura 16) variando: 1) el disolvente, 2) la dosis de irradiación, 3) la concentración de monómero en disolución y 4) la relación molar de monómeros.

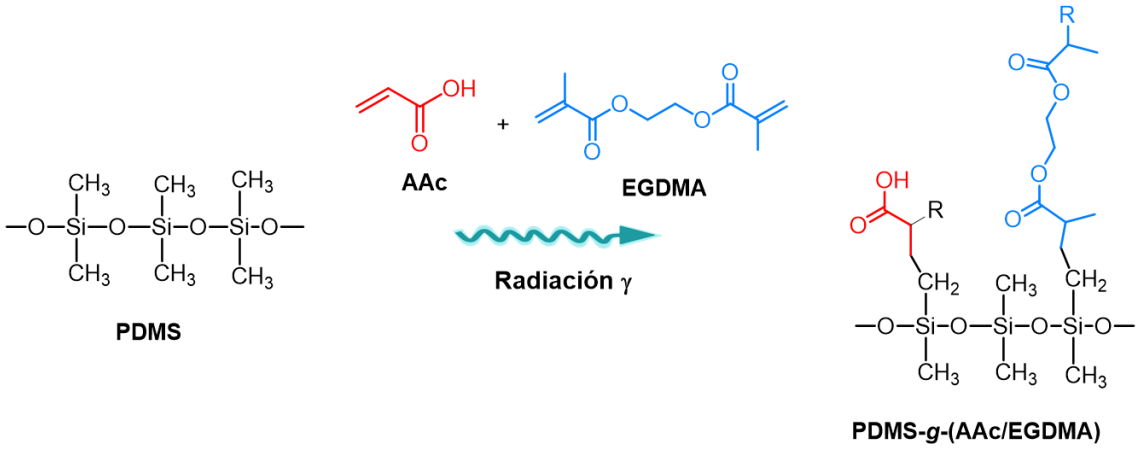

Figura 16. Esquema general de le reacción de injerto sobre la PDMS.

La reacción puede darse de diferentes maneras, es decir, la forma de representarla en el esquema puede ser la más predominante, sin embargo, durante la reacción puede darse primero el injerto de un monómero y posteriormente, sobre ese injerto, la reacción del otro. Se tiene conocimiento de la reactividad del AAc utilizando la radiación, sin embargo, no para el EGDMA. Conocer estas constantes (*r*) podrían ayudar a conocer el mecanismo de reacción por el cual se está llevando a cabo la reacción de injerto.

4.1.1. Elección del disolvente

La reacción de polimerización se llevó a cabo en disolventes de distinta polaridad empleando una concentración de 10% *v/v* de la mezcla de monómeros, con una relación AAc:EGDMA equimolar de éstos, a una dosis de 50 kGy. En la gráfica de barras mostrada en la Figura 17 se puede observar el grado de injerto en los disolventes utilizados para la reacción de injerto, estos resultados son explicados con el comportamiento del PDMS en estos disolventes.

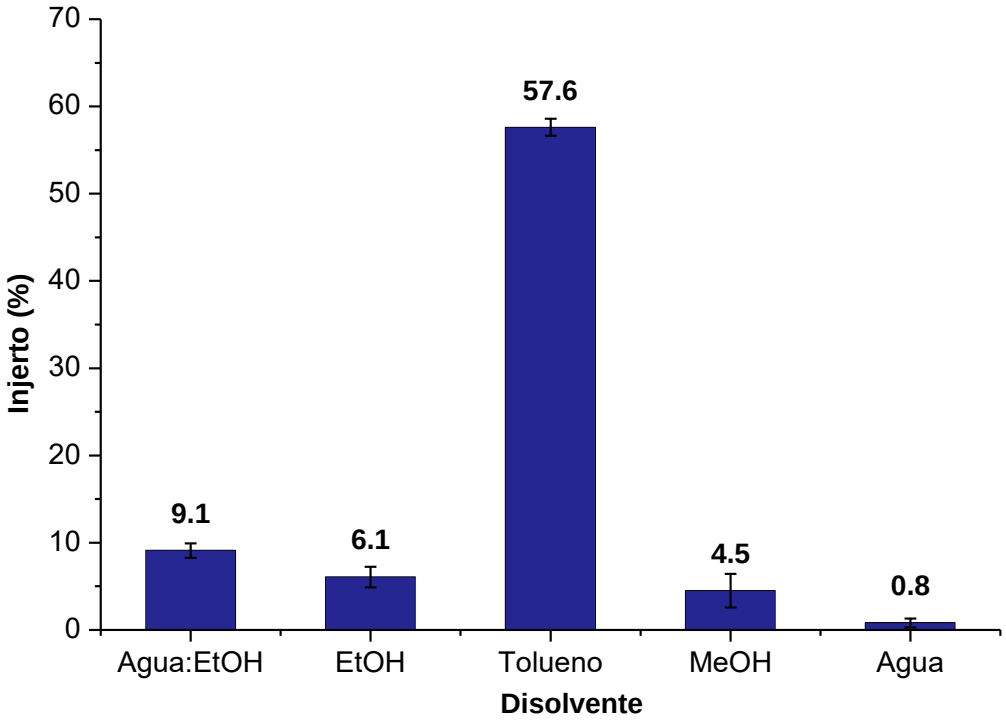

Figura 17. Efecto del disolvente en la reacción de injerto de AAc/EGDMA sobre películas de PDMS.

Está reportado el hinchamiento del PDMS en una gran variedad de disolventes. Lee *et al*. en 2003 reportaron la difusión de estos disolventes a través de la matriz de PDMS (véase la Tabla 4) donde se destaca la gran hidrofobicidad de este polímero y una gran afinidad hacia el tolueno [88]. Considerando esto, al estar en una fase homogénea, el monómero y el disolvente, este sólo difunde a través de las cadenas del polímero con ayuda del disolvente del que está hecha la solución. Por su alta hidrofobicidad, la reacción de injerto empleando agua como disolvente no procede exitosamente, obteniendo injertos por debajo del 1%, atribuido también a que en agua el EGDMA es inmiscible y sólo el AAc es miscible.

Tabla 4. Hinchamiento del PDMS en los disolventes empleados

Disolvente	Hinchamiento	Disolvente	Hinchamiento
Agua	0 %	Tolueno	30 %
Metanol	2 %	Etanol	5 %

Debido a que el tolueno difunde con mayor facilidad a través del PDMS provocando un hinchamiento de la película, este favorece la llegada de la mezcla AAc:EGDMA al interior del polímero. De esta manera, al ser irradiada la ampolleta con la solución de monómero(s) y silicona, los radicales formados en los componentes de la reacción se encuentran con mayor facilidad, y se hace un injerto de AAc/EGDMA dentro de la película, favoreciendo una reacción de injerto en bulto o masa. Esto quiere decir que hay crecimiento de cadenas de polímero dentro de la película y no únicamente en la superficie, como se representa en la Figura 18.

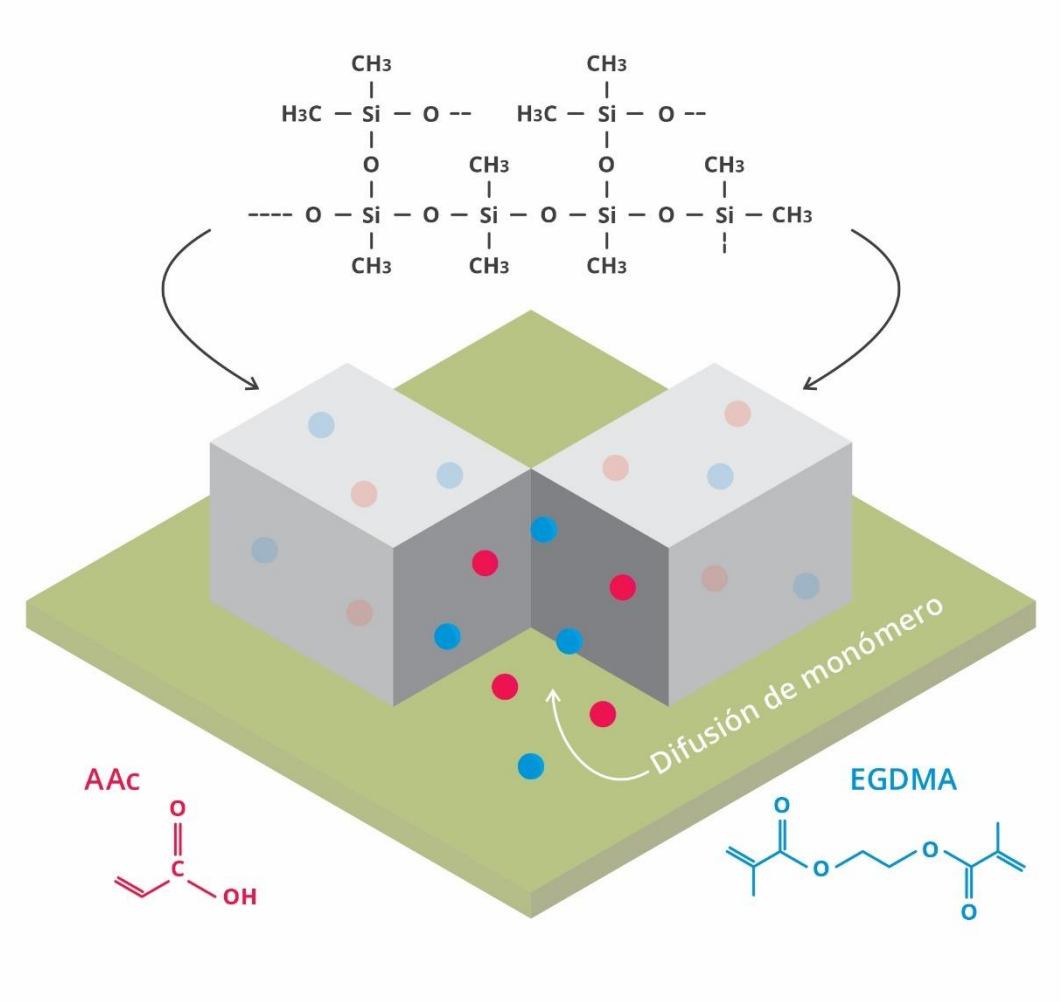

Figura 18. Difusión de monómero a través de la película de PDMS y representación del injerto en masa y en superficie.

De esta manera, las reacciones de polimerización realizadas en tolueno resultan en injertos mayores al 50%, aunado también al hecho de que hay completa solubilidad de los monómeros en este disolvente. Por el contrario, las reacciones en agua, MeOH y EtOH condujeron a la obtención de injertos en superficie, dado que no hubo difusión de monómeros al interior de la película. Además, por la baja afinidad de estos disolventes con el PDMS no hay una buena interacción entre los radicales formados al momento de irradiar la muestra, decayendo el grado de injerto a menos de 7%. También, la baja solubilidad de la mezcla AAc:EGDMA en los alcoholes reduce la probabilidad de colisión de los radicales de los monómeros con los radicales del PDMS ya que favorecen la terminación de la polimerización por la ruptura homolítica del enlace O-H de este grupo funcional.

Es por eso que al llevar a cabo la reacción en la mezcla agua:EtOH hay más injerto, dado que el EtOH interactúa con la superficie del polímero y solubiliza al EGDMA y, el agua favorece la solubilidad del AAc, alcanzando injertos cercanos al 12%. De acuerdo con la utilidad de la película, se selecciona el disolvente adecuado, para llevar a cabo la reacción de polimerización, dado que la respuesta en solución es distinta para una película con injerto en masa o con injerto en superficie.

4.1.2. Efecto de la dosis de radiación y concentración de monómero: Tolueno

La reacción de injerto se realizó en tolueno para la obtención de las películas que se utilizarán para la retención y liberación de agentes antimicrobianos orgánicos. Para este análisis se emplearon distintas dosis de irradiación que no sobrepasarán los 100 kGy (por la reticulación y degradación de la silicona). El efecto de la dosis se estudió: 1) en las cinco relaciones molares propuestas de AAc:EGDMA y 2) con el AAc, la concentración fue fijada en 10% *v/v* en tolueno como disolvente. Para facilitar la identificación de las muestras y películas se utilizaron las claves representadas en la Tabla 5.

Tabla 5. Relación molar AAc:EGDMA para las distintas películas de PDMS modificadas.

Material	Clave	Relación molar
PDMS-*g*-AAc	PDMS-*g*-AAc	1:0
PDMS-*g*-(AAc/EGDMA)	PDMS-1	1:1
	PDMS-2	2:1
	PDMS-3	3:1
	PDMS-4	4:1
	PDMS-5	5:1
P(AAc/EGDMA)	P(AAc/EGDMA)	1:1

*para los experimentos con plata únicamente se utilizaron las películas PDMS-3 y PDMS-5, modificadas en agua:etanol.

En el proceso de injerto se encontró que el grado de injerto depende directamente de la cantidad de dosis absorbida y de la concentración de monómeros, justo como se ha reportado para el injerto de acrilatos sobre matrices de PDMS [89]. Los primeros resultados sobre el injerto de AAc sobre la película de PDMS muestran que mediante polimerización simultánea (concentración: 10% *v/v*) se producen injertos bajos (línea azul en Figura 19a) en comparación con los que se obtienen cuando se hace el injerto utilizando el método de pre-irradiación oxidativa [80]. Esto debido a la alta reactividad del ácido acrílico, ya que al ser irradiado la formación de homopolímero se ve favorecida. Sin embargo, este comportamiento es distinto al aumentar la concentración y mantener fija la dosis en 10 kGy (línea azul en Figura 19b), ya que hay un incremento en el grado de injerto, alcanzando casi el 100%, dado que al aumentar la concentración hay más probabilidad de contacto entre los radicales formados en el PDMS y los monómeros.

Es importante señalar que las películas con injerto mayor a 50% son quebradizas al tacto y poseen una alta capacidad de absorber aguay son susceptibles a degradarse en el medio, por la alta hidrofilicidad del PAAc. Estas propiedades indeseables limitan su aplicación para sistemas biomédicos o biocompatibles, por lo tanto, es más deseable obtener injertos menores. De igual manera, cuando se utilizan dosis por encima de 10 kGy se obtienen películas frágiles debido a que el injerto alcanza casi el 30%.

Por el contrario, al adicionar EGDMA al sistema se logran obtener grados de injerto distintos. En la Figura 19a, la línea continua roja representa el comportamiento de la reacción de injerto en función de la dosis de la película PDMS-1, y se puede observar cómo se obtienen mayores injertos cuando se incrementa la relación AAc:EGDMA (línea continua negra PDMS-5). Los grados de

injerto para las distintas relaciones molares son siempre mayores que cuando se utiliza una relación equimolar, el estudio se realizó para todas las películas PDMS-1 a PDMS-5[§]. Así con el decremento de la cantidad del EGDMA, el grado de injerto aumenta considerablemente debido a que el EGDMA posee dos grupos metacrilato disponibles para reaccionar. Esto se puede explicar con el hecho de que mientras más EGDMA esté disponible en la matriz, la probabilidad de la formación del homopolímero PAAc disminuye, ya que la posibilidad de que dos moléculas de AAc reaccionen entre ellas se reduce. En la reacción de la película con condiciones equimolares (PDMS-1) el injerto es menor que en las demás dado que se favorece la formación de copolímero no enlazado a la película. El injerto no excede del 40% cuando se añade EGDMA al sistema como componente estequiométrico. La probabilidad de terminación de la reacción de polimerización es doble, debido a los dos aceptores de radicales. Es por eso por lo que cuando el sistema contiene menos EGDMA, hay injertos mucho mayores.

En todos los casos de modificación, se utilizó tolueno como disolvente, lo que permitió la difusión de los monómeros al interior de la película de PDMS. Así al formarse los radicales en el PDMS y en los monómeros, hubo una alta probabilidad de reaccionar entre sí, favoreciendo la reacción, alcanzando injertos altos.

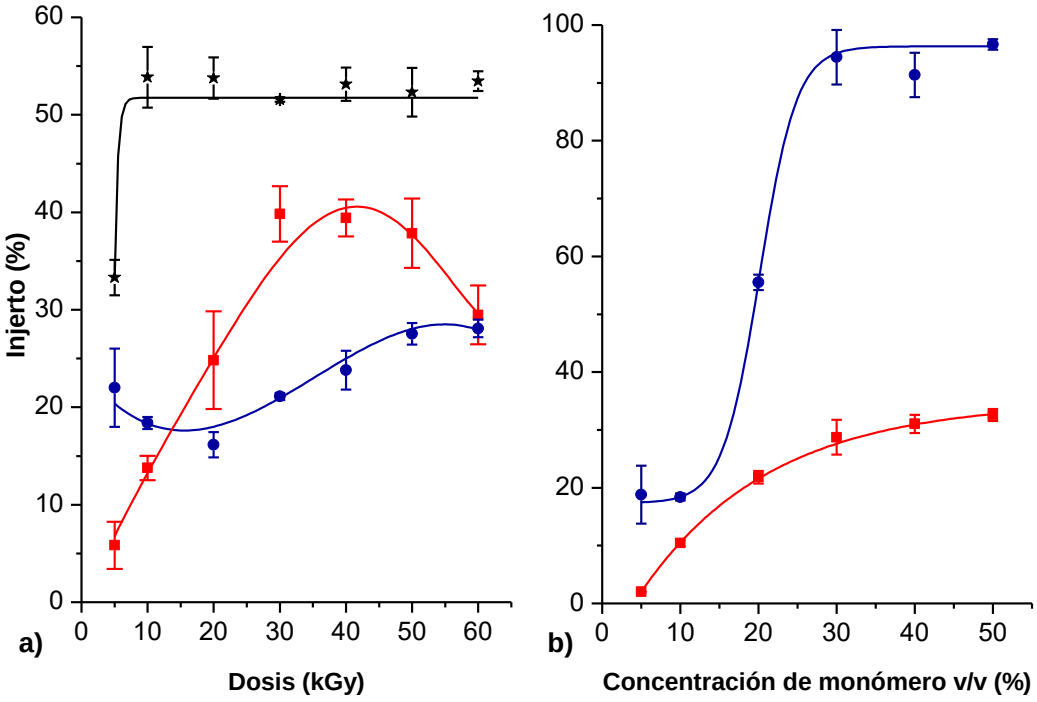

Figura 19. Grado de injerto de las películas modificadas en tolueno (—) PDMS-*g*-AAc; (—) PDMS-1 y (—) PDMS-5 en función de a) la concentración de monómero y b) dosis.
*PDMS-1 y PDMS-5 contienen mezcla de monómeros AAc:EGDMA

[§] Para todos los gráficos véase la sección de Anexos

4.1.3. Efecto de la dosis de radiación y concentración de monómero: Agua:EtOH

Se realizó la modificación de las películas utilizando la mezcla agua:EtOH 1:1, utilizando las relaciones AAc:EGDMA 3:1 y 5:1, a una concentración mayor, de 20% *v/v*; únicamente variando la dosis de radiación (véase Figura 20).

Los resultados demostraron que la reacción se comporta distinto a aquellas modificadas en tolueno, donde el grado de injerto aumenta con dosis más altas. Sin embargo, para estas condiciones (disolvente: agua:EtOH, 20% *v/v*), las películas que se modificaron con relación molar 3:1, el mayor grado de injerto se alcanza con dosis de 25 y 30 kGy. Al aumentar la dosis a 40 y 50 kGy el injerto cae a 6 y 3%, respectivamente. Esto se ve reflejado en el comportamiento de las películas en agua, y su hinchamiento límite.

La caída del grado de injerto puede ser atribuida a la formación de copolímero, ya que este no alcanza a interactuar con las cadenas del PDMS, y es evidentemente en la cantidad de residuo que se genera de la reacción. Con estos resultados, se encontraron las condiciones de reacción óptimas para la inmovilización de AgNP's utilizando radiación, la cual requiere un disolvente polar: mezcla agua y etanol. Las concentración de monómeros fija en 20% *v/v* y una relación molar AAc:EGDMA 3:1.

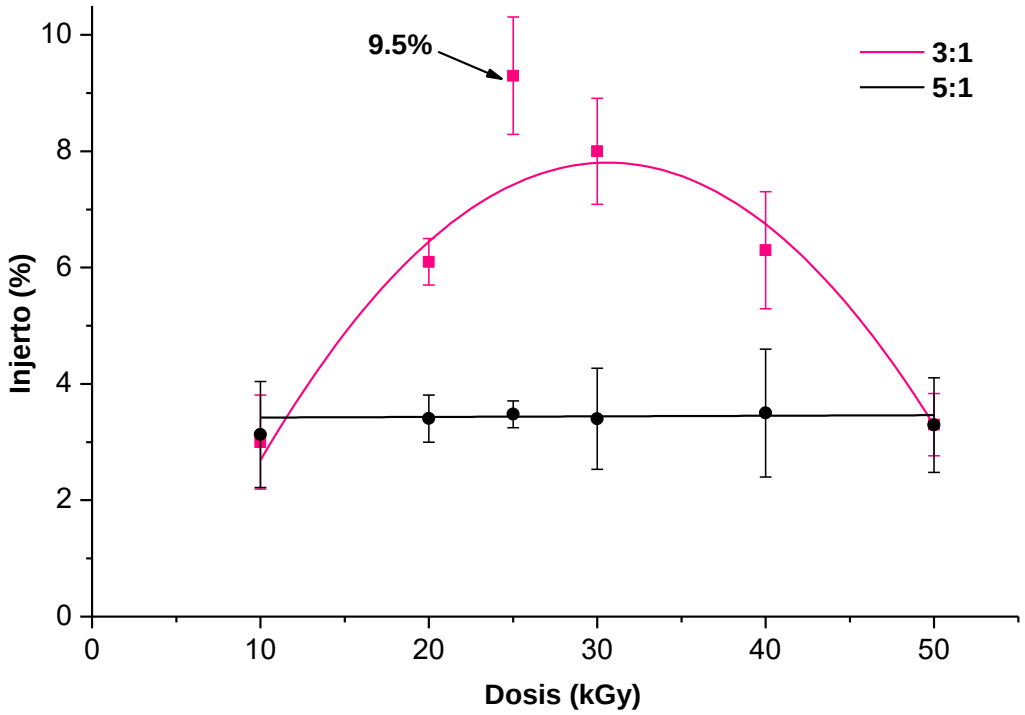

Figura 20. Grado de injerto de las películas modificadas en agua:EtOH como disolvente en función de la dosis, (—) PDMS-3 y (—) PDMS-5.

4.2. Caracterización de las películas

Las películas modificadas por ambos métodos se caracterizaron utilizando métodos espectroscópicos convencionales para identificar cambios estructurares en la matriz polimérica. Además, se llevaron a cabo otras técnicas de caracterización para los polímeros de injerto, como

las pruebas de hinchamiento y su respuesta a ambientes con valores de pH distintos. Dentro de estas pruebas también se encuentran otras técnicas comunes como la prueba de ángulo de contacto para evaluar cambios en la hidrofilicidad de la superficie del polímero.

4.2.1. Espectroscopía Infrarroja

Se evaluaron las películas modificadas mediante FTIR-ATR con el objetivo de identificar la aparición de nuevos grupos funcionales, posteriores a la reacción de polimerización. En el conjunto de espectros mostrados a continuación se pueden observar los espectros correspondientes a los materiales analizados. En el espectro del PDMS de partida se logran identificar dos bandas de alta intensidad, en ~1000 y ~750 cm^{-1}, correspondientes a alargamiento Si-O-Si y al balanceo Si-CH_3 (barra azul y amarilla, en Figura 21).

Adicionalmente, la banda de baja intensidad en ~2900 cm^{-1} se atribuye a alargamiento C-H típico para hidrocarburos alifáticos, por lo que es detectable en los tres espectros; mientras que en los espectros correspondientes al material modificado y al copolímero se observan diferencias significativas en comparación con el PDMS de partida. Dado que el AAc y el EGDMA poseen en su estructura grupos carbonílicos, se logró identificar la aparición de la banda correspondiente al alargamiento C=O en ~1700 cm^{-1} en las películas modificadas con la mezcla de monómeros y con el AAc puro (barra violeta). De esta manera se confirmó la modificación de la película posterior a la irradiación. A modo de comparación se obtuvo el espectro del copolímero P(AAc-*co*-EGDMA) obtenido al irradiar las películas, el cuál muestra las bandas del carbonilo y los metilos, sin embargo, no muestra aquellas que involucran enlaces con silicio, como la PDMS.

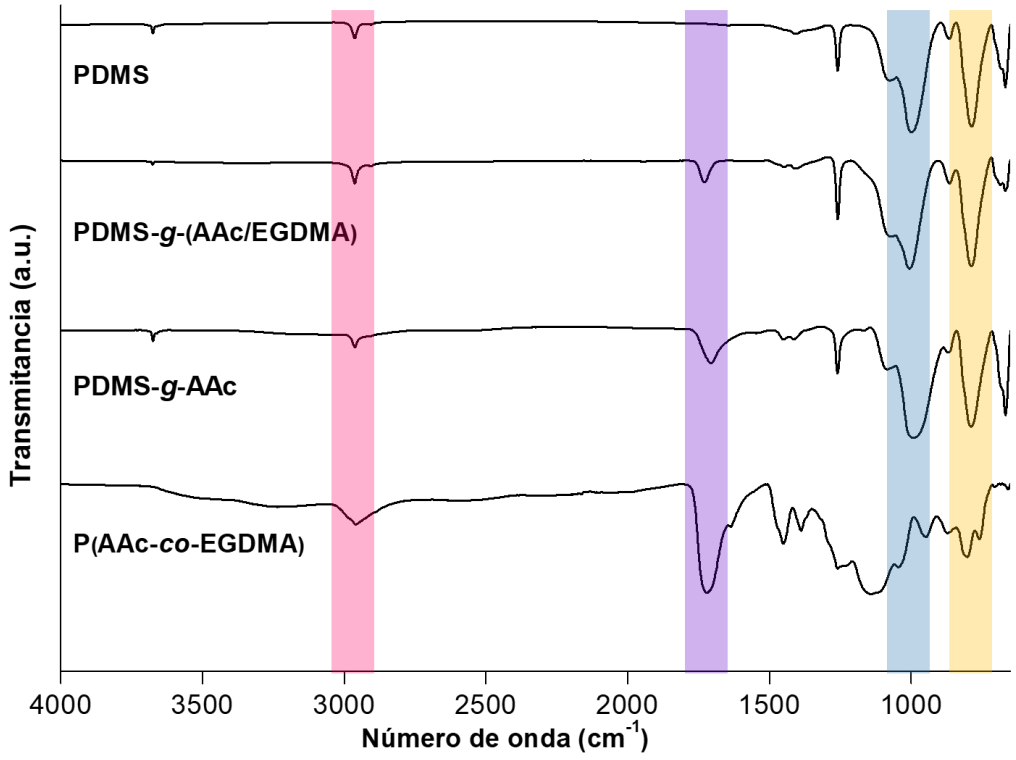

Figura 21. Espectros de FTIR-ATR del PDMS, PDMS-*g*-(AAc/EGDMA), PDMS-*g*-AAc y el copolímero P(AAc-*co*-EGDMA).

Es importante destacar que el experimento se realizó para las películas modificadas con agua:EtOH y con tolueno, y con diferentes porcentajes de injerto, no encontrándose diferencias entre los espectros.

4.2.2. Resonancia Magnética Nuclear en Estado Sólido

Para confirmar la presencia del injerto en la película de PDMS, se llevó a cabo el experimento de RMN en Estado Sólido (NMR-SS, por sus siglas en inglés) (100 MHz) de la película modificada con 30% de injerto en condiciones 3:1 (AAc:EGDMA). El espectro mostró las señales esperadas para los carbonos del PDMS, AAc y EGDMA. En la Figura 22, se observa una señal en 0 ppm que se asignó a los -CH_3 del PDMS (ver anexo 9.2) y en 29.7 ppm a los grupos metileno que se formaron después de la reacción de injerto [70]. El resto de las señales corresponden al injerto de AAc:EGDMA. El grupo carbonilo de los compuestos acrílicos y metacrílicos mostró un desplazamiento químico de 176.0 ppm, que coincide con lo reportado en la literatura [90-91], sin embargo, fue imposible diferenciar el carbonilo proveniente del AAc y el del dimetacrilato, ya que presentan similitudes estructurales. Asimismo, en 19.9 y 62.0 ppm se observan la señal de los metilos y del metileno unido a oxigeno O-CH_2 del EGDMA. Las señales en 44.6 y 38.5 ppm se asignaron a los carbonos α al carbonilo del AAc y EGDMA, respectivamente.

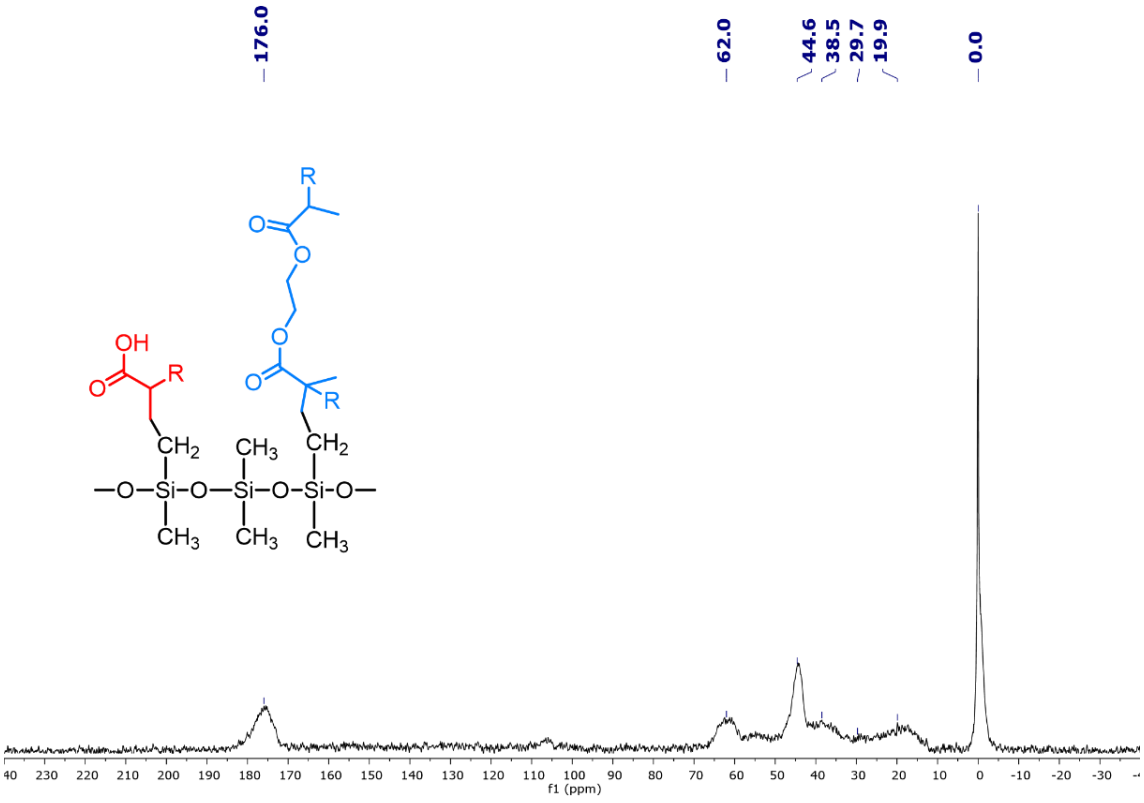

Figura 22. Espectro de SS ^{13}C NMR de la película modificada con AAc:EGDMA.

4.2.3. Análisis térmico

El comportamiento térmico fue diferente para todas las muestras. Sin embargo, todos los materiales presentaron buena estabilidad a altas temperaturas[**]. Esto tiene sentido ya que PDMS posee estabilidad térmica intrínseca [92-93]. Por ejemplo, el PDMS pierde un 10% en peso a 501 °C, mientras que su temperatura de descomposición (T_d) es 588 °C. Por otro lado, se ha reportado que la temperatura de degradación del PAAc es superior a 150 °C con una descarboxilación que se produce a 260-350 °C [80]. Tomando en cuenta estos antecedentes, se realizó un análisis termogravimétrico (TGA) para el copolímero no injertado formado en el medio de reacción PDMS-1a y para todas las diferentes películas de PDMS modificadas utilizando **tolueno** como disolvente. De acuerdo con los resultados de TGA (Figura 23), ambas películas, GY ~10 y 50%, presentan mejor estabilidad térmica que el copolímero poli(AAc/EGDMA) con T_d por encima de los 350 °C; sin embargo, esta temperatura está por debajo de la T_d del PDMS de partida. Para la PDMS-1a (50%) la primera pérdida de peso es cercana a 350 ± 10 °C y la descomposición total se da a los 420 ± 10 °C, para esta película solo una pérdida de masa fue observada.

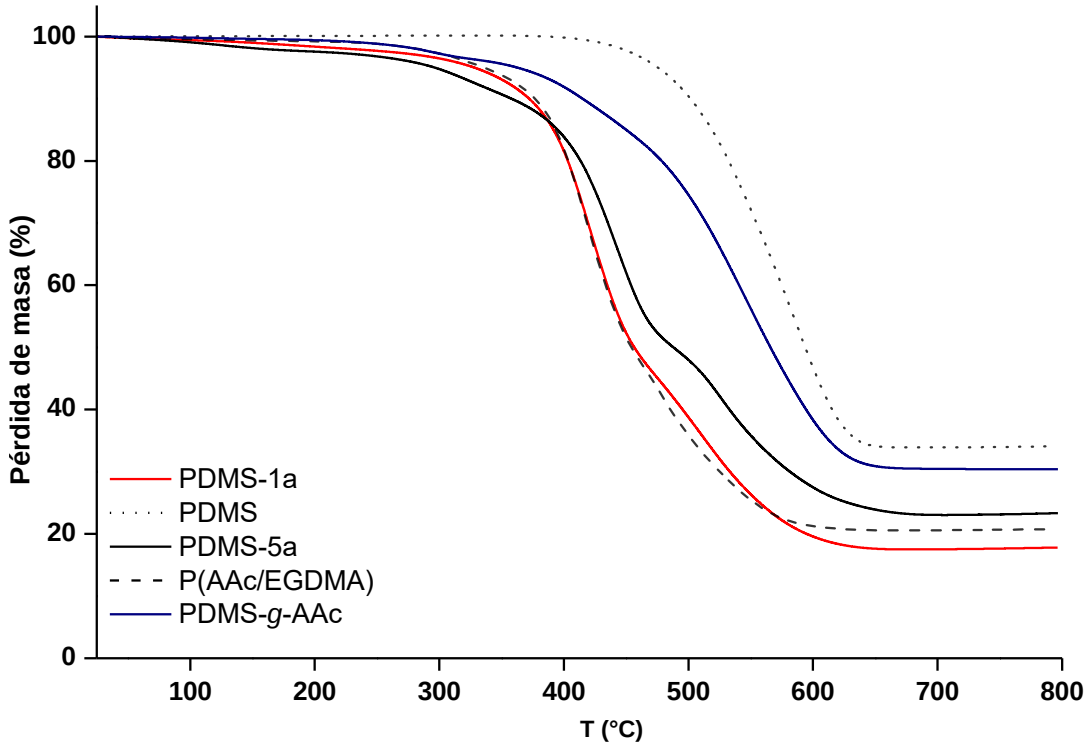

Figura 23. Termogramas para (.....) PDMS, (—) PDMS-*g*-AAc; (—) PDMS-1, (—) PDMS-5 y (– –) P(AAc/EGDMA).

El análisis DSC (Anexo 9.5.) no mostró resultados adicionales. El PDMS sin modificar no mostró transiciones térmicas, mientras que el PDMS-1 50% presentó la transición térmica correspondiente a la temperatura de descomposición de los materiales: en 215 °C para la PDMS-*g*-AAc, 255 °C (PDMS-2a) y 266 °C (PDMS-1a). El copolímero poli(AAc/EGDMA)

[**] Los gráficos se encuentran en el anexo 9.3 y la tabla de temperaturas en 9.4.

tuvo una transición térmica a 50 °C atribuida al acomodo de las cadenas del polímero. Este comportamiento no aparece en las películas modificadas.

4.2.4. Estudios de hidrofilicidad e hinchamiento

Después de realizar la reacción de injerto, las películas modificadas fueron sometidas a la prueba de ángulo de contacto, con el fin de evaluar el cambio en la hidrofilicidad de la superficie. Las muestras analizadas fueron aquellas que se modificaron utilizando **tolueno** como disolvente, el ángulo fue medido al pasar 5 y 10 minutos de que una gota de agua desionizada (DI) que tuvo contacto con la superficie de la película. Los resultados obtenidos se muestran en la Figura 24.

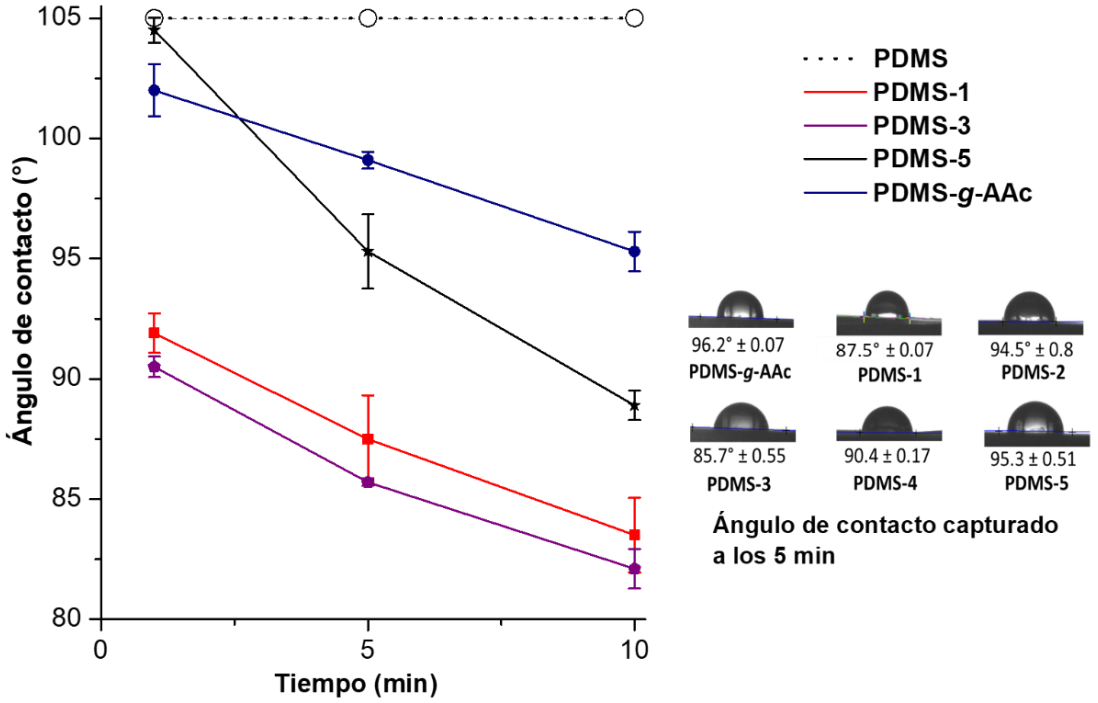

Figura 24. Ángulo de contacto capturado a los 5 y 10 minutos para (---) PDMS, (—) PDMS-*g*-AAc; (—) PDMS-1, (—) PDMS-3 y (—) PDMS-5.

En la imagen se observa que las películas modificadas con diferentes relaciones de monómeros poseen propiedades de hidrofilia en su superficie, comparadas con la película de PDMS sin modificar (105°). Esto debido a que el PAAc es un polímero altamente hidrofílico, con afinidad acuosa. Adicionalmente, el entrecruzante, derivado de metacrilato posee en su estructura fragmentos similares al polietilén glicol (PEG) que también es afín a soluciones acuosas. La adición de estos polímeros en la superficie de la silicona genera que ésta adquiera un ligero carácter hidrofílico, eso es importante ya que demuestra que hay una absorción de agua a través de las cadenas del polímero, esto fue comprobado mediante pruebas de hinchamiento al equilibrio en agua DI y solución salina de fosfatos (PBS).

Las pruebas de hinchamiento se realizaron en agua DI y en solución de PBS, para simular un ambiente fisiológico. Las diferentes películas modificadas (PDMS-1 a PDMS-5, PDMS-*g*-AAc)[††] en la reacción de injerto en tolueno y en agua:EtOH se introdujeron en las soluciones acuosas y se monitoreó a través del tiempo el contenido de agua que absorben hasta llegar al equilibrio, para encontrar el tiempo que tarda la película en absorber agua, a lo que llamaremos "hinchamiento límite". Los resultados obtenidos para las películas PDMS-*g*-AAc, PDMS-1, PDMS-3 y PDMS-5 sintetizadas en tolueno con un injerto de ~50 y ~30% para la PDMS-*g*-AAc, se muestran en la Figura 25.

El grado de hinchamiento (SD) de las películas fue calculado por diferencia de masa, comparado con la masa inicial (W_0) de la película y la masa de la película modificada (W_g). La fórmula general está representada en la Ecuación 2:

$$SD\ (\%) = [(W_g - W_0)/ W_0]100 \qquad \text{(Ecuación 2)}$$

En la Figura 25a se puede observar el comportamiento de las películas en agua DI, donde se alcanzó el máximo de absorción de agua en un tiempo de 24 h, para todas las películas. Es importante destacar que conforme aumenta la relación AAc:EGDMA, el contenido de agua absorbida por la película es mayor, por lo tanto, el EGDMA, en gran proporción genera redes compactas y rígidas, lo que genera menor espacio entre las cadenas del polímero, impidiendo la difusión de agua al interior del injerto polimérico. Incluso, la película modificada sin el dimetacrilato alcanzó hinchamiento de 30%, en 24 horas.

Por otro lado, cuando se llevó a cabo el experimento en solución salina de fosfatos (Figura 25b), las mismas películas tuvieron un comportamiento distinto, hubo un mayor grado de hinchamiento. A modo de comparación se puede observar que la PDMS-1 tuvo un hinchamiento de 4%, en 24 h, en agua DI; en solución de PBS fue de 6.5% en casi 36 h. En el caso de la PDMS-5, en agua DI su SD fue de ~24% y en PBS de 66%. Esto debido al constante intercambio de iones que se da entre la solución y el interior de las cadenas poliméricas, estos son los contraiones de los grupos carboxilato.

En cuanto al comportamiento respecto a la relación AAc:EGDMA, se observó el mismo patrón que en el experimento realizado en agua DI. Conforme aumentó esta relación, el grado de hinchamiento fue mayor. Además, el tiempo que tardaron las películas en absorber el agua fue de casi 36 h, debido al intercambio iónico la difusión de iones fue más lenta y tardó más tiempo en alcanzar el equilibrio.

En el caso de la PDMS-*g*-AAc (línea azul), se observa que no hay un incremento en el contenido de agua, sugiriendo que el EGDMA ayuda a generar redes entrecruzadas que permiten el hinchamiento del polímero, similar a los hidrogeles.

[††] Para todos los gráficos véase la sección de Anexos

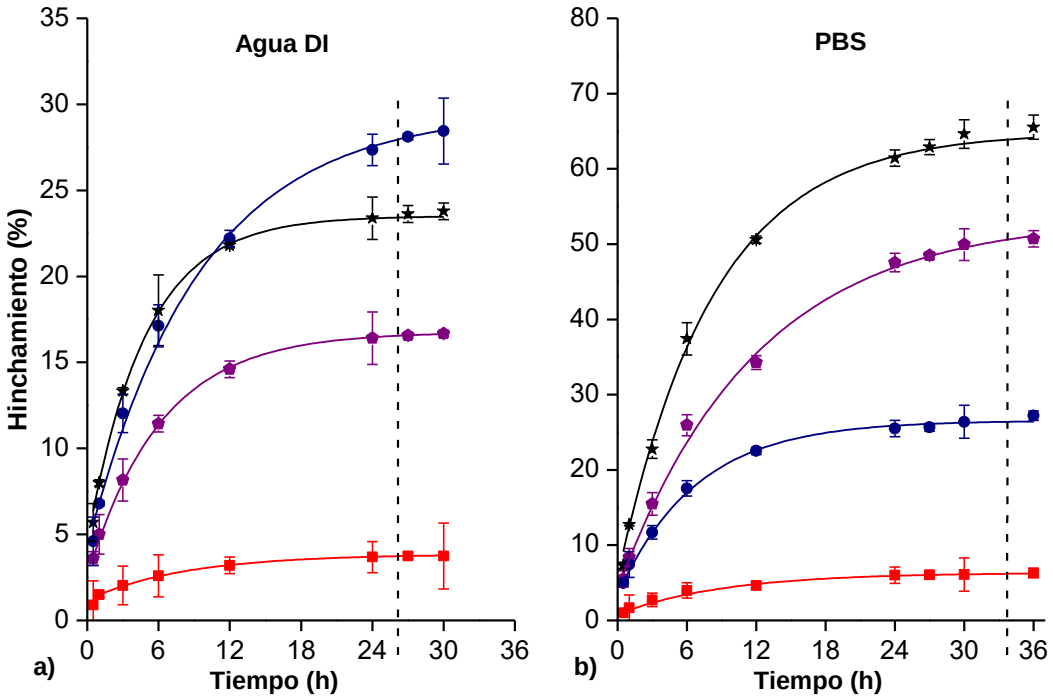

Figura 25. Grado de hinchamiento a través del tiempo para las películas modificadas en tolueno: (—) PDMS-*g*-AAc; (—) PDMS-1, (—) PDMS-3 y (—) PDMS-5 en a) agua DI y b) solución de PBS.

Se le realizó el mismo experimento a la película modificada en **agua:EtOH**. La PDMS-3b con un injerto de 10% (Figura 26), el comportamiento fue similar al de las películas modificadas en tolueno, sin embargo, el equilibrio se alcanzó en menor tiempo. Para el experimento en agua DI el grado de hinchamiento alcanzado fue de casi 4% en poco menos de 24 h, mientras que en solución de PBS el hinchamiento alcanzado fue de ~9%. La diferencia en el grado de hinchamiento se atribuye al mismo fenómeno que en el experimento anterior, dónde se involucra un intercambio iónico.

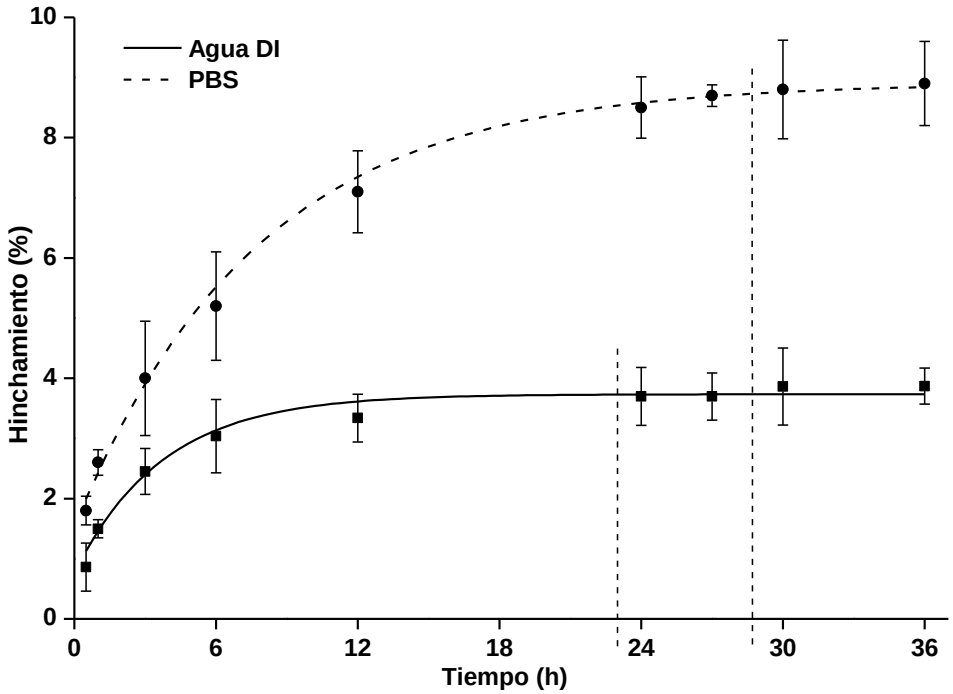

Figura 26. Grado de hinchamiento a través del tiempo para PDMS-3 (modificada en mezcla hidroalcohólica) en agua DI y en solución de PBS.

4.2.5. Sensibilidad al pH

La determinación de las propiedades ácido-base de los materiales tuvo dos objetivos: i) analizar la sensibilidad de las películas modificadas a cambios de pH; y ii) confirmar que se llevó a cabo la reacción de injerto. Estas pruebas se llevaron a cabo para las películas modificadas en **tolueno**, debido a que estas fueron las empleadas para la carga y descarga de ciprofloxacino (parte 2). La sensibilidad al pH se evaluó mediante estudios de hinchamiento con variación de pH, y con titulaciones potenciométricas.

En los estudios de hinchamiento, se utilizaron películas con distinto grado de injerto, 30 y 50%. El hinchamiento fue cuantificado por gravimetría haciendo uso de la Ecuación 2. Las películas fueron expuestas a distinto valor de pH, cada 48 h, asegurando que se alcanzó el equilibrio; y de acuerdo con los resultados de hinchamiento límite en PBS, los resultados se representan en el gráfico de la Figura 27.

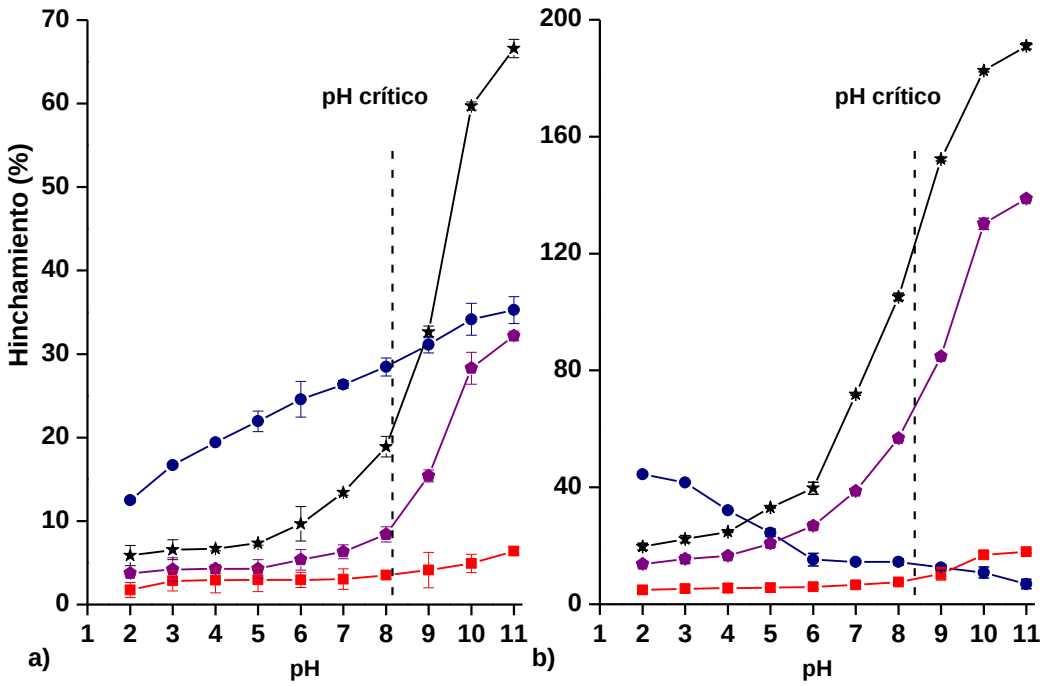

Figura 27. Hinchamiento de las películas modificadas en tolueno con respecto a la variación de pH de (—) PDMS-*g*-AAc; (—) PDMS-1, (—) PDMS-3 y (—) PDMS-5 con injerto de a) 30% y b) 50%.

En cuanto a la respuesta de las películas al cambio de pH, se observó el comportamiento típico del PAAc, dónde el pH crítico[‡‡] es alrededor de pH = 8. Todas las películas tuvieron un comportamiento similar, y se observa que también el hinchamiento depende de la relación molar (AAc:EGDMA), mientras mayor es esta el grado de hinchamiento alcanzado también es mayor, debido al carácter más hidrofílico del ácido acrílico. También, se observó un hinchamiento mucho mayor para aquellas películas que poseen más cantidad de injerto (Figura 25b) lo cual confirma que el hinchamiento es completamente dependiente del grado de injerto, conservando el pH crítico alrededor de 8. Por ejemplo, la PDMS-5 con injerto de 30% tuvo una absorción de agua correspondiente a casi 70% y la misma relación molar, pero con un injerto de 50% alcanzó una absorción de agua de ~200%, muy distintas para la PDMS-1, para la cual los SD fueron de 6 y 20% respectivamente.

Es importante señalar que la PDMS-*g*-AAc (línea azul en ambos gráficos) no tuvo el comportamiento esperado, por el contrario, al ser expuesto a diferentes valores de pH es inestable, incluso la película con mayor injerto comenzó a degradarse a través de los distintos valores del pH.

Este mismo comportamiento se observó en las demás películas al término del experimento, ya que demostraron baja estabilidad a pH mayor a 10. Posterior al experimento de sensibilidad al pH se caracterizaron las películas mediante FTIR-ATR (Figura 28) lo que mostró cambios en la

[‡‡] El pH en el que hay un cambio más notorio en el comportamiento de un polímero hacia el pH, véase sección 2.4.

composición de éstas. Hubo una aparición de bandas correspondientes al alargamiento (~3400 cm^{-1}) y al balanceo (~1500 cm^{-1}) del enlace O-H lo que sugirió la hidrólisis de los ésteres de sistema (EGDMA) y la degradación del injerto.

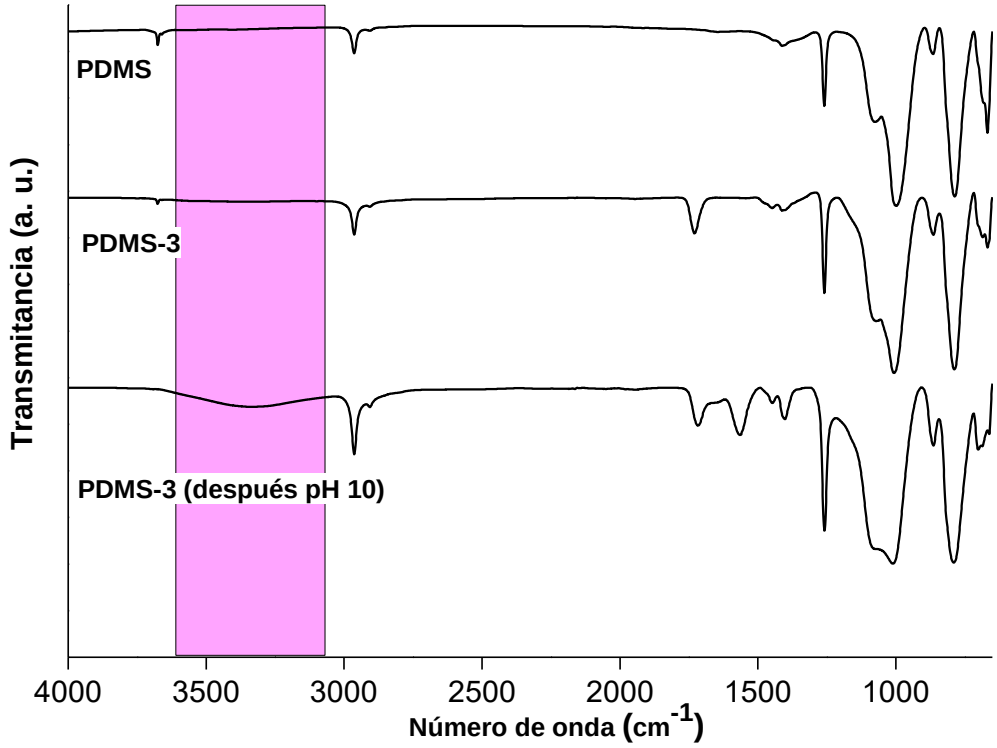

Figura 28. FTIR-ATR del PDMS y PDMS-3 (tolueno) antes y después de estar expuesta a pH básico 10.

Las titulaciones potenciométricas se realizaron para evaluar el comportamiento del par ácido-base ácido acrílico/acrilato de potasio ($HAAc/AAc^-$) que está presente en las cadenas injertadas del PAAc. Se utilizaron las películas con un GY ~ 50% sintetizadas en **tolueno**. La Figura 29 muestra las curvas de titulación para las películas, en donde se muestra un aumento lento del pH en función del titulante agregado (KOH). Esto es común en titulaciones de polielectrolitos pues la interacción de una cantidad elevada de grupos cargados (al desprotonarse) afecta el comportamiento de los otros grupos ácidos alrededor modificando su constante de acidez (pKa) [94–97].

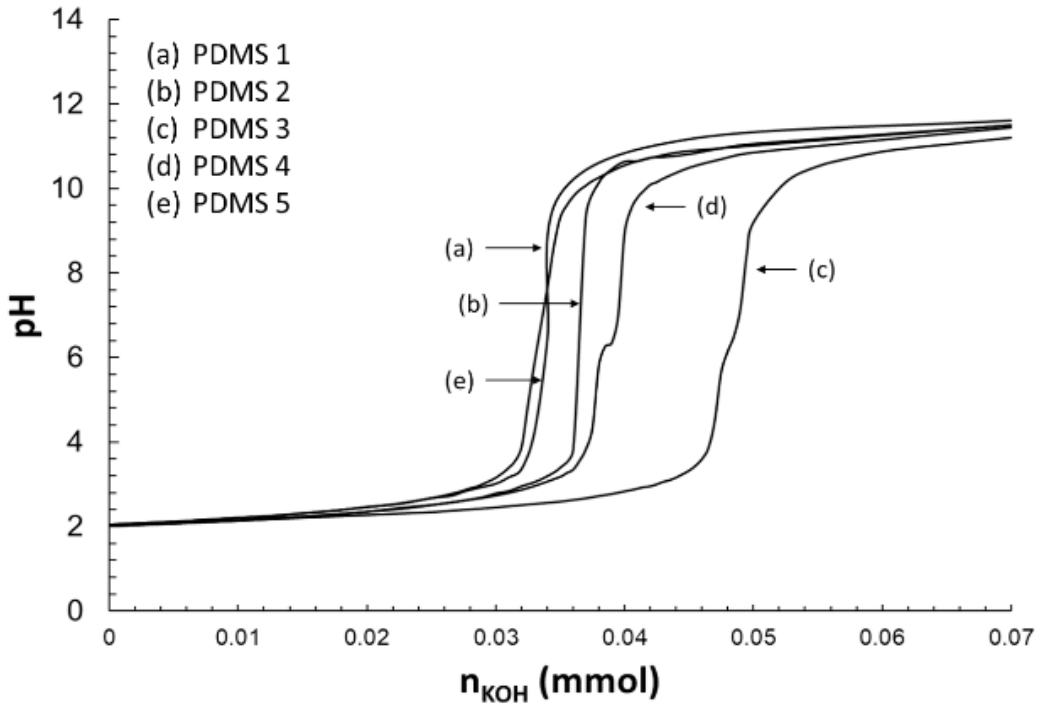

Figura 29. Curvas de titulación ácido-base de las películas.

Para PDMS-1, PDMS-2 y PDMS-3 (AAc:EGDMA 1:1, 2:1, 3:1; respectivamente), el volumen necesario para alcanzar el punto de equivalencia incrementa al aumentar la relación AAc:EGDMA en la mezcla original, lo que indica que hay una mayor cantidad de grupos ácidos en el material modificado. Esto tiene sentido ya que los GY's son mayores cuando la cantidad de AAc aumenta con respecto a EGDMA en las condiciones de reacción (sección 5.1.2).

Por el contrario, para PDMS-4 y PDMS-5, la cantidad de grupos ácidos es aparentemente menor, y esto se atribuye a que una mayor cantidad de AAc en el medio de reacción favorece la homopolimerización del mismo, formando PAAc. Esto es un indicio de que hay una mayor cantidad de EGDMA injertado en la película y éste no tiene grupos ácidos.

La constante de acidez aparente (pKa_{ap}) para todas las películas fue de aproximadamente pKa = 7.5, por arriba de la reportada para el PAAc que es cercano a 5. Sin embargo, este comportamiento es común en polímeros debido a que la estructura del polímero (y sus interacciones intermoleculares) afectan el grado de ionización de este, el cual, directamente afecta el pKa [97–99].

5. PRIMERA SECCIÓN

5.1. Inmovilización de AgNP's *in situ* sobre injerto utilizando radiación γ

Se ha descrito la formación de AgNP's a partir de sales de plata (Ag^{+1}) utilizando la radiación como reductor. La radiación γ se utilizó para llevar a cabo la reacción de injerto y la formación de las AgNP's de manera simultánea. De acuerdo con los resultados previos sobre el injerto utilizando estas condiciones (sección 6.1), se esperaron grados de injerto cercanos al 10%, y de igual manera que las películas sin plata, el mayor grado de injerto se alcanzó con dosis de 25 kGy con una tasa de ~10 kGy h^{-1}.

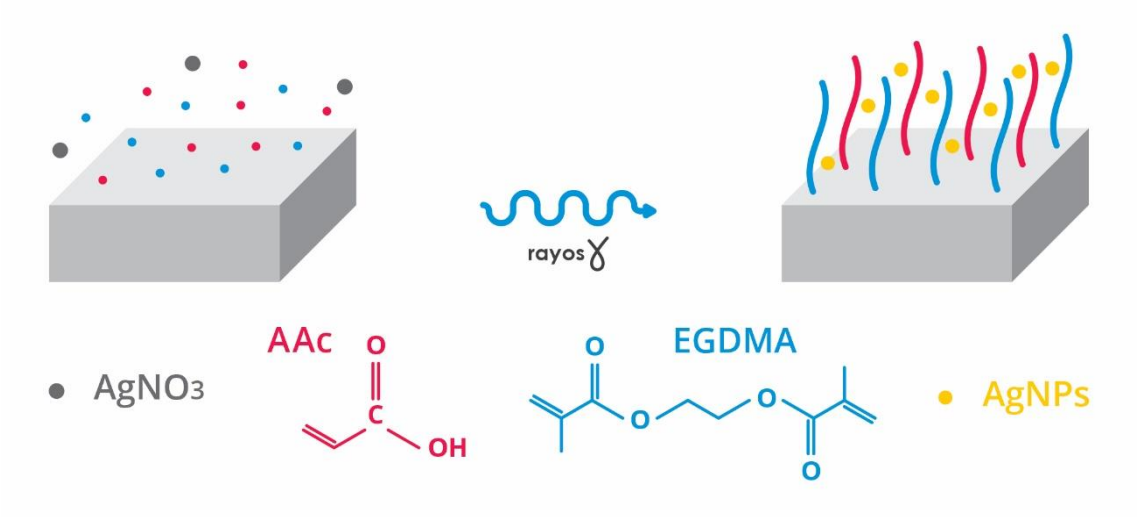

Figura 30. Representación de la reacción de injerto y formación de las AgNP's utilizando la radiación γ.

La reacción se realizó mezclando $AgNO_3$ disuelto en la mezcla **agua:EtOH** 1:1 con 20% *v/v* de la mezcla AAc:EGDMA. El experimento se realizó para dos relaciones molares: 3:1 y 5:1. Está reportada la formación de AgNP's con distintas dosis de radiación, desde 5 hasta cientos de kGy, sin embargo, dado que previamente se han encontrado las condiciones con que se tienen injerto, se probaron esas condiciones encontradas en la sección 4.1 (agua:EtOH 1:1; 20% *v/v* de la mezcla AAc:EGDMA). Para las pruebas preliminares, la concentración del nitrato de plata se mantuvo constante en 5 mM como se ha descrito en ciertos reportes [50,57]. Los resultados obtenidos con variación de dosis son los mostrados en la Figura 31.

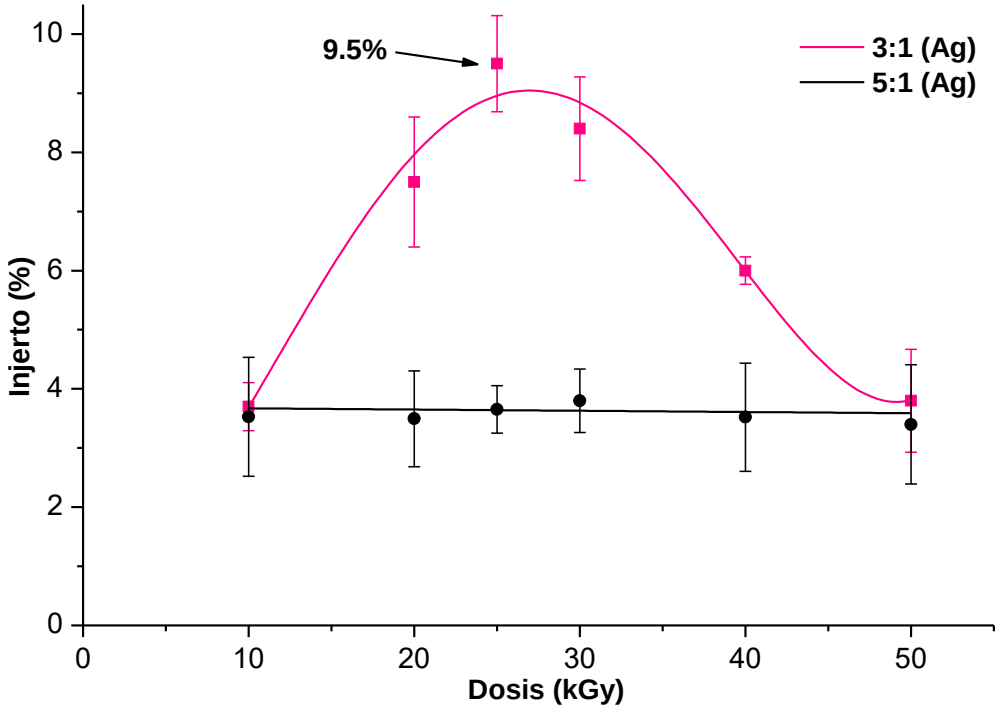

Figura 31. Grado de injerto de las películas modificadas en agua:EtOH (—) PDMS-3 y (—) PDMS-5 en función de la dosis.

Como era de esperarse, los grados de injerto no variaron con respecto a las películas que no contienen plata. El mayor injerto se obtuvo con una dosis de 25 kGy, con una tasa de ~10 kGy h^{-1}. Es importante señalar que para estas reacciones de formación de NP's, el tiempo de exposición a la radiación juega un papel más importante que la dosis total absorbida, ya que se requiere que se vayan acumulando los átomos de plata reducida Ag^0 para la formación de las nanoestructuras.

Pese a que no hay cambios en la cantidad de injerto con la plata, uno de los principales cambios que destacan en las películas modificadas es el cambio en la coloración, conforme a la variación de la dosis y el tiempo de exposición. Esto coincide con lo reportado para diferentes morfologías y tamaños de las NP's [100]. La película obtenida con mayor dosis de radiación se coloreó naranja, mientras que las demás no cambiaron de apariencia. El grado de injerto (GY) no superó el 9%. En la Figura 32 se pueden observar la película de PDMS inicial (a), la película que sólo contiene AAc:EGDMA injertados (b) y la película que contiene injerto AAc:EGDMA+Ag (c), obtenida con relación molar (AAc:EGDMA 3:1), concentración 20% *v/v* y agua:etanol como medio de reacción (PDMS-3).

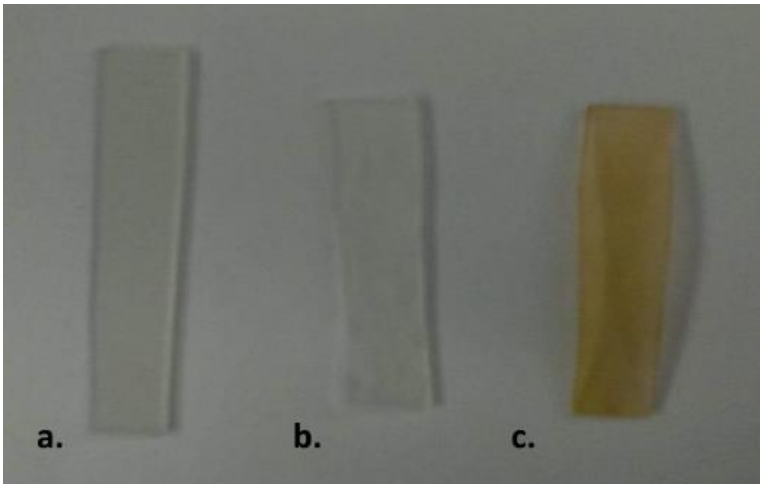

Figura 32. Películas de: a. PDMS; b. PDMS-*g*-(AAc/EGDMA) y c. PDMS-*g*-(AAc/EGDMA)+Ag.

La película PDMS-3c, fue la que se caracterizó debido a que es la que presentó mayor grado de injerto y cambios en la coloración. Se obtuvo el espectro de SS ^{13}C NMR de la película modificada con la mezcla AAc:EGDMA/$AgNO_3$ (5 mM) para observar cambios estructurales en el injerto (Figura 33) o algún corrimiento de las señales correspondientes al carbonilo que aseveraran la coordinación de la plata; sin embargo, el espectro no muestra cambios con respecto al espectro de la película modificada sin plata mostrado en la sección 5.2.2. Esto debido a que la concentración de la sal de plata es baja.

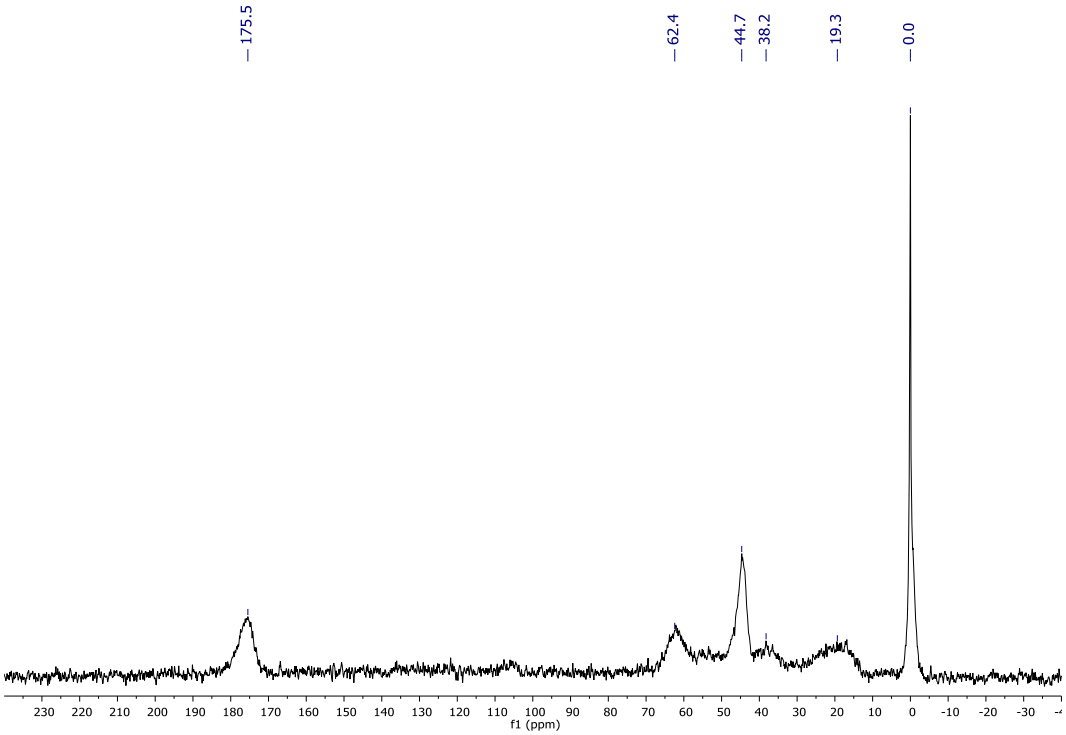

Figura 33. de SS ^{13}C NMR de PDMS-*g*-(AAc/EGDMA)+Ag (5 mM).

También, se obtuvo el espectro de FTIR-ATR de la película PDMS-*g*-(AAc/EGDMA)+Ag (PDMS-3c) y se comparó con las demás películas modificadas sin plata. En la Figura 34 se observa que no hay cambios en las bandas de absorción en el infrarrojo, no hay desplazamiento ni corrimiento de señales. Esto debido a la mínima cantidad de plata que contiene la película.

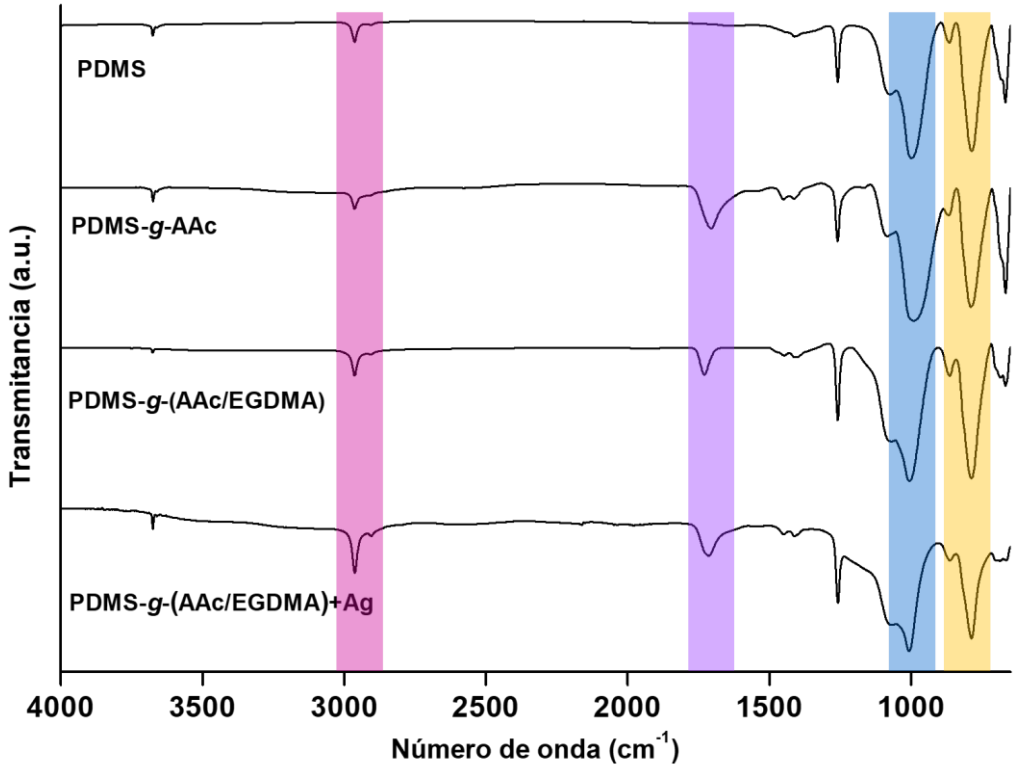

Figura 34. Espectros de FTIR-ATR del PDMS, PDMS-*g*-AAc, PDMS-*g*-(AAc/EGDMA), y PDMS-*g*-(AAc/EGDMA)+Ag.

La comprobación de la presencia de las AgNP's se realizó utilizando la espectroscopia UV de películas, como se muestra en la Figura 35. Se pueden observar los espectros de absorción para la película sin plata y las dos modificadas con diferente relación molar (3:1 y 5:1). En el espectro correspondiente a la película sin plata PDMS-*g*-(AAc/EGDMA) se observa una única banda de absorción alrededor de 430 nm, al igual que para la película PDMS-5. Esta banda puede atribuirse al injerto de AAc sobre la superficie. Sin embargo, para la película que ha sido modificada con la mezcla de monómeros 3:1, y mostró mayor grado de injerto y un cambio en su coloración, se puede percibir la aparición de una nueva banda de absorción alrededor de ~600 nm, lo cual coincide con lo reportado para partículas de plata.

Las dos bandas de absorción tienen concordancia con espectros de UV-Vis de partículas de plata, la absorción de las AgNP's depende de su tamaño, morfología y del medio en el que se hace la medición. Típicamente, las nanopartículas esféricas con diámetro < 20 nm presentan una única banda de plasmón de superficie alrededor de 430 nm, mientras que para las partículas de tamaño mayor (diámetro ~100 nm), semiesféricas o triangulares, la banda de absorción del plasmón de superficie se da alrededor de los ~620 nm [101]. De acuerdo con el espectro, se puede concluir que la película modificada PDMS-*g*-(AAc/EGDMA)+Ag (3:1) posee inmovilizadas en el injerto

una mezcla de nanopartículas y/o agregados de plata en tamaño pequeño (10 y 20 nm) y grande (~100 nm), y es por eso que hay un cambio de coloración en la película.

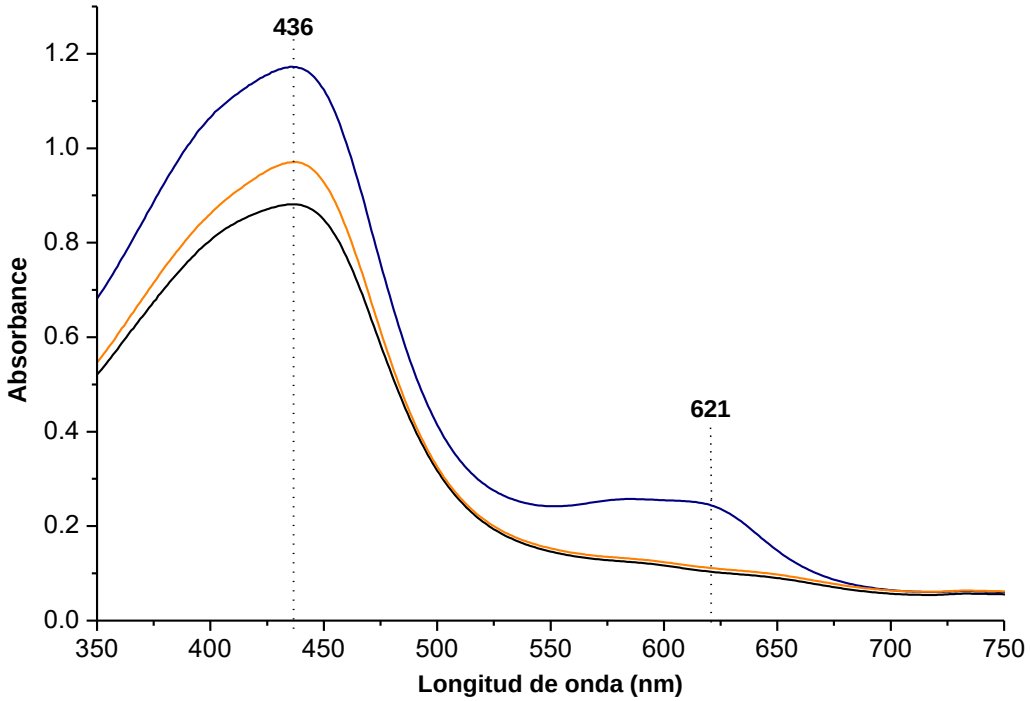

Figura 35. Espectros de UV-Vis de películas para de (—) PDMS-*g*-(AAc/EGDMA) (—) PDMS-*g*-(AAc/EGDMA)+Ag (3:1) y (—) PDMS-*g*-(AAc/EGDMA)+Ag (5:1).

Para este estudio es muy importante modular la concentración de la sal de plata, ya que es otro factor que influye en la morfología y tamaño de los aglomerados. Se encuentran descritos diferentes estudios donde se utiliza desde 1 hasta 100 mM de la sal [50,56,102] y dependiendo de este factor es la morfología y el tamaño de las AgNP's que se obtienen.

Al encontrar que la película modificada con mezcla 3:1 de AAc:EGDMA fue la que retuvo más las nanopartículas o agregados de plata en estado reducido, se procedió a realizar el estudio con diferentes concentraciones molares de $AgNO_3$. La modificación preliminar se había realizado con una concentración fija de 5 mM, para evaluar el efecto de la concentración se utilizaron las siguientes: 1, 5, 10, 20, 30, 40 y 50 mM. El resto de las condiciones experimentales se mantuvieron como en la sección previa: solución de monómero al 20% *v*/*v*, utilizando la mezcla agua:EtOH (1:1) como disolvente. De acuerdo con la Figura 36, se puede observar que no hay cambio en el grado de injerto de las películas, con respecto a las reacciones previas. El GY (%) se mantiene en ~9% en promedio para cada experimento, lo cual indica que la concentración de $AgNO_3$ no interviene en la reacción de polimerización, y la mezcla de monómeros AAc/EGDMA es injertada sobre la superficie del PDMS.

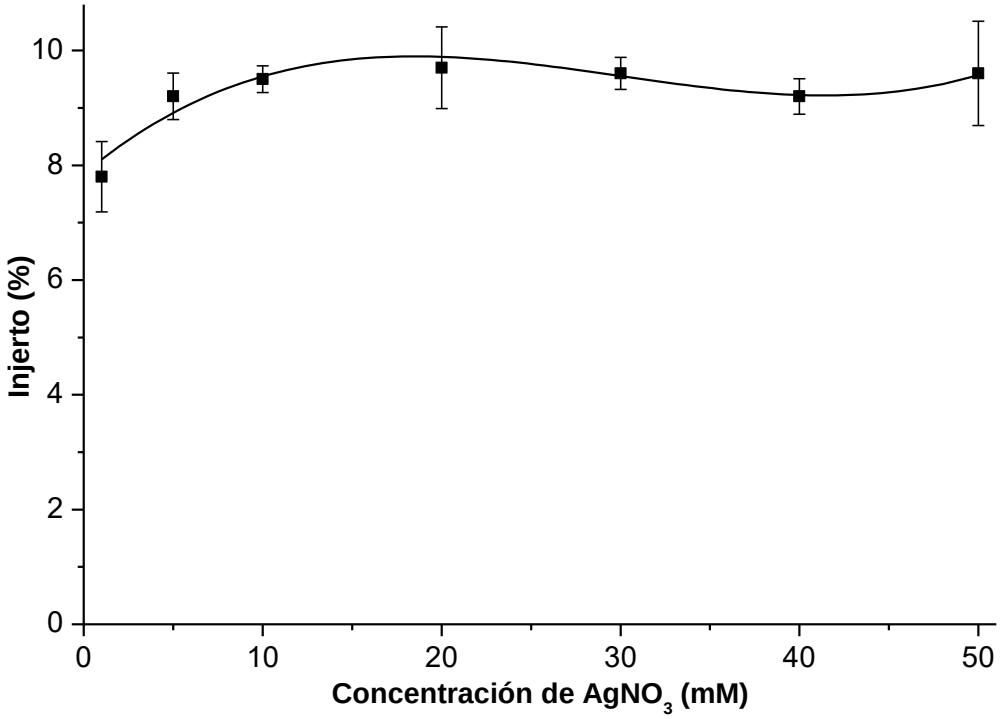

Figura 36. Grado de injerto de (▬)PDMS-*g*-(AAc/EGDMA)+Ag (3:1) en función de la concentración de $AgNO_3$.

Al igual que el primer experimento, la coloración de las películas también cambió. Este cambio fue en función de la concentración del $AgNO_3$, mientras más concentrada estuvo la solución (mayor concentración de la sal de plata), la película adquirió un color más intenso u oscuro, (ver Figura 37), estos resultados nos indican que se están formando partículas de diferente tamaño con respecto a la concentración del nitrato de plata, se sugiere que con mayor concentración de especies Ag^0 formándose en la reacción más grandes los agregados que se forman.

Para observar si había efecto de la intensidad/tasa de radiación *I* (la velocidad con que se irradia una muestra, medida en kGy h^{-1}). En el experimento, la dosis se mantuvo fija en 25 kGy, las dos tasas de irradiación empleadas para este experimento fueron ~5 y 10 kGy h^{-1}. El injerto se mantuvo como en los experimentos anteriores, alrededor de ~9%. Sin embargo, el cambio más drástico fueron las diferencias en el aspecto físico de los materiales, principalmente la coloración.

En la Tabla 5 se pueden observar las condiciones con que se obtuvieron las películas injertadas con AAc:EGDMA y la inmovilización de las AgNP's, junto con la clave para identificarlas en la Figura 37. La película modificada con 1 mM de $AgNO_3$ no presentó cambios en la coloración y no está representada en la Figura.

Tabla 5. Condiciones para la reacción de injerto y formación de AgNP's.

Película	Concentración (mM) $AgNO_3$	Dosis (kGy)	Tasa (kGy h^{-1})
a	NA	NA	NA
b	NA	25	9.6
c	5		5.4
d	10		
e	40		
f	50		
g	5		9.6
h	10		
i	50		

*Relación molar AAc:EGDMA= 3:1; concentración = 20% *v/v*; disolvente= agua:EtOH 1:1.
*Las películas modificadas con 20 y 30 mM de nitrato de plata no se consideraron en esta tabla de claves.
NA= No Aplica

El aspecto físico de las películas puede observarse en la Figura 37, se ven claras diferencias entre las películas obtenidas con poca concentración de la sal de plata y las que se obtuvieron con mayor concentración; así como la variación en la intensidad de radiación.

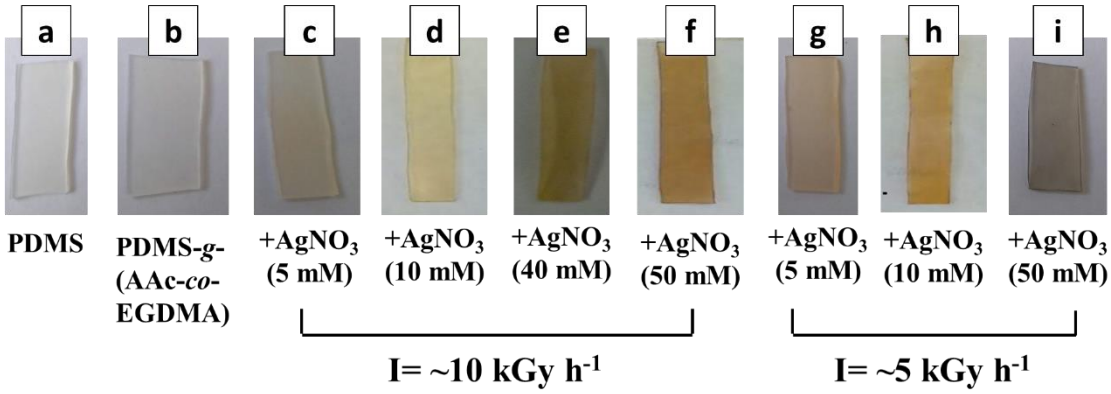

Figura 37. Películas modificadas y su aspecto después de la radiación.

Las películas después de ser irradiadas con diferente concentración de $AgNO_3$, y con la mezcla AAc:EGDMA 3:1, en agua:EtOH, adquirieron coloración naranja y azul. Para confirmar la formación de agregados se empleó de nuevo la espectrofotometría UV-Vis, en los espectros se puede observar que para la película **d** y la película **i**, sigue la aparición de la banda de absorción en ~435 nm que, como habíamos mencionado anteriormente, corresponde a la absorción del plasmón de superficie de las AgNP's esféricas de poco diámetro (alrededor de 10 y 20 nm). En la Figura 38 se muestra el espectro para dos de las películas, aquella que se modificó utilizando la concentración de 50 mM con *I*= ~5 kGy h^{-1} y con 10 mM con *I*= ~10 kGy h^{-1}, para tenerlas como control en la inmovilización de las partículas o agregados de plata.

La película **d**, con 10 mM de concentración de nitrato de plata muestra las mismas dos bandas que la película obtenida en los estudios preliminares mostrados en la Figura 35. La banda de 621 nm se corre 15 nm hacia menor longitud de onda, pero sigue dentro del intervalo que representa la absorción del plasmón de superficie de las partículas de diámetro de 100 nm. Por otro lado, el espectro de absorción de la película **i**, no muestra esta banda, se atribuye a que el experimento se obtuvo con error experimental.

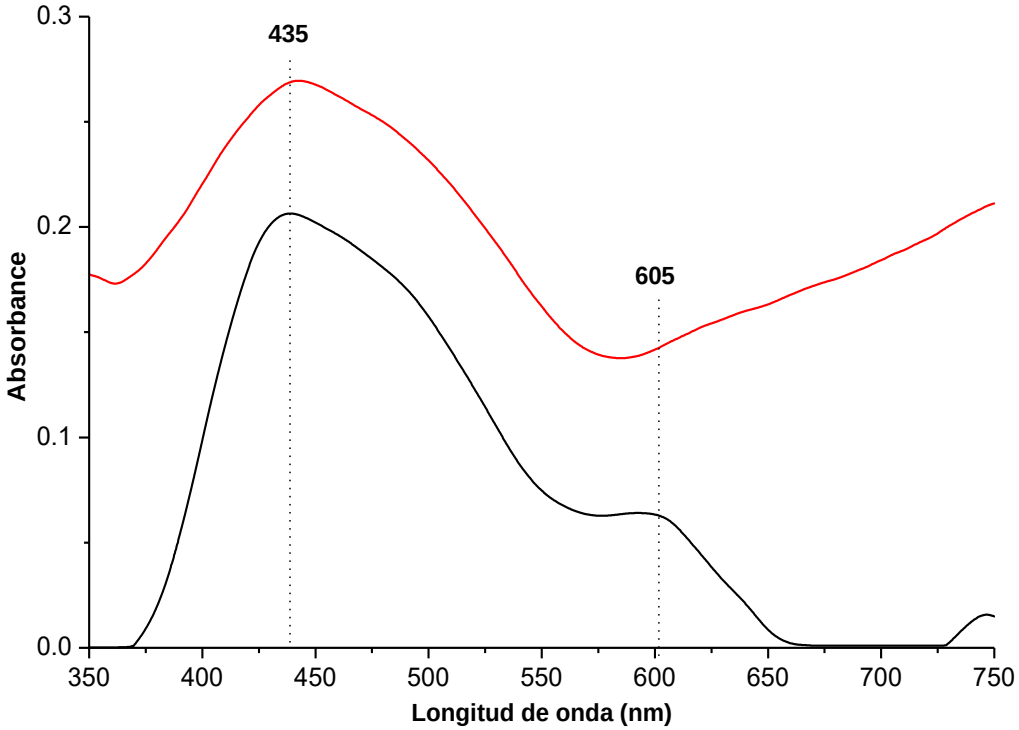

Figura 38. Espectro de UV-Vis de (—) PDMS-*g*-(AAc/EGDMA)+Ag (50 mM) (**i**) y (—) PDMS-*g*-(AAc/EGDMA)+Ag (10 mM) (**d**).

Las películas modificadas con 10, 20 y 30 mM de la sal de plata también tienen aspecto rojizo, la única que sobre pasa esta coloración es la que se obtuvo con 50 mM de nitrato.

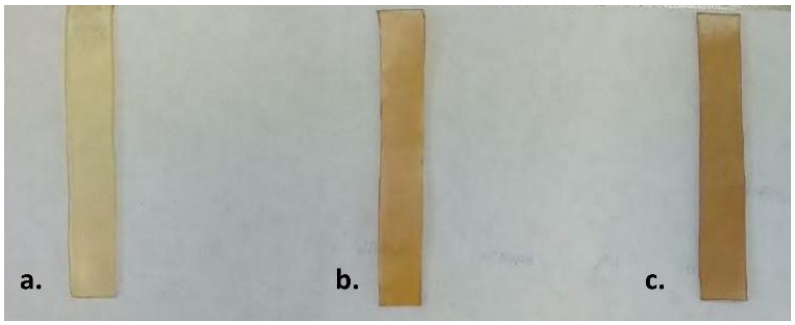

Figura 39. PDMS-*g*-(AAc/EGDMA)+Ag con a. 10 mM, b. 20 mM y c. 30 mM.

Con el objetivo de visualizar cambios en la morfología de la superficie de las distintas películas, se llevó a cabo el análisis por microscopía electrónica de barrido (SEM) para PDMS, PDMS-*g*-(AAc/EGDMA) y PDMS-*g*-(AAc/EGDMA)+Ag con 10 y 50 mM (películas **d** e **i**, ver Figura 38). En la Figura 40 se muestran las micrografías para estos materiales en diferentes aumentos[§§], 250, 500, 1500 y 3000X; conforme hay más aumento se pueden observar más cambios entre las superficies de las películas. En la PDMS se observa una superficie no uniforme, con cierta rugosidad, mientras que el resto de las películas, con injerto de AAc/EGDMA tienen más uniformidad, puede atribuirse a que la reacción de injerto se realiza sobre la superficie y recubre los espacios del PDMS, aun así, se ven porciones con injerto y porciones sin este.

En las micrografías capturadas con mayor aumento se pueden observar con claridad los cambios con respecto a las que tienen o no agregados o partículas de plata. Para la muestra PDMS-*g*-(AAc/EGDMA)+Ag (10 mM) (**d**) coloreada en naranja, se observan agregados de plata en forma esférica y cuasi esférica, que corresponden a los átomos de Ag^0 acumulados en la superficie. Sin embargo, en las micrografías correspondientes a la película modificada con mayor concentración de $AgNO_3$ (50 mM) (**i**) (coloreada en azul, véase Figura 38) se observa mayor concentración de partículas, que tienen un diámetro/tamaño mayor en comparación con la micrografía de **d**, se pueden percibir algunas es forma triangular y menos uniformes en cuanto a la morfología, lo cual coincide con lo previamente reportado y el color que obtuvo la película después de la radiación (más oscura, un poco azul/negro) [103,104].

[§§] Para la película PDMS (sin modificar) se tiene únicamente la micrografía con 500X de aumento.

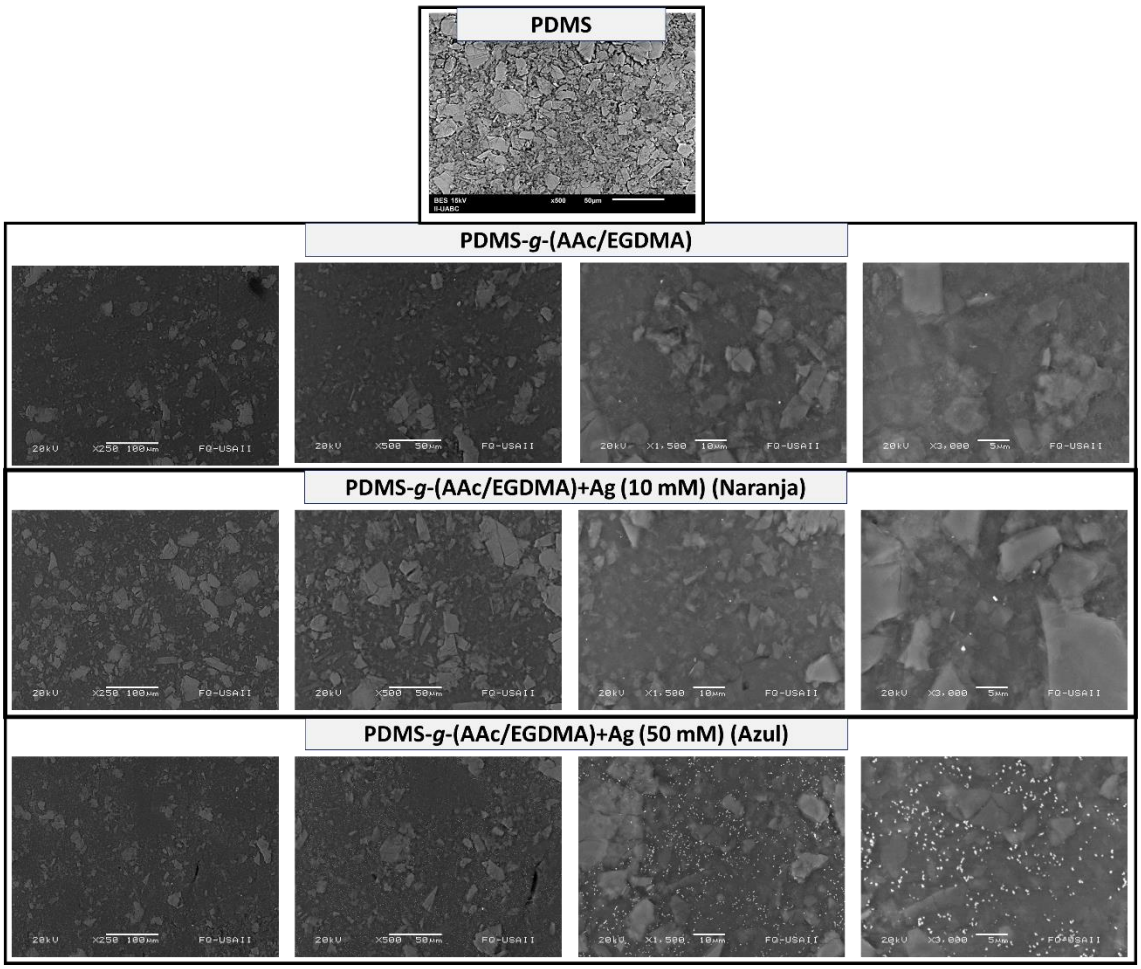

Figura 40. SEM de PDMS, PDMS-*g*-(AAc/EGDMA), PDMS-*g*-(AAc/EGDMA)+Ag modificada con 10 mM de $AgNO_3$ que se coloreó naranja (**d**) y PDMS-*g*-(AAc/EGDMA)+Ag modificada con 10 mM de $AgNO_3$ que se coloreó azul/negro (**i**).

Para confirmar la presencia de plata en estado reducido en las películas, se realizó el análisis elemental de la superficie mediante espectrometría de dispersión de rayos X (EDX), ver Figura 41. Este estudio confirmó la presencia de plata y el injerto AAc/EDGMA sobre la superficie. Las películas con menor concentración de plata PDMS-*g*-(AAc/EGDMA)+Ag (10 mM) que se coloreó naranja (**d**) mostraron menores cantidades de plata, la sección de la superficie con mayor cantidad de plata alcanzó el 4.6%. En contraste, la película PDMS-*g*-(AAc/EGDMA)+Ag (50 mM) que se coloreó azul/negro (**i**) mostró concentraciones más altas de plata en casi toda la superficie, la cantidad más alta fue casi el 6%. Para la película sin plata, no se encontró ninguna cantidad de metal en ningún espectro. La distribución elemental de las películas reveló un contenido en Ag que puede ser suficiente para el propósito indicado de obtener una superficie antimicrobiana [47].

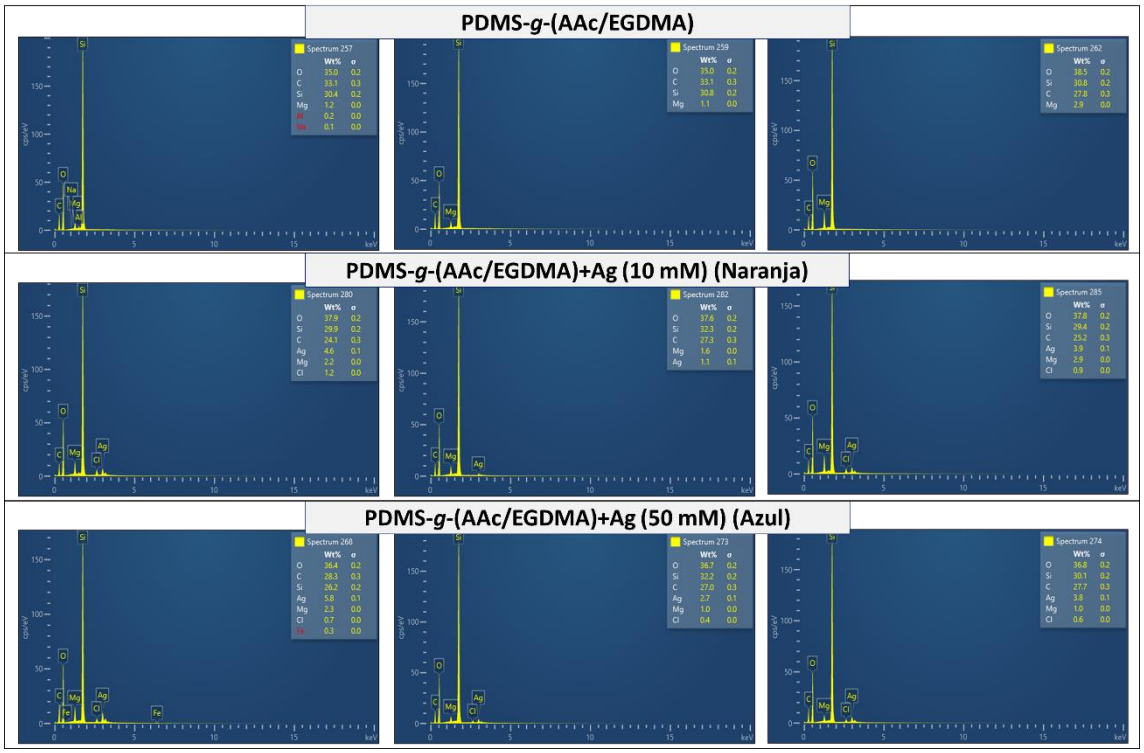

Figura 41. Análisis elemental de PDMS-*g*-(AAc/EGDMA), PDMS-*g*-(AAc/EGDMA)+Ag (10 mM) naranja (**d**) y PDMS-*g*-(AAc/EGDMA)+Ag (50 mM) que se coloreó azul/negro (**i**).

Viabilidad celular

La viabilidad celular se evaluó en pequeños volúmenes de medio de cultivo en contacto directo con fibroblastos del tipo BALB/3T3 (ratón). La citocompatibilidad se determinó con la Ecuación 3 [72]:

$$\text{Citocompatibilidad (\%)} = [\text{Abs}_{muestra}/\text{Abs}_{cont}]100 \qquad \text{(Ecuación 3)}$$

Como se muestra en la Figura 42, la viabilidad celular no se vio afectada por las películas con una baja concentración de plata (10 mM) en esta línea celular, mostró una buena citocompatibilidad >90%, a las 24 h. Es importante resaltar que la viabilidad celular de esa película es cercana al 90%, es decir, la presencia de la sal de plata incrementó la viabilidad celular en comparación con la película modificada sólo con los injertos AAc/EGDMA.

Todas las películas evaluadas tuvieron un GY ~ 10% (AAc/EGDMA), se demuestra que la citocompatibilidad disminuye considerablemente y el injerto más la presencia de la plata sobre la superficie desencadenan la muerte celular [48]. Además, un aumento de la concentración de Ag afecta directamente a la viabilidad celular debido a la citotoxicidad de las nanopartículas, que no desprecian entre células bacterianas y de fibroblastos. La película modificada con 50 mM de nitrato de plata induce la muerte celular, lo que se puede observar ya que la viabilidad celular disminuyó por debajo del 40%, por lo tanto películas modificadas con concentración mayor a 10 mM podrían resultar tóxicas para el ser humano.

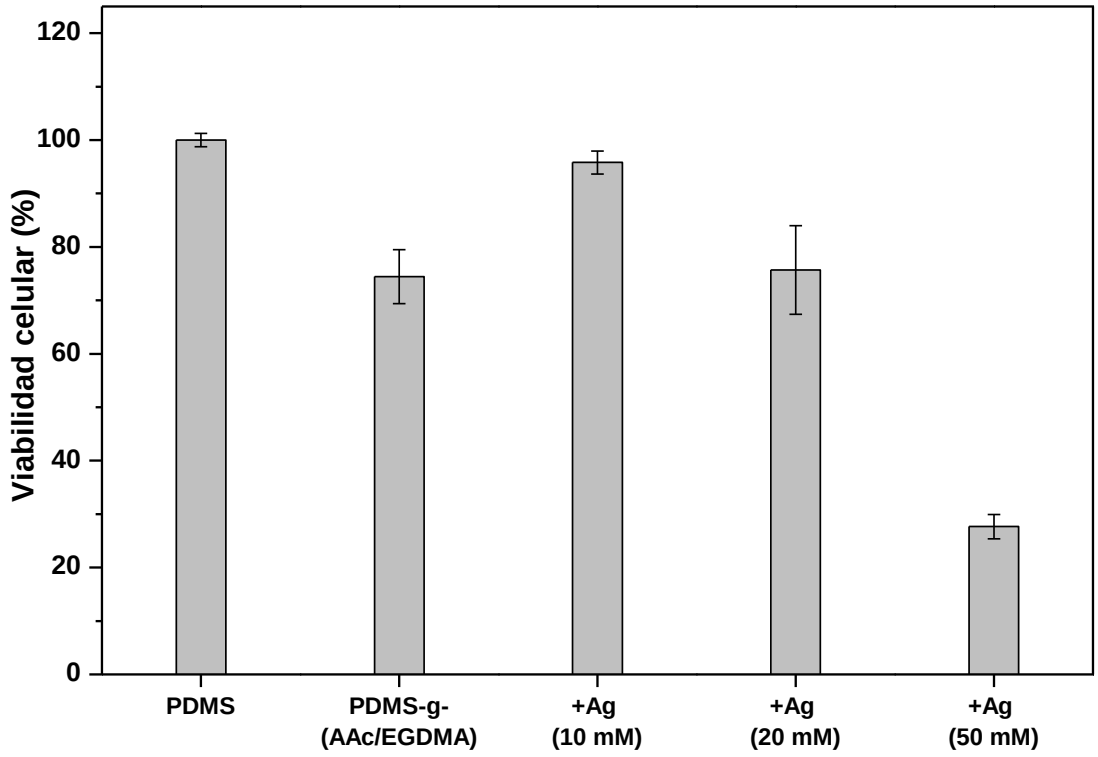

Figura 42. Viabilidad celular de PDMS-*g*-(AAc/EGDMA), y las películas modificadas con 10, 20 y 50 mM de nitrato de plata hacia fibroblastos murinos tipo BALB/3T3.

Pruebas antimicrobianas

Para comprobar que las películas modificadas poseen el efecto bactericida que proporciona la plata, se realizó un estudio contra diferentes bacterias, para la película que mostró una viabilidad celular con fibroblastos de ratón tipo BALB/3T3 mayor al 90%. En el estudio las muestras PDMS-*g*-(AAc/EGDMA)+Ag (10 mM) (I= 10 kGy h^{-1}) (naranja) (**d**), véase Figura 38, fueron probadas contra tres diferentes bacterias, y se comparó el efecto antimicrobiano con la PDMS y la PDMS-*g*-(AAc/EGDMA).

El estudio se llevó a cabo en caldo de cultivo Mueller Hinton con una concentración 0.5 escala McFarland, sumergiendo las películas en el medio. En los estudios preliminares se evaluaron tres bacterias, ya que existen reportes de su efectividad hacia la inhibición del crecimiento de *E. coli* [105-106], *P. aeruginosa* [107], y *S. aureus*, [108], así como estudios sobre su efectividad bactericida e incluso antifúngica [44,109-110].

El reporte de resultados se llevó a cabo midiendo el porcentaje de crecimiento bacteriano, utilizando la lectura de absorbancia a 600 nm, la ecuación utilizada fue la siguiente:

$$\text{Crecimiento bacteriano (\%)} = [Abs_{muestra}/Abs_{cont}]100 \qquad \text{(Ecuación 4)}$$

Las películas PDMS-*g*-(AAc/EGDMA)+Ag (10 mM) (I= 10 kGy h^{-1}) (naranja) (**d**), mostraron tener efectividad contra el crecimiento de las tres bacterias probadas (Figura 43) esta película se comparó con las otras tres muestras, sin plata y sin silicona prístina.

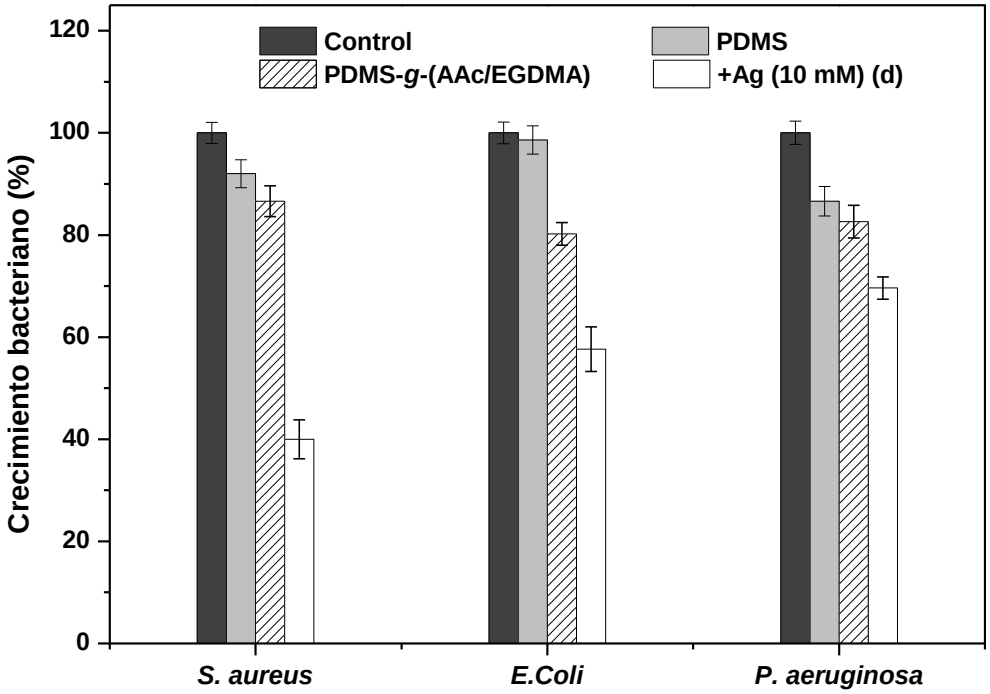

Figura 43. Pruebas de inhibición de crecimiento bacteriano contra *S. aureus*, *E. coli* y *P. aeruginosa*.

Según estos resultados, para la PDMS-3, el PDMS-*g*-(AAc/EGDMA)+Ag (10 mM) (**d**) mostró una mejor inhibición para *S. aureus* en el que el crecimiento bacteriano disminuye hasta un valor de ~ 40% de las células (en comparación con un 100% para otras muestras), después de 24 h. Para *E. coli*, la inhibición fue menos significativa, así como para *P. aeruginosa*, el efecto inhibidor fue menos dramático; sin embargo, todavía se observa una ligera inhibición del crecimiento. La inhibición del crecimiento de *S. aureus* puede haber sido más eficaz que para *E. coli* y *P. aeruginosa*, ya que *S. aureus* es una bacteria gram positiva, incluso si los AgNP's son eficaces contra las bacterias gram negativas; no obstante, la concentración requerida para el efecto antibacteriano en este sistema puede ser mayor, lo que a su vez puede afectar a la biocompatibilidad.

Después de demostrar que el efecto bactericida era más dramático para *S. aureus*, se probó el rendimiento de las películas preparadas con diferentes concentraciones de plata. Para el estudio de cinética de crecimiento bacteriano, se probaron las películas modificadas con 10, 20 y 50 mM de nitrato de plata. La inhibición del crecimiento de esta bacteria se evaluó en función del tiempo como puede verse en la Figura 44. En este gráfico se puede ver claramente que el crecimiento bacteriano de *S. aureus* se inhibe hasta por 48 h, cuando se prueban las películas de menor concentración de plata. Para la película modificada con 50 mM (**i**) se encontró que la absorbancia del medio de cultivo aumenta, lo cual puede atribuirse a la liberación del ion plata Ag^{+1} al medio.

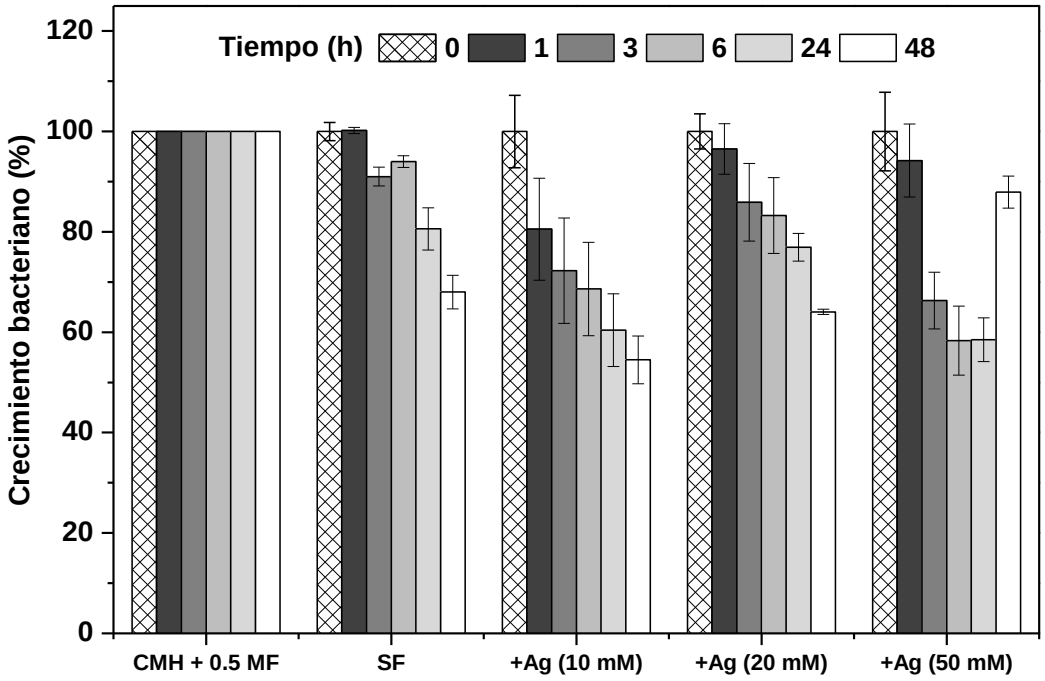

Figura 44. Cinética de crecimiento de *S. aureus* en función del tiempo para PDMS-*g*-(AAc/EGDMA), y las películas modificadas con 10, 20 y 50 mM de nitrato de plata.

6. SEGUNDA SECCIÓN

6.1. Carga y liberación de ciprofloxacino

Como fármaco antibiótico se utilizó el ciprofloxacino (CFX) debido a que tiene un amplio espectro de acción frente a bacterias Gram positivas y negativas. Además, estructuralmente, posee grupos funcionales con los que puede interactuar con otras moléculas de forma no covalente. Estos grupos son sensibles a los cambios de pH (Figura 45), y modular la acidez o basicidad del medio favorece la retención o liberación del propio fármaco.

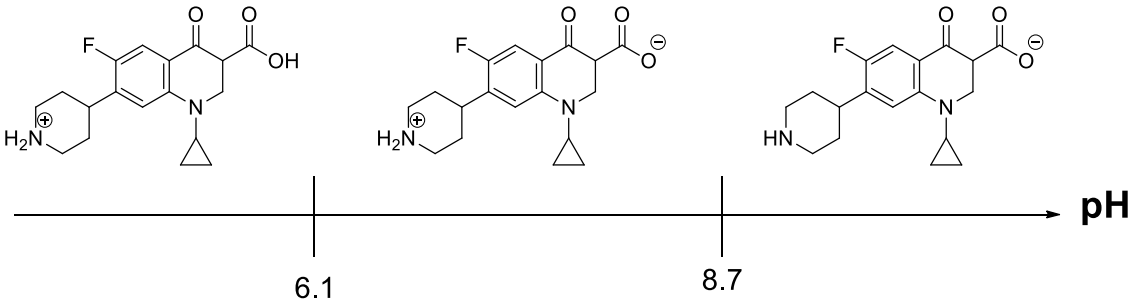

Figura 45. Carácter ácido-base del ciprofloxacino.

Las películas modificadas con **tolueno** en la sección de estudios preliminares se emplearon para inmovilizar ciprofloxacino en un primer paso, y posteriormente, llevar a cabo los experimentos de liberación. La carga se realizó a pH = 7.4, en solución salina de fosfatos (PBS), cuando hay una mayor absorción de agua con un límite de 48 h. Se realizó el experimento con las películas modificadas en **tolueno** PDMS-2, PDMS-3 y PDMS-4,[***] con un injerto de 30%, debido a que no sobrepasan el 20% de hinchamiento en PBS, son estables y con propiedades mecánicas similares a las del PDMS de partida (ver Figura 46). La película PDMS-5 se utilizó para la misma prueba, pero debido a su alta hidrofilicidad e inestabilidad en el medio comenzó a degradarse después de 48 h. El máximo de carga de ciprofloxacino fue de ~0.3 mg por gramo para la película PDMS-3a, mientras que la película PDMS-2a cargó ~0.2 mg.

[***] Preparadas con relación molar AAc:EGDMA 2:1, 3:1, 4:1 y 5:1

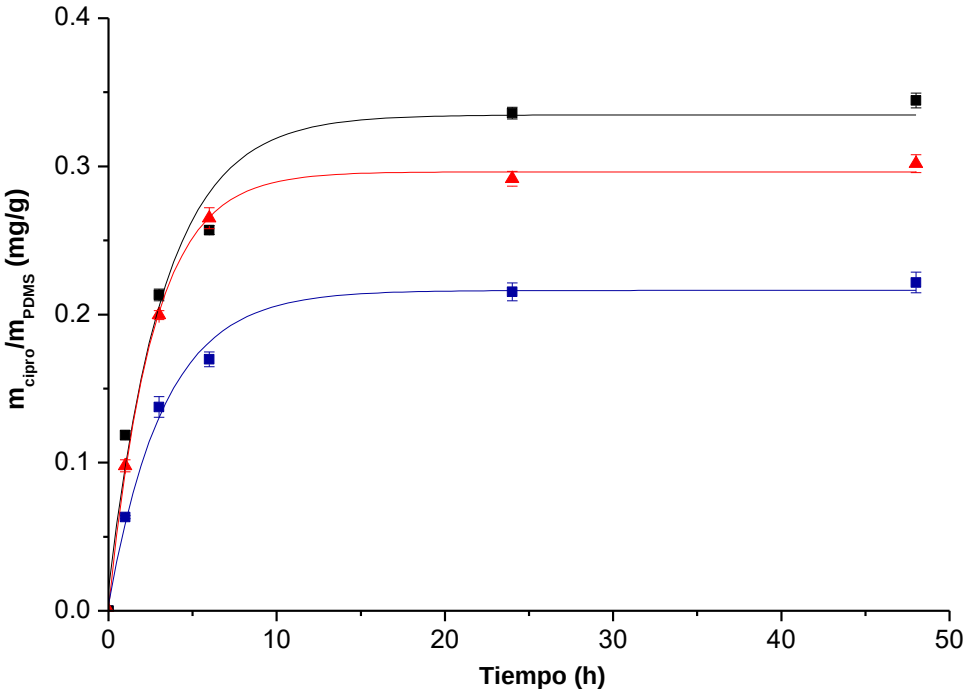

Figura 46. Carga de ciprofloxacino para (—) PDMS-2, (—) PDMS-3 y (—) PDMS-4.

Con respecto a la liberación, las películas liberaron menor ciprofloxacino que el que se cargó (ver Tabla 6). La película que tuvo un mejor porcentaje de liberación fue la PDMS-2a, que liberó 64% del fármaco cargado en un periodo de 48 h. Por el contrario, las PDMS-3a y PDMS-4a, liberaron 31 y 41%, respectivamente; lo cual se puede ver en la Figura 47. La concentración de ciprofloxacino supera la concentración mínima inhibitoria necesaria para bacterias de ambiente hospitalario, misma que se encuentra en el orden de μg mL^{-1}. Por ejemplo, para *E. coli* es de 0.004 - 0.015 μg mL^{-1} y para *S. aureus* de 0.12 – 0.5 μg mL^{-1}.

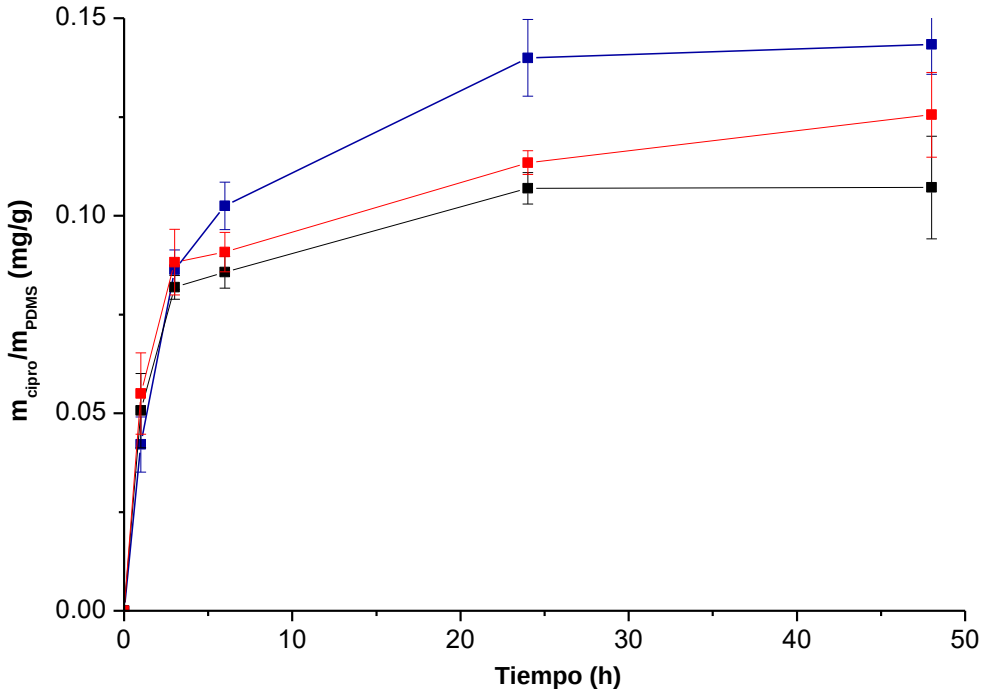

Figura 47. Liberación de ciprofloxacino para (—) PDMS-2, (—) PDMS-3 y (—) PDMS-4.

El perfil de liberación es típico de un mecanismo controlado por difusión, en el caso del sistema PDMS-*g*-(AAc/EGDMA) se estima que la liberación se encuentra controlada por el mecanismo de "contacto con el disolvente", es decir, al entrar en contacto con la solución de PBS, la película se hincha provocando la liberación del ciprofloxacino; esto es completamente dependiente de la estructura química del polímero de injerto (AAc:EGDMA) y del grado de injerto, ya que el hinchamiento es consecuencia de una reacción de ionización.

Tabla 6. Carga y liberación de ciprofloxacino.

Muestra	Carga mg_{cipro}/g_{PDMS}	Liberación mg_{cipro}/g_{PDMS}	% Liberación
PDMS-2a	0.2216 ± 0.01	0.14333 ± 0.0075	64.6 %
PDMS-3a	0.3445 ± 0.005	0.10714 ± 0.013	31.1 %
PDMS-4a	0.3018 ± 0.009	0.12555 ± 0.0107	41.6 %
PDMS-5a	-	-	-

Se probó la eficacia antimicrobiana de las películas modificadas se contra la bacteria gram negativa *E. coli*, debido a que derivados de quinolonas se utilizan en los tratamientos médicos cuando se presenta una infección causada por esta bacteria. Se evaluaron las películas 2, 3, 4 y 5 previamente cargadas con CFX y secadas al vacío.

De acuerdo a los resultados de carga/liberación de CFX (véase Figura 48) la película PDMS-2a, (con relación molar 2:1 AAc:EGDMA) es la que posee un mejor perfil de liberación con respecto a las demás películas, ya que libera más del 64% del fármaco que retiene en la superficie. Esto coincide con los resultados de eficacia antibacteriana, ya que la película PDMS-2a/CFX mostró

mayor efecto bactericida a las 48 h, debido a que la liberación de la CFX es más rápida y se mantiene constante después de 24 h. El resto de las películas también mostró eficacia contra la bacteria, ya que el injerto favorece la retención del CFX en la matriz de silicona, sin embargo, los resultados de liberación no son tan eficientes como para PDMS-2a, y las pruebas de bicompatibilidad con fibroblastos no son satisfactorias para aquellas películas con mayor concentración de AAc.

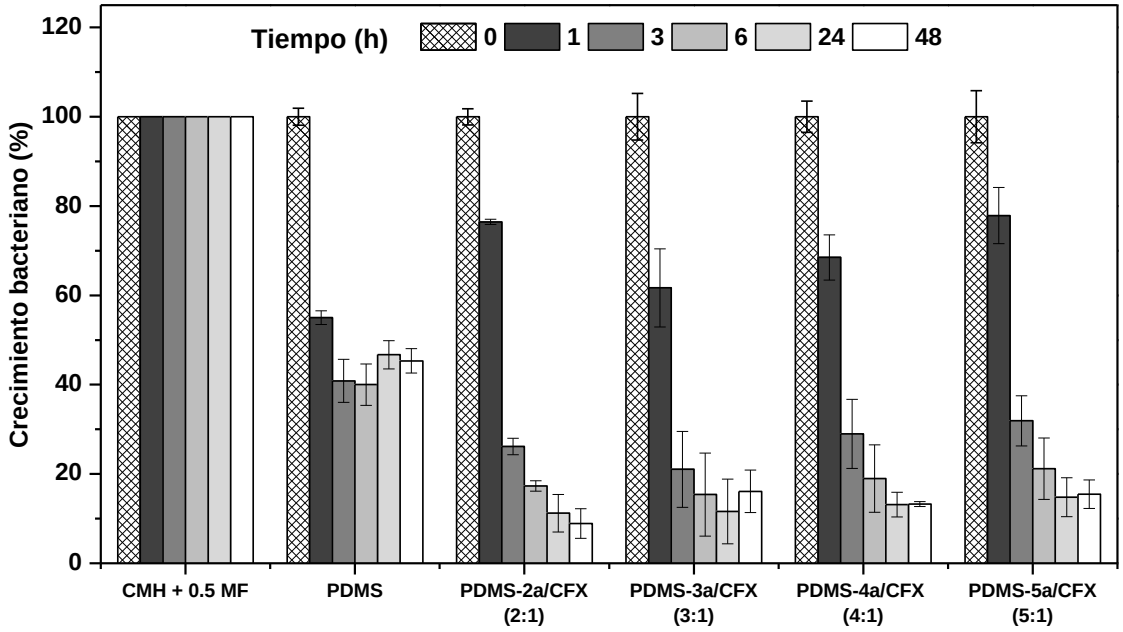

Figura 48. Pruebas de inhibición de crecimiento bacteriano en función del tiempo.

Al igual que en la primera sección (sección 6), la viabilidad celular se evaluó en pequeños volúmenes de medio de cultivo en contacto directo con fibroblastos BALB/3T3 (ratón). La biocompatibilidad se determinó utilizando la Ecuación 3 [72]:

$$\text{Citocompatibilidad (\%)} = [Abs_{muestra}/Abs_{cont}]100 \qquad \text{(Ecuación 3)}$$

Como se muestra en la Figura 49, la viabilidad celular no se vio afectada por las películas con una baja concentración de plata (10 mM) en esta línea celular, mostró una buena citocompatibilidad >90% a las 24 h. Es importante resaltar que la viabilidad celular de esa película es mejor comparada con la película modificada solo con los injertos AAc:EGDMA, todas las películas evaluadas tuvieron un GY ~ 10%, se demuestra que un aumento en el GY sobre la silicona superficie, la citocompatibilidad disminuye considerablemente [48]. Un aumento de la concentración de Ag afecta directamente a la viabilidad celular debido a la citotoxicidad de las nanopartículas. La película modificada con 50 mM de nitrato de plata induce la muerte celular, lo que se puede observar ya que la viabilidad celular disminuyó por debajo del 40%.

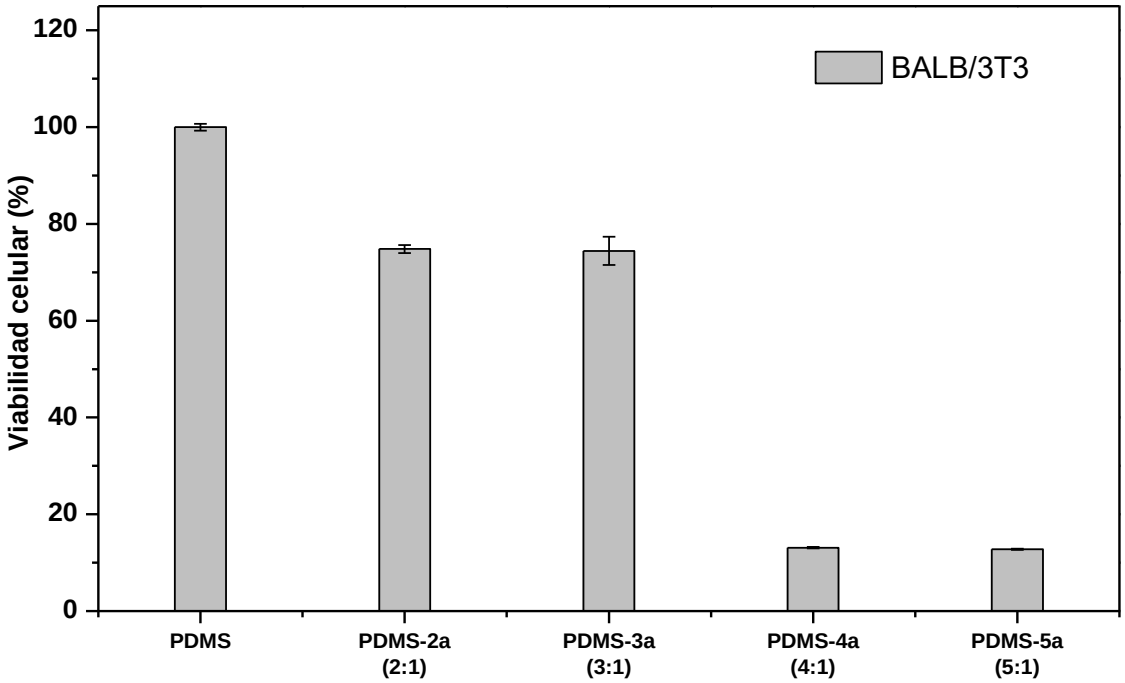

Figura 49. Viabilidad celular de las películas modificadas con AAc:EGDMA en diferente relación molar hacia fibroblastos BALB/3T3.

7. CONCLUSIONES

1. Se logró modificar por método simultáneo de polimerización el PDMS con AAc y EGDMA utilizando tolueno alcanzando injertos más altos (hasta ~50%), mientras que la reacción que se llevó a cabo en mezcla agua:EtOH 1:1 como los injertos fueron menores (~10%). La diferencia en los grados de injerto se atribuye al efecto de la radiación en el disolvente empleado para la reacción de injerto, ya que éste influye en el contacto entre las moléculas de monómero y la matriz de PDMS. La obtención de PDMS-*g*-(AAc/EGDMA) se logró con baja concentración de monómero y dosis no superiores a 50 kGy, para obtener películas con características útiles en dispositivos médicos. La dosis de radiación influye en el grado de injerto que se obtiene en cada reacción, sin embargo, este comportamiento depende también de la relación molar de monómeros. La variación en la relación AAc:EGDMA generó un aumento en la cantidad de injerto muy distinta a la que se obtiene para PDMS-*g*-AAc.

2. Las técnicas espectroscópicas utilizadas mostraron la presencia de la mezcla de monómeros sobre la superficie del PDMS, debido a la similitud estructural entre ambos monómeros no se puede cuantificar la relación de monómeros en el injerto. Lo más característico fue que se encontraron las bandas correspondientes al carbonilo en las técnicas utilizadas. Con respecto al comportamiento térmico no hubo cambios significativos en el TGA de las películas modificadas con respecto al del PDMS de partida, mostrando que el injerto no afecta las propiedades termoestables de la silicona.

3. La superficie de las películas modificadas adoptó la propiedad de hidrofilicidad de la mezcla de monómeros, lo cual se comprobó mediante el estudio de ángulo de contacto, el ángulo disminuyó cerca de 10° con respecto al PDMS que es altamente hidrofóbico (PDMS= 105° y PDMS modificadas ~90°). Las pruebas de hinchamiento en agua desionizada demostraron la capacidad de retener agua de las películas modificadas, lo cual indica que se le ha añadido hidrofilicidad.

4. El comportamiento de las películas en agua desionizada y en solución biológica simulada (PBS) no es el mismo, se alcanzan hinchamientos más altos en solución salina en mayor tiempo. Similar al hinchamiento encontrado al hacer las pruebas de sensibilidad al pH, donde también se demostró la baja estabilidad de las películas PDMS-*g*-AAc con injerto mayor a 30%, y de todas al llegar a pH de 10.

Primera Sección:

1. Se logró reducir Ag^{+1} a Ag^{0} utilizando radiación γ de manera simultánea con la reacción de injerto de los monómeros AAc/EGDMA. La reacción procedió utilizando la relación molar 3:1 y el medio hidroalcohólico como disolvente (agua:EtOH). La reacción de injerto procedió de la misma manera independiente de la concentración de nitrato de plata, el grado de injerto para todos los experimentos fue de ~9.5%. La variación en la concentración de la sal de plata generó un cambio en la coloración de las películas, lo cual puede estar asociado con la morfología y el tamaño de las partículas formadas.
2. La presencia de la plata en estado reducido se comprobó experimentalmente con UV-Vis de películas y SEM/EDX, se encontraron las bandas de absorción λ = ~430 y ~620 nm correspondientes a nanopartículas de plata esféricas de bajo diámetro (10-20 nm) y partículas semiesféricas, amorfas o triangulares de mayor tamaño (~100 nm), respectivamente.

3. La viabilidad celular evaluada con fibroblastos de ratón se mantuvo mayor al 90% para la película PDMS-*g*-(AAc/EGDMA)+Ag (10 mM), mientras que las películas modificadas con mayor concentración de nitrato de plata provocan la muerte celular. Las películas que mantienen mayor viabilidad celular se sometieron a pruebas antimicrobianas contra tres *S. aureus*, *E. coli* y *P. aeruginosa*, mostrando un efecto bactericida contra las tres. Sin embargo, tuvo mayor efecto contra *S. aureus*, y las pruebas de cinética de crecimiento bacteriano demostraron que el efecto dura hasta las 48 h.

Segunda Sección:

- Las películas modificadas con relación molar 2:1; 3:1 y 4:1 de AAc:EGDMA con un 30% de injerto cargaron ciprofloxacino. La película PDMS-2 fue la que mostró mayor eficiencia de liberación, alcanzando una liberación del 64%, que corresponde a 0.14 mg/g, por encima de la concentración mínima inhibitoria para patógenos comunes.
- Todas las películas mostraron un efecto bactericida contra *E. coli*, a las 48 h y una viabilidad celular únicamente se mantuvo mayor al 85% para la película PDMS-2/CFX.

PUBLICACIONES

[1] **Velazco-Medel, M. A.**, Camacho-Cruz, L. A., & Bucio, E. "Modification of PDMS with acrylic acid and acrylic acid/ethylene glycol dimethacrylate by simultaneous polymerization assisted by gamma radiation" *Radiation Physics and Chemistry*, **2020,** 171 (December 2019), 108754. DOI: 10.1016/j.radphyschem.2020.108754

[2] Camacho-Cruz, L. A., **Velazco-Medel, M. A.**, Cruz-Gómez G. A., and Emilio Bucio. "Antimicrobial Polymers" In *Advanced Antimicrobial Materials and Applications*, **2020**, Springer, USA. DOI: 10.1007/978-981-15-7098-8_1

[3] **Velazco-Medel, M. A.**, Camacho-Cruz, L. A., Lugo-González, J. C. & Bucio, E. "Antifungal polymers for medical applications" *Medical Devices & Sensors*, **2020**, (October). DOI: 10.1002/mds3.10134

[4] **Velazco Medel, M. A.**, Camacho Cruz, L. A., Duarte Peña, L., and Emilio Bucio. "Properties of Aerogels" In *Aerogels I: Preparation, Properties and Applications*, 84, **2020**, (pp. 172-200), Materials Research Forum LLC: Materials Research Foundations. DOI: 10.21741/9781644900994-7

[5] Camacho-Cruz, L. A., **Velazco-Medel, M. A.**, & Bucio, E. "Aqueous polymerizations" In *Green Sustainable Process for Chemical and Environmental Engineering and Science*, **2020**, (pp. 275–318). Elsevier, DOI: 10.1016/B978-0-12-819542-0.00009-9

[6] **Velazco-Medel, M. A.**, Camacho-Cruz, L. A., & Bucio, E. "Modification of relevant polymeric materials for medical applications and devices" *Medical Devices & Sensors*, **2020**, DOI: 10.1002/mds3.10073.

[7] Camacho-Cruz LA, **Velazco-Medel MA**, Parra-Delgado H, Bucio E. "Functionalization of cotton gauzes with poly(N-vinylimidazole) and quaternized poly(N-vinylimidazole) with gamma radiation to produce medical devices with pH-buffering and antimicrobial properties" *Cellulose*, **2021**, *28*, 3279–3294, DOI: 10.1007/s10570-021-03725-w.

[8] **Velazco-Medel, M. A.**; Camacho-Cruz, L. A.; Magaña, H.; Palomino, K.; Bucio, E. "Simultaneous Grafting Polymerization of Acrylic Acid and Silver Aggregates Formation by Direct Reduction Using γ Radiation onto Silicone Surface and Their Antimicrobial Activity and Biocompatibility" *Molecules* **2021**, *26*, 2859. DOI: 10.3390/ molecules26102859.

8. REFERENCIAS

[1] M.F. Maitz, Applications of synthetic polymers in clinical medicine, Biosurface and Biotribology. 1 (2015) 161–176. https://doi.org/10.1016/j.bsbt.2015.08.002.

[2] A.J.T. Teo, A. Mishra, I. Park, Y.J. Kim, W.T. Park, Y.J. Yoon, Polymeric Biomaterials for Medical Implants and Devices, ACS Biomater. Sci. Eng. 2 (2016) 454–472. https://doi.org/10.1021/acsbiomaterials.5b00429.

[3] M. Pérez-Calixto, P. Diaz-Rodriguez, A. Concheiro, C. Alvarez-Lorenzo, G. Burillo, Amino-functionalized polymers by gamma radiation and their influence on macrophage polarization, React. Funct. Polym. 151 (2020) 104568. https://doi.org/10.1016/j.reactfunctpolym.2020.104568.

[4] D. Mack, H. Rohde, L.G. Harris, A.P. Davies, M.A. Horstkotte, J.K.-M. Knobloch, Biofilm Formation in Medical Device-Related Infection, Int. J. Artif. Organs. 29 (2006) 343–359. https://doi.org/10.1177/039139880602900404.

[5] C. von Eiff, B. Jansen, W. Kohnen, K. Becker, Infections Associated with Medical Devices, Drugs. 65 (2005) 179–214. https://doi.org/10.2165/00003495-200565020-00003.

[6] C. Costa-Orlandi, J. Sardi, N. Pitangui, H. de Oliveira, L. Scorzoni, M. Galeane, K. Medina-Alarcón, W. Melo, M. Marcelino, J. Braz, A. Fusco-Almeida, M. Mendes-Giannini, Fungal Biofilms and Polymicrobial Diseases, J. Fungi. 3 (2017) 22. https://doi.org/10.3390/jof3020022.

[7] J. V. Desai, A.P. Mitchell, D.R. Andes, Fungal Biofilms, Drug Resistance, and Recurrent Infection, Cold Spring Harb. Perspect. Med. 4 (2014) a019729–a019729. https://doi.org/10.1101/cshperspect.a019729.

[8] Q. Yu, Y. Zhang, H. Wang, J. Brash, H. Chen, Anti-fouling bioactive surfaces, Acta Biomater. 7 (2011) 1550–1557. https://doi.org/10.1016/j.actbio.2010.12.021.

[9] J.W. Costerton, Bacterial Biofilms: A Common Cause of Persistent Infections, Science (80-.). 284 (1999) 1318–1322. https://doi.org/10.1126/science.284.5418.1318.

[10] I. De-la-Pinta, M. Cobos, J. Ibarretxe, E. Montoya, E. Eraso, T. Guraya, G. Quindós, Effect of biomaterials hydrophobicity and roughness on biofilm development, J. Mater. Sci. Mater. Med. 30 (2019) 77. https://doi.org/10.1007/s10856-019-6281-3.

[11] J. Smith, P.M. Fratamico, G. Uhlich, Molecular mechanisms involved in biofilm formation by food-associated bacteria, in: Biofilms Food Beverage Ind., Elsevier, 2009: pp. 42–98. https://doi.org/10.1533/9781845697167.1.42.

[12] P.M. Rose, V. Cantrill, M. Benohoud, A. Tidder, C.M. Rayner, R.S. Blackburn, Application of Anthocyanins from Blackcurrant (Ribes nigrum L.) Fruit Waste as Renewable Hair Dyes, J. Agric. Food Chem. 66 (2018) 6790–6798. https://doi.org/10.1021/acs.jafc.8b01044.

[13] N. Rabin, Y. Zheng, C. Opoku-Temeng, Y. Du, E. Bonsu, H.O. Sintim, Biofilm formation mechanisms and targets for developing antibiofilm agents, Future Med. Chem. 7 (2015) 493–512. https://doi.org/10.4155/fmc.15.6.

[14] N. Rabin, Y. Zheng, C. Opoku-Temeng, Y. Du, E. Bonsu, H.O. Sintim, Biofilm formation mechanisms and targets for developing antibiofilm agents, Future Med. Chem. 7 (2015) 493–512. https://doi.org/10.4155/fmc.15.6.

[15] Z. Khatoon, C.D. McTiernan, E.J. Suuronen, T.-F. Mah, E.I. Alarcon, Bacterial biofilm formation on implantable devices and approaches to its treatment and prevention, Heliyon. 4 (2018) e01067. https://doi.org/10.1016/j.heliyon.2018.e01067.

[16] I. Francolini, G. Donelli, Prevention and control of biofilm-based medical-device-related infections, FEMS Immunol. Med. Microbiol. 59 (2010) 227–238. https://doi.org/10.1111/j.1574-695X.2010.00665.x.

[17] J.M. Goddard, J.H. Hotchkiss, Polymer surface modification for the attachment of bioactive compounds, Prog. Polym. Sci. 32 (2007) 698–725. https://doi.org/10.1016/j.progpolymsci.2007.04.002.

[18] B. Zdyrko, I. Luzinov, Polymer brushes by the "grafting to" method, Macromol. Rapid Commun. 32 (2011) 859–869. https://doi.org/10.1002/marc.201100162.
[19] S. Chatterjee, P.C. leung Hui, Review of stimuli-responsive polymers in drug delivery and textile application, Molecules. 24 (2019). https://doi.org/10.3390/molecules24142547.
[20] C. Alvarez-Lorenzo, C.A. Garcia-Gonzalez, E. Bucio, A. Concheiro, Stimuli-responsive polymers for antimicrobial therapy: drug targeting, contact-killing surfaces and competitive release, Expert Opin. Drug Deliv. 13 (2016) 1109–1119. https://doi.org/10.1080/17425247.2016.1178719.
[21] M. Wei, Y. Gao, X. Li, M.J. Serpe, Stimuli-responsive polymers and their applications, Polym. Chem. 8 (2017) 127–143. https://doi.org/10.1039/c6py01585a.
[22] H. Almeida, M.H. Amaral, P. Lobão, Temperature and pH stimuli-responsive polymers and their applications in controlled and selfregulated drug delivery, J. Appl. Pharm. Sci. 2 (2012) 01–10. https://doi.org/10.7324/JAPS.2012.2609.
[23] M. Rizwan, R. Yahya, A. Hassan, M. Yar, A. Azzahari, V. Selvanathan, F. Sonsudin, C. Abouloula, pH Sensitive Hydrogels in Drug Delivery: Brief History, Properties, Swelling, and Release Mechanism, Material Selection and Applications, Polymers (Basel). 9 (2017) 137. https://doi.org/10.3390/polym9040137.
[24] F. Reyes-Ortega, pH-responsive polymers: properties, synthesis and applications, in: Smart Polym. Their Appl., Elsevier, 2014: pp. 45–92. https://doi.org/10.1533/9780857097026.1.45.
[25] G. Lin, S. Chang, H. Hao, P. Tathireddy, M. Orthner, J. Magda, F. Solzbacher, Osmotic swelling pressure response of smart hydrogels suitable for chronically implantable glucose sensors, Sensors Actuators B Chem. 144 (2010) 332–336. https://doi.org/10.1016/j.snb.2009.07.054.
[26] K.D. Schulze, S.M. Hart, S.L. Marshall, C.S. O'Bryan, J.M. Urueña, A.A. Pitenis, W.G. Sawyer, T.E. Angelini, Polymer Osmotic Pressure in Hydrogel Contact Mechanics, Biotribology. 11 (2017) 3–7. https://doi.org/10.1016/j.biotri.2017.03.004.
[27] H. Wang, G.L. Rempel, PH-responsive polymer core-shell nanospheres for drug delivery, J. Polym. Sci. Part A Polym. Chem. 51 (2013) 4440–4450. https://doi.org/10.1002/pola.26860.
[28] D. Schmaljohann, Thermo- and pH-responsive polymers in drug delivery, Adv. Drug Deliv. Rev. 58 (2006) 1655–1670. https://doi.org/10.1016/j.addr.2006.09.020.
[29] A. Kumar, P.K. Vemula, P.M. Ajayan, G. John, Silver-nanoparticle-embedded antimicrobial paints based on vegetable oil, Nat. Mater. 7 (2008) 236–241. https://doi.org/10.1038/nmat2099.
[30] A. Das, A. Kumar, N.B. Patil, C. Viswanathan, D. Ghosh, Preparation and characterization of silver nanoparticle loaded amorphous hydrogel of carboxymethylcellulose for infected wounds, Carbohydr. Polym. 130 (2015) 254–261. https://doi.org/10.1016/j.carbpol.2015.03.082.
[31] F. Costa, I.F. Carvalho, R.C. Montelaro, P. Gomes, M.C.L. Martins, Covalent immobilization of antimicrobial peptides (AMPs) onto biomaterial surfaces, Acta Biomater. 7 (2011) 1431–1440. https://doi.org/10.1016/j.actbio.2010.11.005.
[32] A. Muñoz-Bonilla, M. Fernández-García, Polymeric materials with antimicrobial activity, Prog. Polym. Sci. 37 (2012) 281–339. https://doi.org/10.1016/j.progpolymsci.2011.08.005.
[33] A. Jain, L.S. Duvvuri, S. Farah, N. Beyth, A.J. Domb, W. Khan, Antimicrobial Polymers, Adv. Healthc. Mater. 3 (2014) 1969–1985. https://doi.org/10.1002/adhm.201400418.
[34] H. Palza, Antimicrobial polymers with metal nanoparticles, Int. J. Mol. Sci. 16 (2015) 2099–2116. https://doi.org/10.3390/ijms16012099.
[35] A. Llorens, E. Lloret, P.A. Picouet, R. Trbojevich, A. Fernandez, Metallic-based micro and nanocomposites in food contact materials and active food packaging, Trends Food Sci. Technol. 24 (2012) 19–29. https://doi.org/10.1016/j.tifs.2011.10.001.
[36] Y. Zare, I. Shabani, Polymer/metal nanocomposites for biomedical applications, Mater.

Sci. Eng. C. 60 (2016) 195–203. https://doi.org/10.1016/j.msec.2015.11.023.
[37] F. López-Saucedo, G.G. Flores-Rojas, J. López-Saucedo, B. Magariños, C. Alvarez-Lorenzo, A. Concheiro, E. Bucio, Antimicrobial silver-loaded polypropylene sutures modified by radiation-grafting, Eur. Polym. J. 100 (2018) 290–297. https://doi.org/10.1016/j.eurpolymj.2018.02.005.
[38] F. López-Saucedo, G.G. Flores-Rojas, E. Bucio, C. Alvarez-Lorenzo, A. Concheiro, O. González-Antonio, Achieving antimicrobial activity through poly(N-methylvinylimidazolium) iodide brushes on binary-grafted polypropylene suture threads, MRS Commun. 7 (2017) 938–946. https://doi.org/10.1557/mrc.2017.121.
[39] M.A. Busolo, P. Fernandez, M.J. Ocio, J.M. Lagaron, Novel silver-based nanoclay as an antimicrobial in polylactic acid food packaging coatings, Food Addit. Contam. Part A. 27 (2010) 1617–1626. https://doi.org/10.1080/19440049.2010.506601.
[40] H. Song, B. Li, Q.-B. Lin, H.-J. Wu, Y. Chen, Migration of silver from nanosilver–polyethylene composite packaging into food simulants, Food Addit. Contam. Part A. 74 (2011) 1–5. https://doi.org/10.1080/19440049.2011.603705.
[41] J.A. Lemire, J.J. Harrison, R.J. Turner, Antimicrobial activity of metals: mechanisms, molecular targets and applications, Nat. Rev. Microbiol. 11 (2013) 371–384. https://doi.org/10.1038/nrmicro3028.
[42] A.C. Burdușel, O. Gherasim, A.M. Grumezescu, L. Mogoantă, A. Ficai, E. Andronescu, Biomedical applications of silver nanoparticles: An up-to-date overview, Nanomaterials. 8 (2018). https://doi.org/10.3390/nano8090681.
[43] K. Gudikandula, S. Charya Maringanti, Synthesis of silver nanoparticles by chemical and biological methods and their antimicrobial properties, J. Exp. Nanosci. 11 (2016) 714–721. https://doi.org/10.1080/17458080.2016.1139196.
[44] J.R. Morones, J.L. Elechiguerra, A. Camacho, K. Holt, J.B. Kouri, J.T. Ramírez, M.J. Yacaman, The bactericidal effect of silver nanoparticles, Nanotechnology. 16 (2005) 2346–2353. https://doi.org/10.1088/0957-4484/16/10/059.
[45] A. Petica, S. Gavriliu, M. Lungu, N. Buruntea, C. Panzaru, Colloidal silver solutions with antimicrobial properties, Mater. Sci. Eng. B. 152 (2008) 22–27. https://doi.org/10.1016/j.mseb.2008.06.021.
[46] B. Tylkowski, A. Trojanowska, M. Nowak, L. Marciniak, R. Jastrzab, Applications of silver nanoparticles stabilized and/or immobilized by polymer matrixes, Phys. Sci. Rev. 2 (2017). https://doi.org/10.1515/psr-2017-0024.
[47] Y. Rodríguez Nuñez, R. Castro, F. Arenas, Z. López-Cabaña, G. Carreño, V. Carrasco-Sánchez, A. Marican, J. Villaseñor, E. Vargas, L. Santos, E. Durán-Lara, Preparation of Hydrogel/Silver Nanohybrids Mediated by Tunable-Size Silver Nanoparticles for Potential Antibacterial Applications, Polymers (Basel). 11 (2019) 716. https://doi.org/10.3390/polym11040716.
[48] A.I. El-Batal, F.M. Mosallam, G.S. El-Sayyad, Synthesis of Metallic Silver Nanoparticles by Fluconazole Drug and Gamma Rays to Inhibit the Growth of Multidrug-Resistant Microbes, J. Clust. Sci. 29 (2018) 1003–1015. https://doi.org/10.1007/s10876-018-1411-5.
[49] X. Ping, M. Wang, G. Xuewu, Surface modification of poly(ethylene terephthalate) (PET) film by gamma-ray induced grafting of poly(acrylic acid) and its application in antibacterial hybrid film, Radiat. Phys. Chem. 80 (2011) 567–572. https://doi.org/10.1016/j.radphyschem.2010.12.011.
[50] N. Eghbalifam, M. Frounchi, S. Dadbin, Antibacterial silver nanoparticles in polyvinyl alcohol/sodium alginate blend produced by gamma irradiation, Int. J. Biol. Macromol. 80 (2015) 170–176. https://doi.org/10.1016/j.ijbiomac.2015.06.042.
[51] S. Gupta, P. Uhlmann, M. Agrawal, S. Chapuis, U. Oertel, M. Stamm, Immobilization of Silver Nanoparticles on Responsive Polymer Brushes, Macromolecules. 41 (2008) 2874–2879. https://doi.org/10.1021/ma800204h.
[52] Y.K. Sung, S.W. Kim, Recent advances in polymeric drug delivery systems, Biomater.

Res. 24 (2020) 12. https://doi.org/10.1186/s40824-020-00190-7.
[53] G.G. Flores-Rojas, F. López-Saucedo, E. Bucio, Gamma-irradiation applied in the synthesis of metallic and organic nanoparticles: A short review, Radiat. Phys. Chem. 169 (2020) 107962. https://doi.org/10.1016/j.radphyschem.2018.08.011.
[54] P. Chen, L. Song, Y. Liu, Y. e. Fang, Synthesis of silver nanoparticles by γ-ray irradiation in acetic water solution containing chitosan, Radiat. Phys. Chem. 76 (2007) 1165–1168. https://doi.org/10.1016/j.radphyschem.2006.11.012.
[55] Y. Liu, S. Chen, L. Zhong, G. Wu, Preparation of high-stable silver nanoparticle dispersion by using sodium alginate as a stabilizer under gamma radiation, Radiat. Phys. Chem. 78 (2009) 251–255. https://doi.org/10.1016/j.radphyschem.2009.01.003.
[56] H.H. Mansour, M. Eid, M.B. El-Arnaouty, Effect of silver nanoparticles synthesized by gamma radiation on the cytotoxicity of doxorubicin in human cancer cell lines and experimental animals, Hum. Exp. Toxicol. 37 (2018) 38–50. https://doi.org/10.1177/0960327116689717.
[57] K. Naghavi, E. Saion, K. Rezaee, W.M.M. Yunus, Influence of dose on particle size of colloidal silver nanoparticles synthesized by gamma radiation, Radiat. Phys. Chem. 79 (2010) 1203–1208. https://doi.org/10.1016/j.radphyschem.2010.07.009.
[58] V.H. Pino-Ramos, A. Ramos-Ballesteros, F. López-Saucedo, J.E. López-Barriguete, G.H.C. Varca, E. Bucio, Radiation Grafting for the Functionalization and Development of Smart Polymeric Materials, Top. Curr. Chem. 374 (2016). https://doi.org/10.1007/s41061-016-0063-x.
[59] F. Abbasi, H. Mirzadeh, A.A. Katbab, Modification of polysiloxane polymers for biomedical applications: A review, Polym. Int. 50 (2001) 1279–1287. https://doi.org/10.1002/pi.783.
[60] B. Pavlović, D.D. Božić, J. Milovanović, A. Jotić, V. Djukić, S. Djukić, N. Konstantinović, I. Ćirković, Quantification of biofilm formation on silicone intranasal splints: An in vitro study, Acta Microbiol. Immunol. Hung. 63 (2016) 301–311. https://doi.org/10.1556/030.63.2016.006.
[61] J.S. Yang, G.H. Hsiue, Synthesis of Acrylic Acid Grafted Silicone Rubber via Preirradiation Graft Copolymerization and Its Physical and Dielectric Properties, J. Appl. Polym. Sci. 61 (1996) 221–229. https://doi.org/10.1002/(SICI)1097-4628(19960711)61:2<221::AID-APP5>3.3.CO;2-K.
[62] K.A. Montoya-Villegas, A. Ramírez-Jiménez, A. Zizumbo-López, S. Pérez-Sicairos, B. Leal-Acevedo, E. Bucio, A. Licea-Claverie, Controlled surface modification of silicone rubber by gamma-irradiation followed by RAFT grafting polymerization, Eur. Polym. J. 134 (2020) 109817. https://doi.org/10.1016/j.eurpolymj.2020.109817.
[63] H. Keshvari, H. Mirzadeh, P. Mansoori, F. Orang, M.T. Khorasani, Collagen Immobilization onto Acrylic Acid Laser-grafted Silicone for Using as Artificial Skin: In Vitro, Iran. Polym. J. 17 (2008) 171–182.
[64] S.-D. Lee, G.-H. Hsiue, C.-Y. Kao, Preparation and characterization of a homobifunctional silicone rubber membrane grafted with acrylic acid via plasma-induced graft copolymerization, J. Polym. Sci. Part A Polym. Chem. 34 (1996) 141–148. https://doi.org/10.1002/(SICI)1099-0518(19960115)34:1<141::AID-POLA15>3.0.CO;2-L.
[65] A.S. Palsule, S.J. Clarson, C.W. Widenhouse, Gamma irradiation of silicones, J. Inorg. Organomet. Polym. Mater. 18 (2008) 207–221. https://doi.org/10.1007/s10904-008-9205-0.
[66] R.S. Maxwell, R. Cohenour, W. Sung, D. Solyom, M. Patel, The effects of γ-radiation on the thermal, mechanical, and segmental dynamics of a silica filled, room temperature vulcanized polysiloxane rubber, Polym. Degrad. Stab. 80 (2003) 443–450. https://doi.org/10.1016/S0141-3910(03)00028-4.
[67] H.I. Meléndez-Ortiz, C. Alvarez-Lorenzo, A. Concheiro, V.M. Jiménez-Páez, E. Bucio, Modification of medical grade PVC with N-vinylimidazole to obtain bactericidal surface,

Radiat. Phys. Chem. 119 (2016) 37–43. https://doi.org/10.1016/j.radphyschem.2015.09.014.

[68] H. Magaña, K. Palomino, J.M. Cornejo-Bravo, C. Alvarez- Lorenzo, A. Concheiro, E. Bucio, Radiation-grafting of acrylamide onto silicone rubber films for diclofenac delivery, Radiat. Phys. Chem. 107 (2015) 164–170. https://doi.org/10.1016/j.radphyschem.2014.10.011.

[69] G.G. Flores-Rojas, F. López-Saucedo, E. Bucio, T. Isoshima, Covalent immobilization of lysozyme in silicone rubber modified by easy chemical grafting, MRS Commun. 7 (2017) 904–912. https://doi.org/10.1557/mrc.2017.115.

[70] V.H. Pino-Ramos, G.G. Flores-Rojas, C. Alvarez-Lorenzo, A. Concheiro, E. Bucio, Graft copolymerization by ionization radiation, characterization, and enzymatic activity of temperature-responsive SR-g-PNVCL loaded with lysozyme, React. Funct. Polym. 126 (2018) 74–82. https://doi.org/10.1016/j.reactfunctpolym.2018.03.002.

[71] G.G. Flores-Rojas, F. López-Saucedo, M. Quezada-Miriel, E. Bucio, Grafting of glycerol methacrylate onto silicone rubber using γ-rays: Derivatization to 2-oxoethyl methacrylate and immobilization of lysozyme, MRS Commun. 8 (2018) 199–206. https://doi.org/10.1557/mrc.2018.16.

[72] H. Magaña, C.D. Becerra, A. Serrano-Medina, K. Palomino, G. Palomino-Vizcaíno, A. Olivas-Sarabia, E. Bucio, J.M. Cornejo-Bravo, Radiation Grafting of a Polymeric Prodrug onto Silicone Rubber for Potential Medical/Surgical Procedures, Polymers (Basel). 12 (2020) 1297. https://doi.org/10.3390/polym12061297.

[73] S.Q. Wei, Y.P. Bai, L. Shao, A novel approach to graft acrylates onto commercial silicones for release film fabrications by two-step emulsion synthesis, Eur. Polym. J. 44 (2008) 2728–2736. https://doi.org/10.1016/j.eurpolymj.2008.04.025.

[74] J. Zhou, D.A. Khodakov, A. V. Ellis, N.H. Voelcker, Surface modification for PDMS-based microfluidic devices, Electrophoresis. 33 (2012) 89–104. https://doi.org/10.1002/elps.201100482.

[75] I. Wong, C.M. Ho, Surface molecular property modifications for poly(dimethylsiloxane) (PDMS) based microfluidic devices, Microfluid. Nanofluidics. 7 (2009) 291–306. https://doi.org/10.1007/s10404-009-0443-4.

[76] K.T. Lim, S.E. Webber, K.P. Johnston, Synthesis and characterization of poly(dimethyl siloxane)-poly[alkyl (meth)acrylic acid] block copolymers, Macromolecules. 32 (1999) 2811–2815. https://doi.org/10.1021/ma981658o.

[77] H. Yang, Z. Hou, Homogenous Grafted Poly(acrylic acid) Brushes on ultra-flat Polydimethlysiloxane (PDMS) Films by UV Irradiation, Nano Biomed. Eng. 3 (2011) 42–46. https://doi.org/10.5101/nbe.v3i1.p42-46.

[78] C.C. Ferraz, G.H.C. Varca, J.C. Ruiz, P.S. Lopes, M.B. Mathor, A.B. Lugão, E. Bucio, Radiation-grafting of thermo- and pH-responsive poly(N-vinylcaprolactam-co-acrylic acid) onto silicone rubber and polypropylene films for biomedical purposes, Radiat. Phys. Chem. 97 (2014) 298–303. https://doi.org/10.1016/j.radphyschem.2013.12.027.

[79] S.E. Park, Y.C. Nho, H. Il Kim, Preparation of poly(polyethylene glycol methacrylate-co-acrylic acid) hydrogels by radiation and their physical properties, Radiat. Phys. Chem. 69 (2004) 221–227. https://doi.org/10.1016/S0969-806X(03)00473-0.

[80] S. Cabana, C.S. Lecona-Vargas, H.I. Meléndez-Ortiz, A. Contreras-García, S. Barbosa, P. Taboada, B. Magariños, E. Bucio, A. Concheiro, C. Alvarez-Lorenzo, Silicone rubber films functionalized with poly(acrylic acid) nanobrushes for immobilization of gold nanoparticles and photothermal therapy, J. Drug Deliv. Sci. Technol. 42 (2017) 245–254. https://doi.org/10.1016/j.jddst.2017.04.006.

[81] Y.M. Mohan, T. Premkumar, K. Lee, K.E. Geckeler, Fabrication of silver nanoparticles in hydrogel networks, Macromol. Rapid Commun. 27 (2006) 1346–1354. https://doi.org/10.1002/marc.200600297.

[82] X. Ping, M. Wang, G. Xuewu, Surface modification of poly(ethylene terephthalate) (PET) film by gamma-ray induced grafting of poly(acrylic acid) and its application in

antibacterial hybrid film, Radiat. Phys. Chem. (2011). https://doi.org/10.1016/j.radphyschem.2010.12.011.

[83] K.K. Patel, M. Tripathi, N. Pandey, A.K. Agrawal, S. Gade, M.M. Anjum, R. Tilak, S. Singh, Alginate lyase immobilized chitosan nanoparticles of ciprofloxacin for the improved antimicrobial activity against the biofilm associated mucoid P. aeruginosa infection in cystic fibrosis, Int. J. Pharm. 563 (2019) 30–42. https://doi.org/10.1016/j.ijpharm.2019.03.051.

[84] M. He, Y. Zhou, S. Nie, P. Lu, H. Xiao, Y. Tong, Q. Liao, R. Wang, Synthesis of Amphiphilic Copolymers Containing Ciprofloxacin and Amine Groups and Their Antimicrobial Performances As Revealed by Confocal Laser-Scanning Microscopy and Atomic-Force Microscopy, J. Agric. Food Chem. 66 (2018) 8406–8414. https://doi.org/10.1021/acs.jafc.8b01759.

[85] X. Liu, L.H. Nielsen, S.N. Kłodzińska, H.M. Nielsen, H. Qu, L.P. Christensen, J. Rantanen, M. Yang, Ciprofloxacin-loaded sodium alginate/poly (lactic-co-glycolic acid) electrospun fibrous mats for wound healing, Eur. J. Pharm. Biopharm. 123 (2018) 42–49. https://doi.org/10.1016/j.ejpb.2017.11.004.

[86] B. Blanco-Fernandez, M. Lopez-Viota, A. Concheiro, C. Alvarez-Lorenzo, Synergistic performance of cyclodextrin–agar hydrogels for ciprofloxacin delivery and antimicrobial effect, Carbohydr. Polym. 85 (2011) 765–774. https://doi.org/10.1016/j.carbpol.2011.03.042.

[87] D.M. Campoli-Richards, J.P. Monk, A. Price, P. Benfield, P.A. Todd, A. Ward, Ciprofloxacin, Drugs. 35 (1988) 373–447. https://doi.org/10.2165/00003495-198835040-00003.

[88] J.N. Lee, C. Park, G.M. Whitesides, Solvent Compatibility of Poly(dimethylsiloxane)-Based Microfluidic Devices, Anal. Chem. 75 (2003) 6544–6554. https://doi.org/10.1021/ac0346712.

[89] G.G. Flores-Rojas, E. Bucio, Radiation-grafting of ethylene glycol dimethacrylate (EGDMA) and glycidyl methacrylate (GMA) onto silicone rubber, Radiat. Phys. Chem. 127 (2016) 21–26. https://doi.org/10.1016/j.radphyschem.2016.05.015.

[90] T. Miyoshi, K. Takegoshi, K. Hikichi, High-resolution solid state 13C n.m.r. study of the interpolymer interaction, morphology and chain dynamics of the poly(acrylic acid)/poly(ethylene oxide) complex, Polymer (Guildf). 38 (1997) 2315–2320. https://doi.org/10.1016/S0032-3861(96)00799-9.

[91] Ü. Akbey, R. Graf, Y.G. Peng, P.P. Chu, H.W. Spiess, Solid-State NMR investigations of anhydrous proton-conducting acid-base poly(acrylic acid)- poly(4-vinyl pyridine) polymer blend system: A study of hydrogen bonding and proton conduction, J. Polym. Sci. Part B Polym. Phys. 47 (2009) 138–155. https://doi.org/10.1002/polb.21623.

[92] D. Fallahi, H. Mirzadeh, M.T. Khorasani, Physical, mechanical, and biocompatibility evaluation of three different types of silicone rubber, J. Appl. Polym. Sci. 88 (2003) 2522–2529. https://doi.org/10.1002/app.11952.

[93] T. Kaneko, S. Ito, T. Minakawa, N. Hirai, Y. Ohki, Degradation mechanisms of silicone rubber under different aging conditions, Polym. Degrad. Stab. 168 (2019) 108936. https://doi.org/10.1016/j.polymdegradstab.2019.108936.

[94] M.S. Bodnarchuk, K.E.B. Doncom, D.B. Wright, D.M. Heyes, D. Dini, R.K. O'Reilly, Polyelectrolyte pKa from experiment and molecular dynamics simulation, RSC Adv. 7 (2017) 20007–20014. https://doi.org/10.1039/c6ra27785c.

[95] I. Borukhov, D. Andelman, R. Borrega, M. Cloitre, L. Leibler, H. Orland, Polyelectrolyte Titration: Theory and Experiment, (2000) 1–13. http://arxiv.org/abs/cond-mat/0005306.

[96] A.K. Narayanan Nair, A. Martinez Jimenez, S. Sun, Complexation Behavior of Polyelectrolytes and Polyampholytes, J. Phys. Chem. B. 121 (2017) 7987–7998. https://doi.org/10.1021/acs.jpcb.7b04582.

[97] C. Zhao, S. Nie, M. Tang, S. Sun, Polymeric pH-sensitive membranes - A review, Prog. Polym. Sci. 36 (2011) 1499–1520. https://doi.org/10.1016/j.progpolymsci.2011.05.004.

[98] A. Rojas-Hernández, N. Rodríguez-Laguna, E.L. Ibarra-Montaño, A. Aníbal Sánchez-Hernández, Determination of pKa Values for Acrylic, Methacrylic and Itaconic Acids by 1H and 13C NMR in Deuterated Water, J. Appl. Solut. Chem. Model. 4 (2015) 7–18. https://doi.org/10.6000/1929-5030.2015.04.01.2.

[99] S. Mafé, V. García-Morales, P. Ramírez, Estimation of pKa shifts in weak polyacids using a simple molecular model: Effects of strong polybases, hydrogen bonding and divalent counterion binding, Chem. Phys. 296 (2004) 29–35. https://doi.org/10.1016/j.chemphys.2003.09.033.

[100] R. He, X. Qian, J. Yin, Z. Zhu, Preparation of polychrome silver nanoparticles in different solvents, J. Mater. Chem. 12 (2002) 3783–3786. https://doi.org/10.1039/b205214h.

[101] R. Desai, V. Mankad, S.K. Gupta, P.K. Jha, Size distribution of silver nanoparticles: UV-visible spectroscopic assessment, Nanosci. Nanotechnol. Lett. 4 (2012) 30–34. https://doi.org/10.1166/nnl.2012.1278.

[102] W.H. Eisa, Y.K. Abdel-Moneam, Y. Shaaban, A.A. Abdel-Fattah, A.M. Abou Zeid, Gamma-irradiation assisted seeded growth of Ag nanoparticles within PVA matrix, Mater. Chem. Phys. 128 (2011) 109–113. https://doi.org/10.1016/j.matchemphys.2011.02.076.

[103] A. Abedini, M. P. Susthitha, R.D. Abdul, H.A. Muhammad Azmi, S. Shaari, Radiolytic formation of highly luminescent triangular Ag nanocolloids, J. Radioanal. Nucl. Chem. 307 (2016) 985–991. https://doi.org/10.1007/s10967-015-4223-1.

[104] S.S. Mansouri, S. Ghader, Experimental study on effect of different parameters on size and shape of triangular silver nanoparticles prepared by a simple and rapid method in aqueous solution, Arab. J. Chem. 2 (2009) 47–53. https://doi.org/10.1016/j.arabjc.2009.07.004.

[105] S. Pal, Y.K. Tak, J.M. Song, Does the antibacterial activity of silver nanoparticles depend on the shape of the nanoparticle? A study of the gram-negative bacterium Escherichia coli, Appl. Environ. Microbiol. 73 (2007) 1712–1720. https://doi.org/10.1128/AEM.02218-06.

[106] I. Sondi, B. Salopek-Sondi, Silver nanoparticles as antimicrobial agent: A case study on E. coli as a model for Gram-negative bacteria, J. Colloid Interface Sci. 275 (2004) 177–182. https://doi.org/10.1016/j.jcis.2004.02.012.

[107] R. Salomoni, P. Léo, A.F. Montemor, B.G. Rinaldi, M.F.A. Rodrigues, Antibacterial effect of silver nanoparticles in Pseudomonas aeruginosa, Nanotechnol. Sci. Appl. 10 (2017) 115–121. https://doi.org/10.2147/NSA.S133415.

[108] Y. Qing, L. Cheng, R. Li, G. Liu, Y. Zhang, X. Tang, J. Wang, H. Liu, Y. Qin, Potential antibacterial mechanism of silver nanoparticles and the optimization of orthopedic implants by advanced modification technologies, Int. J. Nanomedicine. 13 (2018) 3311–3327. https://doi.org/10.2147/IJN.S165125.

[109] N. Durán, M. Durán, M.B. de Jesus, A.B. Seabra, W.J. Fávaro, G. Nakazato, Silver nanoparticles: A new view on mechanistic aspects on antimicrobial activity, Nanomedicine Nanotechnology, Biol. Med. 12 (2016) 789–799. https://doi.org/10.1016/j.nano.2015.11.016.

[110] M. Rai, A. Yadav, A. Gade, Silver nanoparticles as a new generation of antimicrobials, Biotechnol. Adv. 27 (2009) 76–83. https://doi.org/10.1016/j.biotechadv.2008.09.002.

9. ANEXOS

9.1. Grado de injerto variando la dosis para la reacción con distintas condiciones

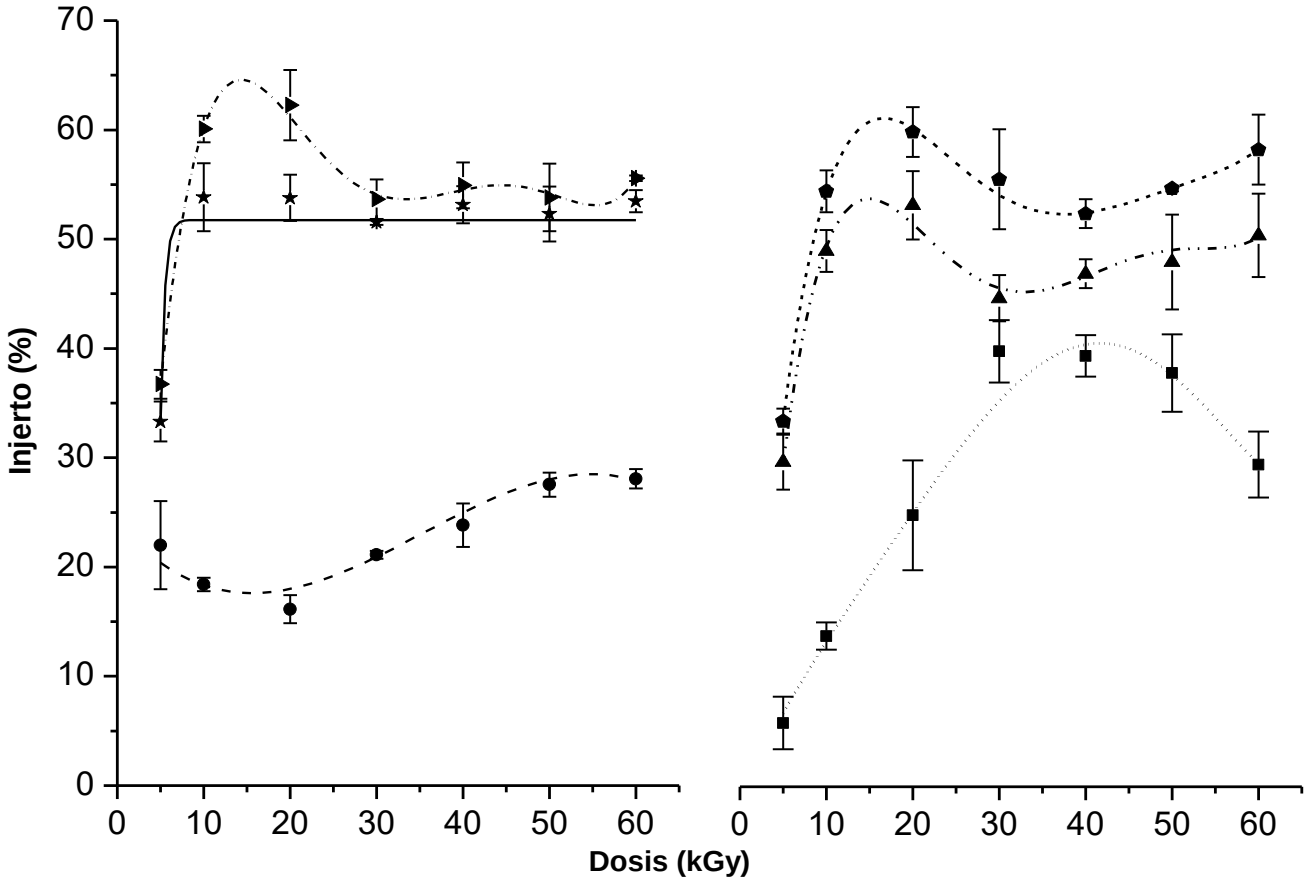

9.2. Espectro SS ^{13}C NMR PDMS

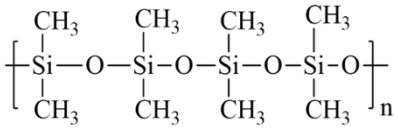

Polidimetilsiloxano

9.3. Termogramas de las películas

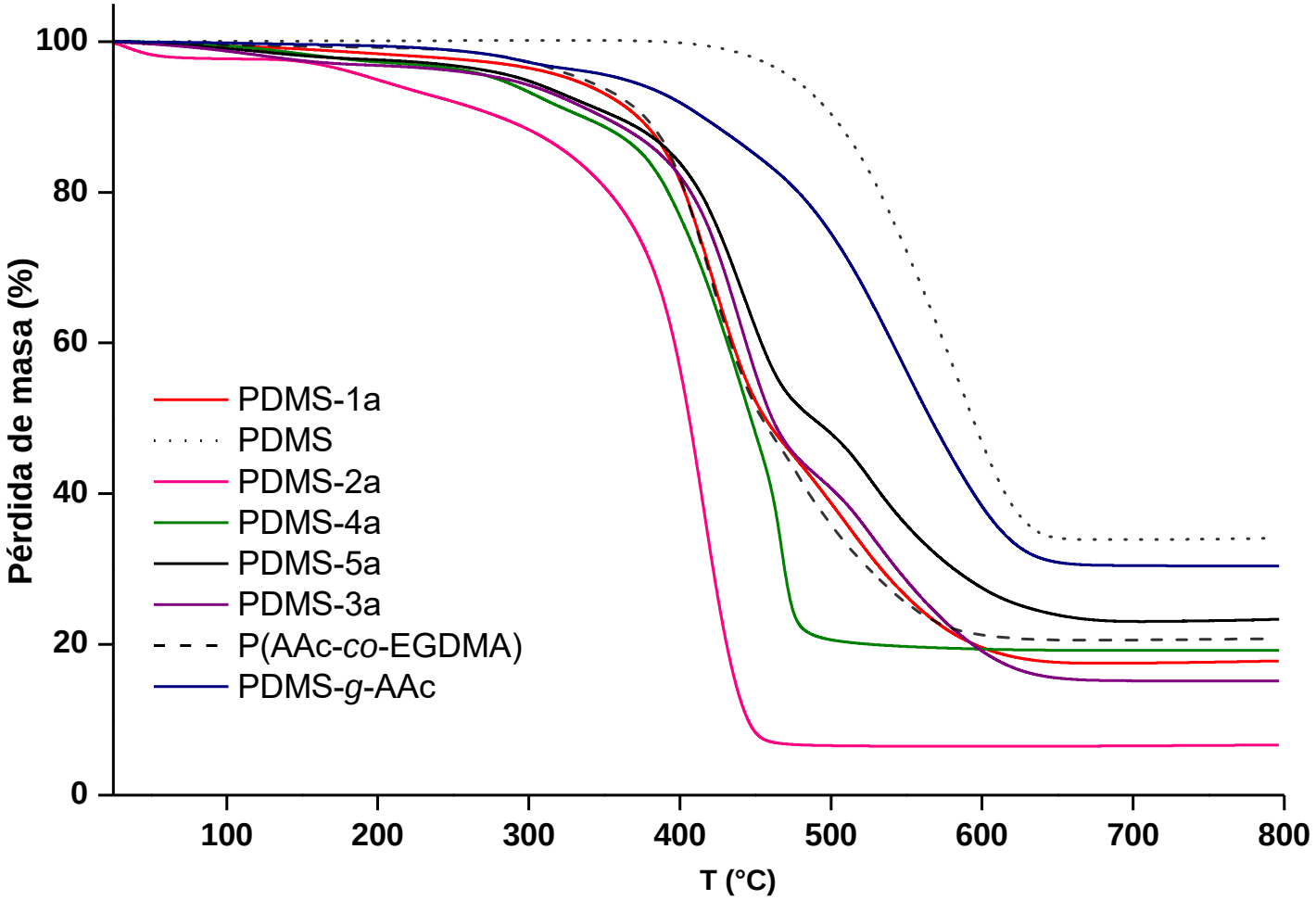

9.4. Tabla de temperaturas de degradación de las películas, obtenido mediante TGA.

Tabla 5. Temperaturas de descomposición de las películas obtenido mediante TGA.

Muestra	10% pérdida de masa (°C)	Temperatura de descomp. (°C)	Residuo a 800°C (% masa)
PDMS	501	588	34
PDMS-1a 10%	426	295, 555, 619	32
PDMS-1a 50%	372	421, 512	17
AAc/EGDMA (1:1)	271	413	1.2

9.5. Termograma DSC

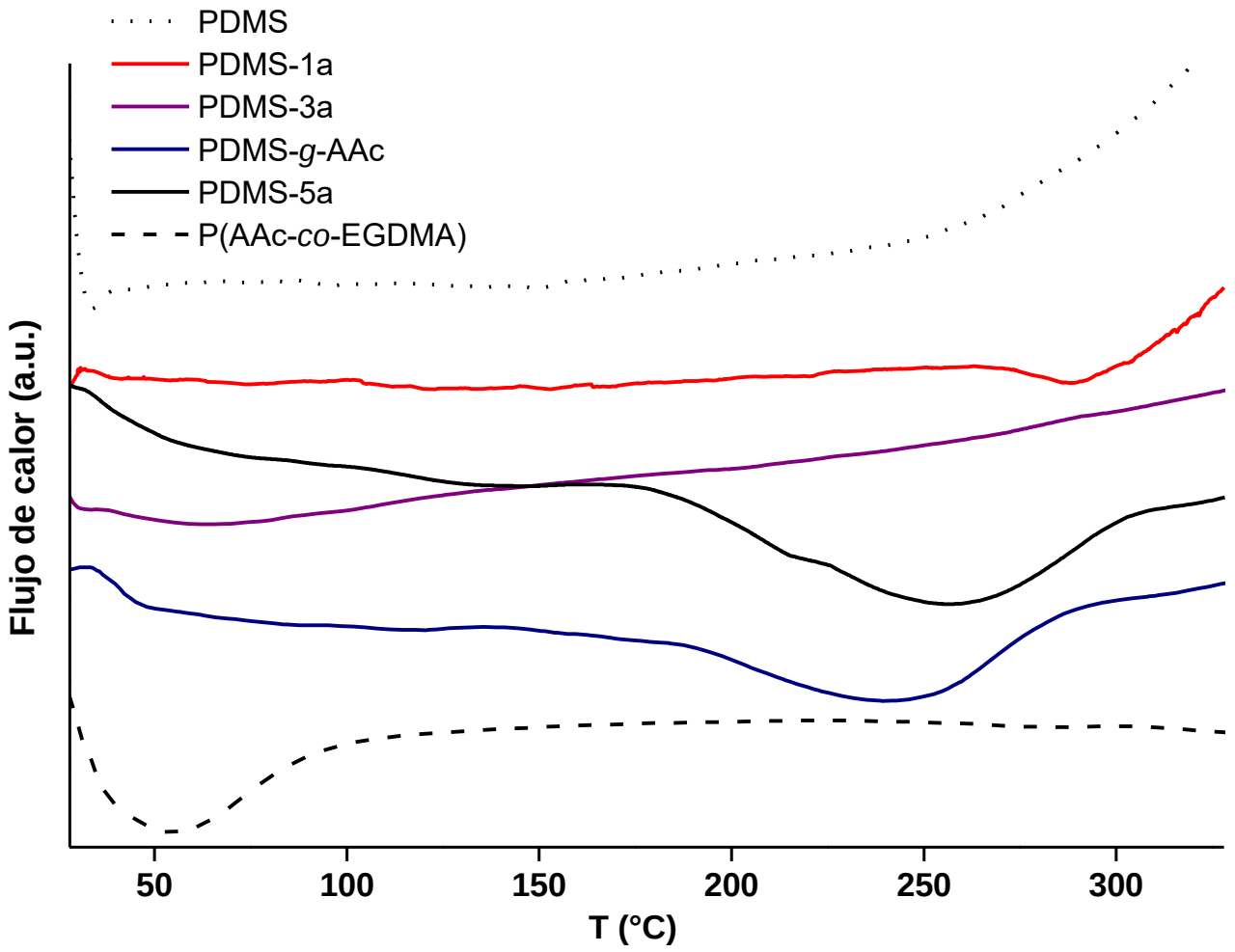

9.6. Curva de calibración de ciprofloxacino

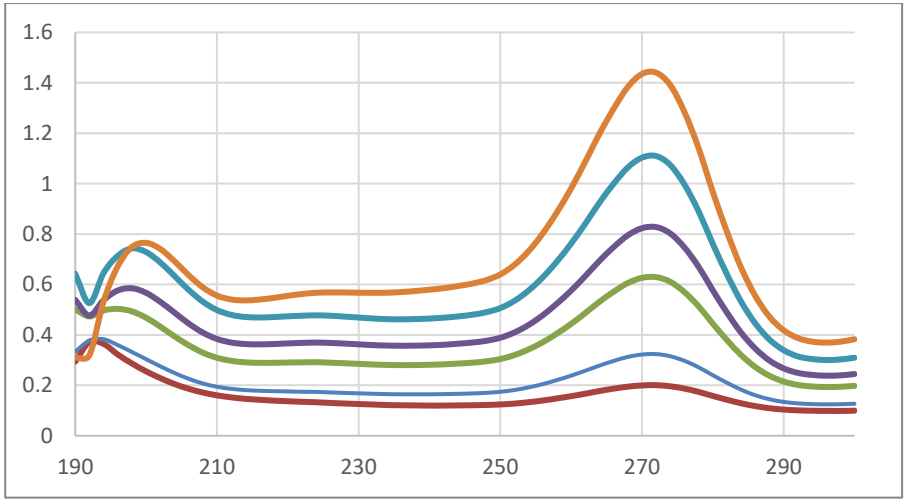

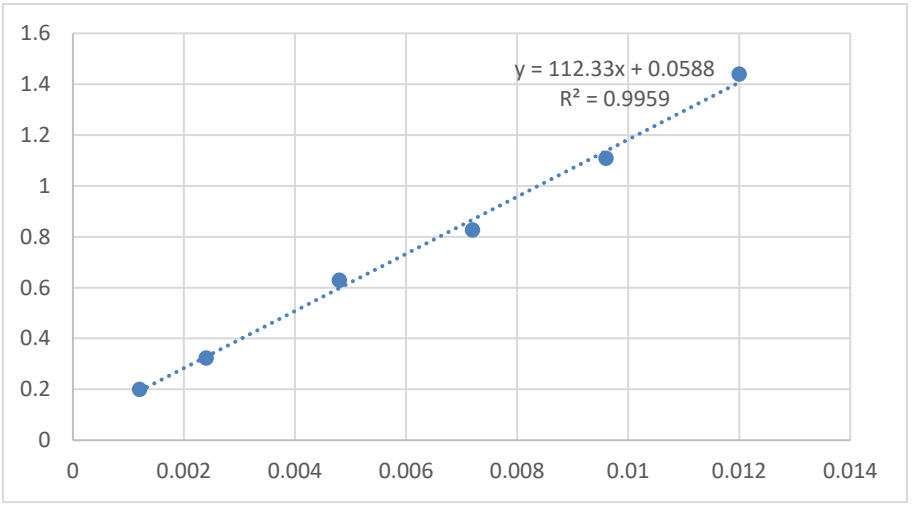

Conc (mg/mL)	A
0.0012	0.200591
0.0024	0.323819
0.0048	0.629451
0.0072	0.827766
0.0096	1.109522
0.012	1.440389

Radiation Physics and Chemistry 171 (2020) 108754

Contents lists available at ScienceDirect

Radiation Physics and Chemistry

journal homepage: www.elsevier.com/locate/radphyschem

Modification of PDMS with acrylic acid and acrylic acid/ethylene glycol dimethacrylate by simultaneous polymerization assisted by gamma radiation

M.A. Velazco-Medel**, L.A. Camacho-Cruz, E. Bucio*

Departamento de Química de Radiaciones y Radioquímica, Instituto de Ciencias Nucleares, Universidad Nacional Autónoma de México, Circuito Exterior, Ciudad Universitaria, CDMX, 04510, Mexico

ARTICLE INFO

Keywords:
Polydimethylsiloxane
Grafting
pH responsiveness
Crosslinking
Swelling
Hydrophilicity

ABSTRACT

The addition of hydrophilic functional groups to hydrophobic polymers has been extensively used for the development of new medical devices with potential applications both for antibacterial substrates and for biocompatible materials. Having this into account, this work sought to modify PDMS films by grafting a copolymer of acrylic acid and ethylene glycol dimethacrylate (AAc/EGDMA) to increase the hydrophilicity of the films, and thus modifying the swelling properties of PDMS in water. The effect of the molar ratio between AAc/EGDMA and the crosslinking of these grafted groups on the properties of these materials was evaluated by performing swelling studies both in water and pH buffer solutions and contact angle measurements. Potentiometric titrations were employed to estimate acid group availability on the PDMS-*g*-(AAc-*co*-EGDMA) films with different grafting yields.

1. Introduction

Polydimethylsiloxane (PDMS) is an organosilicon polymer which is also commonly known as silicone rubber. Materials based on PDMS are critical in the development of biomedical devices due to their high biocompatibility, poor hydrophilicity, and useful mechanical properties such as its glass transition temperature (T_g) and high moduli (Abbasi et al., 2002). Even when the properties of PDMS are very convenient, the modification of this material to improve its characteristics and to add uses to PDMS substrates has been vastly explored (Pinto et al., 2010; Li et al., 2012). One of the most useful approaches for modifying polymer matrixes is the grafting of additional molecules which may contain functional groups that enhance the properties of the original matrix. The grafted groups may be either small molecules or macromolecules with different functionalities and microstructures (Flores-Rojas et al., 2017; Lee and Vörös, 2005).

PDMS has been previously modified by grafting macromolecules that may swell upon changes on the chemical environment (pH, temperature, etc.). These functional macromolecules include mixed-responsive polymers which add multiple characteristics to the modified matrix. Block-copolymers and terpolymers have also been grafted onto PDMS, in these examples each section of the copolymer responds to specific stimuli, conferring further applications to these polymeric materials (Flores-Rojas et al., 2018).

One important strategy for the modification of polymeric matrices has been the use of ionizing radiation (Jaganathan et al., 2015; Cao et al., 2017; Pino-Ramos et al., 2018) because this procedure involves the use of mild reaction conditions and it avoids the use of chemical initiators which often contaminate the final product. Through this method, when a material interacts with ionizing radiation, unstable radical groups are formed within the material which then may lead to conventional free-radical polymerizations. Through this method good results have been obtained for polymer grafting in many matrices, including PDMS (Keshvari et al., 2008; Valencia-Mora et al., 2016; Melendez-Ortiz et al., 2015). There exist two main methods to modify a polymeric substrate using ionizing radiation: Simultaneous/direct method and oxidative pre-irradiation. The first method involves the interaction of the whole reaction system (polymer matrix + monomers + solvent) with ionizing radiation to produce reactive sites within the polymer matrix which then allow for the graft polymerization to take place. Oxidative pre-irradiation, on the other hand, involves the interaction of just the polymer matrix with the radiation in presence of oxygen to form unstable organic peroxides and hydroperoxides that may be later cleaved in the presence of a monomer to initiate a

* Corresponding author.
** Corresponding author.
E-mail addresses: marlene.velazco@correo.nucleares.unam.mx (M.A. Velazco-Medel), ebucio@nucleares.unam.mx (E. Bucio).

https://doi.org/10.1016/j.radphyschem.2020.108754
Received 7 November 2019; Received in revised form 4 December 2019; Accepted 2 February 2020
Available online 05 February 2020
0969-806X/

polymerization reaction. In both methods, the presence of reactive radical groups in solution may form both grafted polymer chains and homopolymer chains.

Poly(acrylic acid) (PAAc) is extensively used due to its impressive absorbent properties and its acid-base behavior. Both the monomer and its corresponding polymer have carboxylic acid groups that allow the formation of hydrogen bonds between polymer chains (when the pH is below its p*K*a value of ~4.5); nevertheless, when the pH is above the p*K*a value for the acid groups, the polymer structure is now composed of carboxylate groups which promote chain-chain repulsion which allows for the absorption of water and greater swelling properties. Acrylic acid (AAc) has been grafted onto PDMS by different initiation methods (Keshvari et al., 2008; Wei et al., 2008; Lee et al., 1996; Shahsavan et al., 2015; Salati et al., 2011); however, when using ionizing radiation, the grafting of this monomer has only been studied by using the oxidative pre-irradiation pathway (Yang and Hsiue, 1996; Yang and Hou, 2011; García-Vargas et al., 2014; Cabana et al., 2017). This is due to the high reactivity of AAc, that causes the formation of high amounts of PAAc homopolymer and low amounts of grafted macromolecules.

Ethylene glycol dimethacrylate (EGDMA) has been used as crosslinking agent to create controlled-shape polymers with 3D-structures. This monomer has been previously combined with AAc to form crosslinked copolymers with high swelling that confers them the property of retaining small molecules or even larger macromolecules like proteins. (Akhtar et al., 2015; Shafiei et al., 2017). Although EGDMA is extremely stable in neutral media, at basic pH, ester hydrolysis occurs slowly. The hydrolysis of different acrylic and methacrylic esters has been reported (Orekhov et al., 2018; Fujisawa and Kadoma, 2012) and this characteristic may be used for drug delivery systems. Previously, a binary poly(ethylene glycol dimethacrylate-*co*-glycidyl methacrylate) copolymer was grafted using gamma radiation into PDMS (PDMS-*g*-(EGDMA-*co*-GMA)) by Flores-Rojas and Bucio, 2016. In this work they showed that by decreasing the ratio of EGDMA/GMA, the grafting yield increases considerably due to the high reactivity of glycidyl methacrylate that promotes homopolymer formation rather than grafting reaction. This last fact may be a potential solution for the poor grafts of AAc that have been observed onto PDMS.

Considering the potential reactivity improvements and the applications of this crosslinking agent, we were interested in the use this biester to obtain PDMS modified with EGDMA and AAc thorugh direct irradiation. Variable reactions (see Table 1) conditions were used to evaluate the effect of varying the ratio AAc/EGDMA in the grafting yields, and how this affected the acid-base properties of the materials. To fulfill these objectives, swelling behavior, potentiometric titrations, and wettability tests were performed to the materials.

2. Experimental section

2.1. Materials

PDMS films (1 × 4 cm) with a density ranging from 1.1 to 1.5 g cm^{-3} and a thickness of 1 mm were purchased from Good-fellow (Huntingdon, UK). Ethylene glycol dimethacrylate and acrylic acid were acquired from Sigma-Aldrich Co. (St Louis MO, USA). All the monomers were purified under vacuum distillation before used. Toluene (analytical grade) was obtained from Baker Mexico and was used without further purification. Buffer solutions were prepared using sodium phosphate, boric acid, sodium carbonate, and citric acid purchased from Sigma-Aldrich Co. (St Louis MO, USA).

Table 1
AAc/EGDMA ratio in the different modified PDMS films.

	ID	AAc/EGDMA ratio
PDMS-*g*-AAc	PDMS-*g*-AAc	1:0
PDMS-*g*-(AAc-*co*-EGDMA)	PDMS-1	1:1
	PDMS-2	2:1
	PDMS-3	3:1
	PDMS-4	4:1
	PDMS-5	5:1
P(AAc-*co*-EGDMA)	P(AAc-*co*-EGDMA)	1:1

2.2. Radiation polymerization

PDMS-films were introduced in an ampoule containing 10 mL of an AAc/EGDMA mixture varying between 5 to 50% (v/v) in toluene as a solvent, the monomer ratio (AAc/EGDMA) was modified also to check the concentration effect of EGDMA in the stability and pH-response of the grafted-films. Then, the ampoules were degassed by freeze-thaw cycles (4 times each 10 min), subsequently the ampoules were sealed and later exposed to variable doses of ^{60}Co γ-radiation using a Gammabeam 651PT available in the Institute of Nuclear Sciences (ICN) at the National Autonomous University of Mexico (UNAM) to initiate the polymerization reaction.

After exposing the films to radiation, the grafted PDMS films (PDMS-*g*-(AAc-*co*-EGDMA)) were washed in different solvents to remove occluded solvent, monomer and copolymer residues. To assure that no toluene or monomer residues remained in the grafted films, the films were washed up to 5 times with deionized water until no visible precipitated toluene was observed and the swelling of PDMS due to its interaction with toluene was negligible. Finally, the samples were dried under vacuum (-80 kPa) at 50 °C and weighed.

The grafting yield (GY) was calculated from weight difference between pristine PDMS (W_0) and grafted-PDMS (W_g), the general formula is shown in Eq. (1):

$$GY\ (\%) = [(W_g - W_0)/W_0\ ]100 \quad \text{(Eq. 1)}$$

The same procedure was employed to prepare PDMS-*g*-AAc films. The monomer concentrations and absorbed doses were varied to compare grafting yields under a varying set of conditions. All the experiments were repeated thrice and the standard error of the mean (SEM) was calculated for all measurements.

2.3. Fourier transform infrared spectroscopy-attenuated total reflectance spectroscopy (FTIR-ATR)

FTIR-ATR spectra of materials were obtained using a PerkinElmer Spectrum 100 spectrometer (Perkin Elmer Cetus Instruments, Norwalk, CT) with 16 scans. All the materials were dried under vacuum prior to the measurements.

2.4. Thermal analysis

For further characterization, thermogravimetric analysis (TGA) and differential scanning calorimetry (DSC) studies were performed to the samples. TGA measurements were carried out on a TAinstruments TGA Q50 ramping from 25 to 800 °C at a heating rate 10 °C/min under a nitrogen atmosphere. DSC analysis was performed in a TAinstruments 2010 DSC calorimeter, the thermal history and the occluded solvent of the samples were removed with a pre-heating cycle ramping up from 25 to 100 °C at 10 °C/min under a nitrogen atmosphere with a second heating ramp from 25 to 350 °C at 10 °C/min. All the materials were dried under vacuum prior to the measurements.

2.5. Contact angle

A Kruss DSA 100 drop shape analyzer (Matthews NC, USA) was used to measure the contact angle of the films with water. The contact angle was recorded at 5 and 10 min after a bi-distilled water droplet had been deposited onto the dry samples. All the experiments were repeated thrice and the standard error of the mean (SEM) was calculated for all

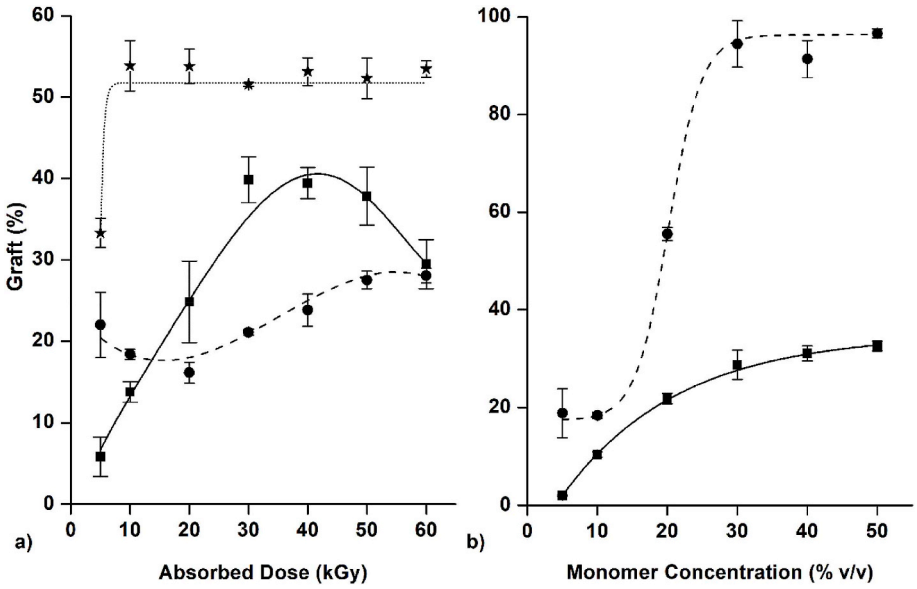

Fig. 1. Grafting yields of (– –) PDMS-*g*-AAc; (———) PDMS-1 and (.....) PDMS-5. a) Fixed monomer concentration: 10% v/v and 1:1 AAc/EGDMA. b) Fixed dose: 10 kGy.

measurements.

2.6. Equilibrium water content and swelling behavior

Ionic solutions with varying ionic strengths were tested to evaluate the swelling behavior of the PDMS-films. The equilibrium water content (EWC%) was measured in three different environments: deionized water, in a 0.13 M NaCl solution, and in a phosphate buffer solution at pH = 7.4 (simulating blood environment). pH-responsiveness of the PDMS-films was evaluated by measuring the swelling degree in buffer solutions with pH values ranging from 2 to 10 (2-3: H_3PO_4/NaH_2PO_4, 4-5: $H_2CO_3/NaHCO_3$, 6-7: NaH_2PO_4/Na_2HPO_4 and 8-10: $B(OH)_3/Na_2B_4O_7$) during 48 h each, the excess of water was removed using filter paper and then the films were weighted. The swelling degree (SD) was calculated using the Equation (2):

$$SD\ (\%) = [(W_S - W_g)/W_g\ ]100 \qquad \text{(Eq. 2)}$$

W_g and W_s represent the mass of the grafted and the swollen film respectively. All the experiments were repeated thrice and the standard error of the mean (SEM) was calculated for all measurements.

2.7. Potentiometric titrations

Potentiometric pH titrations were performed using a HANNA HI4212 potentiometer with a combined glass pH electrode (HANNA HI 1331B) that was calibrated through a standard three-point calibration using Fisher Scientific reference pH buffers (pH = 4.0, 7.0, 10.0). A constant mass of functionalized PDMS was weighed (~0.2 g) and placed in DI water in constant stirring. KOH 0.01 mol/L was slowly added until reaching an added base volume of twice the volume needed to reach the equivalence point while monitoring the pH with the potentiometer. The initial pH of the titration was manually set to a value of two for all samples.

3. Results and discussion

3.1. Preparation of PDMS-g-AAc and PDMS-g-(AAc-co-EGDMA)

All PDMS-*g*-(AAc-*co*-EGDMA) films were prepared by the simultaneous irradiation method by varying the monomer ratio, the concentration of the monomers, the solvent, and the absorbed dose, aiming to analyze the effect of the EGDMA concentration in the hydrophilic properties of modified PDMS. PDMS-*g*-AAc films were prepared by the simultaneous method as control samples to compare their response with the binary films and to set a precedent for the preparation of these materials by the direct irradiation method. Additionally, residual copolymer: P(AAc-*co*-EGDMA) was isolated from PDMS-1 both at 10 and 50 kGy and 10% v/v reaction conditions for further comparisons.

For the grafting process, the grafting yield depends directly of the absorbed dose and on the monomer concentration as it was expected (Flores-Rojas and Bucio, 2016). The first results show that by using simultaneous polymerization at 10% v/v of concentration in toluene, lower GYs are produced (Fig. 1) than the ones obtained by previously reported pre-irradiation methods (Cabana et al., 2017). This is due to the high reactivity of AAc which favors the formation of the homopolymer. However, this behavior changes at higher concentrations at a fixed dose of 10 kGy where the GYs reach about 100%. This is due to the easy contact between a greater number of radicals formed in the polymer matrix and the monomer. At this point, the modified films present breakability and poor swelling properties which limits their applicability; therefore, lower grafting yields are desirable. The samples prepared with doses above 10 kGy presented the poor mechanical properties because of excessive grafting yields; therefore, the concentration was varied at a dose of 10 kGy. This effect also happened with concentrations above 10% v/v so the effect of the dose was

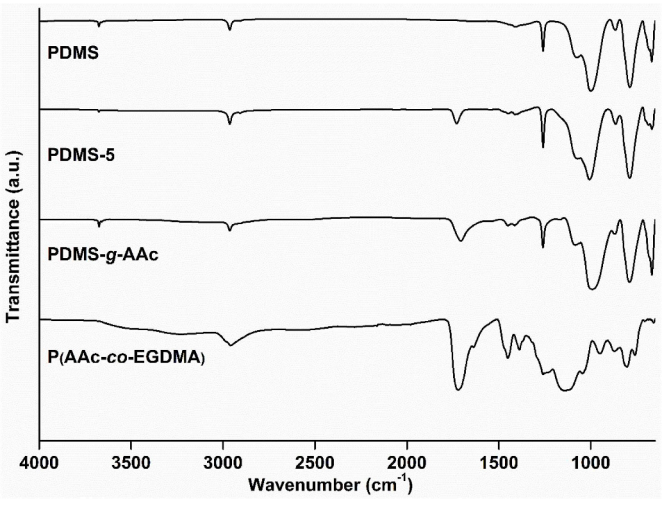

Fig. 2. FTIR-ATR spectra of the different modified PDMS films.

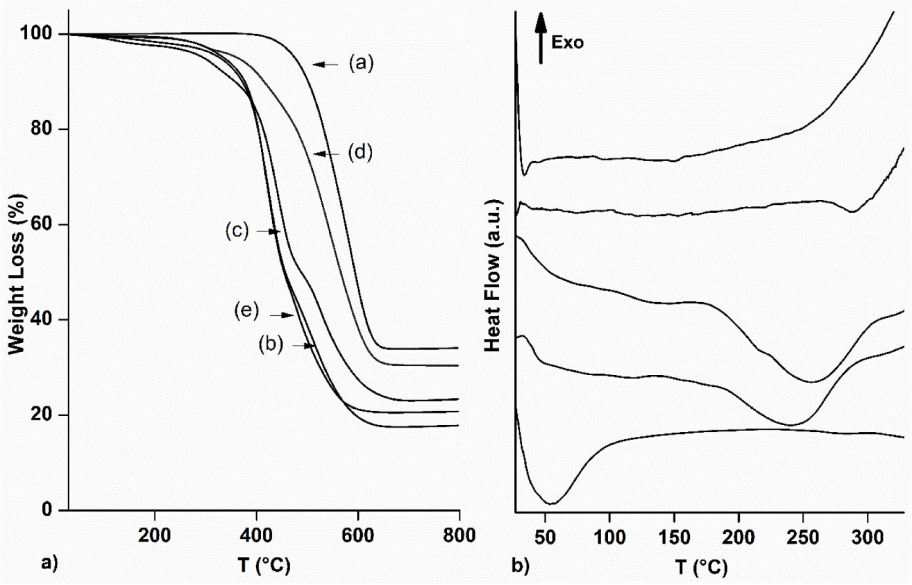

Fig. 3. Thermal behavior analysis by **a)** TGA and **b)** DSC of (a) PDMS; (b) PDMS-1; (c) PDMS-5; (d) PDMS-*g*-AAc and (e) P(AAc-*co*-EGDMA).

evaluated at this concentration.

Different grafting yields were obtained when EGDMA is added to the system. In Fig. 1a, the continuous line represents the behavior of the system as a function of the dose. As observed, when the monomers' molar ratio (AAc/EGDMA) is increased, the grafting yields are higher than the ones from the samples obtained using an equimolar ratio. This happened for all the ratios tested (PDMS-1 to PDMS-5).[1] When the amount of cross-linking agent is decreased, the GYs increased considerably. This could be explained by the fact that when more EGDMA is available in the matrix, the probability of formation of PAAc homopolymer is lower because there is less chance that two molecules of AAc react with each other within the solution. In all cases, the use of toluene as solvent allows for the diffusion of monomers into the bulk of PDMS matrix which increases the interactions between the PDMS matrix and the monomers, allowing for high GYs.

To observe the effect of the variation of the monomer concentration, films grafted at equimolar conditions (AAc/EGDMA, 1:1) and films with only AAc were tested. In Fig. 1b the GYs as a function of monomers' concentrations for PDMS-1 (continuous line) and PDMS-*g*-AAc (dashed line) are shown, as it is observed, GYs increase considerably above a concentration of 10% v/v for films grafted with only AAc; however, for equimolar AAc/EGDMA GYs did not exceed ~40%. This could be explained by the fact that more monomers interact with the bulk of PDMS by diffusion if the concentration of the monomers is increased. In this case, AAc reacts readily with PDMS radicals; however, when EGDMA is present, there is a greater probability of termination reactions which limit chain sizes and thus GYs.

3.2. Characterization of modified PDMS films

FTIR-ATR spectra (Fig. 2) confirmed that the grafting reaction was successful, since there exist clear differences between PDMS and PDMS-*g*-(AAc-*co*-EGDMA) films. The spectrum of pristine PDMS showed strong bands at ~1000 cm^{-1} and ~750 cm^{-1} corresponding to the Si–O–Si stretching and Si–CH_3 bending vibrations, respectively (Fig. 2, PDMS). The short band in ~2900 cm^{-1} is attributed to the typical band for C–H stretching and it is present in all the spectra. After radiation polymerization, practically all the modified PDMS films present roughly the same spectrum [Fig. 2, PDMS-*g*-(AAc-*co*-EGDMA)] because even though the GY changes, the concentration of the functional groups on the PDMS matrix is low, so small changes in concentration of the functional groups do not greatly affect the spectrum. The graph shows an absorption band at ~1720 cm^{-1} which represents the stretching of the carbonyl group, this signal is also present in the copolymer [Fig. 2, P(AAc-*co*-EGDMA], confirming the presence of this group on the functionalized PDMS matrix.

Thermal behavior was different for all the samples; however, all the materials had good thermal stability. This makes sense since PDMS possesses intrinsic thermal stability (Fallahi et al., 2003; Kaneko et al., 2019). For instance, the temperature at which pure PDMS loses 10% weight is 501 °C, while its decomposition temperature is 588 °C. In addition, the degradation temperature of PAAc is reported to be above 150 °C with a decarboxylation occurring at 260–350 °C (Cabana et al., 2017). With this information, thermogravimetric analysis (TGA) was performed for the non-grafted copolymer formed in the PDMS-1 reaction media and to all the different modified PDMS films.

According to the results of TGA (Fig. 3a), all PDMS-*g*-(AAc-*co*-EGDMA) films with GY ~50% present better thermal stability than the copolymer but worse than pristine PDMS, the first weight lost is near 350 ± 10 °C and the total decomposition is at 420 ± 10 °C, only one loss of mass was observed. This indicates that the formation of a copolymer, suggesting that the grafting occurred not only on the surface of the material, but also on its bulk.[2]

DSC analysis (Fig. 3b) showed no additional results. Pristine PDMS did not show any thermal transitions; on the other hand, the modified PDMS presents the thermal transition corresponding to the decomposition temperature at 215 °C (PDMS-*g*-AAc), 255 °C (PDMS-2) and 266 °C (PDMS-1). The copolymer P(AAc-*co*-EGDMA) had a thermal transition at 50 °C attributed to the rearrangement of the polymer chains, this behavior does not appear in the modified PDMS.

3.3. Hydrophilicity studies: contact angle

Since the cross-linked hydrogels of PAAc have superabsorbent capacity, we evaluated the effect in the hydrophilicity of the modified surface. PDMS is extremely hydrophobic due to its dangling methyl groups which do not allow water into the matrix; nevertheless, when

[1] For additional information see supporting information Fig. S1.

[2] For additional TGA results for functionalized samples please see Supporting Information Fig. S2.

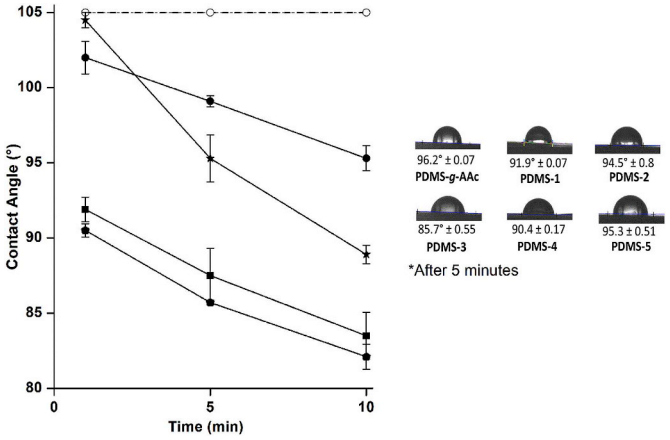

Fig. 4. Contact angle for (---○---) PDMS; (—●—) PDMS-*g*-AAc, (—■—) PDMS-1, (—⬟—) PDMS-3 and (—★—) PDMS-5.

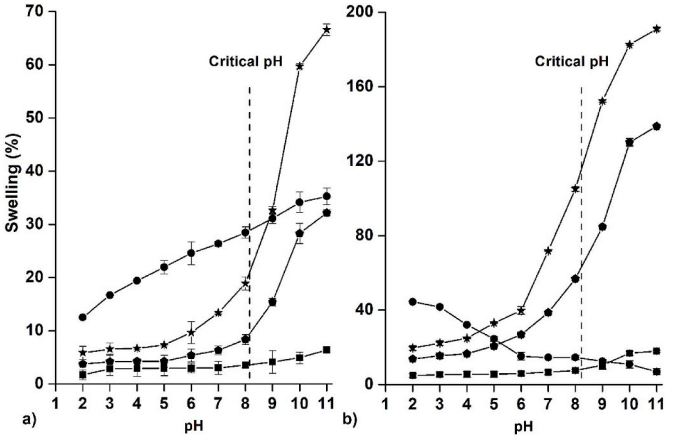

Fig. 6. Swelling behavior in buffer solution for (—●—) PDMS-*g*-AAc, (—■—) PDMS-1, (—⬟—) PDMS-3 and (—★—) PDMS-5 with a) GY ~50% and b) 30%.

this polymer matrix is modified with hydrophilic functional groups, the surface may become able retain water or other polar solvents.

Using contact angle measurements, the surface wettability of the different films was studied. The introduction of EGDMA to the systems produces an increase in the cross-linking degree. By using contact angle, the effect of this cross-linking in the wettability of the surface of the films may be analyzed.

Samples with GY of ~50% of all different monomer ratios were compared, the angle was measured at 5 and 10 min, Fig. 4 shows the contact angle as a function of time, and a representation of the experiment at 5 min. Initially, the difference between the films is not noticeable; however, after 5 and then 10 min, the contact angle decreased significantly. The results depend directly on the crosslinking degree. For instance, when the monomer ratio (AAc/EGDMA) is decreased, the contact angle decreases, due to the higher concentration of acrylic acid and the reduced expected crosslinking degree.

3.4. Hydrophilicity studies: equilibrium water content

To analyze the equilibrium water content (EWC%) of the modified PDMS films, swelling studies were performed in different aqueous solutions (with varying the ionic strengths). In these studies, films with low and high GYs were evaluated. The swelling behavior varies importantly when ions are present in the water and it depends directly on the GY of the films. The difference between the assays in DI water and in the buffer solution are due to the increase in repulsion interactions between charged groups of the modified PDMS and the ions in the media.

PDMS-*g*-AAc behaved differently than the films modified with AAc and EGDMA. As seen on Fig. 5, PDMS-*g*-AAC had the same swelling behavior in both DI water and in a buffer solution. This may indicate that the presence of EGDMA on films PDMS-1 through 5 increases repulsion interactions which promote higher EWC%.

As we can see in the Fig. 5, samples finished swelling sooner in DI water (24 h) than in the buffer solution (33 h). According to these results, the subsequent pH tests in buffer solutions were carried out taking 36 h as limit SD.

Confirming the results of thermal analysis and contact angle measurements, PDMS-5 swelled dramatically in comparison with the other films. Therefore, a considerable amount of AAc is present within PDMS matrix and not only at its surface.

3.5. pH sensitivity: swelling behavior

After verifying that the swelling behavior was different in buffer conditions than in DI water, swelling as a function of pH was evaluated.

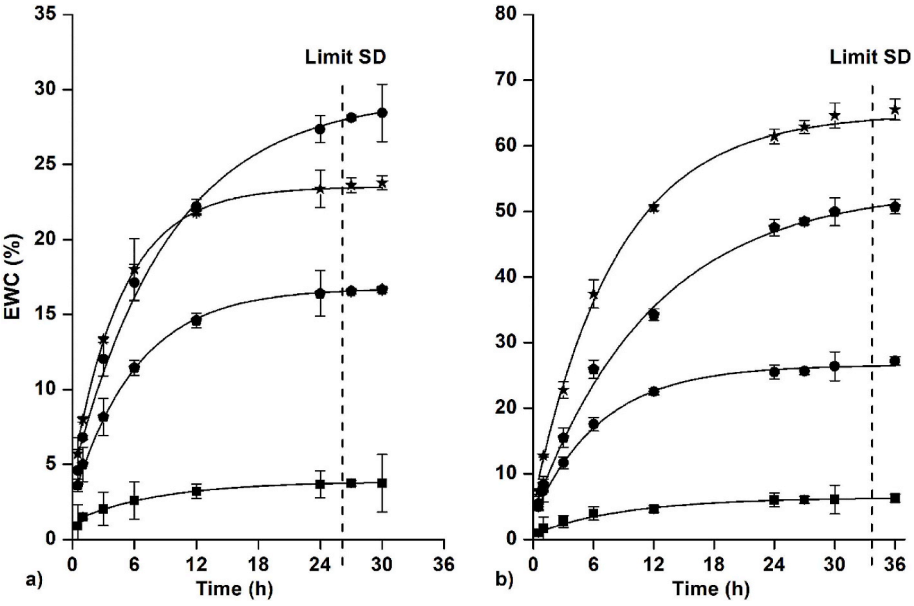

Fig. 5. Equilibrium water content for (—●—) PDMS-*g*-AAc, (—■—) PDMS-1, (—⬟—) PDMS-3 and (—★—) PDMS-5 in a) deionized water and b) phosphate buffer (ionic strength = 0.13 M).

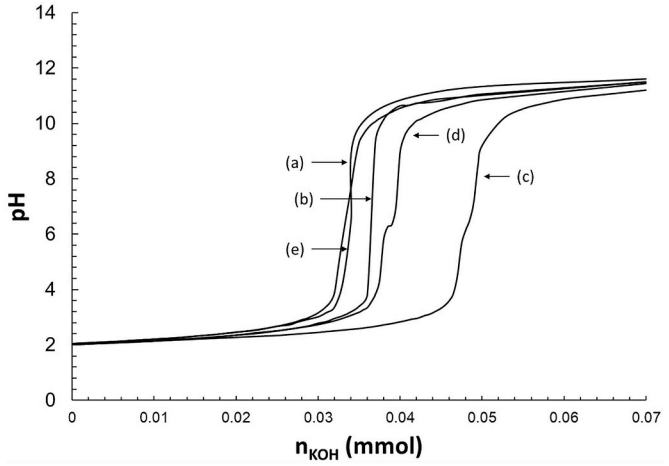

Fig. 7. Potentiometric titrations for of (a) PDMS-1; (b) PDMS-2; (c) PDMS-3; (d) PDMS-4 and (d) PDMS-5.

In the Fig. 6, it is shown that at pH = 8, the increase in SD directly correlated with the GY and the amount of the acrylic acid in the reaction media. PDMS-5 presented a greater water gain than the rest of films; nevertheless, the sizes of all the films increased considerably when GY was ~50%. Water absorption is significantly different for the samples with 30 and 50% of GY, PDMS-1 with lower GY shows a limit SD of 6% at pH =11 while the film with more graft had a SD of 18% due to absorbed water.

It is important to mention that the dramatic swelling of the films for grafts in the order of 50% are not useful for medical applications. Grafts above 30% show the same response at pH = 8 but they do not increase their size detrimentally.

PDMS-*g*-AAc showed low stability in water due to the solubility of PAAc in aqueous media, when pH increases, the films loses weight and become porous. This behavior is only present in the films with a GY above 50%. PDMS-*g*-AAc with lower GY presents the typical pH sensitivity for PAAc with a critical pH value of 8 in a similar fashion to PDMS modified with both AAc and EGDMA.

It is important to remark that the hydrolysis of acrylate esters occurs above pH 10. At this pH the films began to lose stability, since hydrolysis was promoted. The appearance of hydroxyl groups due to hydrolysis is identified using FTIR-ATR, see supporting information Fig. S3.

3.6. pH sensitivity: potentiometric titrations

Potentiometric titrations were performed to evaluate the behavior of the acid-base pair acrylic acid/potassium acrylate (HAAc/AAc^-) that is present in the grafted chains of the PAAc. For films with a GY ~50%, as seen in Fig. 7, for PDMS-1, PDMS-2, and PDMS-3 (AAc:EGDMA 1:1, 2:1, 3:1 respectively), the volume needed to reach the equivalent point increases with increasing amount of AAc in the original mixture, which indicates that there is a greater amount of acid groups on the modified material, this makes sense since GYs are higher when the amount of AAc increases with respect to EGDMA in the reaction conditions. In contrast, for PDMS-4 and PDMS-5, the amount of acid groups is apparently lower, and this is attributed to the fact that a greater amount of AAc in the media when the reaction was performed favors homopolymerization of itself to form PAAc, thus a greater amount of the grafted groups are composed of EGDMA which has no acid-base properties.

4. Conclusion

The functionalization of PDMS with the copolymer EGDMA and AAc using toluene as a solvent was successfully performed by using the simultaneous radiation method. The obtained materials showed varying characteristics depending on the molar ratio between AAc and the crosslinking agent EGDMA. It was found that the inclusion of EGDMA in the surface and bulk of the PDMS matrix provides stability to the system in aqueous conditions, while the interaction with the dissolved ions allowed for high water retentions reaching swelling ratios above 100%. In contrast, when the films were only grafted with AAc, water stability was compromised, this was verified by the weight loss suffered in aqueous conditions. Additionally, PDMS-*g*-AAc did not change its behavior when interacting with ions, suggesting that the EGDMA/AAc graft generates greater repulsion in the swollen polymer matrix than pure AAc.

Acid-base titrations and contact angle measurements confirmed that the diffusion of AAc into the polymers' matrix is favored by the solvent, and the grafts of acidic groups are mainly in the bulk of the PDMS rather than on the surface. Finally, it is important to remark that the materials retain the convenient thermal stability of pure PDMS.

CRediT authorship contribution statement

M.A. Velazco-Medel: Writing - original draft, Methodology, Formal analysis, Investigation, Visualization. **L.A. Camacho-Cruz:** Writing - review & editing, Visualization. **E. Bucio:** Conceptualization, Supervision, Investigation, Resources, Visualization.

Declaration of competing interest

The authors declare that they have no known competing financial interests or personal relationships that could have appeared to influence the work reported in this paper.

Acknowledgement

The authors thank to CONACYT-Mexico (CVU 696062) for supported M. A Velazco-Medel and Dirección General de Asuntos del Personal Académico, Universidad Nacional Autónoma de México under Grant IN202320, and to MSc Benjamín Leal from ICN-UNAM for technical assistance.

Appendix A. Supplementary data

Supplementary data to this article can be found online at https://doi.org/10.1016/j.radphyschem.2020.108754.

References

Abbasi, F., Mirzadeh, H., Katbab, A.A., 2002. Bulk and surface modification of silicone rubber for biomedical applications. Polym. Int. 51, 882–888. https://doi.org/10.1002/pi.1069.

Akhtar, M.F., Ranjha, N.M., Hanif, M., 2015. Effect of ethylene glycol dimethacrylate on swelling and on metformin hydrochloride release behavior of chemically crosslinked pH-sensitive acrylic acid-polyvinyl alcohol hydrogel. DARU J. Pharmacol. Sci. 23, 1–10. https://doi.org/10.1186/s40199-015-0123-8.

Cabana, S., Lecona-Vargas, C.S., Meléndez-Ortiz, H.I., Contreras-García, A., Barbosa, S., Taboada, P., Magariños, B., Bucio, E., Concheiro, A., Alvarez-Lorenzo, C., 2017. Silicone rubber films functionalized with poly(acrylic acid) nanobrushes for immobilization of gold nanoparticles and photothermal therapy. J. Drug Deliv. Sci. Technol. 42, 245–254. https://doi.org/10.1016/j.jddst.2017.04.006.

Cao, J., Zuo, Y., Wang, D., Zhang, J., Feng, S., 2017. Functional polysiloxanes: a novel synthesis method and hydrophilic applications. New J. Chem. 41, 8546–8553. https://doi.org/10.1039/c7nj01294b.

Fallahi, D., Mirzadeh, H., Khorasani, M.T., 2003. Physical, mechanical, and biocompatibility evaluation of three different types of silicone rubber. J. Appl. Polym. Sci. 88, 2522–2529. https://doi.org/10.1002/app.11952.

Flores-Rojas, G.G., Bucio, E., 2016. Radiation-grafting of ethylene glycol dimethacrylate (EGDMA) and glycidyl methacrylate (GMA) onto silicone rubber. Radiat. Phys. Chem. 127, 21–26. https://doi.org/10.1016/j.radphyschem.2016.05.015.

Flores-Rojas, G.G., López-Saucedo, F., Bucio, E., Isoshima, T., 2017. Covalent immobilization of lysozyme in silicone rubber modified by easy chemical grafting. MRS Commun. 7, 904–912. https://doi.org/10.1557/mrc.2017.115.

Flores-Rojas, G.G., López-Saucedo, F., Quezada-Miriel, M., Bucio, E., 2018. Grafting of

glycerol methacrylate onto silicone rubber using γ-rays: derivatization to 2-oxoethyl methacrylate and immobilization of lysozyme. MRS Commun. 8, 199–206. https://doi.org/10.1557/mrc.2018.16.

Fujisawa, S., Kadoma, Y., 2012. Relationships between base-catalyzed hydrolysis rates or glutathione reactivity for acrylates and methacrylates and their NMR spectra or heat of formation. Int. J. Mol. Sci. 13, 5789–5800. https://doi.org/10.3390/ijms13055789.

García-Vargas, M., González-Chomón, C., Magariños, B., Concheiro, A., Alvarez-Lorenzo, C., Bucio, E., 2014. Acrylic polymer-grafted polypropylene sutures for covalent immobilization or reversible adsorption of vancomycin. Int. J. Pharm. 461 (1–2), 286–295. https://doi.org/10.1016/j.ijpharm.2013.11.060.

Jaganathan, S.K., Balaji, A., Vellayappan, M.V., Subramanian, A.P., John, A.A., Asokan, M.K., Supriyanto, E., 2015. Radiation-induced surface modification of polymers for biomaterial application. J. Mater. Sci. 50, 2007–2018. https://doi.org/10.1007/s10853-014-8718-x.

Kaneko, T., Ito, S., Minakawa, T., Hirai, N., Ohki, Y., 2019. Degradation mechanisms of silicone rubber under different aging conditions. Polym. Degrad. Stabil. 168, 108936. https://doi.org/10.1016/j.polymdegradstab.2019.108936.

Keshvari, H., Mirzadeh, H., Mansoori, P., Orang, F., Khorasani, M.T., 2008. Collagen immobilization onto acrylic acid laser-grafted silicone for using as artificial skin: in vitro. Iran. Polym. J. (Engl. Ed.) 17, 171–182.

Li, M., Neoh, K.G., Xu, L.Q., Wang, R., Kang, E.-T., Lau, T., Olszyna, D.P., Chiong, E., 2012. Surface modification of silicone for biomedical applications requiring long-term antibacterial, antifouling, and hemocompatible properties. Langmuir 28, 16408–16422. https://doi.org/10.1021/la303438t.

Lee, S., Vörös, J., 2005. An aqueous-based surface modification of poly(dimethylsiloxane) with poly(ethylene glycol) to prevent biofouling. Langmuir 21, 11957–11962. https://doi.org/10.1021/la051932p.

Lee, S.-D., Hsiue, G.-H., Kao, C.-Y., 1996. Preparation and characterization of a homo-bifunctional silicone rubber membrane grafted with acrylic acid via plasma-induced graft copolymerization. J. Polym. Sci. Part A Polym. Chem. 34, 141–148. https://doi.org/10.1002/(SICI)1099-0518(19960115)34:1<141::AID-POLA15>3.0.CO;2-L.

Melendez-Ortiz, H.I., Alvarez-Lorenzo, C., Concheiro, A., Bucio, E., 2015. Grafting of N-vinyl caprolactam and methacrylic acid onto silicone rubber films for drug-eluting products. J. Appl. Polym. Sci. 132. https://doi.org/10.1002/app.41855.

Orekhov, D.V., Kazantsev, O.A., Sivokhin, A.P., Savinova, M.V., 2018. Features of the acid-catalyzed hydrolysis of mono- and poly(ethylene glycol) methacrylates. Eur. Polym. J. 100, 18–24. https://doi.org/10.1016/j.eurpolymj.2018.01.010.

Pino-Ramos, V.H., Flores-Rojas, G.G., Alvarez-Lorenzo, C., Concheiro, A., Bucio, E., 2018. Graft copolymerization by ionization radiation, characterization, and enzymatic activity of temperature-responsive SR-g-PNVCL loaded with lysozyme. React. Funct. Polym. 126, 74–82. https://doi.org/10.1016/j.reactfunctpolym.2018.03.002.

Pinto, S., Alves, P., Matos, C.M., Santos, A.C., Rodrigues, L.R., Teixeira, J.A., Gil, M.H., 2010. Poly(dimethyl siloxane) surface modification by low pressure plasma to improve its characteristics towards biomedical applications. Colloids Surf. B Biointerfaces 81, 20–26. https://doi.org/10.1016/j.colsurfb.2010.06.014.

Salati, A., Keshvari, H., Karkhaneh, A., Taranejoo, S., 2011. Design and fabrication of artificial skin: chitosan and gelatin immobilization on silicone by poly acrylic acid graft using a plasma surface modification method. J. Macromol. Sci. Part B Phys. 50 (10), 1972–1982.

Shafiei, A., Kalbasi, R.J., Beheshtiha, S., Heravi, M.M., Yahya, S., 2017. Preparation, characterisation, drug loading and release properties of a novel KIT-6/poly(AA-EGDMA) nanocomposite. Micro & Nano Lett. 13, 213–218. https://doi.org/10.1049/mnl.2017.0451.

Shahsavan, H., Quinn, J., D'Eon, J., Zhao, B., 2015. Surface modification of polydimethylsiloxane elastomer for stable hydrophilicity, optical transparency and film lubrication. Colloid. Surface. Physicochem. Eng. Aspect. 482, 267–275. https://doi.org/10.1016/j.colsurfa.2015.05.024.

Valencia-Mora, R.A., Zavala-Lagunes, E., Bucio, E., 2016. Grafting of thermo-sensitive N-vinylcaprolactam onto silicone rubber through the direct radiation method. Radiat. Phys. Chem. 124, 155–158. https://doi.org/10.1016/j.radphyschem.2015.11.003.

Wei, S.Q., Bai, Y.P., Shao, L., 2008. A novel approach to graft acrylates onto commercial silicones for release film fabrications by two-step emulsion synthesis. Eur. Polym. J. 44, 2728–2736. https://doi.org/10.1016/j.eurpolymj.2008.04.025.

Yang, H., Hou, Z., 2011. Homogenous grafted poly(acrylic acid) brushes on ultra-flat polydimethlysiloxane (PDMS) films by UV irradiation. Nano Biomed. Eng. 3, 42–46. https://doi.org/10.5101/nbe.v3i1.p42-46.

Yang, J.S., Hsiue, G.H., 1996. Synthesis of acrylic acid grafted silicone rubber via pre-irradiation graft copolymerization and its physical and dielectric properties. J. Appl. Polym. Sci. 61, 221–229. https://doi.org/10.1002/(SICI)1097-4628(19960711)61:2<221::AID-APP5>3.3.CO;2-K.

molecules

MDPI

Article

Simultaneous Grafting Polymerization of Acrylic Acid and Silver Aggregates Formation by Direct Reduction Using γ Radiation onto Silicone Surface and Their Antimicrobial Activity and Biocompatibility

Marlene A. Velazco-Medel [1,*], Luis A. Camacho-Cruz [1], Héctor Magaña [2], Kenia Palomino [2] and Emilio Bucio [1,*]

[1] Departamento de Química de Radiaciones y Radioquímica, Instituto de Ciencias Nucleares, Universidad Nacional Autónoma de México, Circuito Exterior, Ciudad 7 Universitaria, Ciudad de México 04510, Mexico; c-camacho-la@comunidad.unam.mx

[2] Faculty of Chemical Sciences and Engineering, Autonomous University of Baja California, University Boulevard No. 14418, Otay Mesa, Tijuana 22390, Mexico; hector.magana@uabc.edu.mx (H.M.); kenia.palomino@uabc.edu.mx (K.P.)

* Correspondence: marlene.velazco@correo.nucleares.unam.mx (M.A.V.-M.); ebucio@nucleares.unam.mx (E.B.); Tel.: +52-(55)-5622-4674-9 (E.B.)

Citation: Velazco-Medel, M.A.; Camacho-Cruz, L.A.; Magaña, H.; Palomino, K.; Bucio, E. Simultaneous Grafting Polymerization of Acrylic Acid and Silver Aggregates Formation by Direct Reduction Using γ Radiation onto Silicone Surface and Their Antimicrobial Activity and Biocompatibility. *Molecules* **2021**, *26*, 2859. https://doi.org/10.3390/molecules26102859

Academic Editors: Juan Luis Vivero-Escoto and Miguel Mendez-Rojas

Received: 15 April 2021
Accepted: 9 May 2021
Published: 12 May 2021

Abstract: The modification of medical devices is an area that has attracted a lot of attention in recent years; particularly, those developments which search to modify existing devices to render them antimicrobial. Most of these modifications involve at least two stages (modification of the base material with a polymer graft and immobilization of an antimicrobial agent) which are both time-consuming and complicate synthetic procedures; therefore, as an improvement, this project sought to produce antimicrobial silicone (PDMS) in a single step. Using gamma radiation as both an energy source for polymerization initiation and as a source of reducing agents in solution, PDMS was simultaneously grafted with acrylic acid and ethylene glycol dimethacrylate (AAc:EGDMA) while producing antimicrobial silver nanoparticles (AgNPs) onto the surface of the material. To obtain reproducible materials, experimental variables such as the effect of the dose, the intensity of radiation, and the concentration of the silver salt were evaluated, finding the optimal reaction conditions to obtain materials with valuable properties. The characterization of the material was performed using electronic microscopy and spectroscopic techniques such as ^{13}C-CPMAS-SS-NMR and FTIR. Finally, these materials demonstrated good antimicrobial activity against *S. aureus* while retaining good cell viabilities (above 90%) for fibroblasts BALB/3T3.

Keywords: silicone; grafting; silver nanoparticles; radiation; antimicrobial; cytocompatibility

1. Introduction

Silicone elastomers (a.k.a. silicone rubbers, silicones, polydimethylsiloxane, PDMS) are polymers which possess properties that are very important for the development of devices on medicine [1–3]. For instance, these materials are biocompatible, readily accessible, and easy to manipulate. Despite these advantages, PDMS by itself is prone to microbial contamination through the formation of pathogenic biofilms on its surface [4,5], triggering infections in patients who may already be compromised [6]. This stark disadvantage can be mitigated by the modification of PDMS via grafting, strategy which has already been used extensively to improve the properties of many materials by modifying the characteristics of materials with behaviors such as biocompatibility, hydrophilicity, conductivity, and antimicrobial activities [1–3].

One of the most common strategies to provide antimicrobial activity to surfaces (e.g., carbon nanomaterials [7,8], inorganic substrates [9,10], and polymeric substrates [11]) is

the immobilization of antimicrobial agents through interactions between the antimicrobials and grafted polymer chains onto the base material or by covalent attachment of the antimicrobial to the surface of the base material [12,13]. These antimicrobial agents may be both organic (classical molecular antibiotics) or inorganic (metallic particles) in nature; however, the latter have attracted more attention because the use of classical antibiotics still increase concerns for bacterial antibiotic resistance [14,15]. Most inorganic antimicrobial compounds are metal salts or metal nanoparticles, such as those containing copper, titanium, zinc, and silver, whose biggest advantage is the fact that they can not only be used by themselves, but they can also be combined onto organic substrates such as polymers, or even work alongside other antimicrobials on complicated substrates. For example, Pissinis et al. (2018) performed the functionalization of Ti/TiO_2 surfaces with a mixture of ampicillin and silver nanoparticles (AgNPs) to stop the propagation of Gram-positive *S. aureus* [16]. This is one of many examples employing metals as antibacterial substances.

One system which has shown great effectiveness as an antibacterial substrate is silver. Silver ions, colloidal silver, and AgNPs have demonstrated cytotoxicity against several pathogens because when this metal interacts with the nitrogenous bases of nucleic acids, it produces oxidative stress in cells [17–20]. Because of this, silver salts have already been encapsulated in medical devices to avoid infections, such as catheters or wound dresses. AgNPs have also been immobilized in silicone and other medical-grade polymers [21].

Several strategies for the production of AgNPs onto polymer substrates have been reported [22–26]. For example, the synthesis of AgNPs in-between polyacrylic acid grafts has already been achieved by chemical reduction of Ag^+ to form hybrid materials [27]. In this example, it is worthy to note that polyacrylic acid grafts not only support the silver particles, but also provide stabilization comparable to citrate or alginate ions in other systems [28,29]. The immobilization of AgNPs onto PDMS has also been thoroughly studied by different deposition techniques. The most conventional pathways are by the diffusion of $AgNO_3$ inside the elastomer and subsequent interaction with a reducing agent, such as $NaBH_4$ or sodium citrate [30,31], the diffusion of preformed nanoparticles inside a polymer, or the electrodeposition onto the polymeric surface [32]. For example, López-Saucedo et al., 2018 immobilized preformed AgNPs onto medical grade polytetrafluorethylene to avoid bacterial adhesion [33] and Pazos-Ortiz et al., 2017 used polycaprolactone fibers to retain AgNPs [34]. Additional techniques have been used to attach or immobilize these particles to silicone elastomers, for example, the synthesis of composites of PDMS + AgNPs [35] or the presence of polymers or stabilizers in the process [36].

Although these strategies are both effective to produce antimicrobial substrates using silver, practically all these implementations need at least two synthetic steps; namely, the grafting of a functional molecule or polymer able to support the nanoparticles, the immobilization of silver as nanoparticles or ions, and, in case of first immobilizing silver ions, their reduction to produce silver nanoparticles. Therefore, the search of simplified synthetic pathways is an important goal. A solution to this dilemma would be the simultaneous grafting of polymeric chains, and the direct reduction of silver ions in the reaction media. To achieve this goal, we considered the possibility of using high-energy radiation as a pathway to polymerization initiation and direct reduction of silver ions.

Several stimuli-responsive polymers have been grafted onto different polymer matrixes using radiation [37,38]; for example, acrylic acid has been grafted onto silicone using gamma radiation, laser emission, and plasma. Cabana et al., 2017 achieved the retention of gold nanoparticles to add antimicrobial properties [39]. Alongside this, direct reduction of silver ions to AgNPs using high-energy radiation is possible in aqueous or polar media because when radiation interacts with these solvents, reductive species such as hydrogen radicals ($H^{\cdot}$) and solvated electrons (e^{-}_{aq}) are readily formed [40–45].

Previous reports on this topic mainly focus on the study of the effects of the radiation dose, radiation intensity, and salt concentration on the morphology and size of the synthesized. With these studies it has been discovered that the formation of these metallic nanoparticles is highly dependent on synthesis time and irradiation dose [41,42,46].

The most remarkable aspect to note is the effect of the dose in the shape of the particle; for instance, Abedini et al. (2016) reported that reactions conducted at doses of 30 kGy promote the formation of spherical particles. However, at higher doses, nanoplates or triangular particles are formed [41]. Despite this, changes in morphology do not affect AgNPs' antimicrobial effects [47].

Profiting from the benefits of AgNPs addition to polymer matrices, this project proposes the use of ionizing radiation (coming from a ^{60}Co radioactive source) to perform the simultaneous reduction of Ag^{+} and polymerization of AAc and EDGMA for the in-situ immobilization of AgNPs. By altering variables during the synthetic procedure such as concentration of the monomers, concentration of the silver ions, and irradiation dose, different materials were obtained and characterized with techniques such as SEM microscopy with EDX elemental analysis, FTIR, and ^{13}C-CPMAS-SS-NMR. Subsequent antimicrobial and biocompatibility tests were performed to test the applicability of these novel materials.

2. Results and Discussion

2.1. Grafting Reaction and Silver Particle Formation Assisted by Gamma Radiation

As we previously reported [48], the choice of solvent is crucial to obtain bulk or surface grafts in a polymer matrix. For metal immobilization, it is necessary to obtain polymer chains on the base surface to favor the nanoparticle formation onto the surface rather than inside the bulk. Silicone films (SF) are highly hydrophobic; therefore, polar solvents do not interact with PDMS, thus the choice of the solvent should be carried out so that there is low (but not null) diffusion inside the matrix. To select the solvent, it is then necessary to reference previous studies on the swelling of PDMS on different solvents [49]. The grafting reaction was carried out through this analysis in a solvent mixture (EtOH:H_2O). A low concentration of the mixture of monomers (20% v/v) was used to prevent solubility issues with the monomers, and monomer molar ratios of 3:1 and 5:1 (AAc:EGDMA) were tested on preliminary experiments.

The effect of the irradiation dose was tested by irradiating the samples at different doses with an intensity of ~10 kGy h^{-1}. The highest grafting yield was obtained with an irradiation dose of 25 kGy. Higher doses did not further increase the yield; however, the reactions did not proceed at these doses. This may be due to rapid termination rates at these higher irradiation doses. Grafting yields (GY) of about 10% were obtained by irradiating the monomer solution and the SF simultaneously, using the 3:1 monomer ratio (red line in Figure 1a). For the 5:1 ratio, the grafting reaction did not proceed because the formation of the unbounded polymer is preferred, the highest GY with this condition was 2.5%.

FOR PEER REVIEW 4 of 16

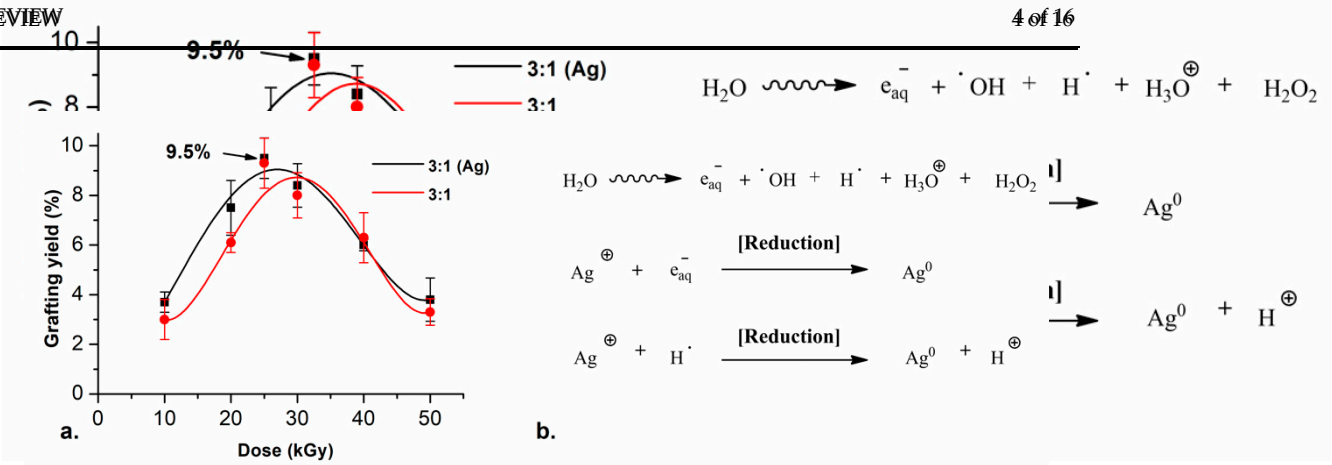

Figure 1. (**a**) Grafting yield of (—) SF-g-(AAc-EGDMA) + Ag and (—) SF-g-(AAc-EGDMA) in function of the dose with monomer concentration fixed at 20% (v/v) and (**b**) Irradiation-reduction mechanism of silver reduction.

Figure 1. (**a**) Grafting yield of (—) SF-g-(AAc-EGDMA) + Ag and (—) SF-g-(AAc-EGDMA) in function of the dose with monomer concentration fixed at 20% (v/v) and (**b**) Irradiation-reduction mechanism of silver reduction.

The atom agglomeration drives the growth of small spherical and quasi-spherical particles in the nanoscale. The acrylic acid moieties of the monomer decrease the pH of the reaction medium to 5, thus the hydrogen radical is the main reducing agent for silver in these conditions. Additionally, the polycarboxylic acids in the polymer graft work as

The atom agglomeration drives the growth of small spherical and quasi-spherical particles in the nanoscale. The acrylic acid moieties of the monomer decrease the pH of the reaction medium to 5, thus the hydrogen radical is the main reducing agent for silver

For the systems containing silver, the same synthetic conditions used before were evaluated, but adding different concentrations of $AgNO_3$ to the reaction media. With all tested conditions, the grafting reaction and the reduction of the silver ions were reached successfully in one step. Furthermore, the presence of the silver nitrate (5 mM) did not change the GY on the films. The highest GY with these conditions was 9.5%, which was equivalent to the grafting yield corresponding to the reaction without the silver salt (black line in Figure 1a). The most notable change in the films was that they turned colorful, from clear to yellow and orange, similar to other reported elastomer + AgNPs [35].

The reduction reaction of silver ions was carried out by an irradiation–reduction mechanism assisted by gamma radiation. The radiolysis of the water promotes different reactive species (Figure 1b), which react with the silver salt and trigger a redox reaction.

The atom agglomeration drives the growth of small spherical and quasi-spherical particles in the nanoscale. The acrylic acid moieties of the monomer decrease the pH of the reaction medium to 5, thus the hydrogen radical is the main reducing agent for silver in these conditions. Additionally, the polycarboxylic acids in the polymer graft work as stabilizers in the reactions which allow the retention of the AgNPs between the chains in the graft.

2.2. Characterization of the Films

FTIR-ATR spectra (Figure 2a) show changes regarding the initial SF but not between the film SF-*g*-(AAc-*co*-EGDMA) compared with the SF-*g*-(AAc-*co*-EGDMA) + Ag. According to these spectra, we can conclude that there is polymer graft present on both surfaces after the radiation, even when there is silver in the system, there are no changes in the absorption bands which correspond to the typical functional groups reported for silicone modified with AAc [50,51].

The spectrum of pristine SF showed strong bands corresponding to the Si-O-Si stretching and Si-CH_3 bending vibrations at ~1000 cm^{-1} and ~750 cm^{-1}, respectively (Figure 1b, SF). The short band at ~2900 cm^{-1} is attributed to the typical band for C-H stretching, present in all the spectra. The absorption band at ~1710 cm^{-1} is a characteristic band for the C=O stretching confirming the presence of this group on the functionalized versions of SF.

Aac:EGDMA grafting onto SF was confirmed further with equilibrium water content (EWC%) tests. In these tests, SF-*g*-(AAc-*co*-EGDMA) with GY~9.5% demonstrated swelling properties in deionized water (DI water) and phosphate buffer saline (PBS) solution (in contrast to pure SF); this fact aided to confirm the AAc grafts onto the SF. The EWC% for the films in DI water and PBS was ~3.7 (24 h) and 8.8% (30 h), respectively (for graphs, see Supplementary Material). Although DI water and PBS both have a pH above the pKa of AAc (pKa 4.7), the dissolved salts in the PBS change the ionic strength in the solution, which trigger a variation in the osmotic pressure inside and outside of the graft. This change conduces to the ion flow from the solution to the free volume between polymeric chains, this effect is similar as other hydrogel swelling behaviors [52].

Additional to EWC% studies, contact angle studies of the three films after 5 min showed that both SF-*g*-(AAc-*co*-EGDMA) (GY ~9.5%) and SF-*g*-(AAc-*co*-EGDMA) + Ag (GY ~9.5%) increased the surface wettability against DI (Figure 2b). The contact angle decreases from 105° (SF), which means the surface is highly hydrophobic, to 95° in the modified films, confirming a hydrophilic AAc graft onto the surface, as we reported in our last work [48]. The angle did not change between films with and without silver; thus, allowing us to conclude that silver does not affect the water absorption. Although silver was expected to increase hydrophilicity because of the metal–oxygen interactions, since the measurement was made almost instantaneously (after 5 min, to avoid the evaporation of the drop) no changes in the hydrophilicity between the two films were found.

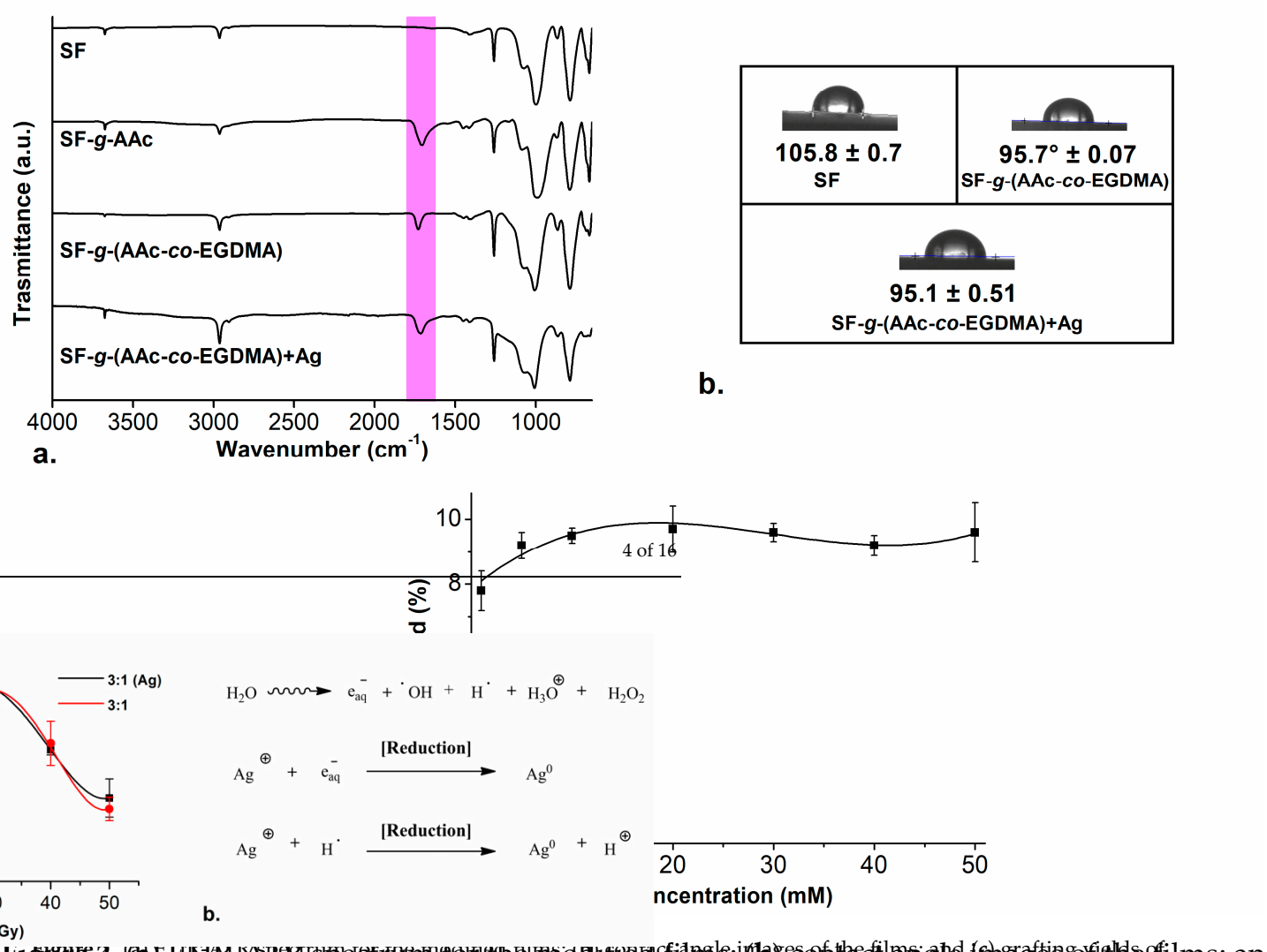

Figure 2. (**a**) FTIR-ATR spectrum for the modified films; (**b**) contact angle images of the films; and (**c**) grafting yields of (—) SF-*g*-(AAc-*co*-EGDMA) + Ag and (- - -) SF-*g*-(AAc-*co*-EGDMA) as a function of the concentration of $AgNO_3$.

Reports claim that the reaction time in the synthesis of AgNPs plays an essential role in their shape and size and thus the time was fixed for all reactions; therefore, to obtain higher doses (input energy to the system), the intensity of the radiation (I = [kGy/h]) was varied instead of time to control this variable for the following experiments. Two different radiation intensities were tested, and when I was decreased from 10 to 5 kGy h^{-1}, the color

zation of the Films

R spectra (Figure 2a) show changes regarding the initial SF but not between AAc-*co*-EGDMA) compared with the SF-*g*-(AAc-*co*-EGDMA) + Ag. According pectra, we can conclude that there is polymer graft present on both surfaces ation, even when there is silver in the system, there are no changes in the nds which correspond to the typical functional groups reported for silicone AAc [50,51].

ctrum of pristine SF showed strong bands corresponding to the Si-O-Si Si-CH_3 bending vibrations at ~1000 cm^{-1} and ~750 cm^{-1}, respectively (Figure hort band at ~2900 cm^{-1} is attributed to the typical band for C-H stretching, the spectra. The absorption band at ~1710 cm^{-1} is a characteristic band for ching confirming the presence of this group on the functionalized versions

MA grafting onto SF was confirmed further with equilibrium water content . In these tests, SF-*g*-(AAc-*co*-EGDMA) with GY~9.5% demonstrated swell- in deionized water (DI water) and phosphate buffer saline (PBS) solution

In the case of ^{13}C-CPMAS-SS-NMR spectra (see Supplementary Material) the signal observed at 0 ppm is assigned to the pendant -CH_3 chains of SF and the signal at 29.7 ppm corresponds to the methylene groups that were formed after the grafting reaction [53]. The rest of the signals correspond to the AAc:EGDMA graft. The carbonyl group of acrylic acids in the polymer graft [54] is not possible to differentiate the carbonyl from AAc and EGDMA in the spectra. However, they present structural similarities. In addition, at 19.9 and 42.0 ppm, the signals correspond to methyl and methylene groups of EGDMA are observed. The signals at 44.6 and 38.5 ppm were assigned to the α-carbons and the carbonyl groups in AAc and EGDMA, respectively.

The effect of silver nitrate concentration on the grafting reaction was also evaluated. The simultaneous reaction was performed in the same conditions but altering the concentration of the salt. As in the first experiments, the synthesized films at different concentrations of $AgNO_3$ became colorful, starting from a concentration above 5 mM of silver salt the films became orange with different intensities, similar to the color of the aqueous dispersion of small spherical and quasi-spherical AgNPs [55,56]. For all the reactions, the AAc:EGDMA GY was between ~8% and ~9.5%. The increase in the concentration of the silver nitrate in the reaction did not affect the grafting yield in the films (check Figure 2c), the amount of AAc:EGDMA graft onto the surface is still the same, and EWC% and hydrophilicity tests also confirm this.

different colors depending on the intensity of radiation (see Figure 3a). The typical coloration for aqueous colloids with spherical AgNPs with diameter <20 nm is usually yellow, while for particles bigger than 100 nm the coloration is most often blue [30,41,57]. The formation of bigger particles at 50 mM and lower intensity of radiation can be attributed to the increase in the time of exposure which promotes effective silver reduction and formation of bigger aggregates, according to Abedini et al., 2016.

Silver nanoparticles have a surface plasmon resonance (SPR) depending on the shape and size of the particle which can be detected by UV-Visible Spectroscopic analysis. The presence of the nanoparticles was confirmed in the films by that technique. The spectra in Figure 3b,c show the typical bands for SRP of AgNPs.

The spherical nanoparticles yielded a SPR peak at 435 nm, similar to the value previously reported for spherical and quasi-spherical AgNPs with sizes below 20 nm [30]. It is noticeable that an additional band in 605 nm appeared, which is typical for triangular silver nanoplates or quasi-spherical AgNPs with a bigger size (~100 nm). The formation of the bigger particles occurred in the experiments with a higher concentration of $AgNO_3$ and increased radiation exposure (I = ~5 kGy h). This can be explained with the continuous reduction reactions happening while the radiation where silver clusters are easier to form.

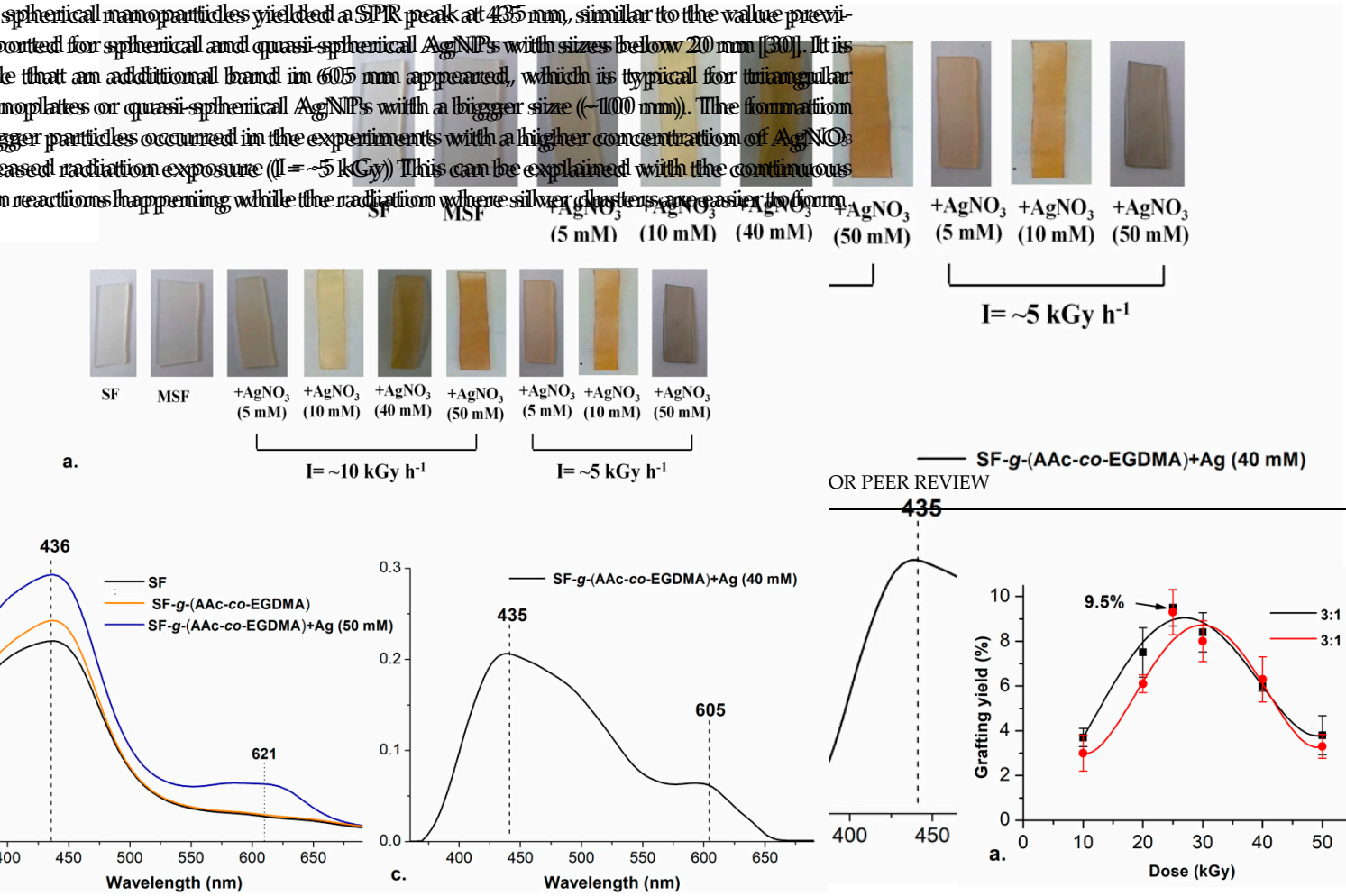

Figure 1. (**a**) Films prepared with different intensity of radiation and concentration of $AgNO_3$; (**b**) UV-Vis spectra of (—) SF, (—) SF-*g*-(AAc-*co*-EGDMA) and (—) SF-*g*-(AAc-*co*-EGDMA) + Ag (50 mM); and (**c**) UV-Vis spectrum of SF-*g*-(AAc-*co*-EGDMA) + Ag (10 mM).

Due to the thickness of the films, images from transmission microscopy could not be obtained; however, scanning electron microscopy (SEM) was successful. The obtained micrographs show the morphologies of the films' surfaces before (Figure 4a) and after the modification processes. The roughness of the films does not increase substantially, which was expected since the grafting percentage was low (max GY = 9.5%) (Figure 4b). However, the presence of silver particles is evident when looking at the images corresponding

The spherical nanoparticles yielded a SPR peak at 435 nm, similar to the value previously reported for spherical and quasi-spherical AgNPs with sizes below 20 nm [30]. It is noticeable that an additional band in 605 nm appeared, which is typical for triangular silver nanoplates or quasi-spherical AgNPs with a bigger size (~100 nm). The formation of the bigger particles occurred in the experiments with a higher concentration of $AgNO_3$ and increased radiation exposure (I = ~5 kGy) This can be explained with the continuous reduction reactions happening while the radiation where silver clusters are easier to form.

ER REVIEW 7 of 16

Due to the thickness of the films, images from transmission microscopy could not be obtained; however, scanning electron microscopy (SEM) was successful. The obtained micrographies show the morphologies of the films' surfaces before (Figure 4a) and after the modification processes. The roughness of the films does not increase substantially, which was expected since the grafting percentage was low (with GYs ~9.5%) (Figure 4b). However, the presence of silver particles is evident when looking at the images corresponding to the silver-functionalized materials. As expected, the amount of silver that can be observed depends on the concentration of silver used in the synthesis of the material (Figure 4c,d). Changes in the color of the films may be attributed to these silver aggregates or clusters inside or outside of the pores of the graft [58].

to the silver-functionalized materials. As expected, the amount of silver that can be observed depends on the concentration of silver used in the synthesis of the material (Figure 4c,d). Changes in the color of the films may be attributed to these silver aggregates or clusters inside or outside of the pores of the graft [58].

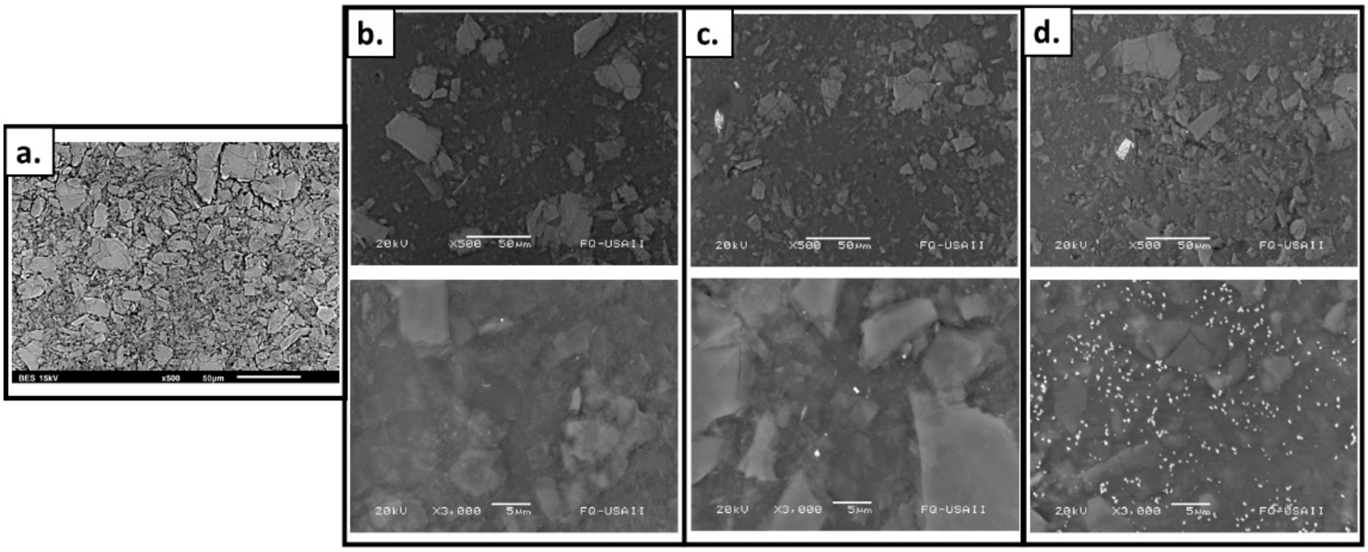

Figure 4. SEM images of (**a**) SF; (**b**) SF-*g*-(AAc-*co*-EGDMA); (**c**) SF-*g*-(AAc-*co*-EGDMA) + Ag (10 mM); and (**d**) SF-*g*-(AAc-*co*-EGDMA) + Ag (50 mM).

Figure 4. SEM images of (**a**) SF; (**b**) SF-*g*-(AAc-*co*-EGDMA); (**c**) SF-*g*-(AAc-*co*-EGDMA) + Ag (10 mM); and (**d**) SF-*g*-(AAc-*co*-EGDMA) + Ag (50 mM).

Additionally, the energy-dispersive X-ray spectrometry (EDX) information confirmed the presence of silver and the AAc:EDGMA graft on the surface. Films with a lower concentration of silver (Figure 5b) showed correspondingly lower amounts of silver. The section of the surface with a higher amount of silver reached 4.6%. In contrast, the blue film, synthesized using 50 mM of silver nitrate showed higher concentrations of silver in almost all the surface, the higher amount was nearly 6% (Figure 5c). For the film without silver, no amount of the metal was found in any spectra (Figure 5a). The elemental distributions for the films revealed a silver content that may be adequate concerning the development of antimicrobial surfaces [59].

Additionally, the energy-dispersive X-ray spectrometry (EDX) information confirmed the presence of silver and the AAc:EDGMA graft on the surface. Films with a lower concentration of silver (Figure 5b) showed correspondingly lower amounts of silver. The section of the surface with a higher amount of silver reached 4.6%. In contrast, the blue film, synthesized using 50 mM of silver nitrate showed higher concentrations of silver in almost all the surface, the higher amount was nearly 6% (Figure 5c). For the film without silver, no amount of the metal was found in any spectra (Figure 5a). The elemental distributions for the films revealed a silver content that may be adequate concerning the development of antimicrobial surfaces [59].

film, synthesized using 50 mM of silver nitrate showed higher concentrations of silver in almost all the surface, the higher amount was nearly 6% (Figure 5c). For the film without silver, no amount of the metal was found in any spectra (Figure 5a). The elemental distributions for the films revealed a silver content that may be adequate concerning the development of antimicrobial surfaces [59].

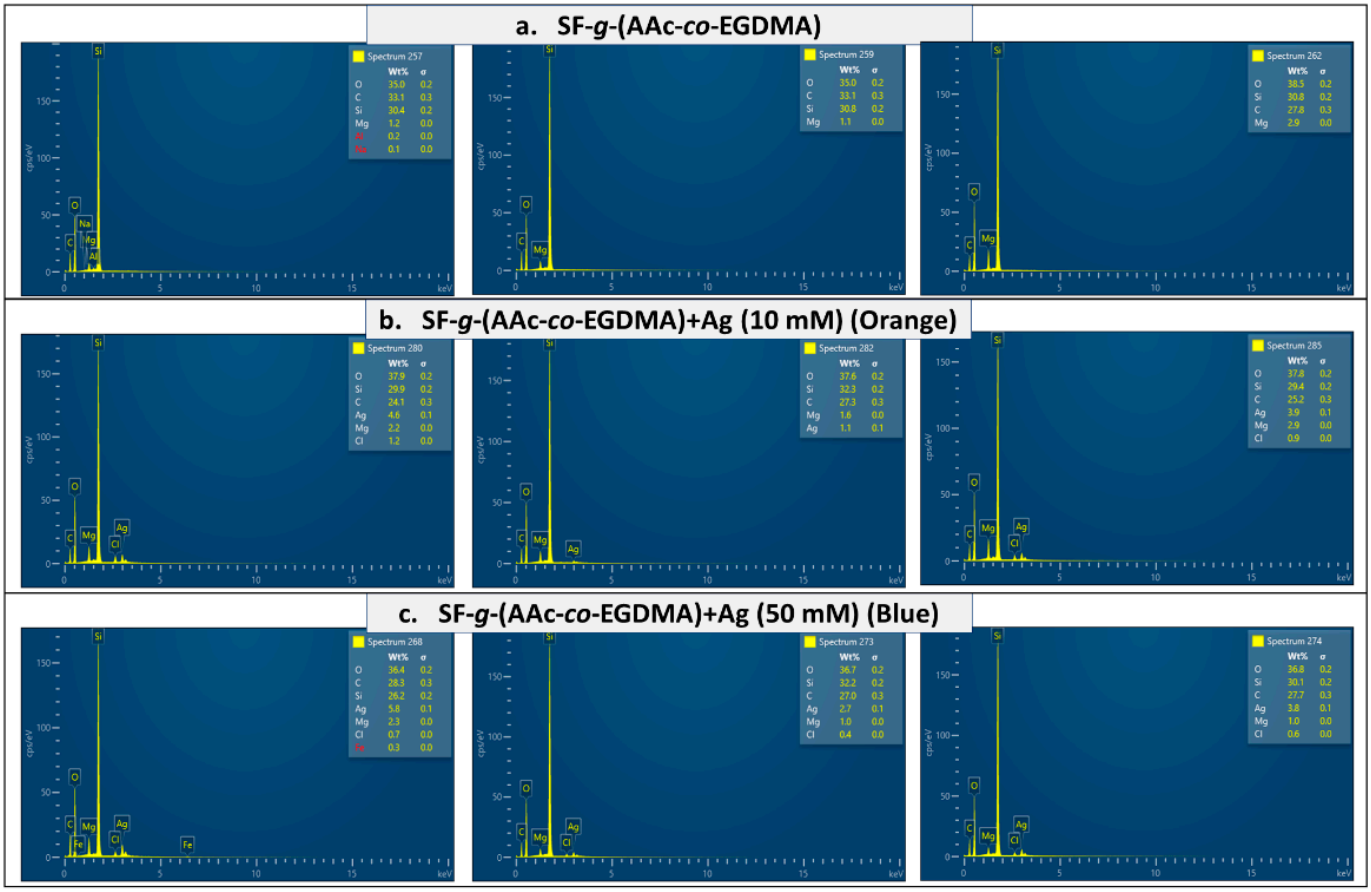

Figure 5. EDX spectra of (**a**) SF-*g*-(AAc-*co*-EGDMA), (**b**) SF-*g*-(AAc-*co*-EGDMA) + Ag (10 mM), and (**c**) SF-*g*-(AAc-*co*-EGDMA) + Ag (50 mM).

To test for the stability of the materials, the films were exposed to atmospheric oxygen and water for 12 months and monitored periodically. Both tests were performed in the absence of light. The films remained without color changes for 12 months, suggesting the absence of oxidation reactions which would have darkened the samples. FTIR-ATR and UV-Vis spectra were recorded after 6 months and very similar spectral data was obtained (see Supplementary Material). In an aqueous solution, the diffusion of silver outside the polymer to the solution was not detected by absorbance measurements, this supports the fact that the particles and aggregates are occluded into the AAc grafts may be by a carboxylate-AgNP interaction in DI water and buffer solutions.

2.3. Antimicrobial Test

The film: SF-*g*-(AAc-*co*-EGDMA) + Ag (10 mM) (orange) was used for preliminary antimicrobial analyses against Gram-positive and Gram-negative bacteria. The results were compared between this sample, the film without silver and pristine silicone. As seen in Figure 6a, UV–Vis results confirmed growth inhibition due to the presence of SF-*g*-(AAc-*co*-EGDMA) + Ag (10 mM) for the three bacteria after 24 h according to absorbance measurements.

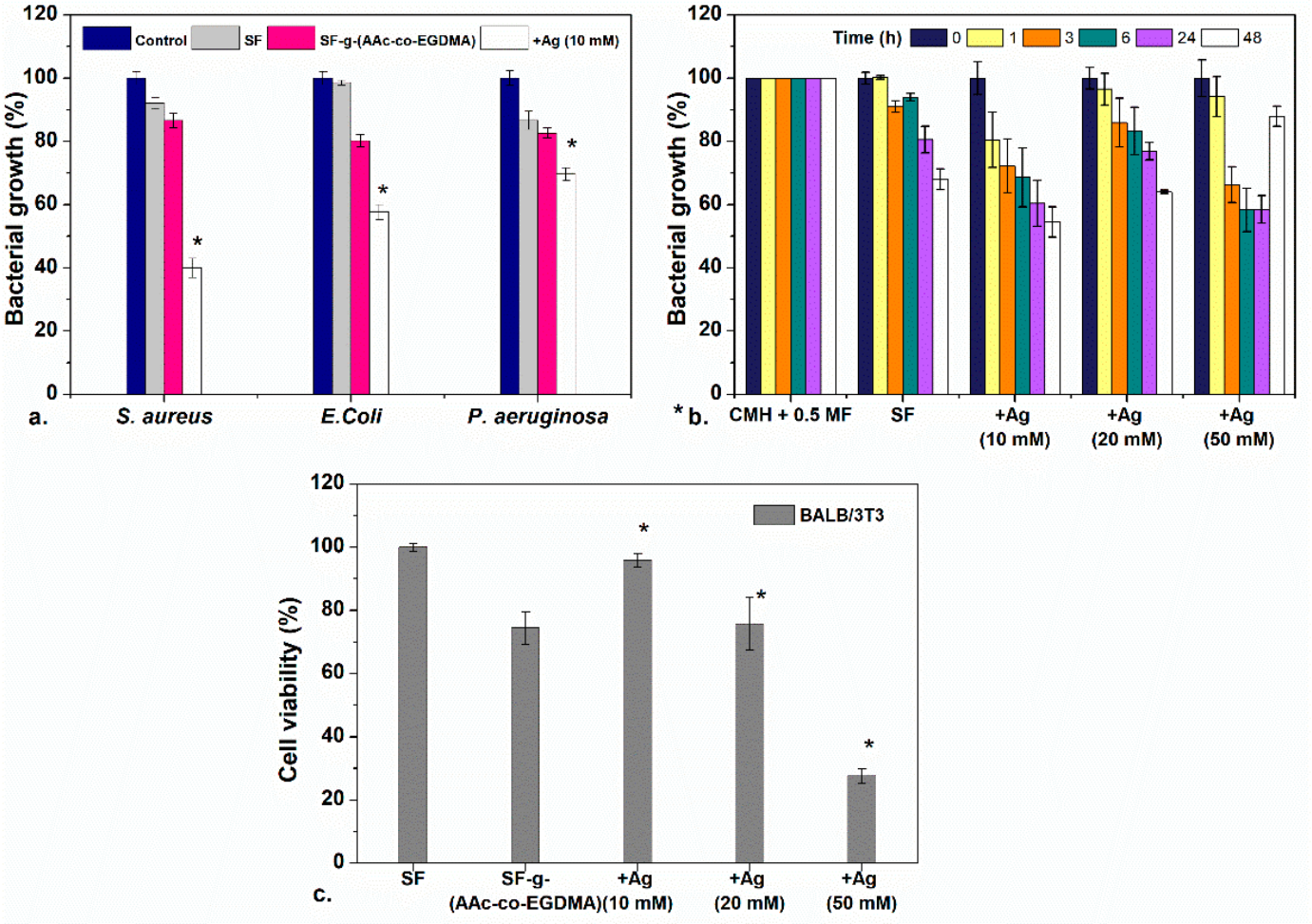

Figure 6. (**a**) Antimicrobial evaluation against three bacteria of SF, SF-*g*-(AAc-*co*-EGDMA), and SF-*g*-(AAc-*co*-EGDMA) + Ag. (**b**) Antimicrobial effect of SF-*g*-(AAc-*co*-EGDMA) + Ag with different concentrations of Ag as a function of the time against *S. aureus*, and (**c**) cytocompatibility of the films in fibroblast cultures after 24 h. Statistically significant differences between control samples and modified materials are highlighted with a *.

3. Experimental Section

3.1. Materials and Methods

Silicone films (1 × 4 cm) with a density ranging from 1.1 to 1.5 g cm^{-3} and a thickness of 1 mm were purchased from Good-fellow (Huntingdon, UK). Silver nitrate (99.9%), ethylene glycol dimethacrylate, and acrylic acid were acquired from Sigma-Aldrich Co. (St. Louis, MO, USA). All the monomers were purified under vacuum distillation before used. Deionized water and ethanol (analytical grade) were obtained from Baker Mexico and were used without further purification.

3.2. Grafting Reaction and Silver Reduction Assisted by Radiation

As preliminary experiments, silicone films (SF) were introduced in an ampoule containing 8 mL of an AAc:EGDMA mixture in 3:1 and 5:1 ratios (SF-*g*-(AAc-*co*-EGDMA)). The monomer concentrations tested were 10 and 20% (*v*/*v*) in EtOH:H_2O (1:1) mixture as a solvent.

In silicone films with silver immobilization (SF-*g*-(AAc-*co*-EGDMA) + Ag), different

According to these results, SF-*g*-(AAc-*co*-EGDMA) + Ag (10 mM) showed better inhibition for *S. aureus* in which the bacterial growth decreases up to a value of ~40% of cells (in comparison to 100% for other samples) after 24 h. For *E. coli*, the inhibition was less significant, as well as for *P. aeruginosa*, the inhibiting effect was less dramatic; however, slight growth inhibition is still observed, which is common for silver modified materials. To examine if these differences are significant, a one-way ANOVA difference of means test with a confidence level of $p = 0.01$ was performed (see Section 3 and Supplementary Material) between the culture media containing a pristine SF, and assays involving either the control or modified films.

One accepted mechanism for the antimicrobial effect of the AgNPs is that they attach to the cell wall of bacteria and disrupt the biochemical processes of the cell. The nanoparticles can pass through the cell wall and affect the environment inside the bacterium triggering cell death [40]. The difference between the thickness in the cell wall is apparent that directly influences the bactericidal effect of the particles when those penetrate the membrane and get inside the cell; nevertheless, this antimicrobial effect can be reached only by contact too as it has been previously demonstrated by microscopy [61]. The linkage between the metallic particle and the cell wall can be conducted by electrostatic forces between these two entities, but this depends on the coating of the particle. For instance, particles coated with polycarboxylates are normally negatively charged [62,63]. Therefore, these particles

may interact with the proteins in the cell wall causing irreversible changes in the cell wall structure and cell morphology; these changes conduct to cell death [20,64,65].

Figure 6a shows inhibition for both Gram-negative (*E. coli* and *P. aeruginosa*) and Gram-positive *S. aureus*. Despite what previous reports suggest, the antibacterial effect was dramatic for *S. aureus* than *E. coli* and *P. aeruginosa*, even though *S. aureus* is a Gram-positive bacteria. The higher bactericidal effect against *S. aureus* can be attributed to the antimicrobial mechanism is by direct contact between the cell wall and the AgNP surface, as it has been reported for Gram-positive *S. epidermidis* in glass surfaces modified with AgNPs which showed antibacterial effect by cell/surface contact [66,67]. For Gram-negative bacteria the main antimicrobial mechanism is attributed to the release of silver ions Ag^+ produced by oxidation of AgNPs [68]. Something beyond the scope of this paper which is interesting to remark is that although inhibition of Gram-positive bacteria due to the presence of AgNPs is not unprecedented, the behavior seen on this work unexpected for these materials and it would be interesting to investigate further in follow-up investigations.

After demonstrating that the bactericidal activity was more effective for *S. aureus*, the performance of the SF prepared with different concentrations of silver was tested. The bacterial growth inhibition was evaluated as a function of time (Figure 6b). This graph shows that the bacterial growth of *S. aureus* is inhibited for up to 48 h when testing the lower silver concentration films. The three tested films showed bactericidal effect after 24 and 48 h. There are no differences in the results between the films with lower and higher concentration of silver.

As it may be noted, the inhibition of the film prepared with a concentration of 50 mM $AgNO_3$ has an apparent anomalous increase in bacterial growth at 48 h. This can be explained as an interference effect of the oxidation of AgNPs and aggregation of silver oxide in the presence of light and oxygen, which increase the absorbance of the medium (silver oxides are black insoluble solids) and could be confused with bacterial growth on absorbance measurements. This effect is not seen in materials with lower concentrations of silver because the oxidation and aggregation are more probable in materials with more concentrations of silver.

The antibacterial effect of the AgNPs depends on the particle size; small-diameter particles have a larger area and thus more contact with the bacteria. For that reason, the films prepared with 10 mM of silver nitrate with an excess of small spherical particles showed the same effect as the films containing more Ag (50 mM), because the effect is due to the size of the nanoparticles rather than to the concentration.

2.4. Cytocompatibility

Cell viability was evaluated in small volumes of growth medium in direct contact with BALB/3T3 (mouse). As shown in Figure 5c, cell viability in this cell line was unaffected for the films with a low concentration of silver (10 mM), for these samples, good cytocompatibility (>90%) was observed at 24 h. It is important to remark that the cell viability of that film is better than that of film modified only with the AAc:EGDMA grafts. All the evaluated films had a GY ~10%, and it is shown that with an increase in the GY onto the silicone surface, the cytocompatibility decreases considerably [69]. An increase in Ag concentration directly affects the cell viability due to the cytotoxicity of the nanoparticles. The film modified with 50 mM of silver nitrate induces cell death, which can be seen since the cell viability decreased below 40%. Fibroblasts are adherent cells; thus, they need to be attached to a surface to function, therefore the fact that they survived in solution is a good sign. In comparison to other studies in which lower cytocompatibilities have been found, the cytocompatibility of these materials is acceptable [70].

3. Experimental Section

3.1. Materials and Methods

Silicone films (1 × 4 cm) with a density ranging from 1.1 to 1.5 g cm^{-3} and a thickness of 1 mm were purchased from Good-fellow (Huntingdon, UK). Silver nitrate (99.9%),

ethylene glycol dimethacrylate, and acrylic acid were acquired from Sigma-Aldrich Co. (St. Louis, MO, USA). All the monomers were purified under vacuum distillation before used. Deionized water and ethanol (analytical grade) were obtained from Baker Mexico and were used without further purification.

3.2. Grafting Reaction and Silver Reduction Assisted by Radiation

As preliminary experiments, silicone films (SF) were introduced in an ampoule containing 8 mL of an AAc:EGDMA mixture in 3:1 and 5:1 ratios (SF-*g*-(AAc-*co*-EGDMA)). The monomer concentrations tested were 10 and 20% (*v*/*v*) in EtOH:H_2O (1:1) mixture as a solvent.

In silicone films with silver immobilization (SF-*g*-(AAc-*co*-EGDMA) + Ag), different solutions with a concentration of silver nitrate were used (1, 5, 10, 20, 30, 40, and 50 mM) the $AgNO_3$ was dissolved in the monomer/EtOH:H_2O solutions. Monomer concentration was fixed at 20% *v/v* in a ratio 3:1 (AAc:EGDMA). The ampoules were deoxygenated by displacing oxygen with Argon for 20 min subsequently the ampoules were sealed and later exposed to variable doses of ^{60}Co γ-radiation (I = ~5 and ~10 kGy h^{-1}) using a Gammabeam 651PT available in the Institute of Nuclear Sciences (ICN) at the National Autonomous University of Mexico (UNAM) to initiate the polymerization reaction. After exposing the films to radiation, all the modified SF were washed in different solvents to remove the occluded solvent, $AgNO_3$, monomer, and copolymer residues. Finally, the samples were dried under vacuum (−80 kPa) at 40 °C and weighed.

The grafting yield (GY) was calculated from the weight difference between pristine PDMS (m_0) and grafted-PDMS (m_g), the general formula is shown in Equation (1):

$$\text{GY (\%)} = [(m_g - m_0)/m_0]100 \quad (1)$$

All the experiments were repeated thrice, and the standard error of the mean (Err) was calculated for all measurements.

3.3. Characterization

To check for a successful modification of the materials the Fourier Transform Infrared Spectroscopy Attenuated Total Reflectance Spectroscopy (FTIR ATR) using a Perkin-Elmer Spectrum 100 spectrometer (Perkin Elmer Cetus Instruments, Norwalk, CT, USA). All the materials were dried under a vacuum before the measurements. The characterization of the surfaces was made using UV-VIS spectroscopy using an Ocean Optics HR4000CG-UV-NIR, and the Scanning Electron Microscopy (SEM) in a JEOL JSM 5900 LV with graphite recovering at 20 kV and energy-dispersive X-ray spectrometry (EDX). Since both FTIR ATR measurements are performed on the solid state, sample preparation only consisted of the aforementioned vacuum dry.

The equilibrium water content (EWC%) was measured in deionized water for 48 h each, the excess of water was removed using filter paper and then the films were weighted. The swelling degree (SD) was calculated using Equation (2):

$$\text{SD (\%)} = [(m_S - m_g)/m_g]100 \quad (2)$$

m_g and m_s represent the mass of the grafted and the swollen film, respectively. All the experiments were repeated thrice, and the standard error of the mean (Err) was calculated for all measurements.

For contact angle a Kruss DSA 100 drop shape analyzer (Matthews, NC, USA) was used, the angle was recorded at 5 min after deionized water droplet had been deposited into the dry samples. All the experiments were made thrice.

3.4. Bacterial-Growth Inhibition Tests

Small pieces of SF, SF-*g*-(AAc-*co*-EGDMA), SF-*g*-(AAc-*co*-EGDMA) + Ag (1 cm^2 and 100 mg), were placed in tubes containing *Staphylococcus aureus* (ATCC 25,923), *Escherichia*

coli (ATCC 25,922), or *Pseudomonas aeruginosa* (ATCC 27,853) in Muller–Hinton agar at a concentration of approximately 1.5×10^8 CFU mL^{-1} (0.5 McFarland) and then incubated at 37 °C for 3, 6, 12, 24, and 48 h. Control cultures with and without bacteria were also prepared with this method. To quantify bacterial growth, light absorption by the culture media was measured in a UV–Vis spectrophotometer at wavelengths ranging from 450 to 800 nm. Absorbance at 600 nm was used to compare bacterial growth in all the systems as stated in the literature [71]. All bacterial-growth inhibition tests were performed three times and a one-way ANOVA difference of means test ($p = 0.01$) was conducted to evaluate the statistical significance of the results at 24 h. The details of the ANOVA test are presented in the Supplementary Material. For these assays, since the means were expected to be different if growth inhibition was achieved; therefore, these were the proposed hypotheses for the statistical test:

$$H_0: \%\ Growth_{SF} = \%\ Growth_{SF\text{-}g\text{-}(AAc\text{-}co\text{-}EDGMA)} = \%\ Growth_{SF\text{-}g\text{-}(AAc\text{-}co\text{-}EDGMA)\ +\ Ag}$$

$$H_a: \%\ Growth_{SF} \neq \%\ Growth_{SF\text{-}g\text{-}(AAc\text{-}co\text{-}EDGMA)} \neq \%\ Growth_{SF\text{-}g\text{-}(AAc\text{-}co\text{-}EDGMA)\ +\ Ag}$$

Post-hoc (Tukey test) tests allowed to determine which of the samples had indeed different ability to stop growth inhibition for each bacteria.

3.5. Cytocompatibility Essays

The cytocompatibility tests were performed using a murine embryonic fibroblast cell line BALB/3T3 (ATCC CCL-163, Manassas, VA, USA). The fibroblast cell line was cultured in Dulbecco's modified Eagle's medium (DMEM) with FBS 10% (fetal bovine serum), penicillin-streptomycin (1% *w*/*v*), and gentamicin (10 µg/mL). Experiments were performed in 96 well plates with 50,000 cells mL^{-1} for 12 h incubated in a humidified atmosphere of 5% CO2 at 37 °C. SF-g-(AAc-co-EGDMA), and SF-g-(AAc-co-EGDMA) + Ag films (0.25 × 0.20 cm), were submerged in the cell media for 24 h in culture standard conditions. After this time, the films were removed and cell viability was determined using a MTT kit (Roche, Switzerland). All experiments were performed thrice and compared with cells without films as a negative control. Finally, absorbances were obtained using a Multiskan FC, Thermo Scientific spectrophotometer at 620 nm. Cytocompatibility (%) is calculated as follows:

$$\text{Cytocompatibility (\%)} = [A_{sample}/A_{cont}]100 \quad (3)$$

All cytocompatibility tests were performed three times and a one-way ANOVA difference of means test ($p = 0.01$) was conducted to evaluate the statistical significance of the results at 24 h. The details of the ANOVA test are presented in the Supplementary Material. For these assays, since the means were expected to be different if growth inhibition was achieved; therefore, these were the proposed hypotheses for the statistical test:

H_0: % Cell $viability_{SF}$ = % Cell $viability_{SF\text{-}g\text{-}(AAc\text{-}co\text{-}EDGMA)}$ = % Cell $viability_{SF\text{-}g\text{-}(AAc\text{-}co\text{-}EDGMA)\ +\ Ag\ (10\ mM)}$ = % Cell $viability_{SF\text{-}g\text{-}(AAc\text{-}co\text{-}EDGMA)}$ + Ag (20 mM) = % Cell $viability_{SF\text{-}g\text{-}(AAc\text{-}co\text{-}EDGMA)\ +\ Ag\ (50\ mM)}$.

H_a: % Cell $viability_{SF} \neq$ % Cell $viability_{SF\text{-}g\text{-}(AAc\text{-}co\text{-}EDGMA)} \neq$ % Cell $viability_{SF\text{-}g\text{-}(AAc\text{-}co\text{-}EDGMA)\ +\ Ag\ (10\ mM)} \neq$ % Cell $viability_{SF\text{-}g\text{-}(AAc\text{-}co\text{-}EDGMA)\ +\ Ag\ (20\ mM)} \neq$ % Cell $viability_{SF\text{-}g\text{-}(AAc\text{-}co\text{-}EDGMA)\ +\ Ag\ (50\ mM)}$ post-hoc (Tukey test) tests allowed to determine which of the samples had differences in their cytocompatibility.

4. Conclusions

The simultaneous polymer grafting and silver reduction using gamma radiation were successfully reached in ethanol:water solution. With the analysis of the obtained materials, it was possible to determine the necessary conditions to obtain reproducible grafts while also determining the synthetic conditions that allow for AgNPs to form within the polymer grafts. The presence of silver on the SF was verified by EDX elemental analysis, UV-vis determination of plasmon resonance, and SEM microscopy. As suggested through the

change of color of the films from clear to orange, the formation of spherical or quasi-spherical AgNPs.

The modified films SF-*g*-(AAc-*co*-EGDMA) + Ag showed good antimicrobial activity against *S. aureus* and some antimicrobial activity of *E. coli* and *P. aeruginosa* while maintaining and a cytocompatibility (above 90%) as long as the concentration of silver was 10 mM or lower.

Supplementary Materials: The following are available online, Figure S1: EWC% for the films in DI water and PBS; Figure S2: ^{13}C CPMAS SS NMR spectra of the different films; Figure S3: FTIR-ATR spectrum of the SF-*g*-(AAc-*co*-EGDMA) + Ag (50 mM) recorded after 12 months; Figure S4: UV-Vis spectrum of the SF-*g*-(AAc-*co*-EGDMA) + Ag (50 mM) recorded after 12 months.

Author Contributions: Conceptualization, M.A.V.-M.; Data curation, M.A.V.-M.; Formal analysis, M.A.V.-M.; Funding acquisition, E.B.; Investigation, M.A.V.-M.; Methodology, M.A.V.-M., L.A.C.-C. and K.P.; Resources, H.M. and E.B.; Supervision, H.M. and E.B.; Visualization, M.A.V.-M.; Writing—original draft, M.A.V.-M.; Writing—review and editing, M.A.V.-M. and L.A.C.-C. All authors have read and agreed to the published version of the manuscript.

Funding: Dirección General de Asuntos del Personal Académico, Universidad Nacional Autónoma de México under Grant IN202320 (México). Call for basic scientific research CONACYT 2017–2018 del "Fondo Sectorial de Investigación para la educación CB2017-2018" (Grant A1-S-29789). Thanks to CONACyT for the doctoral scholarships provided for Marlene Alejandra Velazco Medel (696062/583700) and Luis Alberto Camacho Cruz (916557).

Data Availability Statement: Data sharing is not applicable to this article.

Acknowledgments: The authors thanks G. Cedillo from IIM-UNAM for technical assistance with NMR determination, A. Camacho from the Department of Microbiology of Faculty of Chemistry at UNAM for technical support, I. Puente Lee from USAII-UNAM for the technical assistance for scanning electron microscopy, R. Sato from ICAT-UNAM for UV-Vis, and also ML Escamilla from ICN-UNAM for technical assistance.

Conflicts of Interest: The authors declare no conflict of interest.

Sample Availability: Samples of the compounds are not available from the authors.

References

1. Xiao, Y.; Yu, X.-D.; Xu, J.-J.; Chen, H.-Y. Bulk modification of PDMS microchips by an amphiphilic copolymer. *Electrophoresis* **2007**, *28*, 3302–3307. [CrossRef]
2. Zhou, J.; Khodakov, D.A.; Ellis, A.V.; Voelcker, N.H. Surface modification for PDMS-based microfluidic devices. *Electrophoresis* **2012**, *33*, 89–104. [CrossRef]
3. Shahsavan, H.; Quinn, J.; D'Eon, J.; Zhao, B. Surface modification of polydimethylsiloxane elastomer for stable hydrophilicity, optical transparency and film lubrication. *Colloids Surfaces A Physicochem. Eng. Asp.* **2015**, *482*, 267–275. [CrossRef]
4. Zander, Z.K.; Becker, M.L. Antimicrobial and Antifouling Strategies for Polymeric Medical Devices. *ACS Macro Lett.* **2018**, *7*, 16–25. [CrossRef]
5. Li, M.; Neoh, K.G.; Xu, L.Q.; Wang, R.; Kang, E.-T.; Lau, T.; Olszyna, D.P.; Chiong, E. Surface Modification of Silicone for Biomedical Applications Requiring Long-Term Antibacterial, Antifouling, and Hemocompatible Properties. *Langmuir* **2012**, *28*, 16408–16422. [CrossRef] [PubMed]
6. Von Eiff, C.; Jansen, B.; Kohnen, W.; Becker, K. Infections Associated with Medical Devices. *Drugs* **2005**, *65*, 179–214. [CrossRef]
7. Tran, D.L.; Le Thi, P.; Thi, T.T.H.; Park, K.D. Graphene oxide immobilized surfaces facilitate the sustained release of doxycycline for the prevention of implant related infection. *Colloids Surf. B Biointerfaces* **2019**, *181*, 576–584. [CrossRef] [PubMed]
8. De Saravia, S.G.G.; Rastelli, S.E.; Angulo-Pineda, C.; Palza, H.; Viera, M.R. Anti-adhesion and antibacterial activity of silver nanoparticles and graphene oxide-silver nanoparticle composites. *Matéria (Rio Jan.)* **2020**, *25*. [CrossRef]
9. Kierys, A.; Sienkiewicz, A.; Grochowicz, M.; Kasperek, R. Polymer-amino-functionalized silica composites for the sustained-release multiparticulate system. *Mater. Sci. Eng. C* **2018**, *85*, 114–122. [CrossRef] [PubMed]
10. Ghilini, F.; Rodríguez González, M.C.; Miñán, A.G.; Pissinis, D.E.; Creus, A.H.; Salvarezza, R.C.; Schilardi, P.L. Highly Stabilized Nanoparticles on Poly-l-Lysine-Coated Oxidized Metals: A Versatile Platform with Enhanced Antimicrobial Activity. *ACS Appl. Mater. Interfaces* **2018**, *10*, 23657–23666. [CrossRef] [PubMed]
11. Alvarez-Lorenzo, C.; Garcia-Gonzalez, C.A.; Bucio, E.; Concheiro, A. Stimuli-responsive polymers for antimicrobial therapy: Drug targeting, contact-killing surfaces and competitive release. *Expert Opin. Drug Deliv.* **2016**, *13*, 1109–1119. [CrossRef] [PubMed]

12. Pinto, S.; Alves, P.; Matos, C.M.; Santos, A.C.; Rodrigues, L.R.; Teixeira, J.A.; Gil, M.H. Poly(dimethyl siloxane) surface modification by low pressure plasma to improve its characteristics towards biomedical applications. *Colloids Surf. B Biointerfaces* **2010**, *81*, 20–26. [CrossRef]
13. Felice, B.; Seitz, V.; Bach, M.; Rapp, C.; Wintermantel, E. Antimicrobial polymers: Antibacterial efficacy of silicone rubber–titanium dioxide composites. *J. Compos. Mater.* **2017**, *51*, 2253–2262. [CrossRef]
14. Alex, J.; González, K.; Kindel, T.; Bellstedt, P.; Weber, C.; Heinekamp, T.; Orasch, T.; Guerrero-Sanchez, C.; Schubert, U.S.; Brakhage, A.A. Caspofungin Functionalized Polymethacrylates with Antifungal Properties. *Biomacromolecules* **2020**, *21*, 2104–2115. [CrossRef] [PubMed]
15. Neu, H.C. Overview of mechanisms of bacterial resistance. *Diagn. Microbiol. Infect. Dis.* **1989**, *12*, 109–116. [CrossRef]
16. Pissinis, D.E.; Benítez, G.A.; Schilardi, P.L. Two-step biocompatible surface functionalization for two-pathway antimicrobial action against Gram-positive bacteria. *Colloids Surf. B Biointerfaces* **2018**, *164*, 262–271. [CrossRef] [PubMed]
17. Salomoni, R.; Léo, P.; Montemor, A.F.; Rinaldi, B.G.; Rodrigues, M.F.A. Antibacterial effect of silver nanoparticles in Pseudomonas aeruginosa. *Nanotechnol. Sci. Appl.* **2017**, *10*, 115–121. [CrossRef]
18. Petica, A.; Gavriliu, S.; Lungu, M.; Buruntea, N.; Panzaru, C. Colloidal silver solutions with antimicrobial properties. *Mater. Sci. Eng. B* **2008**, *152*, 22–27. [CrossRef]
19. Varaprasad, K.; Mohan, Y.M.; Ravindra, S.; Reddy, N.N.; Vimala, K.; Monika, K.; Sreedhar, B.; Raju, K.M. Hydrogel-silver nanoparticle composites: A new generation of antimicrobials. *J. Appl. Polym. Sci.* **2010**, *115*, 1199–1207. [CrossRef]
20. Sondi, I.; Salopek-Sondi, B. Silver nanoparticles as antimicrobial agent: A case study on E. coli as a model for Gram-negative bacteria. *J. Colloid Interface Sci.* **2004**, *275*, 177–182. [CrossRef] [PubMed]
21. Chutrakulwong, F.; Thamaphat, K.; Tantipaibulvut, S.; Limsuwan, P. In Situ Deposition of Green Silver Nanoparticles on Urinary Catheters under Photo-Irradiation for Antibacterial Properties. *Processes* **2020**, *8*, 1630. [CrossRef]
22. El-Shishtawy, R.M.; Asiri, A.M.; Abdelwahed, N.A.M.; Al-Otaibi, M.M. In situ production of silver nanoparticle on cotton fabric and its antimicrobial evaluation. *Cellulose* **2011**, *18*, 75–82. [CrossRef]
23. Niu, Y.; Guo, T.; Yuan, X.; Zhao, Y.; Ren, L.-X. An injectable supramolecular hydrogel hybridized with silver nanoparticles for antibacterial application. *Soft Matter* **2018**, *14*, 1227–1234. [CrossRef]
24. Kalaivani, R.; Maruthupandy, M.; Muneeswaran, T.; Hameedha Beevi, A.; Anand, M.; Ramakritinan, C.M.; Kumaraguru, A.K. Synthesis of chitosan mediated silver nanoparticles (Ag NPs) for potential antimicrobial applications. *Front. Lab. Med.* **2018**, *2*, 30–35. [CrossRef]
25. Fazly Bazzaz, B.S.; Khameneh, B.; Jalili-Behabadi, M.-M.; Malaekeh-Nikouei, B.; Mohajeri, S.A. Preparation, characterization and antimicrobial study of a hydrogel (soft contact lens) material impregnated with silver nanoparticles. *Contact Lens Anterior Eye* **2014**, *37*, 149–152. [CrossRef]
26. López-Barriguete, J.E.; Flores-Rojas, G.G.; López-Saucedo, F.; Isoshima, T.; Bucio, E. Improving thermo-responsive hydrogel films by gamma rays and loading of Cu and Ag nanoparticles. *J. Appl. Polym. Sci.* **2021**, *138*, 49841. [CrossRef]
27. Ping, X.; Wang, M.; Xuewu, G. Surface modification of poly(ethylene terephthalate) (PET) film by gamma-ray induced grafting of poly(acrylic acid) and its application in antibacterial hybrid film. *Radiat. Phys. Chem.* **2011**, *80*, 567–572. [CrossRef]
28. Liu, Y.; Chen, S.; Zhong, L.; Wu, G. Preparation of high-stable silver nanoparticle dispersion by using sodium alginate as a stabilizer under gamma radiation. *Radiat. Phys. Chem.* **2009**, *78*, 251–255. [CrossRef]
29. Pan, J.; Zhang, Z.; Zhan, Z.; Xiong, Y.; Wang, Y.; Cao, K.; Chen, Y. In situ generation of silver nanoparticles and nanocomposite films based on electrodeposition of carboxylated chitosan. *Carbohydr. Polym.* **2020**, *242*, 116391. [CrossRef] [PubMed]
30. Chen, Y.; Wang, C.; Ma, Z.; Su, Z. Controllable colours and shapes of silver nanostructures based on pH: Application to surface-enhanced Raman scattering. *Nanotechnology* **2007**, *18*, 325602. [CrossRef]
31. Pyatenko, A.; Yamaguchi, M.; Suzuki, M. Synthesis of Spherical Silver Nanoparticles with Controllable Sizes in Aqueous Solutions. *J. Phys. Chem. C* **2007**, *111*, 7910–7917. [CrossRef]
32. Akhavan, B.; Bakhshandeh, S.; Najafi-Ashtiani, H.; Fluit, A.C.; Boel, E.; Vogely, C.; Van Der Wal, B.C.H.; Zadpoor, A.A.; Weinans, H.; Hennink, W.E.; et al. Direct covalent attachment of silver nanoparticles on radical-rich plasma polymer films for antibacterial applications. *J. Mater. Chem. B* **2018**, *6*, 5845–5853. [CrossRef] [PubMed]
33. López-Saucedo, F.; Flores-Rojas, G.G.; Magariños, B.; Concheiro, A.; Alvarez-Lorenzo, C.; Bucio, E. Radiation grafting of poly(methyl methacrylate) and poly(vinylimidazole) onto polytetrafluoroethylene films and silver immobilization for antimicrobial performance. *Appl. Surf. Sci.* **2019**, *473*, 951–959. [CrossRef]
34. Pazos-Ortiz, E.; Roque-Ruiz, J.H.; Hinojos-Márquez, E.A.; López-Esparza, J.; Donohué-Cornejo, A.; Cuevas-González, J.C.; Espinosa-Cristóbal, L.F.; Reyes-López, S.Y. Dose-Dependent Antimicrobial Activity of Silver Nanoparticles on Polycaprolactone Fibers against Gram-Positive and Gram-Negative Bacteria. *J. Nanomater.* **2017**, *2017*, 4752314. [CrossRef]
35. Li, C.; Liu, M.; Yan, L.; Liu, N.; Li, D.; Liu, J.; Wang, X. Silver nanoparticles/polydimethylsiloxane hybrid materials and their optical limiting property. *J. Lumin.* **2017**, *190*. [CrossRef]
36. Kim, J.H.; Park, H.; Seo, S.W. In situ synthesis of silver nanoparticles on the surface of PDMS with high antibacterial activity and biosafety toward an implantable medical device. *Nano Converg.* **2017**, *4*, 33. [CrossRef] [PubMed]
37. Camacho-Cruz, L.A.; Velazco-Medel, M.A.; Parra-Delgado, H.; Bucio, E. Functionalization of cotton gauzes with poly(N-vinylimidazole) and quaternized poly(N-vinylimidazole) with gamma radiation to produce medical devices with pH-buffering and antimicrobial properties. *Cellulose* **2021**, *28*, 3279–3294. [CrossRef]

38. Audifred-Aguilar, J.C.; Pino-Ramos, V.H.; Bucio, E. Synthesis and characterization of hydrophilically modified Tecoflex® polyurethane catheters for drug delivery. *Mater. Today Commun.* **2021**, *26*, 101894. [CrossRef]
39. Cabana, S.; Lecona-Vargas, C.S.; Meléndez-Ortiz, H.I.; Contreras-García, A.; Barbosa, S.; Taboada, P.; Magariños, B.; Bucio, E.; Concheiro, A.; Alvarez-Lorenzo, C. Silicone rubber films functionalized with poly(acrylic acid) nanobrushes for immobilization of gold nanoparticles and photothermal therapy. *J. Drug Deliv. Sci. Technol.* **2017**, *42*, 245–254. [CrossRef]
40. Eisa, W.H.; Abdel-Moneam, Y.K.; Shaaban, Y.; Abdel-Fattah, A.A.; Abou Zeid, A.M. Gamma-irradiation assisted seeded growth of Ag nanoparticles within PVA matrix. *Mater. Chem. Phys.* **2011**, *128*, 109–113. [CrossRef]
41. Abedini, A.; Menon, P.S.; Daud, A.R.; Hamid, M.A.A.; Shaari, S. Radiolytic formation of highly luminescent triangular Ag nanocolloids. *J. Radioanal. Nucl. Chem.* **2015**, *307*, 985–991. [CrossRef]
42. Abedini, A.; Bakar, A.A.A.; Larki, F.; Menon, P.S.; Islam, M.S.; Shaari, S. Recent Advances in Shape-Controlled Synthesis of Noble Metal Nanoparticles by Radiolysis Route. *Nanoscale Res. Lett.* **2016**, *11*, 287. [CrossRef]
43. El-Batal, A.I.; Haroun, B.M.; Farrag, A.A.; Baraka, A.; El-Sayyad, G.S. Synthesis of Silver Nanoparticles and Incorporation with Certain Antibiotic Using Gamma Irradiation. *Br. J. Pharm. Res.* **2014**, *4*, 1341–1363. [CrossRef]
44. Siegel, J.; Lyutakov, O.; Polívková, M.; Staszek, M.; Hubáček, T.; Švorčík, V. Laser-assisted immobilization of colloid silver nanoparticles on polyethyleneterephthalate. *Appl. Surf. Sci.* **2017**, *420*, 661–668. [CrossRef]
45. Chen, P.; Song, L.; Liu, Y.; Fang, Y.-E. Synthesis of silver nanoparticles by γ-ray irradiation in acetic water solution containing chitosan. *Radiat. Phys. Chem.* **2007**, *76*, 1165–1168. [CrossRef]
46. Naghavi, K.; Saion, E.; Rezaee, K.; Yunus, W.M.M. Influence of dose on particle size of colloidal silver nanoparticles synthesized by gamma radiation. *Radiat. Phys. Chem.* **2010**, *79*, 1203–1208. [CrossRef]
47. Pal, S.; Tak, Y.K.; Song, J.M. Does the Antibacterial Activity of Silver Nanoparticles Depend on the Shape of the Nanoparticle? A Study of the Gram-Negative Bacterium Escherichia coli. *Appl. Environ. Microbiol.* **2007**, *73*, 1712–1720. [CrossRef]
48. Velazco-Medel, M.A.; Camacho-Cruz, L.A.; Bucio, E. Modification of PDMS with acrylic acid and acrylic acid/ethylene glycol dimethacrylate by simultaneous polymerization assisted by gamma radiation. *Radiat. Phys. Chem.* **2020**, *171*, 108754. [CrossRef]
49. Lee, J.N.; Park, C.; Whitesides, G.M. Solvent Compatibility of Poly(dimethylsiloxane)-Based Microfluidic Devices. *Anal. Chem.* **2003**, *75*, 6544–6554. [CrossRef] [PubMed]
50. Keshvari, H.; Ourang, F.; Mirzadeh, H.; Khorasani, M.T.; Mansouri, P. Collagen Immobilization onto Acrylic Acid Laser-grafted Silicone for Using as Artificial Skin: In Vitro. *Iran. Polym. J.* **2008**, *17*, 171–182.
51. Völcker, N.; Klee, D.; Höcker, H.; Langefeld, S. Functionalization of silicone rubber for the covalent immobilization of fibronectin. *J. Mater. Sci. Mater. Electron.* **2001**, *12*, 111–119. [CrossRef] [PubMed]
52. Drozdov, A.D.; Christiansen, J.D. The effects of pH and ionic strength on equilibrium swelling of polyampholyte gels. *Int. J. Solids Struct.* **2017**, *110*, 192–208. [CrossRef]
53. Pino-Ramos, V.H.; Flores-Rojas, G.G.; Alvarez-Lorenzo, C.; Concheiro, A.; Bucio, E. Graft copolymerization by ionization radiation, characterization, and enzymatic activity of temperature-responsive SR- g -PNVCL loaded with lysozyme. *React. Funct. Polym.* **2018**, *126*, 74–82. [CrossRef]
54. Akbey, Ü.; Graf, R.; Peng, Y.G.; Chu, P.P.; Spiess, H.W. Solid-State NMR investigations of anhydrous proton-conducting acid-base poly(acrylic acid)-poly(4-vinyl pyridine) polymer blend system: A study of hydrogen bonding and proton conduction. *J. Polym. Sci. Part B Polym. Phys.* **2009**, *47*, 138–155. [CrossRef]
55. González, A.L.; Noguez, C.; Beránek, J.; Barnard, A.S. Size, Shape, Stability, and Color of Plasmonic Silver Nanoparticles. *J. Phys. Chem. C* **2014**, *118*, 9128–9136. [CrossRef]
56. Yaqub Qazi, U.; Shervani, Z.; Javaid, R. Green Synthesis of Silver Nanoparticles by Pulsed Laser Irradiation: Effect of Hydrophilicity of Dispersing Agents on Size of Particles. *Front. Nanosci. Nanotechnol.* **2018**, *4*. [CrossRef]
57. Wijaya, Y.N.; Kim, J.; Choi, W.M.; Park, S.H.; Kim, M.H. A systematic study of triangular silver nanoplates: One-pot green synthesis, chemical stability, and sensing application. *Nanoscale* **2017**, *9*, 11705–11712. [CrossRef] [PubMed]
58. Ghorab, F.; Es'Haghi, Z.; Sheikh, N.; Akhavan, A. Gamma Irradiation Surface Modified Polypropylene-Based Hollow Fiber with Silver Nanoparticles and Its Impact on the Properties of Treated Membrane. *Plasmonics* **2019**, *14*, 1253–1260. [CrossRef]
59. Guzman, M.; Dille, J.; Godet, S. Synthesis and antibacterial activity of silver nanoparticles against gram-positive and gram-negative bacteria. *Nanomed. Nanotechnol. Biol. Med.* **2012**, *8*, 37–45. [CrossRef]
60. Dakal, T.C.; Kumar, A.; Majumdar, R.S.; Yadav, V. Mechanistic Basis of Antimicrobial Actions of Silver Nanoparticles. *Front. Microbiol.* **2016**, *7*, 1831. [CrossRef]
61. Khalandi, B.; Asadi, N.; Milani, M.; Davaran, S.; Abadi, A.J.N.; Abasi, E.; Akbarzadeh, A. A Review on Potential Role of Silver Nanoparticles and Possible Mechanisms of their Actions on Bacteria. *Drug Res.* **2016**, *67*, 70–76. [CrossRef]
62. Abbaszadegan, A.; Ghahramani, Y.; Gholami, A.; Hemmateenejad, B.; Dorostkar, S.; Nabavizadeh, M.; Sharghi, H. The Effect of Charge at the Surface of Silver Nanoparticles on Antimicrobial Activity against Gram-Positive and Gram-Negative Bacteria: A Preliminary Study. *J. Nanomater.* **2015**, *2015*, 720654. [CrossRef]
63. Pallavicini, P.; Dacarro, G.; Taglietti, A. Self-Assembled Monolayers of Silver Nanoparticles: From Intrinsic to Switchable Inorganic Antibacterial Surfaces. *Eur. J. Inorg. Chem.* **2018**, *2018*, 4846–4855. [CrossRef]
64. Raffi, M.; Hussain, F.; Bhatti, T.M.; Akhter, J.I.; Hameed, A.; Hasan, M.M. Antibacterial Characterization of Silver Nanoparticles against E. Coli ATCC-15224. *J. Mater. Sci. Technol.* **2008**, *24*, 192–196.

65. Bondarenko, O.; Ivask, A.; Käkinen, A.; Kurvet, I.; Kahru, A. Particle-Cell Contact Enhances Antibacterial Activity of Silver Nanoparticles. *PLoS ONE* **2013**, *8*, e64060. [CrossRef]
66. Taglietti, A.; Arciola, C.R.; D'Agostino, A.; Dacarro, G.; Montanaro, L.; Campoccia, D.; Cucca, L.; Vercellino, M.; Poggi, A.; Pallavicini, P.; et al. Antibiofilm activity of a monolayer of silver nanoparticles anchored to an amino-silanized glass surface. *Biomaterials* **2014**, *35*, 1779–1788. [CrossRef]
67. Taglietti, A.; Diaz Fernandez, Y.A.; Amato, E.; Cucca, L.; Dacarro, G.; Grisoli, P.; Necchi, V.; Pallavicini, P.; Pasotti, L.; Patrini, M. Antibacterial Activity of Glutathione-Coated Silver Nanoparticles against Gram Positive and Gram Negative Bacteria. *Langmuir* **2012**, *28*, 8140–8148. [CrossRef]
68. Holt, K.B.; Bard, A.J. Interaction of Silver(I) Ions with the Respiratory Chain of Escherichia coli: An Electrochemical and Scanning Electrochemical Microscopy Study of the Antimicrobial Mechanism of Micromolar Ag+. *Biochemistry* **2005**, *44*, 13214–13223. [CrossRef] [PubMed]
69. Cornejo-Bravo, J.M.; Palomino, K.; Palomino-Vizcaino, G.; Pérez-Landeros, O.M.; Curiel-Alvarez, M.; Valdez-Salas, B.; Bucio, E.; Magaña, H. Poly(*N*-vinylcaprolactam) and Salicylic Acid Polymeric Prodrug Grafted onto Medical Silicone to Obtain a Novel Thermo- and pH-Responsive Drug Delivery System for Potential Medical Devices. *Materials* **2021**, *14*, 1065. [CrossRef] [PubMed]
70. Pérez-Calixto, M.; Diaz-Rodriguez, P.; Concheiro, A.; Alvarez-Lorenzo, C.; Burillo, G. Amino-functionalized polymers by gamma radiation and their influence on macrophage polarization. *React. Funct. Polym.* **2020**, *151*, 104568. [CrossRef]
71. McBirney, S.E.; Trinh, K.; Wong-Beringer, A.; Armani, A.M. Wavelength-normalized spectroscopic analysis of Staphylococcus aureus and Pseudomonas aeruginosa growth rates. *Biomed. Opt. Express* **2016**, *7*, 4034–4042. [CrossRef] [PubMed]

Received: 13 December 2019 | Revised: 19 February 2020 | Accepted: 19 February 2020

DOI: 10.1002/mds3.10073

MINI-REVIEW

MEDICAL DEVICES & SENSORS WILEY

Modification of relevant polymeric materials for medical applications and devices

Marlene A. Velazco-Medel | Luis A. Camacho-Cruz | Emilio Bucio

Departamento de Química de Radiaciones y Radioquímica, Instituto de Ciencias Nucleares, Universidad Nacional Autónoma de México, Circuito Exterior, Ciudad Universitaria, México, México

Correspondence
Emilio Bucio and Luis A. Camacho-Cruz, Departamento de Química de Radiaciones y Radioquímica, Instituto de Ciencias Nucleares, Universidad Nacional Autónoma de México, Circuito Exterior, Ciudad Universitaria, México CDMX 04510, México.
Emails: ebucio@nucleares.unam.mx (EB); c-camacho-la@comunidad.unam.mx (LAC)

Abstract

The present review compiles different biomedical relevant polymers that have been modified to enhance their properties, giving hydrophilicity to their surfaces, antifouling properties to avoid bacterial adhesion, biocompatibility, incorporation of drug delivery systems and the improving of their mechanical properties to use them in the manufacturing of medical devices as prosthesis or implants, or other medical applications as wound dressers or scaffolds to cell culture. Other content of this work is a general description of the different techniques to modify and graft molecules, biomolecules and other polymers onto polymeric matrices in order to obtain high-performance biomaterials and medical devices.

KEYWORDS

biocompatibility, drug delivery, grafting, hydrophilicity, polymeric medical devices

1 | INTRODUCTION

Nowadays, it is important to create new materials to improve the quality of life for human health. The development of materials for medical applications is, undoubtedly, one of the most important research fields recently aiming at the production and modification of devices with new features or better properties.

One approach to enhance existing devices is their modification to provide them with additional properties, thus obtaining more sophisticated and useful devices to covering the basic needs of medical procedures. For the manufacturing of medical devices, it is important to take advantage of biocompatible components like polymers (Caló & Khutoryanskiy, 2015; Love, 2017; Maitz, 2015; Teo et al., 2016). Some polymeric materials make a possible wide range of examples used in medical device design, such a broad number of catheter-like devices, implants, gastric bags, valves, sutures and wound dressings. These materials are produced with different families of polymers, commonly called biocompatible polymers, which have been so versatile as to be successfully used as artificial organs and drug delivery systems (Gupta, Vermani, & Garg, 2002).

Many polymers are used in medicine; for example, natural polymers such as protein derivatives (collagen, gelatin or agar) and polysaccharides (chitosan, cellulose or trehalose), or synthetic polymers such as polyesters or polyurethanes. Many of these were initially developed as plastics, elastomers and fibres for non-medical applications. However, with the modification of these polymeric materials being aimed at improving the mechanical behaviour, antimicrobial and drug delivery properties, immunological acceptance, shelf life, and biocompatibility; these materials have rapidly dominated medical applications. With new developments, some of these medical materials have been modified with antimicrobial moieties to avoid microbe adhesion to avoid infections caused by bacterial growth on the polymer surface (Sun, Babar Shahzad, Li, Wang, & Xu, 2015).

Problems such as microbial contamination and low stability of polymeric devices have been confronted by adding components that prevent biofilm formation or by coupling drug delivery systems to existing polymeric substrates (Sall, Ayé, Bottzeck, Praud, & Blache, 2018; Schönemann et al., 2019; Utrata-Wesoek, 2013; Yu, Zhang, Wang, Brash, & Chen, 2011). Bacterial adherence to catheters or valves in treatments is one of the main causes of nosocomial disease; particullarly, infections caused by *Pseudomonas aeruginosa* or *Staphylococcus aureus* are common in hospital patients (Campoccia, Montanaro, & Arciola, 2013; Tunney, Gorman, & Patrick, 2002). Therefore, the surface modification of these polymeric materials made of poly(vinyl chloride) (PVC), polyurethane (PU) or polydimethylsiloxane (PDMS or silicone) is a strategy to avoid this problem

(Ikada, 1994; Uyama, Kato, & Ikada, 1998). Additional to this, protein-repellent surfaces have been very important for devices that come in contact with blood to prevent bacterial adhesion and thrombosis (Nagase & Horiguchi, 2011). Some examples of these modifications include the incrustation of antimicrobial nanoparticles (NPs) derived from metals (Cabana et al., 2017; López-Saucedo et al., 2018; López-Saucedo, Flores-Rojas, Magariños, et al., 2019; Palza, 2015) or the development of polymeric materials that include immobilized proteins or enzymes that also may offer bactericidal properties to the surfaces. For instance, lysozyme is the most commonly used enzyme to provide a high antimicrobial activity to materials (Flores-Rojas, López-Saucedo, Bucio, & Isoshima, 2017; Flores-Rojas, López-Saucedo, Quezada-Miriel, & Bucio, 2018).

Another important application is the crafting of drug delivery systems. Polymers with donor–acceptor hydrogen bond groups are used to bind drugs that can later be delivered to a specific environment by the action of stimuli-responsive polymers. These drug releases can be controlled either by diffusion or by a specific stimulus; for example, the pH sensibility of some derivatives from acrylates or amides causes changes to their chain conformations triggering the delivery of molecules occluded between polymer chains; a similar response is obtained with thermo-sensible polymers, where the collapse of chains is reached when temperature changes (Alvarez-Lorenzo, Garcia-Gonzalez, Bucio, & Concheiro, 2016; Gandhi, Paul, Sen, & Sen, 2015; López-Saucedo, Flores-Rojas, Meléndez-Ortiz, et al., 2019; Priya James, John, Alex, & Anoop, 2014).

Other varieties of polymers used for biomedical applications are used to produce artificial organs in tissue engineering and implant fabrication (Tang et al., 2014) by using polymers that favour cell growth. For this aim, polymers must interact with membrane proteins allowing for normal cell functions to be achieved even when cells interact with the polymer. In the last decade, tissue-engineering strategies repair and regeneration was revolutionized by the combination of stem cells with scaffold-based therapy; thereby, the research about polymers for scaffolds has achieved the creation of new biocompatible macromolecules. For bone tissues and cartilage, polymers such as collagen, chitosan, gelatin, cellulose and polycaprolactone have been modified with hyaluronic acid, polycarbonates and poly(lactic acid); there even exists metal prosthesis grafted with polymers that avoid biofilm formation (Orapiriyakul, Young, Damiati, & Tsimbouri, 2018).

In the case of the skin and wound dressings, the modification of polymer such as chitosan, poly(lactic acid), collagen, chondroitin sulphate and polyamides has been employed using different techniques. Currently, the inclusion of monomers with similar chemical properties to skin tissue has been tested, such is the case of zwitterionic polymers. The grafting of these systems has allowed for the creation of materials mimicking artificial skin or skin regeneration (Keshvari, Mirzadeh, Mansoori, Orang, & Khorasani, 2008; Salati, Keshvari, Karkhaneh, & Taranejoo, 2011; Tang et al., 2014). Stimuli-responsive polymers and hydrogels combined with biocompatible macromolecules are also used for skin regeneration. Self-healing polymers such as polyamide derivatives are grafted onto chitosan or hyaluronic acid due to its self-healing properties, giving a polymer used as a glue for wounds (Chattopadhyay & Raines, 2014). Most of the polymers mentioned before are extensively used, for their ease of processability, controllable mechanical properties, availability of reactive functional groups and minimal foreign body rejections.

All these novel applications and uses of polymers that have been achieved through chemical modification are extremely relevant to modern medicine, and this review intends to present recent advancement in this field. Table 1 shows a list of some of the different synthetic and natural polymers that have been modified to provide them with uses associated with medical applications and devices. In the following sections, highlights of modern applications of some of the most relevant polymeric materials are analysed individually to present a wider panorama of some of the applications of these materials.

2 | STIMULI-RESPONSIVE POLYMERS FOR MEDICAL APPLICATIONS

Stimuli-responsive or smart polymers cover those polymers that respond to a single or multiple physical or chemical stimulus such as pH, temperature, light intensity, ionic strength, electric or magnetic fields, and biochemical stimuli. These responses induce macroscopic effects in the material, such as polymer chain collapse, swelling, colour changes, solubility or solution-to-gel transitions depending on the physical and conformational state of polymer chains.

These kinds of polymers have been an interesting research field in the last decades as they possess properties that make them very promising materials for many applications. The introduction of these polymers in biomedicine has allowed for the creation of shape-memory polymers used in the preparation of minimally invasive surgical devices (Hardy, Palma, Wind, & Biggs, 2016), biosensors for clinical diagnosis (Adhikari & Majumdar, 2004), nanocarriers for drug delivery systems, wound repair helpers (Li et al., 2017), etc.

For example, pH-sensitive polymers suffer changes in the volume between their chains when the polymers are exposed to different pH values. This is due to electrostatic repulsion between charged groups, which promotes the increase in the free space between chains, allowing for better water absorption and increasing its water content capability. This behaviour is exploited for drug release taking advantage of the different pH environments in the gastric system. Figure 1 shows the response of acidic polymers in basic media; red balls represent molecules occluded in the polymer matrix before the pH changes. Several of these polymers have been grafted in other metallic and polymeric matrices to provide additional properties to other systems, even some polymers with dual response have been synthesized, with the use of monomers from different nature and sensible to distinct stimuli.

The combination of different smart polymers facilitates the fabrication of responsive hydrogels with desired properties. Hydrogels are 3D polymer-based systems that exhibit swelling properties and show

TABLE 1 Polymers with biomedical applications

Polymer	Medical application	References
Synthetic		
Polyethylene	• Orthopaedic implants • Catheters	Bongiovanni, Di Gianni, Priola, and Pollicino (2007), Gopanna, Rajan, Thomas, and Chavali (2019), Zhang et al. (2007), Zheng et al. (2016)
Expanded poly(tetrafluoroethylene)	• Suture • Catheters	Coad, Lu, and Meagher (2012), Jansen and Kohnen (1995), Liu, Munisso, et al. (2018), López-Saucedo, Flores-Rojas, Magariños, et al. (2019)
Polyamides	• Artificial skin • Suture • Orthopaedic implants • Tissue engineering • Drug delivery systems	Kumaresan, Gandhinathan, Ramu, Ananthasubramanian, and Pradheepa (2016), Shah Hosseini et al. (2018), Shrestha et al. (2016), Winnacker et al. (2019), Zhang et al. (2016)
Polypropylene	• Surgical suture fibres • Suture	Gopanna et al. (2019), López-Saucedo et al. (2017), López-Saucedo et al. (2018), RâpĂ, Matei, Ghioca, Cincu, and Niculescu (2016), Saxena et al. (2011)
Poly(ethylene terephthalate)	• Catheters • Vascular grafts • Suture	Li et al. (2007), Wang et al. (2007)
Polydimethylsiloxane derivatives	• Catheters • Intrauterine device • Gastric bag • Tubes • Valves	Abbasi et al. (2001), Alauzun et al. (2010), Cabana et al. (2017), Dong et al. (2011), Flores-Rojas et al. (2018), Frost, Reynolds, and Meyerhoff (2005)
Poly(methyl methacrylate)	• Dental implants • Contact lens	Miyashita et al. (2013), Rivkin (2014)
Polyurethane	• Short-term implant • Catheters	Ates, Koytepe, Karaaslan, Balcioglu, and Gulgen (2014), Barde et al. (2018), Roohpour et al. (2012)
Poly(vinyl chloride)	• Catheters • Valves	Asadinezhad et al. (2010), Lafarge, Kébir, Schapman, and Burel (2013), Meléndez-Ortiz et al. (2016), Zuñiga-Zamorano et al. (2018)
Polyalkylthiophenes	• Retinal prosthesis	Gautam and Narayan (2014), Manfredi, Colombo, Barsotti, Benfenati, and Lanzani (2019)
Poly(ethylene glycol)	• Drug delivery systems • Biocompatibility	Lee, Lee, Pyo, Park, and Lee (2010), McCullough and Yadavalli (2013), Winnacker et al. (2019)
Natural		
Protein derivatives (Collagen, gelatin, etc.)	• Biocompatibility	Copes, Pien, Van Vlierberghe, Boccafoschi, and Mantovani (2019), Highley, Prestwich, and Burdick (2016), Meyer (2019), Nishizawa, Takai, and Ishihara (2010)
Polysaccharides derivatives (Cellulose, poly(lactic acid), etc.)	• Drug delivery systems • Wound dressers • Suture	Alauzun et al. (2010), Alvarez-Lorenzo, Bucio, Burillo, and Concheiro (2010), Bergström and Hayman (2016), Cingolani et al. (2018), Concheiro and Alvarez-Lorenzo (2013), de Oliveira Barud et al. (2016), Pillai and Sharma (2010)

a tendency to adsorb water. Hydrogels based on stimuli-responsive polymers are interesting for biomedical applications because they can swell and release molecules in situ under physiological environments (Feksa et al., 2018; Hoare & Kohane, 2008; Vashist, Vashist, Gupta, & Ahmad, 2014). Also, due to their porosity and soft consistency, they closely simulate natural living tissue, more so than any other class of synthetic biomaterials (Holback, Yeo, & Park, 2011).

Other biomedical applications of hydrogels are the preparation of pharmaceutical formulations such as carriers or excipients (Peppas, 2000), and even some commercially available products (Caló & Khutoryanskiy, 2015; Cascone & Lamberti, 2019).

As we mentioned above, the introduction of stimuli-responsive polymers in polymeric matrices provides additional properties to the initial matrix. Synthetic and natural polymers have been modified with these smart materials as seen in Table 2. It is important to mention that the introduction of these materials can be via covalent or non-covalent means.

3 | POLYURETHANES

Polyurethanes (PUs) are commonly used for the manufacturing of biocompatible devices such as heart valves, wound dressings and catheters that are in direct contact with blood and exposed skin. Polyurethanes are widely used in the manufacturing of implants and prostheses in tissue engineering. Polyurethane is a polymer with alternated urethane groups in their structure, and the chemical composition of the urethane functional group and one variation of polyurethane are represented in Figure 2.

Different varieties of polyurethanes have been modified to provide them with additional properties; for example, the synthesis of

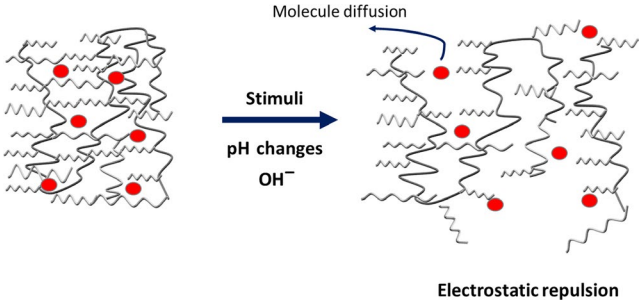

FIGURE 1 Polymer chain repulsion due to the electrostatic charges in the basic groups and molecule diffusion outside the polymer matrix

chitin- and chitosan-based polyurethanes has been explored. The introduction of chitin/chitosan segments into the polymer structure provides biocompatibility to the materials, which allows for some of their applications to be in wound healing, wound dressing, antibacterial coatings, tissue engineering scaffolds and drug delivery systems (Mahanta et al., 2015; Usman et al., 2016).

The modification of PU with these polymers has been performed by conventional chemistry, using coupling reactions (Liu, Munisso, et al., 2018), free-radical polymerization (Calvete, Holguín, & Luna, 2015), plasma-induced polymerization (Fujimoto, Inoue, & Ikada, 1993; Myung, Yeom, Jang, Choi, & Cho, 2005; Shourgashti, Khorasani, & Khosroshahi, 2010), UV radiation (Zia, Zuber, Mahboob, Sultana, & Sultana, 2010) and with other non-conventional mechanisms (Guan, Gao, Feng, & Sheng, 2000).

The surface modification of PUs for medical purposes has been directed towards increasing the biocompatibility, enzyme immobilization or cell adhesion (Ahmad, 2018; Wang & Wang, 2012). Small molecules, peptides and other polymers have been grafted into different variations of polyurethane matrices. For example, segmented

TABLE 2 Some stimuli-responsive polymers with potential biomedical applications

Polymer	Biomedical application	References
Temperature-sensitive polymers		
• Poly(*N*-substituted acrylamide) • Poly(vinyl amide) • Poly(vinyl ether)s • Poly(*N*-vinylcaprolactam)	These polymers are sensitive to the temperature and change their microstructural features in response to change in temperature. These polymers present a critical solution temperature	Almeida, Amaral, and Lobão (2012), Gandhi et al. (2015), Klouda (2015), Schmaljohann (2006)
pH-sensitive polymers		
Polyacid: • Poly(acrylic acids) • Poly(methacrylic acids) • Polybasic • Poly(N-dialkylaminoethyl methacrylate) • Poly(ethyl pyrrolidine methacrylate) • Poly(4-vinyl pyridine)	Polymers that can swell or dilute at changes in the pH, taking advantage of the differences in pH that occur at several body sites, being capable to respond to metabolic states and/or physiological variations	Fundueanu, Constantin, Bucatariu, and Ascenzi (2017), Kamoun et al. (2018), Kyriakides et al. (2002)
Photosensitive polymers		
Chomophores attached to polymers • Azobenzenes • Spiropyran • *o*-nitrobenzyl derivatives • 2-naphtoquinone-3-methides	Materials that response to light, at different wavelength triggering changes in the macromolecular structure allowing changes in the absorption spectra and colour	Aguilar and San Román (2014)
Polymer hydrogels		
• Poly(acrylates) • Chitosan derivatives • Poly(*N*-substituted acrylamides) • Poly(ethylene glycol) derivatives • Poly(2-hydroxyethyl methacrylate) • Poly(vinyl alcohol) • Gelatin	Hydrogels that exhibit swelling properties and show a high tendency to adsorb water	Anirudhan, Divya, and Nima (2016), Huang et al. (2018), Lee, Lee, Le Thi, Oh, and Park (2018), Pellá et al. (2018), Tu et al. (2019)
Shape-memory polymers		
• Poly(ethylene glycol) diacrylate (PEGDA) hydrogel onto a poly(DL-lactide-co-glycolide) (PLGA) blend • Gelatin	These materials can fix one or more temporary shapes and recover to their remembered permanent shape under suitable stimuli	Korde and Kandasubramanian (2020), Liang et al. (2019)
Self-healing polymers		
• Poly(amide)s derivatives • Ureidopyrimidinone (UPy)-type polymers	Materials that present self-repair properties due to the physical and chemical properties of the functional groups present in the polymeric matrix, favoured by supramolecular interactions	Campanella, Döhler, and Binder (2018), Duan (2015), Lim, Lin, Xue, and Loh (2019), Phadke et al. (2012), Qian et al. (2019)

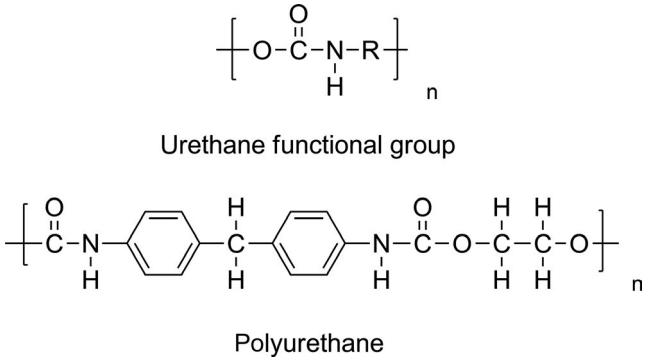

FIGURE 2 Urethane and polyurethane structures

poly(ester-urethane) (SPEU) was modified with poly(ethylene glycol) (PEG) via condensation and Michael addition reactions using chemical linkers to favour PEG attach, and the final SPEU-PEG, represented in Figure 3, demonstrated improved resistance to protein adsorption and good resistance to platelet adhesion, indicating enhanced surface haemocompatibility (Liu, Munisso, et al., 2018).

There exist other studies about modified PU with different polymers, such as acrylic acid (AAc) (Butruk-Raszeja, Trzaskowska, Kuźminska, & Ciach, 2016; Myung et al., 2005), gelatin (Losi et al., 2015), 2-hydroxyethyl acrylate (HEA) (Guan et al., 2000), poly(ethylene oxide) (Han, Park, & Kim, 1998) and polydimethylsiloxane (Pinchuk, Martin, Esquivel, & Macgregor, 1988; Shourgashti et al., 2010), used for medical applications. As it is the case of the HEA grafted PU were proved as scaffold for the promotion of human endothelial cell adhesion and growth.

4 | POLYETHYLENE AND POLYPROPYLENE

Polyethylene and polypropylene (PE and PP) (Figure 4) are the least complex polymeric materials as they are made from very simple aliphatic vinylic compounds. Depending on the polymerization methodology, these materials may be produced with many different properties, which may be useful in many contexts. Due to their aliphatic nature, these polymers are very hydrophobic, which limits their applications on medical devices. However, both polymers are very important as materials for bone implants. Many of the modifications of these materials are then aimed at improving their hydrophilicity (Kissin, 2012; Maier & Calafut, 1998).

An important example of polyethylene and propylene modification has been the grafting of hydrophilic of functional molecules onto this substrate by the exposure of a PE or PP film to either high-energy electrical discharges or ionizing radiation to produce reactive groups that can be later reacted with functional molecules or with additional monomers to produce covalently bound surfaces. Through this procedure, PE has been previously grafted with poly(acrylamide) and poly(2-bromoethylacrylate) to form hydrophilic and charged PE films (Bucio & Burillo, 1996; Suzuki, Kishida, Ikada, & Iwata, 1986). PP has also been modified through a two-step procedure to graft acrylic acid to further modify the substrate with biopolymers such as chitosan and cellulose, and *N*-isopropylacrylamide with acrylic acid by these types of procedures to obtain materials that have pH and thermal sensitivity or that may act as metal ion adsorbents (Hernández-Aguirre, Núñez-Pineda, Tapia-Tapia, & Espinosa, 2016; Ramírez-Fuentes, Bucio, & Burillo, 2007). Some of these examples are illustrated in Figure 5.

An additional example of the modification of PE was the impregnation of gentamicin-loaded chitosan onto porous UHMWPE (ultra-high-molecular-weight polyethylene) for sustain release of this drug in implants used for hip replacement (Manoj Kumar et al., 2017). On the other hand, for PP modification, layer-by-layer plasma-enhanced chemical vapour deposition has been successfully used to deposit hydrophilic substrates such as carboxylic acid groups from the decomposition of anhydrides, or positively charged amines. The deposited substrates in this work were crafted as polyelectrolytes to increase the hydrophilicity of the samples and to allow for further modification of the films with functional molecules (Hachim & Brown, 2018).

5 | POLYDIMETHYLSILOXANE

Polydimethylsiloxane (PDMS) is an organosilicon polymer, which is also commonly known as silicone rubber, and its general structure is

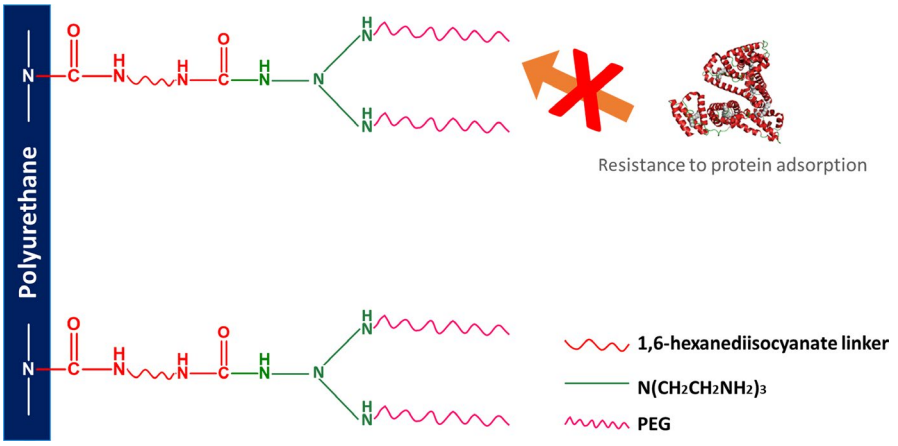

FIGURE 3 Representation of the grafting PEG onto SPEU synthesized by Liu, Munisso, et al. (2018) for avoiding protein adsorption improving haemocompatibility

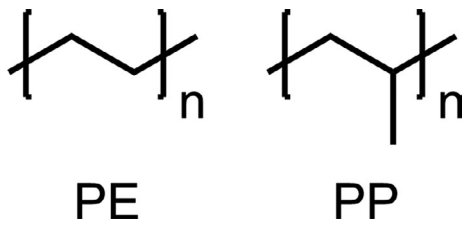

FIGURE 4 Representation of polyethylene and polypropylene

represented in Figure 6. The development of biomedical devices and materials based on PDMS has been vastly explored due to its high biocompatibility, hydrophobicity and useful mechanical properties such as its glass transition temperature (T*g*) and high moduli (Abbasi, Mirzadeh, & Katbab, 2001). In addition, some modifications have been carried out to PDMS to improve its characteristics and uses (Li et al., 2012), and these modifications have been achieved using different techniques, such as conventional chemical reactions (Alauzun et al., 2010; Mazumder, 2017; Wei, Bai, & Shao, 2008), plasma-induced polymerization (Lee, Hsiue, & Kao, 1996; Salati et al., 2011) and ionizing radiation (Flores-Rojas et al., 2018; Pino-Ramos, Flores-Rojas, Alvarez-Lorenzo, Concheiro, & Bucio, 2018; Xiong et al., 2015) among others.

For biomedical purposes, several synthetic and natural polymers, peptides and small molecules have been attached to PDMS matrices and films. For example, surface modification to avoid biofilm formation has been explored, the addition via *grafting* of stimuli-responsive polymers such as acrylates derivatives, poly(ethylene glycol), acrylamide derivatives or *N*-vinyl caprolactam to favour the metal nanoparticle immobilization or the antimicrobial drugs delivery (Cabana et al., 2017; Cao, Wu, Wang, Shi, & Li, 2018; Lee & Vörös, 2005; Li, Zhai, Yi, Gao, & Ha, 1999; Li et al., 2012; Melendez-Ortiz, Alvarez-Lorenzo, Concheiro, & Bucio, 2015; Völcker, Klee, Höcker, & Langefeld, 2001).

Skin mimicking is one challenge of tissue engineering for transplants and wound repair; for this aim, silicone has been modified to take advantage of its biocompatibility. A zwitterionic-type polymer was grafted onto silicone surface using ozone-induced radical polymerization. The addition of *N*,*N*-dimethyl-*N*-methacryloyloxyethyl-*N*-(3-sulfopropyl) ammonium (SBMA) as it is represented in Figure 7 provides haemocompatibility due to its ionic character and the sulphonate group in its structure, and it also rejected platelet adhesion to avoid blood coagulation and thrombosis around this material (Yuan et al., 2004). The same material was prepared by Cao and coworkers in 2018 using vacuum ultraviolet (VUV) irradiation to graft SBMA with a cross-linking agent to obtain a 3D comb-like layer onto the silicone surface that exhibits better hydrophilic stability, antibacterial adhesion properties and biocompatibility due to better coverage of the surface. Additionally, Cabana et al. (2017) grafted acrylic acid onto silicone using gamma radiation, and the resulting PDMS-*g*-AAc demonstrates good gold nanoparticles loading, obtaining an antifouling material used for photothermal therapy.

Other biocompatible molecules and peptides have been attached on the PDMS surface in order to simulate the human skin, and some of them are hyaluronic acid, chitosan, gelatin and collagen (Alauzun et al., 2010; Mazumder, 2017; Yue, Liu, Molino, & Wallace, 2011); these immobilizations have been made using other polymers to attach them or they are directly covalent bonded to the PDMS matrix.

Polyacrylic acid (PAAc) has been grafted onto silicone to provide hydrophilicity to the surface, and for its acid-base behaviour, the functional groups allow the drug or metal nanoparticles loading. Collagen was immobilized onto acrylic acid grafted into silicone, and this material was evaluated as artificial skin (Keshvari et al., 2008); a chitosan/gelatin mixture was covalently bonded to carboxylic groups of PAAc mimicking artificial skin too (Salati et al., 2011).

6 | ACRYLIC POLYMERS

Acrylic polymers are macromolecules that are formed mainly by the acrylate or methacrylate functional group (Figure 8). These polymers tend to form a versatile set of materials, which also exhibit great biocompatibility, and thus are used extensively on medical applications (Serini, 2012).

The uses of acrylic polymers include scaffold materials for tissue growth, adhesives for the treatment of wounds, cement-like materials for bone prostheses and materials for the fabrication of

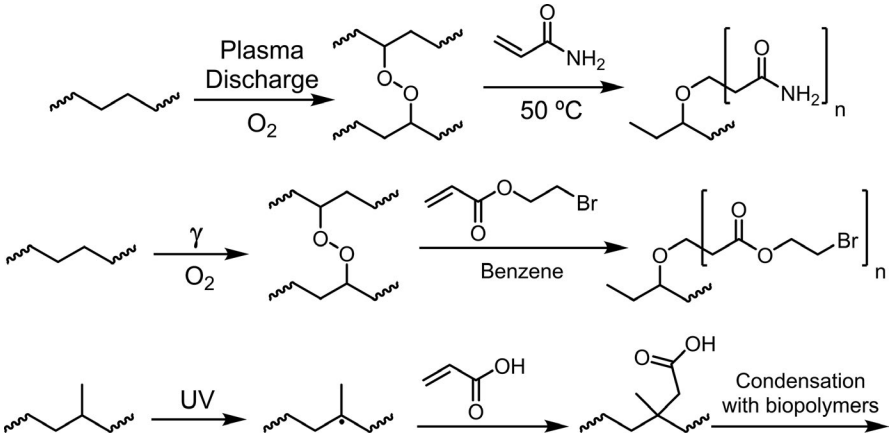

FIGURE 5 Examples of PE/PP modification for biomedical applications

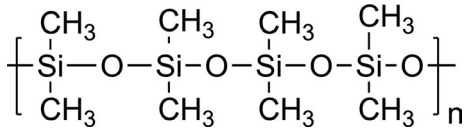

FIGURE 6 General structure of polydimethylsiloxane

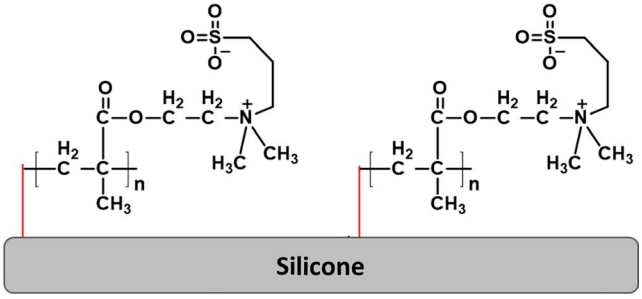

FIGURE 7 PDMS-*g*-SBMA with haemocompatibility and low protein adhesion, and the red line represents the different initiators used in any work

contact lenses. These materials are convenient and are readily used in current medical treatments; however, many efforts have arisen to modify the properties of these materials mainly to improve biocompatibility, mechanical resistance or antibacterial properties. In this section, a compilation of recent developments in the modification of acrylic materials is presented (Serrano-Aroca, 2017).

6.1 | Improvements for bone cement

Bone cement is a necessary component for filling the space between prosthesis and the surrounding bones. The most common formulation of bone cement is a 1:2 mixture of poly(methyl methacrylate) (PMMA) and liquid MMA with a polymerization initiator (Benzoyl peroxide) to promote curing (Román, Vázquez Lasa, Aguilar, & Boesel, 2008; Serrano-Aroca, 2017). This is a very resourceful formulation; however, the polymerization of MMA releases big amounts of heat, and bone cement does not bind permanently to bone and tends to loosen or break over time. To improve the mechanical properties of these materials, many classical bone cement formulations include fibres, ceramics or metal particles as filling materials to form composites. However, recently, the addition of chemical agents or the copolymerization of MMA with functional monomers to improve both mechanical properties and biocompatibility has been an area of great interest. For instance, MMA and other polyfunctional acrylic monomers have been copolymerized with thiol groups of hydroxylamine groups as cross-linking groups that may improve the mechanical properties of the acrylic materials (Ciucurel & Sefton, 2011; Forghani et al., 2018).

Another development is the inclusion of filling materials that have been chemically modified or that include chemical compounds that may improve the mechanical properties of the cement. For example, PMMA has been modified with strontium-doped calcium polyphosphate properties coated with polydopamine to promote bone growth and to improve the binding ability of calcium polyphosphate to PMMA (Liu et al., 2019). Another example of the modification of these materials is the encapsulation of octyl cyanoacrylate adhesive into polyurethane to include this adhesive as an extra curing material onto PMMA bone cement (Brochu, Chyan, & Reichert, 2012).

Finally, some developments have sought to reduce the polymerization temperature of the bone cement mixture. For example, by including poly(ethylene glycol) (PEG) to the blend, the heat of polymerization is absorbed by the PEG, reducing the overall temperature of the treatment (Król & Pielichowska, 2016).

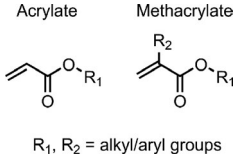

FIGURE 8 Acrylate and methacrylate functional groups

6.2 | Cyanoacrylate-adhesive modification

Cyanoacrylate-based adhesives, also known as 'super-glues', are polymers best known for their strong adhesive force after curing, which are useful in binding damaged tissues without the use of stitching. These materials have been used in medicine extensively because of their practicality and biocompatibility. Although the most common poly(cyanoacrylate) adhesives are composed of *n*-butyl cyanoacrylate or ethyl cyanoacrylate, medical cyanoacrylates are also typically composed of polymers, copolymers or blends of longer-chained cyanoacrylates. Usual developments on the modification of these materials include the copolymerization and blending of pure cyanoacrylate adhesives with other compounds to adjust curing times or to give specific properties to the adhesives (Leggat, Smith, & Kedjarune, 2007; Pascual et al., 1999). A classic example of these modifications is the development of radiopaque cyanoacrylate, which is produced by mixing isobutyl cyanoacrylate with iodophendylate to lengthen the curing time and to produce a radiopaque material for tracking therapeutic embolisms (Cromwell & Kerber, 1980).

6.3 | Modifications for antibacterial properties

Antibacterial properties of acrylic polymers for their direct use for implants and coatings have been researched thoroughly as acrylic polymers are intrinsically good substrates for bacterial adhesion and the formation of harmful bacterial biofilms. Typical modification of acrylic materials for antibacterial purposes is performed by chemical impregnation or copolymerization of antibacterial substances onto acrylic polymers (Gîfu et al., 2019; Wang et al., 2018; Zhou et al., 2019). One example of this is the functionalization of MMA with borneol acrylate to produce a copolymer for implants; in this work, the authors determined the excellent capability of the

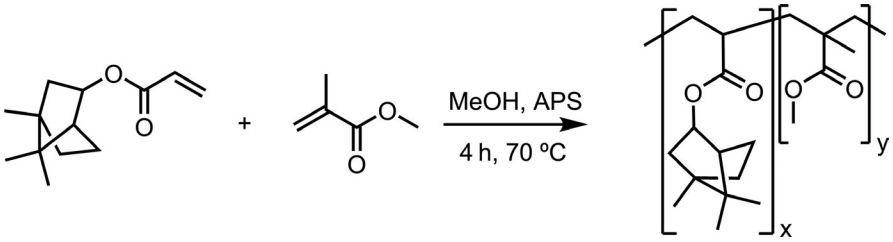

FIGURE 9 Copolymerization of MMA with borneol acrylate

substrate to stop the adhesion of both Gram-negative and Gram-positive bacteria while still retaining biocompatibility for the use of implants, and this reaction is illustrated in Figure 9 (Sun et al., 2016).

6.4 | Other modifications

The modification of acrylic polymers has also had other applications in mind. A notable example is the modification of these materials to promote tissue growth. For example, Más Estellés and collaborators have produced porous materials for tissue engineering by synthetizing cross-linked poly(ethyl acrylate) with ethylene glycol dimethacrylate using compressed Nylon 6 fibres as templates (Más Estellés, Krakovsky, Rodríguez Hernández, Piotrowska, & Monleón Pradas, 2007).

Further modifications of these materials include its uses in ophthalmology where acrylic materials have been often used as substrates for corneal implants or intraocular lenses. In the first field, PMMA for corneal prosthesis was produced by the grafting of (3-aminopropyl)triethoxysilane on PMMA and the functionalization of the dangling amine groups of (3-aminopropyl)triethoxysilane with collagen to increase the biocompatibility of PMMA as core material for the prosthesis (Riau et al., 2015). Another example was the copolymerization of MMA with allyl POSS–PMMA to improve adhesion of human lens epithelial cells after intraocular lens implant to improve the performance and durability of these medical devices (Wang et al., 2014).

7 | POLY(TETRAFLUOROETHYLENE)

Poly(tetrafluoroethylene) (PTFE) is a fluoropolymer (see Figure 10) used for the manufacturing of medical devices due to its inert, transparent and non-toxic characteristics; additionally, it possesses high thermal stability, low friction coefficient and high resistant to UV radiation. This material is usually used for catheters and coating of other materials.

One variety of PTFE is the expanded PTFE (ePTFE) that refers to the mechanical state of the material involving an expansion process, and this variety of PTFE has many medical applications in the development of prosthesis, surgical membranes, medical tubing and stents (Ebnesajjad, 2017; Kajiwara, Hamada, Ichikawa, Ishi, & Yamazaki, 2004).

Both PTFE variations have been modified to add additional characteristics, increase the hydrophilicity and favour cell adhesion. Different techniques are employed to graft other molecules or polymers onto the PTFE surface, for instance plasma, radiation or conventional chemistry. The need of modification of this material is because it may induce thrombosis and intimal hyperplasia due to the lack of an endothelial cell layer (Noh, Baik, Noh, Park, & Lee, 2007; Ren et al., 2015; Tu, Liu, Lee, & Lai, 2005).

Polymers such as PAAc or PEG are used to provide biocompatible features to the PTFE matrix, and the PTFE surface grafted with a high density of PEG has proven to be effective in preventing the adhesion of proteins (Wang & Chen, 2007; Wang, Tan, & Kang, 2000; Zhang et al., 2002). The PEG-grafting reaction onto PTFE was carried out by different techniques, one of the most used is the plasma-induced polymerization; Wang and coworkers 2000 made a PTFE pre-treatment with Ar plasma and subsequently exposure to atmospheric air to form peroxides and hydroperoxides onto the surface, and the peroxide decomposition was activated using UV-induced graft copolymerization, as it is represented in the Figure 11.

The resulting PTFE-*g*-PEGMA decreases protein adsorption, and the effect of protein inhibition is higher when the PEG chain is longer. Another approach to biocompatibility is protein graft; Löhbach et al. (2002) modified PTFE with proteins such as gelatin, fibronectin, *Yersinia enterocolitica* invasin fragment and collagen as cell receptors by covalent bonds; the protein grafting was performed using chemical reactions; the oxidation of the polymer was carried out with an H_2O_2/H_2SO_4 mixture, and then, a nucleophilic reaction allowed the bond formation between a cross-linking agent and the protein; and cell growth was successfully in the PTFE modified with the different proteins compared with the unmodified PTFE.

Following the same objective, the endothelial cell affinity was reached with the modification of PTFE with polar oxygenated and nitrogenated groups using NH_3 flow during UV radiation, and the results showed high cell proliferation when the UV exposure was higher (Gumpenberger et al., 2003). Other successful results that achieved endothelial cell adhesion involve the modification of PTFE

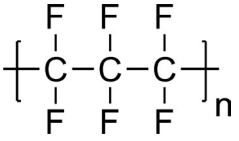

FIGURE 10 Poly(tetrafluoroethylene) structure

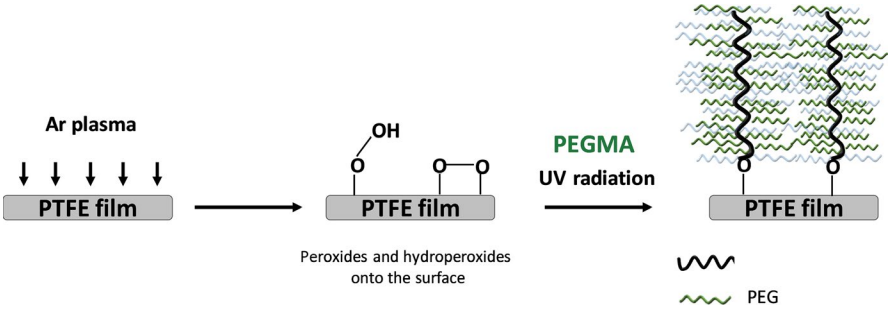

FIGURE 11 PEG plasma/UV-induced graft copolymerization onto PTFE surface

with bioactive molecules such as an arginine–glycine–aspartic acid segment (RGD) and heparin. The grafting reaction consisted of many steps including oxygen plasma treatment, dopamine coating, polyethyleneimine grafting, and RGD or RGD/heparin immobilization. Very favourable effects on endothelial cell attachment, viability and proliferation were obtained due to strong cell–substrate interactions between cells and the peptide (Mi, Jing, Thomsom, & Turng, 2018).

Regarding the prevention of biofilm formation, antimicrobial agents and polymers have been grafted in PTFE films. López-Saucedo, Flores-Rojas, Magariños, et al. (2019) used radiation grafting to add binary copolymer from poly(methyl methacrylate) and poly(vinyl imidazole) for silver immobilization, and the incorporation of silver nanoparticles to the system improves the antimicrobial performance of the modified films against *S. aureus* or *E. coli*.

8 | POLY(VINYL CHLORIDE)

Poly(vinyl chloride) (PVC) (Figure 12) is one of the most used polymers due to its ease of production, low cost and excellent mechanical properties that can be modulated to produce materials with varying characteristics. In the medical industry, PVC is the most used polymeric material because it shows good biocompatibility and its physical properties have been very practical for producing medical devices such as drip chambers, face masks, bags for intravenous fluids and especially plastic tubing for both intravenous and urinary catheters (Hong, 1996).

Although PVC is very useful for medical applications, some issues still exist that have prompted for many researches in improving this polymeric material. For instance, one of the main concerns about the use of commercially available PVC is the inclusion of plasticizers and thermal stabilizers to the material (Navarro et al., 2016). Even when these components are essential for obtaining PVC with usable characteristics, most of these materials may leak into physiological fluids and present a health hazard. Another issue with pure PVC is that this polymer is highly hydrophobic, which may present a challenge with the interactions of PVC with human tissue and may promote the adhesion of proteins and the formation of biofilms onto the substrate. Many modifications of PVC have already been reported in well-documented reviews; therefore, in this review we present some examples from the last decade (Asadinezhad, Lehocký, Sáha, & Mozetič, 2012).

The modification of PVC to improve its antibacterial properties has been achieved through a variety of methods. For example, films composed of a blend of PVC and poly(vinyl acetate) have been produced by typical casting methods and have been mildly effective in inhibiting the growth of Gram-negative bacteria, yeasts and fungi (Abdelghany, Meikhail, & Asker, 2019). Another example of this is the modification of PVC by grafting of quaternized *N*-vinylimidazole by using gamma radiation (Figure 13). This modification was effective in inhibiting the growth of *S. aureus* (Meléndez-Ortiz, Alvarez-Lorenzo, Concheiro, Jiménez-Páez, & Bucio, 2016).

Additional modifications of PVC have had the objective to increase the hydrophilicity of the polymer substrate (Lăzăroaie, Rusen, Mărculescu, Zecheru, & Hubcă, 2010; Tooma et al., 2015). A notable example of these modifications is the modification of PVC with thiosulphate and thiourea via a nucleophilic substitution reaction. This modification was carried out both to evaluate antimicrobial properties of the material and to evaluate improved biocompatibility of modified PVC with human cells (Monika et al., 2015).

9 | POLYCARBONATES

Polycarbonate polymers (PC) are a very important substrate in polymer chemistry due to its good mechanical properties, its good thermal stability, their resistance to hydrolysis, their resistance to gamma radiation (used for sterilization) and their convenient optical properties. These polymers contain a carbonate functional group as seen in Figure 14 and may include any series of functional groups depending on its formation (NIIR Board of Consultants & Engineers, 2006).

Polycarbonate substrates are usually used in housing and tubing of medical equipment, especially in equipment that is used in blood filters, in blood oxygenators and overall tubing that aids in surgical

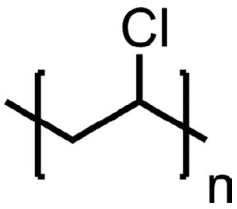

FIGURE 12 Polymeric structure of PVC

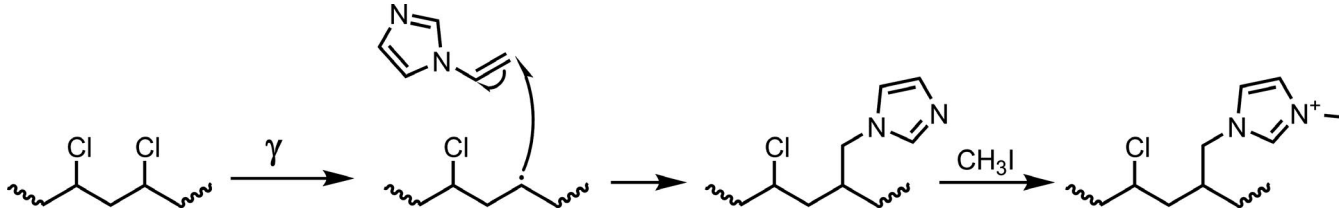

FIGURE 13 Grafting of poly(*N*-vinylimidazole) onto PVC

procedures. As most of these uses require sterile materials, many PC medical devices are sterilized via gamma radiation or exposure to Et_2O; however, contamination after sterilization is not accounted for. Therefore, many of the advancements in PC modification are for antibacterial purposes (Mahendran, Sridharan, Arunmozhidevan, Selvakumar, & Rajasekar, 2016; Rogalsky, Moshynets, Lyoshina, & Tarasyuk, 2014). An important example of this is the inclusion of positively charged amines into specially designed PCs because these approaches have shown to be particularly effective at creating antibacterial surfaces. These custom PCs were prepared by ring-opening polymerization as seen in Figure 15 (Nimmagadda et al., 2017). With this procedure, it was possible to obtain both random and di-block copolymers. Following these advancements, similar works have emerged seeking antibacterial properties via the formation of charged macromolecules (Chin et al., 2018).

Another interesting example of polycarbonate is the nitration of Bisphenol-A polycarbonate (PC BPA) with nitric acid followed by a reduction to form amine groups on the PC to form microprojection arrays capable of detecting biomarkers in vitro and in vivo (Figure 16) (Yeow et al., 2013).

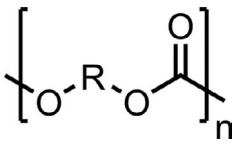

FIGURE 14 Base structure of a polycarbonate

10 | POLYAMIDES

Polyamides are another family of polymers that are produced through polycondensation of diamines with dicarboxylic acids or diacyl halides. Aliphatic polyamides are also typically called 'nylons', and aromatic polyamides are typically called 'aramides'. Nylons (Figure 17) have convenient elastic properties, very good mechanical properties and may be used in biomedical devices because of their biocompatibility as they contain the amide bond that is also naturally present in proteins (proteins are therefore also polyamides). Common uses of nylons on medical devices include filling materials for composites in dental and implant materials and use as membranes, and matrices or scaffolds for cell adhesion. Additionally, nylon fibres are commonly used as suture materials. For both applications, control of polyamide folding and hydrophilicity, and antibacterial properties are very important (Winnacker, 2017). Several reviews have already been crafted that deal with the modification of polyamides with different objectives (Nagase & Horiguchi, 2011; Shmack, Dutschk, & Pisanova, 2000; Winnacker, 2017); therefore, only one recent example of the modification of polyamides is hereby

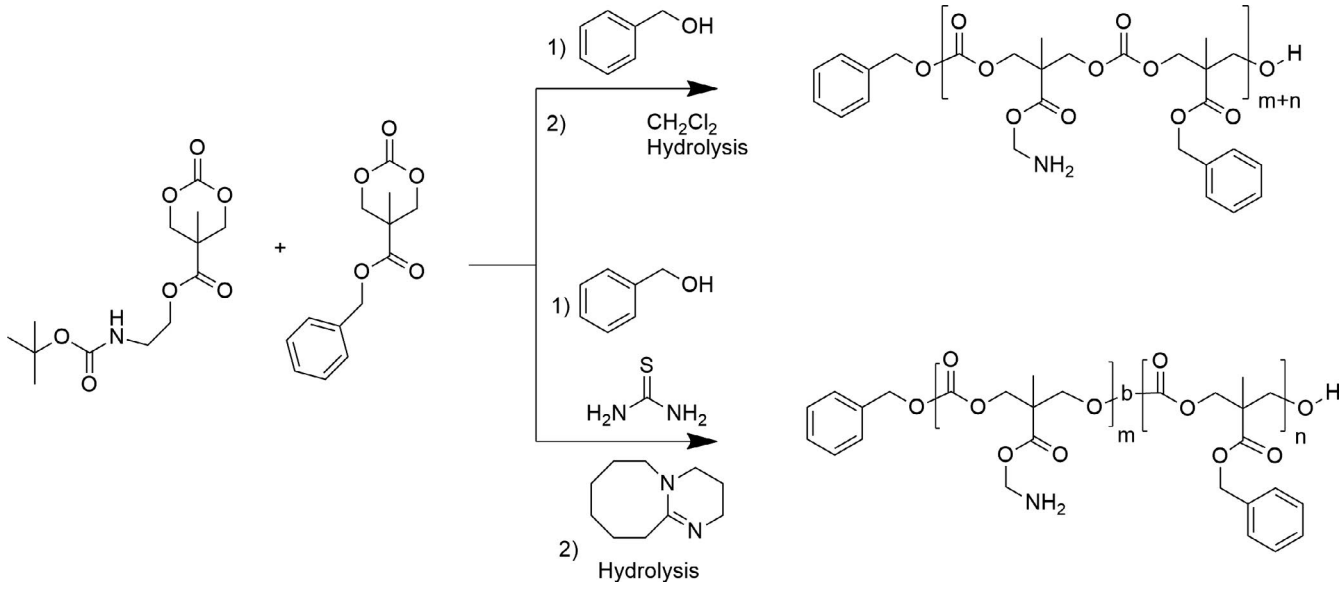

FIGURE 15 Ring-opening polymerization for the formation of PC copolymers

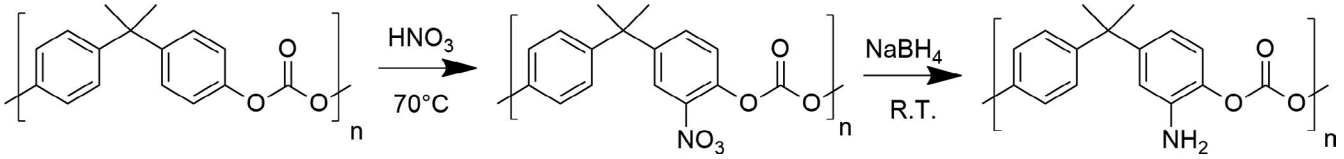

FIGURE 16 Modification of PC BPA with amine groups

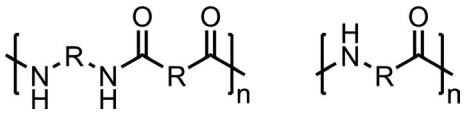

FIGURE 17 Base structure of nylons

presented. In this example, Nylon 6 was modified with collagen via Ar-plasma treatment to study the capability of this substrate for cell proliferation (Kissin, 2012).

11 | CONCLUSIONS

Polymeric materials are crucial for medical device development because of their convenient mechanical properties, good biocompatibility and low cost. Therefore, it is not surprising that these materials are being used increasingly in the medical field. Even when polymeric materials present clear advantages, these materials still present some disadvantages both in mechanical properties and in biocompatibility when interacting with the human body, because of this, new developments in the field of polymer chemistry and new developments involving the modification of existing materials are a very active field. In the last decade, an immense number of examples of polymer modification have arisen, which not only have improved some of the disadvantageous characteristics of the materials, but also have allowed for new uses of polymers in all areas of medicine.

ACKNOWLEDGMENTS

The authors thank CONACyT México (CVU 696062 and CVU 916557) for supported M. A Velazco-Medel and L. A. Camacho-Cruz. We thank Dirección General de Asuntos del Personal Académico, Universidad Nacional Autónoma de México under Grant IN202320.

REFERENCES

Abbasi, F., Mirzadeh, H., & Katbab, A. A. (2001). Modification of polysiloxane polymers for biomedical applications: A review. *Polymer International*, *50*, 1279–1287. https://doi.org/10.1002/pi.783

Abdelghany, A. M., Meikhail, M. S., & Asker, N. (2019). Synthesis and structural-biological correlation of PVC\PVAc polymer blends. *Journal of Materials Research and Technology*, *8*(5), 3908–3916. https://doi.org/10.1016/j.jmrt.2019.06.053

Adhikari, B., & Majumdar, S. (2004). Polymers in sensor applications. *Progress in Polymer Science (Oxford)*, *29*(7), 699–766. https://doi.org/10.1016/j.progpolymsci.2004.03.002

Aguilar, M. R., & San Román, J. (2014). Introduction to smart polymers and their applications. In *Smart polymers and their applications* (2nd Ed., Vol. *15*, pp. 1–11).

Ahmad, S. (2018). Polyurethane: A versatile scaffold for biomedical applications. *Significances of Bioengineering & Biosciences*, *2*(3). 144-146. https://doi.org/10.31031/SBB.2018.02.000536

Alauzun, J. G., Young, S., D'Souza, R., Liu, L., Brook, M. A., & Sheardown, H. D. (2010). Biocompatible, hyaluronic acid modified silicone elastomers. *Biomaterials*, *31*(13), 3471–3478. https://doi.org/10.1016/j.biomaterials.2010.01.069

Almeida, H., Amaral, M. H., & Lobão, P. (2012). Temperature and pH stimuli-responsive polymers and their applications in controlled and selfregulated drug delivery. *Journal of Applied Pharmaceutical Science*, *2*(6), 01–10. https://doi.org/10.7324/JAPS.2012.2609

Alvarez-Lorenzo, C., Bucio, E., Burillo, G., & Concheiro, A. (2010). Medical devices modified at the surface by γ-ray grafting for drug loading and delivery. *Expert Opinion on Drug Delivery*, *7*(2), 173–185. https://doi.org/10.1517/17425240903483174

Alvarez-Lorenzo, C., Garcia-Gonzalez, C. A., Bucio, E., & Concheiro, A. (2016). Stimuli-responsive polymers for antimicrobial therapy: Drug targeting, contact-killing surfaces and competitive release. *Expert Opinion on Drug Delivery*, *13*(8), 1109–1119. https://doi.org/10.1080/17425247.2016.1178719

Anirudhan, T. S., Divya, P. L., & Nima, J. (2016). Synthesis and characterization of novel drug delivery system using modified chitosan based hydrogel grafted with cyclodextrin. *Chemical Engineering Journal*, *284*, 1259–1269. https://doi.org/10.1016/j.cej.2015.09.057

Asadinezhad, A., Lehocký, M., Sáha, P., & Mozetič, M. (2012). Recent progress in surface modification of polyvinyl chloride. *Materials*, *5*(12), 2937–2959. https://doi.org/10.3390/ma5122937

Asadinezhad, A., Novák, I., Lehocký, M., Sedlařík, V., Vesel, A., Junkar, I., … Chodák, I. (2010). An in vitro bacterial adhesion assessment of surface-modified medical-grade PVC. *Colloids and Surfaces B: Biointerfaces*, *77*(2), 246–256. https://doi.org/10.1016/j.colsurfb.2010.02.006

Ates, B., Koytepe, S., Karaaslan, M. G., Balcioglu, S., & Gulgen, S. (2014). Biodegradable non-aromatic adhesive polyurethanes based on disaccharides for medical applications. *International Journal of Adhesion and Adhesives*, *49*, 90–96. https://doi.org/10.1016/j.ijadhadh.2013.12.012

Barde, M., Davis, M., Rangari, S., Mendis, H. C., De La Fuente, L., & Auad, M. L. (2018). Development of antimicrobial-loaded polyurethane films for drug-eluting catheters. *Journal of Applied Polymer Science*, *135*(27), 1–8. https://doi.org/10.1002/app.46467

Bergström, J. S., & Hayman, D. (2016). An overview of mechanical properties and material modeling of polylactide (PLA) for medical applications. *Annals of Biomedical Engineering*, *44*(2), 330–340. https://doi.org/10.1007/s10439-015-1455-8

Bongiovanni, R., Di Gianni, A., Priola, A., & Pollicino, A. (2007). Surface modification of polyethylene for improving the adhesion of a highly fluorinated UV-cured coating. *European Polymer Journal*, *43*(9), 3787–3794. https://doi.org/10.1016/j.eurpolymj.2007.06.037

Brochu, A. B. W., Chyan, W. J., & Reichert, W. M. (2012). Microencapsulation of 2-octylcyanoacrylate tissue adhesive for self-healing acrylic bone cement. *Journal of Biomedical Materials*

Research – Part B Applied Biomaterials, *100B*(7), 1764–1772. https://doi.org/10.1002/jbm.b.32743

Bucio, E., & Burillo, G. (1996). Radiation-grafting of 2-bromoethylacrylate onto polyethylene film by preirradiation method. *Radiation Physics and Chemistry*, *48*(6), 805–810. https://doi.org/10.1016/S0969-806X(96)00066-7

Butruk-Raszeja, B. A., Trzaskowska, P. A., Kuźminska, A., & Ciach, T. (2016). Polyurethane modification with acrylic acid by Ce(IV)-initiated graft polymerization. *Open Chemistry*, *14*(1), 206–214. https://doi.org/10.1515/chem-2016-0020

Cabana, S., Lecona-Vargas, C. S., Meléndez-Ortiz, H. I., Contreras-García, A., Barbosa, S., Taboada, P., … Alvarez-Lorenzo, C. (2017). Silicone rubber films functionalized with poly(acrylic acid) nanobrushes for immobilization of gold nanoparticles and photothermal therapy. *Journal of Drug Delivery Science and Technology*, *42*, 245–254. https://doi.org/10.1016/j.jddst.2017.04.006

Caló, E., & Khutoryanskiy, V. V. (2015). Biomedical applications of hydrogels: A review of patents and commercial products. *European Polymer Journal*, *65*, 252–267. https://doi.org/10.1016/j.eurpolymj.2014.11.024

Calvete, D. P., Holguín, D. F. R., & Luna, M. P. (2015). Grafting polymer based in active polyurethane matrixes via free radical. *Procedia Materials Science*, *9*, 491–495. https://doi.org/10.1016/j.mspro.2015.05.021

Campanella, A., Döhler, D., & Binder, W. H. (2018). Self-healing in supramolecular polymers. *Macromolecular Rapid Communications*, *39*(17), 1700739. https://doi.org/10.1002/marc.201700739

Campoccia, D., Montanaro, L., & Arciola, C. R. (2013). A review of the biomaterials technologies for infection-resistant surfaces. *Biomaterials*, *34*(34), 8533–8554. https://doi.org/10.1016/j.biomaterials.2013.07.089

Cao, Q., Wu, S., Wang, L., Shi, X., & Li, G. (2018). Effects of the morphology of sulfobetaine zwitterionic layers grafted onto a silicone surface on improving the hydrophilic stability, anti-bacterial adhesion properties, and biocompatibility. *Journal of Applied Polymer Science*, *135*(44), 1–9. https://doi.org/10.1002/app.46860

Cascone, S., & Lamberti, G. (2020). Hydrogel-based commercial products for biomedical applications: A review. *International Journal of Pharmaceutics*, *573*, 118803. https://doi.org/10.1016/j.ijpharm.2019.118803

Chattopadhyay, S., & Raines, R. T. (2014). Collagen-based biomaterials for wound healing. *Biopolymers*, *101*(8), 821–833. https://doi.org/10.1002/bip.22486

Chin, W., Zhong, G., Pu, Q., Yang, C., Lou, W., De Sessions, P. F., … Yang, Y. Y. (2018). A macromolecular approach to eradicate multidrug resistant bacterial infections while mitigating drug resistance onset. *Nature Communications*, *9*(1), 1–14. https://doi.org/10.1038/s41467-018-03325-6

Cingolani, A., Casalini, T., Caimi, S., Klaue, A., Sponchioni, M., Rossi, F., & Perale, G. (2018). A methodologic approach for the selection of bio-resorbable polymers in the development of medical devices: The case of poly(L-lactide-co-ε-caprolactone). *Polymers*, *10*(8), 851. https://doi.org/10.3390/polym10080851

Ciucurel, E. C., & Sefton, M. V. (2011). A poloxamine-polylysine acrylate scaffold for modular tissue engineering. *Journal of Biomaterials Science, Polymer Edition*, *22*(18), 2515–2528. https://doi.org/10.1163/092050610X541133

Coad, B. R., Lu, Y., & Meagher, L. (2012). A substrate-independent method for surface grafting polymer layers by atom transfer radical polymerization: Reduction of protein adsorption. *Acta Biomaterialia*, *8*(2), 608–618. https://doi.org/10.1016/j.actbio.2011.10.006

Concheiro, A., & Alvarez-Lorenzo, C. (2013). Chemically cross-linked and grafted cyclodextrin hydrogels: From nanostructures to drug-eluting medical devices. *Advanced Drug Delivery Reviews*, *65*(9), 1188–1203. https://doi.org/10.1016/j.addr.2013.04.015

Copes, F., Pien, N., Van Vlierberghe, S., Boccafoschi, F., & Mantovani, D. (2019). Collagen-Based Tissue Engineering Strategies for Vascular Medicine. *Frontiers in Bioengineering and Biotechnology*, *7*, 166. https://doi.org/10.3389/fbioe.2019.00166

Cromwell, L. D., & Kerber, C. W. (1980). Modification of cyanoacrylate for therapeutic embolization: Preliminary experience. *American Journal of Neuroradiology*, *1*(1), 113–114.

de Oliveira Barud, H. G., da Silva, R. R., da Silva Barud, H., Tercjak, A., Gutierrez, J., Lustri, W. R., … Ribeiro, S. J. L. (2016). A multipurpose natural and renewable polymer in medical applications: Bacterial cellulose. *Carbohydrate Polymers*, *153*, 406–420. https://doi.org/10.1016/j.carbpol.2016.07.059

Dong, Z., Mao, J., Yang, M., Wang, D., Bo, S., & Ji, X. (2011). Phase behavior of poly(sulfobetaine methacrylate)-grafted silica nanoparticles and their stability in protein solutions. *Langmuir*, *27*(24), 15282–15291. https://doi.org/10.1021/la2038558

Duan, J. (2015). Self-healing hydrogels based on carboxymethyl chitosan and acryloyl-6-aminocaproic acid. *Journal of Polymers*, *2015*, 1–6. https://doi.org/10.1155/2015/719529

Ebnesajjad, S. (2017). Medical and Surgical Applications of Expanded PTFE. In S. Ebnesajjad (Ed.), *Expanded PTFE Applications Handbook* (pp. 193–211). Amsterdam: Elsevier. https://doi.org/10.1016/B978-1-4377-7855-7.00009-2

Feksa, L. R., Troian, E. A., Muller, C. D., Viegas, F., Machado, A. B., & Rech, V. C. (2018). Hydrogels for biomedical applications. In A. M. Grumezescu (Ed.), *Nanostructures for the Engineering of Cells, Tissues and Organs* (pp. 403–438). Romania: Elsevier. https://doi.org/10.1016/B978-0-12-813665-2.00011-9

Flores-Rojas, G. G., López-Saucedo, F., Bucio, E., & Isoshima, T. (2017). Covalent immobilization of lysozyme in silicone rubber modified by easy chemical grafting. *MRS Communications*, *7*(4), 904–912. https://doi.org/10.1557/mrc.2017.115

Flores-Rojas, G. G., López-Saucedo, F., Quezada-Miriel, M., & Bucio, E. (2018). Grafting of glycerol methacrylate onto silicone rubber using γ-rays: Derivatization to 2-oxoethyl methacrylate and immobilization of lysozyme. *MRS Communications*, *8*, 199–206. https://doi.org/10.1557/mrc.2018.16

Forghani, A., Garber, L., Chen, C., Tavangarian, F., Tighe, T. B., Devireddy, R., … Hayes, D. (2018). Fabrication and characterization of thiol-triacrylate polymer via Michael addition reaction for biomedical applications. *Biomedical Materials*, *14*(1), 015001. https://doi.org/10.1088/1748-605X/aae684

Frost, M. C., Reynolds, M. M., & Meyerhoff, M. E. (2005). Polymers incorporating nitric oxide releasing/generating substances for improved biocompatibility of blood-contacting medical devices. *Biomaterials*, *26*(14), 1685–1693. https://doi.org/10.1016/j.biomaterials.2004.06.006

Fujimoto, K., Inoue, H., & Ikada, Y. (1993). Protein adsorption and platelet adhesion onto polyurethane grafted with methoxy-poly(ethylene glycol) methacrylate by plasma technique. *Journal of Biomedical Materials Research*, *27*(12), 1559–1567. https://doi.org/10.1002/jbm.820271213

Fundueanu, G., Constantin, M., Bucatariu, S., & Ascenzi, P. (2017). pH/thermo-responsive poly(N-isopropylacrylamide-co-maleic acid) hydrogel with a sensor and an actuator for biomedical applications. *Polymer*, *110*, 177–186. https://doi.org/10.1016/j.polymer.2017.01.003

Gandhi, A., Paul, A., Sen, S. O., & Sen, K. K. (2015). Studies on thermoresponsive polymers: Phase behaviour, drug delivery and biomedical applications. *Asian Journal of Pharmaceutical Sciences*, *10*(2), 99–107. https://doi.org/10.1016/j.ajps.2014.08.010

Gautam, V., & Narayan, K. S. (2014). Polymer optoelectronic structures for retinal prosthesis. *Organogenesis*, *10*(1), 9–12. https://doi.org/10.4161/org.28316

Gîfu, I. C., Maxim, M. E., Cinteza, L. O., Popa, M., Aricov, L., Leontieș, A. R., … Petcu, C. (2019). Antimicrobial activities of hydrophobically

modified poly(acrylate) films and their complexes with different chain length cationic surfactants. *Coatings*, *9* (244), https://doi.org/10.3390/coatings9040244

Gopanna, A., Rajan, K. P., Thomas, S. P., & Chavali, M. (2019). Polyethylene and polypropylene matrix composites for biomedical applications. In V. Grumezescu & A. M. Grumezescu (Eds.), *Materials for Biomedical Engineering*. Romania: Elsevier Inc. https://doi.org/10.1016/b978-0-12-816874-5.00006-2

Guan, J., Gao, C., Feng, L., & Sheng, J. (2000). Surface photo-grafting of polyurethane with 2-hydroxyethyl acrylate for promotion of human endothelial cell adhesion and growth. *Journal of Biomaterials Science, Polymer Edition*, *11*(5), 523–536. https://doi.org/10.1163/156856200743841

Gumpenberger, T., Heitz, J., Bäuerle, D., Kahr, H., Graz, I., Romanin, C., … Leisch, F. (2003). Adhesion and proliferation of human endothelial cells on photochemically modified polytetrafluoroethylene. *Biomaterials*, *24*(28), 5139–5144. https://doi.org/10.1016/S0142-9612(03)00460-5

Gupta, P., Vermani, K., & Garg, S. (2002). Hydrogels: From controlled release to pH-responsive drug delivery. *Drugs Discovery Today*, *7*(10), 569–579. https://doi.org/10.1016/S1359-6446(02)02255-9

Hachim, D., & Brown, B. N. (2018). Surface modification of polypropylene for enhanced layer-by-layer deposition of polyelectrolytes. *Journal of Biomedical Materials Research – Part A*, *106*(7), 2078–2085. https://doi.org/10.1002/jbm.a.36405

Han, D. K., Park, K. D., & Kim, Y. H. (1998). Sulfonated poly(ethylene oxide)-grafted polyurethane copolymer for biomedical applications. *Journal of Biomaterials Science, Polymer Edition*, *9*(2), 163–174. https://doi.org/10.1163/156856298X00497

Hardy, J. G., Palma, M., Wind, S. J., & Biggs, M. J. (2016). Responsive biomaterials: Advances in materials based on shape-memory polymers. *Advanced Materials*, *28*, 5717–5724. https://doi.org/10.1002/adma.201505417

Hernández-Aguirre, O. A., Núñez-Pineda, A., Tapia-Tapia, M., & Espinosa, R. M. G. (2016). Surface modification of polypropylene membrane using biopolymers with potential applications for metal ion removal. *Journal of Chemistry*, *2016*, 1–11. https://doi.org/10.1155/2016/2742013

Highley, C. B., Prestwich, G. D., & Burdick, J. A. (2016). Recent advances in hyaluronic acid hydrogels for biomedical applications. *Current Opinion in Biotechnology*, *40*, 35–40. https://doi.org/10.1016/j.copbio.2016.02.008

Hoare, T. R., & Kohane, D. S. (2008). Hydrogels in drug delivery: Progress and challenges. *Polymer*, *49*(8), 1993–2007. https://doi.org/10.1016/j.polymer.2008.01.027

Holback, H., Yeo, Y., & Park, K. (2011). Hydrogel swelling behavior and its biomedical applications. In S. Rimmer (Ed.), *Biomedical Hydrogels* (pp. 3–24). Amsterdam: Elsevier. https://doi.org/10.1533/9780857091383.1.3

Hong, K. Z. (1996). Poly(Vinyl Chloride) in medical device and packaging applications. *Journal of Vinyl and Additive Technology*, *2*(3), 193–197. https://doi.org/10.1002/vnl.10123

Huang, Z., Delparastan, P., Burch, P., Cheng, J., Cao, Y., & Messersmith, P. B. (2018). Injectable dynamic covalent hydrogels of boronic acid polymers cross-linked by bioactive plant-derived polyphenols. *Biomaterials Science*, *6*(9), 2487–2495. https://doi.org/10.1039/c8bm00453f

Ikada, Y. (1994). Surface modification medical applications. *Biomaterials*, *15*, 725–736.

Jansen, B., & Kohnen, W. (1995). Prevention of biofilm formation by polymer modification. *Journal of Industrial Microbiology*, *15*(4), 391–396. https://doi.org/10.1007/BF01569996

Kajiwara, H., Hamada, T., Ichikawa, Y., Ishi, M., & Yamazaki, I. (2004). Experience with expanded polytetrafluoroethylene (ePTFE Gore-Tex) surgical membrane for coronary artery grafting: Does ePTFE surgical membrane predispose to postoperative mediastinitis? *Artificial Organs*, *28*(9), 840–845. https://doi.org/10.1111/j.1525-1594.2004.07298.x

Kamoun, E. A., Fahmy, A., Taha, T. H., El-Fakharany, E. M., Makram, M., Soliman, H. M. A., & Shehata, H. (2018). Thermo-and pH-sensitive hydrogel membranes composed of poly(N-isopropylacrylamide)-hyaluronan for biomedical applications: Influence of hyaluronan incorporation on the membrane properties. *International Journal of Biological Macromolecules*, *106*, 158–167. https://doi.org/10.1016/j.ijbiomac.2017.08.011

Keshvari, H., Mirzadeh, H., Mansoori, P., Orang, F., & Khorasani, M. T. (2008). Collagen immobilization onto acrylic acid laser-grafted silicone for using as artificial skin: In vitro. *Iranian Polymer Journal*, *17*(3), 171–182.

Kisin, J. V. (2013). *Polyethylene end-use properties and their physical meaning*. Munich: Hanser.

Klouda, L. (2015). Thermoresponsive hydrogels in biomedical applications. *European Journal of Pharmaceutics and Biopharmaceutics*, *97*, 338–349. https://doi.org/10.1016/j.ejpb.2015.05.017

Korde, J. M., & Kandasubramanian, B. (2020). Naturally biomimicked smart shape memory hydrogels for biomedical functions. *Chemical Engineering Journal*, *379*, 122430. https://doi.org/10.1016/j.cej.2019.122430

Król, K., & Pielichowska, K. (2016). Modification of acrylic bone cements by poly(ethylene glycol) with different molecular weight. *Polymers for Advanced Technologies*, *27*(10), 1284–1293. https://doi.org/10.1002/pat.3792

Kumaresan, T., Gandhinathan, R., Ramu, M., Ananthasubramanian, M., & Pradheepa, K. B. (2016). Design, analysis and fabrication of polyamide/ hydroxyapatite porous structured scaffold using selective laser sintering method for bio-medical applications. *Journal of Mechanical Science and Technology*, *30*(11), 5305–5312. https://doi.org/10.1007/s12206-016-1049-x

Kyriakides, T. R., Cheung, C. Y., Murthy, N., Bornstein, P., Stayton, P. S., & Hoffman, A. S. (2002). pH-Sensitive polymers that enhance intracellular drug delivery in vivo. *Journal of Controlled Release*, *78*(1–3), 295–303. https://doi.org/10.1016/S0168-3659(01)00504-1

Lafarge, J., Kébir, N., Schapman, D., & Burel, F. (2013). Design of self-disinfecting PVC surfaces using the click chemistry. *Reactive and Functional Polymers*, *73*(11), 1464–1472. https://doi.org/10.1016/j.reactfunctpolym.2013.08.001

Lăzăroaie, C., Rusen, E., Mărculescu, B., Zecheru, T., & Hubcă, G. (2010). Chemical modification of PVC for polymer matrices with special properties. *UPB Scientific Bulletin, Series B: Chemistry and Materials Science*, *72*(2), 127–140.

Lee, H., Lee, K. D., Pyo, K. B., Park, S. Y., & Lee, H. (2010). Catechol-grafted poly(ethylene glycol) for PEGylation on versatile substrates. *Langmuir*, *26*(6), 3790–3793. https://doi.org/10.1021/la904909h

Lee, S.-D., Hsiue, G.-H., & Kao, C.-Y. (1996). Preparation and characterization of a homobifunctional silicone rubber membrane grafted with acrylic acid via plasma-induced graft copolymerization. *Journal of Polymer Science Part A: Polymer Chemistry*, *34*(1), 141–148. https://doi.org/10.1002/(SICI)1099-0518(19960115)34:1<141:AID-POLA15>3.0.CO;2-L

Lee, S. Y., Lee, Y., Le Thi, P., Oh, D. H., & Park, K. D. (2018). Sulfobetaine methacrylate hydrogel-coated anti-fouling surfaces for implantable biomedical devices. *Biomaterials Research*, *22*(1), 3–9. https://doi.org/10.1186/s40824-017-0113-7

Lee, S., & Vörös, J. (2005). An aqueous-based surface modification of poly(dimethylsiloxane) with poly(ethylene glycol) to prevent biofouling. *Langmuir*, *21*, 11957–11962. https://doi.org/10.1021/la051932p

Leggat, P. A., Smith, D. R., & Kedjarune, U. (2007). Surgical applications of cyanoacrylate adhesives: A review of toxicity. *ANZ Journal of Surgery*, *77*(4), 209–213. https://doi.org/10.1111/j.1445-2197.2007.04020.x

Li, J. X., Wang, J., Shen, L. R., Xu, Z. J., Li, P., Wan, G. J., & Huang, N. (2007). The influence of polyethylene terephthalate surfaces modified by silver ion implantation on bacterial adhesion behavior. *Surface and Coatings Technology*, *201*(19-20), 8155–8159. https://doi.org/10.1016/j.surfcoat.2006.02.069

Li, J., Zhai, M., Yi, M., Gao, H., & Ha, H. (1999). Radiation grafting of thermo-sensitive poly (NIPAAm) onto silicone rubber. *Radiation Physics and Chemistry*, *55*, 173–178.

Li, M., Neoh, K. G., Xu, L. Q., Wang, R., Kang, E.-T., Lau, T., … Chiong, E. (2012). Surface modification of silicone for biomedical applications requiring long-term antibacterial, antifouling, and hemocompatible properties. *Langmuir*, *28*(47), 16408–16422. https://doi.org/10.1021/la303438t

Li, Q., Liu, C., Wen, J., Wu, Y., Shan, Y., & Liao, J. (2017). The design, mechanism and biomedical application of self-healing hydrogels. *Chinese Chemical Letters*, *28*(9), 1857–1874. https://doi.org/10.1016/j.cclet.2017.05.007

Liang, R., Wang, L., Yu, H., Khan, A., Ul Amin, B., & Khan, R. U. (2019). Molecular design, synthesis and biomedical applications of stimuli-responsive shape memory hydrogels. *European Polymer Journal*, *114*, 380–396. https://doi.org/10.1016/j.eurpolymj.2019.03.004

Lim, J. Y. C., Lin, Q., Xue, K., & Loh, X. J. (2019). Recent advances in supramolecular hydrogels for biomedical applications. *Materials Today Advances*, *3*, 100021. https://doi.org/10.1016/j.mtadv.2019.100021

Liu, L., Gao, Y., Zhao, J., Yuan, L., Li, C., Liu, Z., & Hou, Z. (2018). A mild method for surface-grafting PEG onto segmented poly(ester-urethane) film with high grafting density for biomedical purpose. *Polymers*, *10*(10), 1125. https://doi.org/10.3390/polym10101125

Liu, X., Cheng, C., Peng, X. U., Xiao, H., Guo, C., Wang, X. U., … Yu, X. (2019). A promising material for bone repair: PMMA bone cement modified by dopamine-coated strontium-doped calcium polyphosphate particles. *Royal Society Open Science*, *6*(10), 1-10. https://doi.org/10.1098/rsos.191028

Liu, Y., Munisso, M. C., Mahara, A., Kambe, Y., Fukazawa, K., Ishihara, K., & Yamaoka, T. (2018). A surface graft polymerization process on chemically stable medical ePTFE for suppressing platelet adhesion and activation. *Biomaterials Science*, *6*(7), 1908–1915. https://doi.org/10.1039/c8bm00364e

López-Saucedo, F., Flores-Rojas, G. G., Bucio, E., Alvarez-Lorenzo, C., Concheiro, A., & González-Antonio, O. (2017). Achieving antimicrobial activity through poly(N-methylvinylimidazolium) iodide brushes on binary-grafted polypropylene suture threads. *MRS Communications*, *7*(4), 938–946. https://doi.org/10.1557/mrc.2017.121

López-Saucedo, F., Flores-Rojas, G. G., López-Saucedo, J., Magariños, B., Alvarez-Lorenzo, C., Concheiro, A., & Bucio, E. (2018). Antimicrobial silver-loaded polypropylene sutures modified by radiation-grafting. *European Polymer Journal*, *100*, 290–297. https://doi.org/10.1016/j.eurpolymj.2018.02.005

López-Saucedo, F., Flores-Rojas, G. G., Magariños, B., Concheiro, A., Alvarez-Lorenzo, C., & Bucio, E. (2019). Radiation grafting of poly(methyl methacrylate) and poly(vinylimidazole) onto polytetrafluoroethylene films and silver immobilization for antimicrobial performance. *Applied Surface Science*, *473*, 951–959. https://doi.org/10.1016/j.apsusc.2018.12.229

López-Saucedo, F., Flores-Rojas, G. G., Meléndez-Ortiz, H. I., Morfín-Gutierrez, A., Luna-Straffon, M. A., & Bucio, E. (2019). Stimuli-Responsive Nanomaterials for Drug Delivery. In S. S. Mohapatra, S. Ranjan, N. Dasgupta, R. K. Mishra, & S. Thomas (Eds.), *Characterization and Biology of Nanomaterials for Drug Delivery* (pp. 375–424). Amsterdam: Elsevier. https://doi.org/10.1016/B978-0-12-814031-4.00014-3

Losi, P., Mancuso, L., Al Kayal, T., Celi, S., Briganti, E., Gualerzi, A., … Soldani, G. (2015). Development of a gelatin-based polyurethane vascular graft by spray, phase-inversion technology. *Biomedical Materials*, *10*(4), 045014. https://doi.org/10.1088/1748-6041/10/4/045014

Love, B. (2017). Polymeric Biomaterials. In B. Love (Ed.), *Biomaterials: A Systems Approach to Engineering Concepts* (pp. 205–238). Michigan: Elsevier. https://doi.org/10.1016/B978-0-12-809478-5.00009-2

Mahanta, A. K., Mittal, V., Singh, N., Dash, D., Malik, S., Kumar, M., & Maiti, P. (2015). Polyurethane-grafted chitosan as new biomaterials for controlled drug delivery. *Macromolecules*, *48*(8), 2654–2666. https://doi.org/10.1021/acs.macromol.5b00030

Mahendran, R., Sridharan, D., Arunmozhidevan, C., Selvakumar, T. A., & Rajasekar, P. (2016). Fabrication and antibacterial effects of polycarbonate/leaf extract based thin films. *Journal of Materials*, *2016*, 1–7. https://doi.org/10.1155/2016/3194154

Maier, C., & Calafut, T. (1998). *Polypropylene: the definitive users guide and databook*. Norwich, NY: Plastics Design Library.

Maitz, M. F. (2015). Applications of synthetic polymers in clinical medicine. *Biosurface and Biotribology*, *1*(3), 161–176. https://doi.org/10.1016/j.bsbt.2015.08.002

Manfredi, G., Colombo, E., Barsotti, J., Benfenati, F., & Lanzani, G. (2019). Photochemistry of organic retinal prostheses. *Annual Review of Physical Chemistry*, *70*(1), 99–121. https://doi.org/10.1146/annurev-physchem-042018-052445

Manoj Kumar, R., Gupta, P., Sharma, S. K., Mittal, A., Shekhar, M., Kumar, V., … Lahiri, D. (2017). Sustained drug release from surface modified UHMWPE for acetabular cup lining in total hip implant. *Materials Science and Engineering C*, *77*, 649–661. https://doi.org/10.1016/j.msec.2017.03.221

Más Estellés, J., Krakovsky, I., Rodríguez Hernández, J. C., Piotrowska, A. M., & Monleón Pradas, M. (2007). Mechanical properties of porous crosslinked poly(ethyl-acrylate) for tissue engineering. *Journal of Materials Science*, *42*(20), 8629–8635. https://doi.org/10.1007/s10853-007-1727-2

Mazumder, M. A. J. (2017). Polydimethylsiloxane substrates with surfaces decorated by immobilized hyaluronic acids of different molecular weight for biomedical applications. *Arabian Journal for Science and Engineering*, *42*, 271–280. https://doi.org/10.1007/s13369-016-2354-5

McCullough, E. J., & Yadavalli, V. K. (2013). Surface modification of fused deposition modeling ABS to enable rapid prototyping of biomedical microdevices. *Journal of Materials Processing Technology*, *213*(6), 947–954. https://doi.org/10.1016/j.jmatprotec.2012.12.015

Melendez-Ortiz, H. I., Alvarez-Lorenzo, C., Concheiro, A., & Bucio, E. (2015). Grafting of N -vinyl caprolactam and methacrylic acid onto silicone rubber films for drug-eluting products. *Journal of Applied Polymer Science*, *132*(17), 41855. https://doi.org/10.1002/app.41855

Meléndez-Ortiz, H. I., Alvarez-Lorenzo, C., Concheiro, A., Jiménez-Páez, V. M., & Bucio, E. (2016). Modification of medical grade PVC with N-vinylimidazole to obtain bactericidal surface. *Radiation Physics and Chemistry*, *119*, 37–43. https://doi.org/10.1016/j.radphyschem.2015.09.014

Meyer, M. (2019). Processing of collagen based biomaterials and the resulting materials properties. *BioMedical Engineering OnLine*, *18*(1), 24. https://doi.org/10.1186/s12938-019-0647-0

Mi, H.-Y., Jing, X., Thomsom, J. A., & Turng, L.-S. (2018). Promoting endothelial cell affinity and antithrombogenicity of polytetrafluoroethylene (PTFE) by mussel-inspired modification and RGD/heparin grafting. *Journal of Materials Chemistry B*, *6*(21), 3475–3485. https://doi.org/10.1039/C8TB00654G

Miyashita, D., Chahud, F., Barros da Silva, G. E., de Albuquerque, V. B., Garcia, D. M., & Cruz, A. A. V. (2013). Tissue ingrowth into perforated polymethylmethacrylate orbital implants: An experimental study. *Ophthalmic Plastic and Reconstructive Surgery*, *29*(3), 160–163. https://doi.org/10.1097/IOP.0b013e318285b4c8

Monika, M., Mahto, S. K., Das, S., Ranjan, A., Singh, S. K., Roy, P., & Misra, N. (2015). Chemical modification of poly(vinyl chloride) for blood and cellular biocompatibility. *RSC Advances*, *5*(56), 45231–45238. https://doi.org/10.1039/C5RA03362D

Myung, S.-W., Yeom, Y.-H., Jang, Y.-M., Choi, H.-S., & Cho, D. (2005). Preparation of a reticulated polyurethane foam grafted with poly(acrylic acid) through atmospheric pressure plasma treatment and its lysozyme immobilization. *Journal of Materials Science: Materials in Medicine*, *16*(8), 745–751. https://doi.org/10.1007/s10856-005-2612-7

Nagase, Y., Horiguchi, K., & Fazel-Rezai, R. (2011). Biocompatible Polyamides and Polyurethanes Containing Phospholipid Moiety. In *Biomedical Engineering - Frontiers and Challenges* (pp. 217–232). Rijeka, Croatia: InTech. https://doi.org/10.5772/22473

Navarro, R., Perrino, M., García, C., Elvira, C., Gallardo, A., & Reinecke, H. (2016). Opening New Gates for the Modification of PVC or Other PVC Derivatives: Synthetic Strategies for the Covalent Binding of Molecules to PVC. *Polymers*, *8*(4), 152. https://doi.org/10.3390/polym8040152

NIIR Board of Consultants and Engineers (2006). *The complete book on medical plastics*. Retrieved from https://books.google.com/books?id=vgK3AgAAQBAJ&pg=PA42&lpg=PA42&dq=condensation+steam+sterilization+medical+plastic&source=bl&ots=TLxdJT3-z-&sig=ud0c0Je7MfBoPLQoiDcJkgKO7R0&hl=en&sa=X&ved=0ahUKEwjf3IyX6dzOAhXBiCwKHW_kDmMQ6AEIWzAJ#v=snippet&q=radel&f=false

Nimmagadda, A., Liu, X., Teng, P., Su, M. A., Li, Y., Qiao, Q., … Cai, J. (2017). Polycarbonates with potent and selective antimicrobial activity toward gram-positive bacteria. *Biomacromolecules*, *18*(1), 87–95. https://doi.org/10.1021/acs.biomac.6b01385

Nishizawa, K., Takai, M., & Ishihara, K. (2010). Stabilization of phospholipid polymer surface with three-dimensional nanometer-scaled structure for highly sensitive immunoassay. *Colloids and Surfaces B: Biointerfaces*, *77*(2), 263–269. https://doi.org/10.1016/j.colsurfb.2010.02.008

Noh, J. H., Baik, H. K., Noh, I., Park, J.-C., & Lee, I.-S. (2007). Surface modification of polytetrafluoroethylene using atmospheric pressure plasma jet for medical application. *Surface and Coatings Technology*, *201*(9–11), 5097–5101. https://doi.org/10.1016/j.surfcoat.2006.07.223

Orapiriyakul, W., Young, P. S., Damiati, L., & Tsimbouri, P. M. (2018). Antibacterial surface modification of titanium implants in orthopaedics. *Journal of Tissue Engineering*, *9*, 204173141878983. https://doi.org/10.1177/2041731418789838

Palza, H. (2015). Antimicrobial polymers with metal nanoparticles. *International Journal of Molecular Sciences*, *16*(1), 2099–2116. https://doi.org/10.3390/ijms16012099

Pascual, B., Gurruchaga, M., Ginebra, M. P., Gil, F. J., Planell, J. A., & Gonî, I. (1999). Influence of the modification of P/L ratio on a new formulation of acrylic bone cement. *Biomaterials*, *20*(5), 465–474. https://doi.org/10.1016/S0142-9612(98)00192-6

Pellá, M. C. G., Lima-Tenório, M. K., Tenório-Neto, E. T., Guilherme, M. R., Muniz, E. C., & Rubira, A. F. (2018). Chitosan-based hydrogels: From preparation to biomedical applications. *Carbohydrate Polymers*, *196*, 233–245. https://doi.org/10.1016/j.carbpol.2018.05.033

Penzel, E., Ballard, N. & Asua, J.M. (2020). Polyacrylates. In *Ullmann's Encyclopedia of Industrial Chemistry* (1-20). https://doi.org/10.1002/14356007.a21_157.pub2

Peppas, N. (2000). Hydrogels in pharmaceutical formulations. *European Journal of Pharmaceutics and Biopharmaceutics*, *50*(1), 27–46. https://doi.org/10.1016/S0939-6411(00)00090-4

Phadke, A., Zhang, C., Arman, B., Hsu, C.-C., Mashelkar, R. A., Lele, A. K., … Varghese, S. (2012). Rapid self-healing hydrogels. *Proceedings of the National Academy of Sciences of the United States of America*, *109*(12), 4383–4388. https://doi.org/10.1073/pnas.1201122109

Pillai, C. K. S., & Sharma, C. P. (2010). Review paper: Absorbable polymeric surgical sutures: Chemistry, production, properties, biodegradability, and performance. *Journal of Biomaterials Applications*, *25*(4), 291–366. https://doi.org/10.1177/0885328210384890

Pinchuk, L., Martin, J. B., Esquivel, M. C., & Macgregor, D. C. (1988). The use of silicone/polyurethane graft polymers as a means of eliminating surface cracking of polyurethane prostheses. *Journal of Biomaterials Applications*, *3*(2), 260–296. https://doi.org/10.1177/088532828800300206

Pino-Ramos, V. H., Flores-Rojas, G. G., Alvarez-Lorenzo, C., Concheiro, A., & Bucio, E. (2018). Graft copolymerization by ionization radiation, characterization, and enzymatic activity of temperature-responsive SR-g-PNVCL loaded with lysozyme. *Reactive and Functional Polymers*, *126*, 74–82. https://doi.org/10.1016/j.reactfunctpolym.2018.03.002

Priya James, H., John, R., Alex, A., & Anoop, K. R. (2014). Smart polymers for the controlled delivery of drugs – A concise overview. *Acta Pharmaceutica Sinica B*, *4*(2), 120–127. https://doi.org/10.1016/j.apsb.2014.02.005

Qian, C., Zhang, T., Gravesande, J., Baysah, C., Song, X., & Xing, J. (2019). Injectable and self-healing polysaccharide-based hydrogel for pH-responsive drug release. *International Journal of Biological Macromolecules*, *123*, 140–148. https://doi.org/10.1016/j.ijbiomac.2018.11.048

Ramírez-Fuentes, Y. S., Bucio, E., & Burillo, G. (2007). Radiation-induced grafting of N-isopropylacrylamide and acrylic acid onto polypropylene films by two step method. *Nuclear Instruments and Methods in Physics Research, Section B: Beam Interactions with Materials and Atoms*, *265*(1), 183–186. https://doi.org/10.1016/j.nimb.2007.08.046

RâpĂ, M., Matei, E., Ghioca, P. N., Cincu, C., & Niculescu, M. (2016). Structural changes of modified polypropylene with thermoplastic elastomers for medical devices applications. *Journal of Adhesion Science and Technology*, *30*(16), 1727–1740. https://doi.org/10.1080/01694243.2015.1132103

Ren, X., Feng, Y., Guo, J., Wang, H., Li, Q., Yang, J., … Li, W. (2015). Surface modification and endothelialization of biomaterials as potential scaffolds for vascular tissue engineering applications. *Chemical Society Reviews*, *44*(15), 5680–5742. https://doi.org/10.1039/C4CS00483C

Riau, A. K., Mondal, D., Yam, G. H. F., Setiawan, M., Liedberg, B., Venkatraman, S. S., & Mehta, J. S. (2015). Surface modification of PMMA to improve adhesion to corneal substitutes in a synthetic core-skirt keratoprosthesis [Research-article]. *ACS Applied Materials and Interfaces*, *7*(39), 21690–21702. https://doi.org/10.1021/acsami.5b07621

Rivkin, A. (2014). A prospective study of non-surgical primary rhinoplasty using a polymethylmethacrylate injectable implant. *Dermatologic Surgery*, *40*(3), 305–313. https://doi.org/10.1111/dsu.12415

Rogalsky, S. P., Moshynets, O. V., Lyoshina, L. G., & Tarasyuk, O. P. (2014). Antimicrobial polycarbonates for biomedical applications. *EPMA Journal*, *5*(S1), A133. https://doi.org/10.1186/1878-5085-5-s1-a133

Román, J. S., Vázquez Lasa, B., Aguilar, M. R., & Boesel, L. F. (2008). Modifications of bone cements. In S. Deb (Ed.), *Orthopaedic bone cements* (pp. 332–357). Amsterdam: Elsevier.

Roohpour, N., Moshaverinia, A., Wasikiewicz, J. M., Paul, D., Wilks, M., Millar, M., & Vadgama, P. (2012). Development of bacterially resistant polyurethane for coating medical devices. *Biomedical Materials*, *7*(1), 015007. https://doi.org/10.1088/1748-6041/7/1/015007

Salati, A., Keshvari, H., Karkhaneh, A., & Taranejoo, S. (2011). Design and fabrication of artificial skin: Chitosan and gelatin immobilization on silicone by poly acrylic acid graft using a plasma surface modification method. *Journal of Macromolecular Science, Part B: Physics*, *50*(10), 1972–1982. https://doi.org/10.1080/00222348.2010.549438

Sall, C., Ayé, M., Bottzeck, O., Praud, A., & Blache, Y. (2018). Towards smart biocide-free anti-biofilm strategies: Click-based synthesis of cinnamide analogues as anti-biofilm compounds against marine

bacteria. *Bioorganic and Medicinal Chemistry Letters*, *28*(2), 155–159. https://doi.org/10.1016/j.bmcl.2017.11.039

Saxena, S., Ray, A. R., Kapil, A., Pavon-Djavid, G., Letourneur, D., Gupta, B., & Meddahi-Pellé, A. (2011). Development of a new polypropylene-based suture: Plasma grafting, surface treatment, characterization, and biocompatibility studies. *Macromolecular Bioscience*, *11*(3), 373–382. https://doi.org/10.1002/mabi.201000298

Schmaljohann, D. (2006). Thermo- and pH-responsive polymers in drug delivery. *Advanced Drug Delivery Reviews*, *58*(15), 1655–1670. https://doi.org/10.1016/j.addr.2006.09.020

Schönemann, E., Koc, J., Aldred, N., Clare, A. S., Laschewsky, A., Rosenhahn, A., & Wischerhoff, E. (2019). Synthesis of novel sulfobetaine polymers with differing dipole orientations in their side chains, and their effects on the antifouling properties. *Macromolecular Rapid Communications*, *41*, 1900447. https://doi.org/10.1002/marc.201900447

Serrano-Aroca, Á., & Reddy, B. (2017). Latest Improvements of Acrylic-Based Polymer Properties for Biomedical Applications. In *Acrylic Polymers in Healthcare* (pp. 75–98). Rijeka, Croatia: Inthech. https://doi.org/10.5772/intechopen.68996

Shah Hosseini, N., Bölgen, N., Khenoussi, N., Yılmaz, Ş. N., Yetkin, D., Hekmati, A. H., … Adolphe, D. (2018). Novel 3D electrospun polyamide scaffolds prepared by 3D printed collectors and their interaction with chondrocytes. *International Journal of Polymeric Materials and Polymeric Biomaterials*, *67*(3), 143–150. https://doi.org/10.1080/00914037.2017.1309541

Shmack, G., Dutschk, V., & Pisanova, E. (2000). Modification of polyamide fibres to improve their biocompatibility. *Fibre Chemistry*, *32*(1), 48–55. https://doi.org/10.1007/BF02359201

Shourgashti, Z., Khorasani, M. T., & Khosroshahi, S. M. E. (2010). Plasma-induced grafting of polydimethylsiloxane onto polyurethane surface: Characterization and in vitro assay. *Radiation Physics and Chemistry*, *79*(9), 947–952. https://doi.org/10.1016/j.radphyschem.2010.04.007

Shrestha, B. K., Mousa, H. M., Tiwari, A. P., Ko, S. W., Park, C. H., & Kim, C. S. (2016). Development of polyamide-6,6/chitosan electrospun hybrid nanofibrous scaffolds for tissue engineering application. *Carbohydrate Polymers*, *148*, 107–114. https://doi.org/10.1016/j.carbpol.2016.03.094

Sun, D., Babar Shahzad, M., Li, M., Wang, G., & Xu, D. (2015). Antimicrobial materials with medical applications. *Materials Technology*, *30*(B2), B90–B95. https://doi.org/10.1179/1753555714Y.0000000239

Sun, X., Qian, Z., Luo, L., Yuan, Q., Guo, X., Tao, L., … Wang, X. (2016). Antibacterial adhesion of poly(methyl methacrylate) modified by borneol acrylate. *ACS Applied Materials and Interfaces*, *8*(42), 28522–28528. https://doi.org/10.1021/acsami.6b10498

Suzuki, M., Kishida, A., Ikada, Y., & Iwata, H. (1986). Graft copolymerization of acrylamide onto a polyethylene surface pretreated with a glow discharge. *Macromolecules*, *19*(7), 1804–1808. https://doi.org/10.1021/ma00161a005

Tang, X., Thankappan, S. K., Lee, P., Fard, S. E., Harmon, M. D., Tran, K., & Yu, X. (2014). Polymeric Biomaterials in Tissue Engineering and Regenerative Medicine. In S. G. Kumbar, C. T. L. And, & M. Deng (Eds.), *Natural and Synthetic Biomedical Polymers*. Amsterdam: Elsevier Inc. https://doi.org/10.1016/B978-0-12-396983-5.00022-3

Teo, A. J. T., Mishra, A., Park, I., Kim, Y. J., Park, W. T., & Yoon, Y. J. (2016). Polymeric Biomaterials for Medical Implants and Devices. *ACS Biomaterials Science and Engineering*, *2*(4), 454–472. https://doi.org/10.1021/acsbiomaterials.5b00429

Tooma, M. A., Najim, T. S., Alsalhy, Q. F., Marino, T., Criscuoli, A., Giorno, L., & Figoli, A. (2015). Modification of polyvinyl chloride (PVC) membrane for vacuum membrane distillation (VMD) application. *Desalination*, *373*, 58–70. https://doi.org/10.1016/j.desal.2015.07.008

Tu, C.-Y., Liu, Y.-L., Lee, K.-R., & Lai, J.-Y. (2005). Surface grafting polymerization and modification on poly(tetrafluoroethylene) films by means of ozone treatment. *Polymer*, *46*(18), 6976–6985. https://doi.org/10.1016/j.polymer.2005.05.116

Tu, Y., Chen, N., Li, C., Liu, H., Zhu, R., Chen, S., … He, L. (2019). Advances in injectable self-healing biomedical hydrogels. *Acta Biomaterialia*, *90*, 1–20. https://doi.org/10.1016/j.actbio.2019.03.057

Tunney, M. M., Gorman, S. P., & Patrick, S. (2002). Infection associated with medical devices. *International Journal of General Systems*, *31*(1), 195–205. https://doi.org/10.2165/00003495-200565020-00003

Usman, A., Zia, K. M., Zuber, M., Tabasum, S., Rehman, S., & Zia, F. (2016). Chitin and chitosan based polyurethanes: A review of recent advances and prospective biomedical applications. *International Journal of Biological Macromolecules*, *86*, 630–645. https://doi.org/10.1016/j.ijbiomac.2016.02.004

Utrata-Wesoek, A. (2013). Antifouling surfaces in medical application. *Polimery/Polymers*, *58*(9), 685–695. https://doi.org/10.14314/polimery.2013.685

Uyama, Y., Kato, K., & Ikada, Y. (1998). Surface Modification of Polymers by Grafting. *Advances in Polymer Science*, *137*, 1–39. https://doi.org/10.1007/3-540-69685-7_1

Vashist, A., Vashist, A., Gupta, Y. K., & Ahmad, S. (2014). Recent advances in hydrogel based drug delivery systems for the human body. *Journal of Materials Chemistry B*, *2*(2), 147–166. https://doi.org/10.1039/C3TB21016B

Völcker, N., Klee, D., Höcker, H., & Langefeld, S. (2001). Functionalization of silicone rubber for the covalent immobilization of fibronectin. *Journal of Materials Science: Materials in Medicine*, *12*(2), 111–119. https://doi.org/10.1023/A:1008938525489

Wang, B., Lin, Q., Shen, C., Tang, J., Han, Y., & Chen, H. (2014). Hydrophobic modification of polymethyl methacrylate as intraocular lenses material to improve the cytocompatibility. *Journal of Colloid and Interface Science*, *431*, 1–7. https://doi.org/10.1016/j.jcis.2014.05.056

Wang, B., Wang, F., Kong, Y., Wu, Z., Wang, R. M., Song, P., & He, Y. (2018). Polyurea-crosslinked cationic acrylate copolymer for antibacterial coating. *Colloids and Surfaces A: Physicochemical and Engineering Aspects*, *549*, 122–129. https://doi.org/10.1016/j.colsurfa.2018.04.012

Wang, C., & Chen, J.-R. (2007). Studies on surface graft polymerization of acrylic acid onto PTFE film by remote argon plasma initiation. *Applied Surface Science*, *253*(10), 4599–4606. https://doi.org/10.1016/j.apsusc.2006.10.014

Wang, J., Li, J., Shen, L., Ling, R., Xu, Z., Zhao, A., … Huang, N. (2007). The biomedical properties of polyethylene terephthalate surface modified by silver ion implantation. *Nuclear Instruments and Methods in Physics Research Section B: Beam Interactions with Materials and Atoms*, *257*(1-2), 141–145. https://doi.org/10.1016/j.nimb.2006.12.137

Wang, P., Tan, K. L., & Kang, E. T. (2000). Surface modification of poly(tetrafluoroethylene) films via grafting of poly(ethylene glycol) for reduction in protein adsorption. *Journal of Biomaterials Science, Polymer Edition*, *11*(2), 169–186. https://doi.org/10.1163/156856200743634

Wang, W., & Wang, C. (2012). Polyurethane for biomedical applications: A review of recent developments. In J. P. Davim (Ed.), *The Design and Manufacture of Medical Devices* (Woodhead P, pp. 115–151). Minnesota: Elsevier. https://doi.org/10.1533/9781908818188.115

Wei, S. Q., Bai, Y. P., & Shao, L. (2008). A novel approach to graft acrylates onto commercial silicones for release film fabrications by two-step emulsion synthesis. *European Polymer Journal*, *44*, 2728–2736. https://doi.org/10.1016/j.eurpolymj.2008.04.025

Winnacker, M. (2017). Polyamides and their functionalization: Recent concepts for their applications as biomaterials. *Biomaterials Science*, *5*(7), 1230–1235. https://doi.org/10.1039/c7bm00160f

Winnacker, M., Beringer, A. J. G., Gronauer, T. F., Güngör, H. H., Reinschlüssel, L., Rieger, B., & Sieber, S. A. (2019). Polyamide/PEG

blends as biocompatible biomaterials for the convenient regulation of cell adhesion and growth. *Macromolecular Rapid Communications*, *40*(12), 1900091. https://doi.org/10.1002/marc.201900091

Xiong, X., Wu, Z., Pan, J., Xue, L., Xu, Y., & Chen, H. (2015). A facile approach to modify poly(dimethylsiloxane) surfaces via visible light-induced grafting polymerization. *Journal of Materials Chemistry B*, *3*(4), 629–634. https://doi.org/10.1039/c4tb01600a

Yeow, B., Coffey, J. W., Muller, D. A., Grøndahl, L., Kendall, M. A. F., & Corrie, S. R. (2013). Surface modification and characterization of polycarbonate microdevices for capture of circulating biomarkers, both in vitro and in vivo. *Analytical Chemistry*, *85*(21), 10196–10204. https://doi.org/10.1021/ac402942x

Yu, Q., Zhang, Y., Wang, H., Brash, J., & Chen, H. (2011). Anti-fouling bioactive surfaces. *Acta Biomaterialia*, *7*(4), 1550–1557. https://doi.org/10.1016/j.actbio.2010.12.021

Yuan, Y., Zang, X., Ai, F., Zhou, J., Shen, J., & Lin, S. (2004). Grafting sulfobetaine monomer onto silicone surface to improve haemocompatibility. *Polymer International*, *53*(1), 121–126. https://doi.org/10.1002/pi.1122

Yue, Z., Liu, X., Molino, P. J., & Wallace, G. G. (2011). Bio-functionalisation of polydimethylsiloxane with hyaluronic acid and hyaluronic acid – Collagen conjugate for neural interfacing. *Biomaterials*, *32*(21), 4714–4724. https://doi.org/10.1016/J.BIOMATERIALS.2011.03.032

Zhang, Q., Wang, C., Babukutty, Y., Ohyama, T., Kogoma, M., & Kodama, M. (2002). Biocompatibility evaluation of ePTFE membrane modified with PEG in atmospheric pressure glow discharge. *Journal of Biomedical Materials Research*, *60*(3), 502–509. https://doi.org/10.1002/jbm.1294

Zhang, S., Yang, Q., Zhao, W., Qiao, B., Cui, H., Fan, J., … Jiang, D. (2016). In vitro and in vivo biocompatibility and osteogenesis of graphene-reinforced nanohydroxyapatite polyamide66 ternary biocomposite as orthopedic implant material. *International Journal of Nanomedicine*, *11*, 3179–3189. https://doi.org/10.2147/IJN.S105794

Zhang, W., Zhang, Y., Ji, J., Yan, Q., Huang, A., & Chu, P. K. (2007). Antimicrobial polyethylene with controlled copper release. *Journal of Biomedical Materials Research Part A*, *83A*(3), 838–844. https://doi.org/10.1002/jbm.a.31436

Zheng, Y., Miao, J., Zhang, F., Cai, C., Koh, A., Simmons, T. J., … Linhardt, R. J. (2016). Surface modification of a polyethylene film for anticoagulant and antimicrobial catheter. *Reactive and Functional Polymers*, *100*(3), 142–150. https://doi.org/10.1016/j.reactfunctpolym.2016.01.013

Zhou, J., Zhang, X., Yan, Y., Hu, J., Wang, H., Cai, Y., & Qu, J. (2019). Preparation and characterization of a novel antibacterial acrylate polymer composite modified with capsaicin. *Chinese Journal of Chemical Engineering*, *27*, 3043–3052. https://doi.org/10.1016/j.cjche.2019.03.024

Zia, K. M., Zuber, M., Mahboob, S., Sultana, T., & Sultana, S. (2010). Surface characteristics of UV-irradiated chitin-based shape memory polyurethanes. *Carbohydrate Polymers*, *80*(1), 229–234. https://doi.org/10.1016/j.carbpol.2009.11.015

Zuñiga-Zamorano, I., Meléndez-Ortiz, H. I., Costoya, A., Alvarez-Lorenzo, C., Concheiro, A., & Bucio, E. (2018). Poly(vinyl chloride) catheters modified with pH-responsive poly(methacrylic acid) with affinity for antimicrobial agents. *Radiation Physics and Chemistry*, *142*, 107–114. https://doi.org/10.1016/j.radphyschem.2017.02.008

How to cite this article: Velazco-Medel MA, Camacho-Cruz LA, Bucio E. Modification of relevant polymeric materials for medical applications and devices. *Med Devices Sens*. 2020;00:e10073. https://doi.org/10.1002/mds3.10073

Received: 27 July 2020 | Revised: 6 September 2020 | Accepted: 17 September 2020

DOI: 10.1002/mds3.10134

MEDICAL DEVICES & SENSORS WILEY

MINI REVIEW

Antifungal polymers for medical applications

Marlene Alejandra Velazco-Medel[1] | Luis Alberto Camacho-Cruz[1] | José Carlos Lugo-González[2] | Emilio Bucio[1]

[1]Departamento de Química de Radiaciones y Radioquímica, Instituto de Ciencias Nucleares, Universidad Nacional Autónoma de México, Universidad Nacional Autónoma de México, CDMX, CDMX 04350, Mexico

[2]Departamento de Química Inorgánica y Nuclear, Facultad de Química, Universidad Nacional Autónoma de México, Universidad Nacional Autónoma de México, CDMX, CDMX 04350, Mexico

Correspondence
Marlene Alejandra Velazco-Medel and Emilio Bucio, Departamento de Química de Radiaciones y Radioquímica, Instituto de Ciencias Nucleares, Universidad Nacional Autónoma de México, Circuito Exterior, Ciudad Universitaria, CDMX 04510, Mexico.
Emails: marlene.velazco@correo.nucleares.unam.mx (MAV); ebucio@nucleares.unam.mx (EB)

Abstract

Fungi-associated infections are very common diseases in humans, and these have increased in immunocompromised population and hospitalized patients. Fungi grow almost in any environment, and they reproduce easily in dirt and wet spaces, and thus, the development of antifungal materials is focused on avoiding fungal infections or inhibiting growth. Polymers used for medical devices are susceptible to microorganism adhesion. Therefore, they have been treated and modified for the inhibition of fungi growth. There are two pathways to deal with these microorganisms, firstly, the synthesis of versatile polymeric materials with antifouling properties, and, secondly, the development of materials for controlled fungicide release. These two approaches have been used in the crafting of food packaging. Additionally, sophisticated polymeric drug delivery systems have allowed the systematic and localized administration of fungicides reducing doses with a prolonged delivery. This general purpose has been accomplished by the synthesis of polymeric composites, grafted polymers or the modification of polymeric fungicides, by the coupling of cationic moieties on polymers, using metallic salts and nanoparticles, and by the loading of fungicides in micelles and metallic nanoparticles. Most of the materials presented on this review are still at an early stage of development. This compilation intends to be a frame of reference for researchers willing to explore this topic since clinical applications of these materials are starting to be increasingly relevant.

KEYWORDS
antifungal, azoles, cationic, fungicide, polymer

1 | INTRODUCTION

The application of polymers as medical devices has steadily increased in almost all medical fields because of the versatility of these materials. Thus, research has focused both on the development of more appropriate materials for specific situations and on the modification of already useful materials for the improvement of their intrinsic properties. Modifications on this kind of materials have increased their potential uses by adapting their mechanical properties to specific needs. Moreover, biocompatibility of the polymeric materials has been improved by the inclusion of certain functional groups, providing responses to physical and chemical stimuli present in physiological conditions.

Until recently, one of the most worrying problems in hospitals has been infections derived from medical devices usage. Typically, this kind of infections was handled with the use of prophylactic and therapeutic treatments with 'classic' (low-molecular weight) antimicrobial agents. This strategy has been effective in most patients suffering from nosocomial infections. However, it has the disadvantage of substantially increasing the probability of antimicrobial-resistant pathogens appearance, which continue to be especially dangerous in hospital environments (Cohen et al., 2017; World Health Organization, n.d.; Zegers et al., 2017). Additionally, due to

the hydrophobic nature and roughness of biocompatible polymers for medical devices (De-la-Pinta et al., 2019), microbe adhesion and biofilm formation is probable on this type of materials, increasing the risk of infection development on the vicinity of these devices (e.g. tissues near wound dressings, urinary catheters, implants, etc.). While treatments with 'classic' antimicrobials could be administered orally or intravenously, a localized effect on the infections is not always attained. Taking these issues into account, one of the most promising strategies is the production of polymeric devices which exhibit antimicrobial properties.

The production of polymers that are able to prevent the growth of pathogens of different species such as bacteria, fungi, algae and yeasts is a huge area of research. This is due to the great variety of techniques used to prevent pathogen growth as well as to the great variety of targeted pathogenic microorganisms (Narayana & Pichika, 2019). Recently, the focus of the research has been the development of antibacterial polymers (polymers which only prevent the growth of bacteria), which have been proven to be biocompatible, effective and able to resolve the issues related to the use of 'classic' antibiotics (Arora & Mishra, 2018). Many other antimicrobial polymers have already proven to be just as useful for combating other kinds of infections produced by both bacteria and other pathogens. Since antimicrobial systems are less considered as focus for the research community, with this mini-review we seek to make a brief compilation of advances in antifungal polymeric medical devices by presenting the most common examples of polymeric antifungals, a brief explanation of general mechanism of action, and their most important classifications.

This review focuses on fungi-associated infections, since the worldwide occurrence of fungal infections has been steadily increasing. Fungal infections caused by drug-resistant organisms are an emerging threat to heavily immunosuppressed patients with haematological malignancies. We chose this topic because the spotlight for reviews about antimicrobial substrates are mainly antibacterial materials and fungal infections are very common in humans, since fungi can grow in wet and dry areas. Additionally, these infections are also associated with drug-resistant fungi and yeasts, and skin infections are the most common fungal diseases in humans (De Pauw, 2011). Some estimates indicate that the rate of fungal disease has surpassed at least one billion infections worldwide, with many strains of fungi causing hospital-related infections and high mortality rates on patients with compromised immune systems such as those with cancer, HIV-positive diagnoses (Bongomin et al., 2017; Fisher et al., 2012) or haematological malignancies (Gamaletsou et al., 2018). Generally, for human infections, the most common fungi and yeasts are *Candida*, *Aspergillus*, *Trichophyton rubrum*, *Blastomyces*, *Saccharomyces*, *Histoplasma* and *Cryptococcus* spp. Thus, the main purpose for this research field is to inhibit their growth and mitigate the diseases. As mentioned before, current treatments for this kind of infections include the administration of organic fungicides such as polyenes, azoles or lipopeptides. Furthermore, some of these compounds are introduced in topic formulations to deal with fungal keratitis or skin infections (Garber, 2001; Pfaller et al., 2006). Unfortunately, just as other pathogens, the increased use of 'classic' antifungals has led to the development of antifungal resistant strains which are even more concerning (Wiederhold, 2017).

Although antifungal polymers have the common characteristic of stopping the propagation of different kinds of fungi, these materials differ substantially on the strategy they use for inhibiting their growth. The difference on their mechanism of action allows the following classification which will be important throughout this review:

- Inclusion of intrinsically antifungal moieties on a polymeric structure. (e.g. quaternized ammonium salts, azole groups).
- Modified polyene macrolides and echinocandins.
- Polymer composites containing metallic or organic antifungal agents.
- Polymer architectures for the release of low-molecular weight antifungals (e.g. inclusion of Amphotericin B on polymeric micelles).

It is important to note, that although all the classifications have their own advantages and disadvantages, each of this kind of antifungal polymers have their own challenges in the design, synthesis, production and applicability. It is important to mention that one of the most challenging steps in finding antifungal agents is coming from the fact that both fungi and mammal cells are eukaryotes, which tend to complicate the finding of non-cytotoxic fungicidal compounds. This is in clear contrast to the situation with antibacterial compounds in which the differentiation between prokaryotic (pathogen) and eukaryotic (mammal) cells allows for easier selectivity (Liu et al., 2013). Although the main difference between prokaryotic and eukaryotic cells is the presence of a nucleus, another important difference is the presence of peptidoglycan in the cell wall. Nevertheless, both antibacterial and antifungal drugs affect cell wall or membrane in similar way, by disruption processes of the cell membranes/walls. It is important, however, to mention that these disruption processes depend greatly on the mechanism of action of each antimicrobial drug, specifically the target enzymes which are activated or deactivated on these processes (e.g. hydrolysis of glycans or electrostatic interactions). At the current stage of development of these materials, the research has focused in finding the appropriate chemical substrates that can be both antifungal and biocompatible. Although this may be an objective numerical indicator of the usefulness of the material in a general scenario, it is not trivial to say which material or type of material will be the best option since each material may be better suited for a specific application. As the research advances, the clinical demands for specific antifungals will help for the discrimination of certain substrates for many uses.

Additional to this classification, it is possible to differentiate between antifungal macromolecular materials by considering their possible applications; for instance, some materials may be better suited for medical devices, while others may be better suited for water purification. These differences in applications are crucial when evaluating the properties of a material and are therefore discussed briefly in each of the sections of this work. As a final point to mention, most of these materials are in an early stage of

development; thus, the applicability of these in a clinical context may be limited to the testing and effectiveness of these materials as medical devices or as drug formulations. Therefore, this review focuses on the production of materials which showed promising antifungal properties and may be later exploited as tangible medical applications.

As a guide to the reader and as a final note to the introduction, we add a brief table of contents to summarize the content of the review. As such, the present review is divided in the following sections:

1. Polymers with antifungal moieties
   (a) Cationic antifungal polymers
   (b) Azoles
2. Fungicide addition to polymers
   (a) Metal-loaded polymers and composites
   (b) Addition of organic-fungicide compounds to polymers
3. Drug delivery systems
4. Polyene macrolides and echinocandins
5. Other antifungal polymers.

2 | POLYMERS WITH ANTIFUNGAL MOIETIES

Low-molecular weight antifungal molecules and the specific moieties which allow for their antifungal activity are well documented and readily used on the medical industry. For instance, topical and oral formulations of clotrimazole, fluconazole and ketoconazole have been commonly used for the treatment of many fungal infections for decades and even have been available as over the counter medications in some of their pharmaceutical forms (Choi et al., 2019; Patton et al., 2001; Sawyer et al., 1975). In contrast, their polymeric counterparts have been only recently researched in a thorough manner and have often been related to the corresponding research on antibacterial polymers. It is important to note that although the inhibition effect of antifungal polymers is the same as the one of low-molecular 'classic' antifungals, their mechanisms of action are usually focused on the vicinity of the cell membranes, since polymer molecules are not prone in migrating within the insides of pathogen cells. In any case, the majority of polymers that have been proven to be antifungal must have cationic moieties so that the polymers have an overall positive charge density which are antifungal via the disruption of fungal cell membranes (e.g. quaternary ammonium and phosphonium salts), or contain moieties which are 'classically antifungal' through inhibition of crucial processes for fungi proliferation (e.g. azole rings), or that exhibit both properties (eg. azolium rings) (Jiao et al., 2017; Long et al., 2017). With this in mind, in this section, for both cationic antifungal polymers and polymers with moieties which 'classically' inhibit fungi proliferation, their summarized mechanisms of action, important examples of each classification and recent advances on each field will be discussed.

FIGURE 1 Ammonium (left) and phosphonium (right) containing polymers, R groups are alkyl or allyl chains, while X is a counterion

2.1 | Cationic antifungal polymers

Cationic polymers and macromolecules are arguably one of the most extensively researched in antimicrobial polymeric materials as these substrates tend to be very effective antibacterials and antifungals. Even though the mechanism of action for this kind of polymers is not universally accorded, it is believed that the positive charge on these macromolecules inhibits the growth of pathogens by disrupting the cell walls and membranes of microorganisms (negative charge), promoting lysis of the contents of the cell. In this sense, both bacteria (especially gram-positive bacteria) and fungi are susceptible to this effect and are therefore often evaluated similarly when testing this kind of polymers. Even when all cationic polymers must bear a positive charged moiety, this characteristic is not enough to effectively disrupt the cell walls of pathogens such as fungi; for that purpose, functional groups that are effective in antifungal polymers must have certain characteristics.

Firstly, one of the most important characteristics of the charged functional groups is their identity since this determines both the synthetic availability of the materials and the potential for modification of a material. In general, the most common cationic moieties of antifungal polymers are quaternized ammonium and phosphonium salts from which ammonium salts are more prevalent. These types of salts are very common due to the existence of an enormous variety of techniques for their synthesis and the inclusion onto polymers (Arora & Mishra, 2018). Most of the salts contain pendant alkyl chains bounded to the heteroatom (nitrogen or phosphorus) (see Figure 1), which may be specifically selected during the synthetic protocol, so that the resulting material has specific behaviours or characteristics. It is important to note that although cell lysis is one of the most common mechanism of action for this kind of substrates, other mechanisms exist that may potentiate the effect of the positive charge and may be modulated by the identity of the alkyl groups attached to ammonium and phosphonium moieties, as well as by the backbone of the polymer. Some examples will be presented in this section (Jiao et al., 2017).

Secondly, one of the most important characteristics of this kind of polymers is the density of positive charge within the macromolecules, which directly affects the effectivity of the polymers in disrupting the cell walls of fungi. In general, more charge density implies a greater disruption capability. This parameter depends on the identity of the backbone of the polymeric material, the amount of charged groups within the polymer backbone, the identity of the charged functional groups, the presence of ramifications on the

polymer substrate or the charged functional group, and on the average molecular weights of the material (Kenawy et al., 2007).

Another important characteristic that influence the behaviour of these polymers against fungi is their hydrophobic/hydrophilic balance. This parameter must be well balanced, since excessively hydrophobic surfaces (including polymer films and medical devices) are susceptible to protein adhesion which may promote fungi biofilm formation and excessively hydrophilic substrates may not only be toxic to pathogenic cells but also to hosts cells. The amphiphilic character may be easily modified by altering the identity of the pendant alkyl chains of ammonium or phosphonium salts. Even though it might not be universal for all polymers, chain sizes between 6 and 8 carbons have shown to be best effective in inhibiting pathogen growth (both bacteria and fungi) without being toxic to mammal cells (Ergene et al., 2018; Muñoz-Bonilla & Fernández-García, 2012; Xue et al., 2014).

A final parameter that is also important to control is the identity of the counterion (anion). This is due to mainly three facts: firstly, the dissociation of the polymer-counterion salt is a very important step in the interaction of the antifungal polymer and the pathogenic cells; therefore, the counterion must not be strongly bounded to the polymeric cation. Secondly, the identity of the counterion (especially the size and chemical characteristics) may affect the hydrophilic/hydrophobic balance of the polymer, especially when using large counterions such as PF_6^-. The third aspect about the counterion is related to the fact that the presence of cationic polymers often disrupts the concentration of essential cations like Na^+, K^+, Mg^{2+} and Ca^{2+}, disrupting the osmotic balance of pathogen cells which may potentiate the antifungal effect. This last effect is related to the mobility that the counterion has within the cell walls and the extracellular environment of the pathogens. The choice of the correct counterion depends on the characteristics of the cationic polymer matrix, and it is often one of the last parameters to be adjusted for these systems (Ergene et al., 2018; Jiao et al., 2017; Xue et al., 2014). Since the rise of antifungal cationic polymers, the search for antifungal polymers has been often associated with the development of antibacterial polymers. Nonetheless, fungi cells are not necessarily susceptible to the same cationic polymers as bacteria, since fungi are not prokaryotic cells like bacteria but eukaryotic cells; meaning that although the cell walls may be similar in composition and charge, the charge density and distribution may differ significatively to that of bacteria (Arslan et al., 2017; Hassan, 2015). Therefore, in recent years, the development and evaluation of specific antifungal polymers has increased with the added advantage that they also may be antibacterial.

One interesting system that has received a lot of attention recently is chitosan, specifically cationic derivatives of this substrate. Chitosan is one of the most abundant natural polysaccharides on the planet (second only to cellulose), and this linear polysaccharide is composed by random structural units of D-glucosamine and *N*-acetyl-D-glucosamine and is obtained through the partial deacetylation of chitin as shown on Figure 2 (Pérez-Calixto et al., 2016). Apart from being extremely abundant and being biocompatible, Shin and collaborators demonstrated that this polymer has intrinsic antimicrobial properties against gram-positive bacteria such as *S. aureus* and possess intrinsic antifungal properties by inhibition of crucial metabolic processes for fungi species such as *C. albicans* and *S. cerevisiae* (Shih et al., 2019). Additionally, chitosan has been used in combination with other antifungal compounds and has been used in the development of fungicide-delivery systems (as it will be discussed in following sections).

Although chitosan by itself presents crucial advantages as an antifungal substrate (at least for common pathogens for humans), its use is limited by its solubility in aqueous (and non-aqueous) media. To overcome this drawback, the most common modification for chitosan is the alkylation of its amino groups to form cationic *N*-substituted chitosan derivatives. This not only allows enhanced solubility of the polysaccharide, but also gives the possibility to freely integrate cationic ammonium or phosphonium moieties to the chitosan polysaccharide backbone.

A recent example of a modification of this nature was presented by Huang Jianying and collaborators, in which a modified antifungal chitosan that could be useful for oral medications was obtained. In this work, the modified chitosan was produced by treating chitosan with 4-chlorobutyryl chloride. The nucleophilic substitution of the obtained *N*-chlorobutyrylchitosan lead to the formation of the ammonium derivative of chitosan, *N*-(1-carboxybutyl-4-pyridinium) chitosan chloride (Figure 3). This modified chitosan derivative was effective in inhibiting the growth of two different fungi species with higher effectiveness than pure chitosan, as shown on Table 1 (Jia et al., 2016).

In another example of chitosan modification, quaternized *N*,*N*,*N*-trimethylchitosan was produced by a two-step method involving the formation of a Schiff base intermediate on the amino group of chitosan, and its reduction followed by methylation with methyl iodide (Tabriz et al., 2019). These chitosan cationic derivatives along

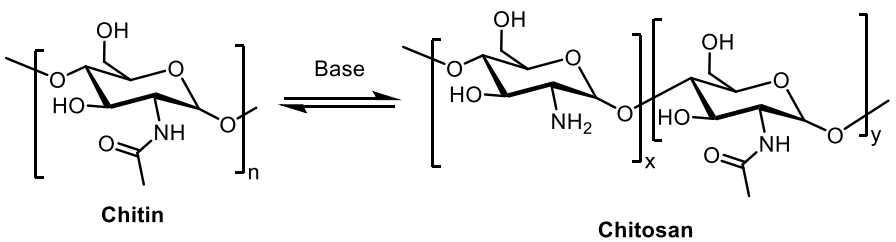

FIGURE 2 Partial deacetylation of chitin to produce chitosan

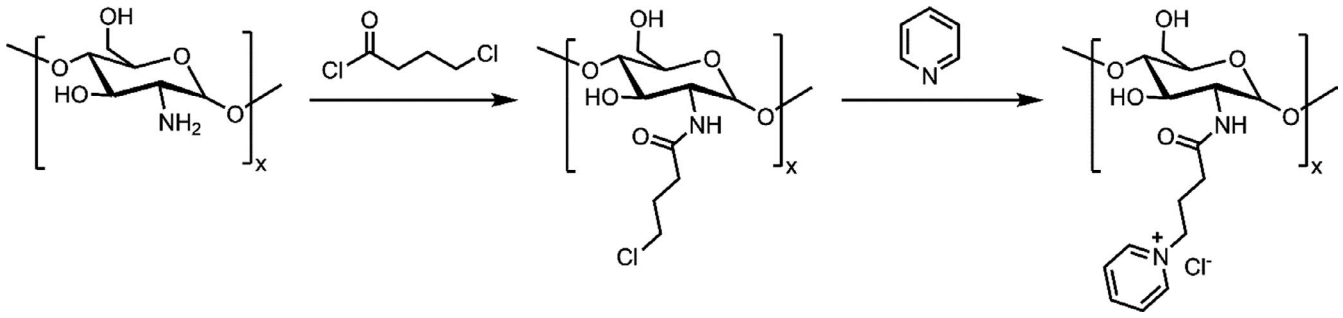

FIGURE 3 Synthetic route for *N*-(1-carboxybutyl-4-pyridinium) chitosan chloride

TABLE 1 MICs and MFCs for pyridine modified chitosan (Jia et al., 2016)

	Chitosan		*N*-(1-carboxybutyl-4-pyridinium) chitosan chloride	
Microorganism	MIC (mg/L)[a]	MFC (mg/L)[b]	MIC (mg/L)	MFC (mg/L)
Botrytis cinerea	0.25	8.00	0.13	4.00
Fulvia fulva	0.25	2.00	0.13	1.00

[a]MIC: Minimum inhibitory concentration. For antimicrobial substances, is the minimum concentration of said substance in solution capable of visibly inhibiting the growth of a pathogen.

[b]MFC: Minimum fungicidal concentration: For antifungal substances, is the minimum concentration of said substance in solution capable of killing at least 99.9% of the initial pathogens in a culture medium.

with pristine chitosan were embedded within polyethersulphone membranes and tested for antifungal activity and hydrophilicity. In all cases, the inclusion of chitosan generated antifungal activities, which were visually detected in petri dish 'zone of inhibition test'[1] with notable results from the membranes that contained quaternized *N*,*N*,*N*-trimethylchitosan, in which there was notorious inhibition of growth of *Aspergillus niger*. According to the results for this research, these membranes may be used for water purification and filtration processes (Tabriz et al., 2019).

A final series of examples of chitosan modification is the work presented by Wenqiang Tan and collaborators from 2017 to 2020. They presented the incorporation of different functional groups onto chitosan with an array of synthetic techniques as a mean to inhibit different species of fungi relevant to agriculture and to improve water solubility of the chitosan derivatives. In this work (Figure 4a), a combination of phosphonium and ammonium salts was introduced by chitosan amine groups alkylation and nucleophilic substitution to form the quaternary alkyl and allyl phosphonium groups (Tan et al., 2017). In another paper (Figure 4b), the research group modified chitosan nitrogen with two methyl groups and a different array of pyridinium groups through Schiff base intermediates to form quaternary ammonium antifungal polymers (Wei et al., 2018). In a follow-up study (Figure 4c), the same research group used azide−−alkyne click reactions to include quaternary ammonium onto chitosan (Tan et al., 2018). In this paper, these substrates demonstrated to be antifungal but not to be completely biocompatible by exhibiting some dose-dependent cytotoxicity. Finally, in 2020, the research group (Figure 4d) used nucleophilic substitution reactions to form urea and pyridine-containing chitosan, and these polymers also proved to be antifungal and also to cause low cytotoxicity on L929 cells with cell viabilities up to 100% (Zhang et al., 2020). For the last two examples, not only antifungal activity was achieved, but also antioxidant and radical scavenging properties. Although these advances are not specifically for human relevant fungi, they showed progresses in pathways to obtain functional antifungal substrates for human use in the future.

Although many of the recent advances on the development of antifungal substrates have been performed onto chitosan, other polymers have also exhibited good activity. For example, another important field for antifungal cationic polymers are derivatives of nylon-3 which are produced by ring-opening polymerization of β-lactams which general structure is depicted on Figure 5. It is important to mention that most of the examples presented in this work involve the synthesis of specially crafted monomers (via chemical modification of the monomers or specialized synthesis of specific monomers) to form systems that could be antimicrobial or even could have other functionalities. However, as with any polymeric system modification, post-polymerization is also possible and may be useful in certain cases (Liu et al., 2014).

These polymers are interesting since they mimic the underlying structures of naturally occurring peptides that aid in the immune response against microbes. However, they lack α-peptide bonds cleavable by natural enzymes coming from some antifungal resistant pathogens. This kind of polymers originally showed good response against bacteria without being toxic to human cells. With further developments, other polymer structures were also found to be toxic to fungi without compromising their biocompatibility. One of the first examples of such systems was produced in 2013, where custom amino-containing β-lactams were copolymerized by anionic ring-opening polymerization to form racemic mixtures of poly-β-peptides (Zhang, Kissounko, et al., 2009). In this work, the produced nylon-3 derivatives were capable of inhibiting the growth of *C. albicans* with MICs as low as 3.1 mg/L and HC_{10}[2] and IC_{10}[3] higher than 400 mg/L for the corresponding polymer. This evidences a very good antifungal activity and very low cytotoxicity. Interestingly, these polymers

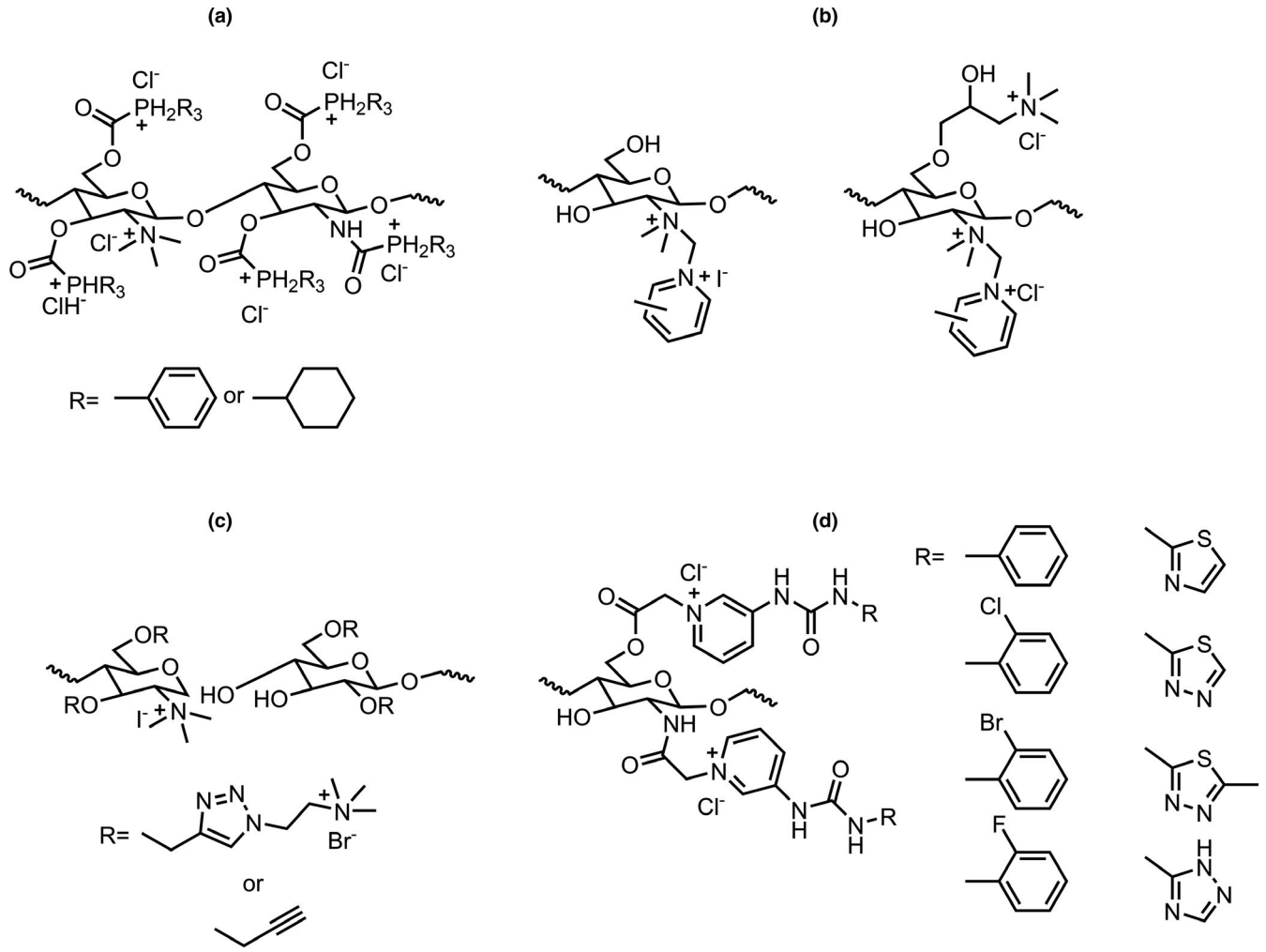

FIGURE 4 Modified derivatives of chitosan which have shown potentiated antifungal properties (Tan et al., 2017, 2018; Wei et al., 2018; Zhang et al., 2020)

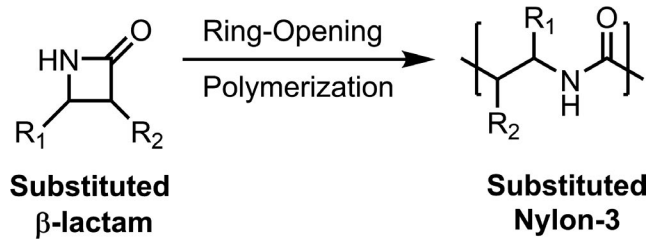

FIGURE 5 Formation of nylon-3 derivatives from ring-opening polymerization of substituted β-lactams

were also very effective antibacterials having MICs for *E. coli*, *B. subtilis*, *E. faecium* and *S. aureus* ranging from ~100 mg/L to ~102 mg/L (Liu et al., 2013). On a follow-up study, Liu and collaborators determined some of the crucial structural components necessary for these compounds to be useful, related to the β-peptide structure, the cationic and hydrophobic balance and how this is related to toxicity against *C. albicans* and some other fungi (Liu et al., 2014).

From these pioneering works, more studies emerged in which different nylon-3 derived copolymers were studied. On one of these studies, the evaluated nylon-3 derivative showed excellent antifungal activity against several organisms from the genera *Candida* and *Cryptococcus*, comparable to fluconazole and amphotericin B (AmB) (Rank et al., 2017, 2018), even showing synergism when used along these antifungals. Unfortunately, these substrates were not effective against *Aspergillus* spp by themselves, but they were shown to enhance the effect of other azole antifungals such as posaconazole and itraconazole against these pathogens. Finally, for this work, the cytotoxicity of the compounds was evaluated and it was concluded that these compounds are still biocompatible up to doses much higher than the determined MICs (Rank et al., 2017). In a follow-up study, the same research group evaluated new derivatives of these compounds obtaining an extensive list of inhibition interactions within several genera of fungi (Rank et al., 2018).

A last notable example of effective antifungal cationic polymers is a member of the well-known guanidines used as antiseptics and antimicrobials in wound dressings, contact lens solutions, gloves, etc. (Ali & Wilson, 2017; Karidurаganavar et al., 2014; Lee et al., 2004; Lim et al., 2008; Niu et al., 2017). In this work, polyhexamethylene guanidine hydrochloride (PHMGH) was evaluated for its

antifungal properties (Figure 6). The authors found that this polymer has comparable MICs to AmB against various fungi species (Table 2), while causing no haemolysis or LDH release at concentrations at least up to 16 times higher than the found MICs (in direct contrast with AmB which is much more toxic to human cells). Additionally, in this work, they elucidated a possible mechanism for its antifungal behaviour which was determined to be pore formation and ion leakage form the cell (Choi et al., 2017). Additional studies regarding both low-molecular weight and polymeric guanidino compounds as antifungals have also shown promising results (Buxbaum et al., 2006; Jana et al., 2005; Manetti et al., 2009). Developments performed on this kind of substrates will represent promising alternative as novel cationic antifungals.

2.2 | Azoles

Azole antifungals are one of the most important developments of the last century in antifungal therapy. Prior to the development and introduction of this new generation of drugs, the majority of therapies against fungal infection implied aggressive side effects and toxicity (Refer to section regarding polyene macrolides). Therefore, 'classic' antifungals, like ketoconazole, fluconazole, clotrimazole, miconazole, itraconzole, voriconazole and posaconazole, all contain an azole in their structures (Allen et al., 2015). Generally, most of these drugs work by inhibiting important metabolic processes of the fungi organisms, such as the production of ergosterol (which is an essential component of fungi cell walls). Therefore, the introduction of these functional groups to polymers has been a recently explored alternative in the field of antifungals. It is important to mention that although these heterocyclic moieties are clearly identified as being effective antifungals, since these heterocyclic functional groups may be alkylated or protonated to form quaternary ammonium salts, they have also been explored as antibacterial materials due to their positive charge (Anderson & Long, 2010; Andersson Trojer et al., 2013; López-Saucedo et al., 2017, 2018; Meléndez-Ortiz et al., 2015, 2016; Yang et al., 2018). In this section, we only present examples of azole-containing polymers which have shown to be effective against fungi. We were interested in presenting azoles on their own section because these functional groups have proven to be very effective as antifungal drugs with minimal side effects and since their mechanism of action is not only due to electrostatic interactions as in the case of cationic antifungals.

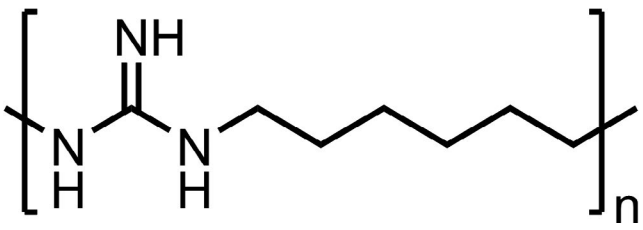

FIGURE 6 Polyhexamethylene guanidine hydrochloride (PHMGH)

TABLE 2 MICs for the guanidine antifungal polymer

Microorganism	MIC (mg/L)	
	PHMGH	AmB
C. albicanis (ATCC 90028)	1.25	2.5
C. parapsilosis (ATCC 22019)	1.25	2.5
M. furgur (KCTC 7744)	2.5	2.5
T. beigelii (KCTC 7707)	1.25	1.25
T. rubrum (KCTC 6345)	2.5	1.25

A first example of polymers containing an imidazole group as antibacterial and antifungal substrate is a 2019 patent in which a series of imidazole ionenes[4] showed to be effective antibacterial and antifungal agents with no significant haemotoxicity (WO 2019/088917 A1, 2019). In 2019, Wei and collaborators obtained different cationic chitosan derivatives through the inclusion of imidazole derivatives bounded to oxygen number 6 of the chitosan structure (Figure 7). These derivatives were demonstrated to have antifungal activity against *Botrytys cinera* and *Gibberella zeae* with good biocompatibility to human HaCaT cells (Wei et al., 2019).

Chun's group has modified polymers with azole groups to add antifungal properties. For example, in 2018, crosslinked polyurethanes (PU) containing imidazole groups were obtained by grafting and crosslinking 4-imidazole acrylic acid using AIBN as an initiator (Figure 8). These polymeric materials were tested for their antifungal properties as well as for their mechanical properties and shape-memory capabilities. Films of this materials were shown to have the ability to attain shape recovery due to the introduction of increasing amounts of the imidazole moiety in the crosslinked structure. Additionally, these films were able to have flexibility even at low temperatures (<10°C) due to the grafting of the imidazole. Finally, some of these materials were demonstrated to be antifungal against a mixture of *C. globosum*, *A. niger*, *P. pinophilium*, *G. virens* and *A. pullulans* (Chung, Kim, et al., 2018).

In addition, the same group modified PU with benzimidazole rings, since benzimidazole avoids fungal growth against a wide spectrum of fungi. The surface modification of this polymer was achieved by a grafting reaction with benzimidazole, 2 hydroxyethyl acrylate and acryllic acid, to increase the hydrophilicity and to facilitate the contact between the fungi and the benzimidazole moiety, see Figure 9. The resulting material showed shape-memory properties with fungi growth inhibition, when tested in a mixture of *Aspergillus niger* (ATCC 9642), *Aureobasidium pullulans* (ATCC 15233), *Chaetomium globosum* (ATCC 6205), *Gliocladium virens* (ATCC 9645) and *Penicillium pinophilum* (ATCC 11797) (Chung, Park, et al., 2018).

A final example of azole-containing polymers was the inclusion of three (triazole) and four nitrogen (tetrazole) rings to produce polymer pipes, which are resistant to corrosion due to bacteria or fungi. For this objective, the authors modified low density polyethylene (LDPE) films with various triazoles and tetrazoles through extrusion. With these, the authors demonstrated significant antifungal activity against *Aspergillus niger*, *Penicillium*

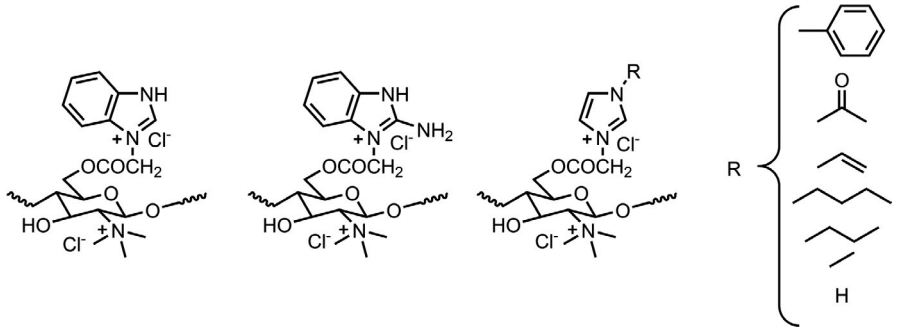

FIGURE 7 Antifungal imidazolium-containing chitosan (Wei et al., 2019)

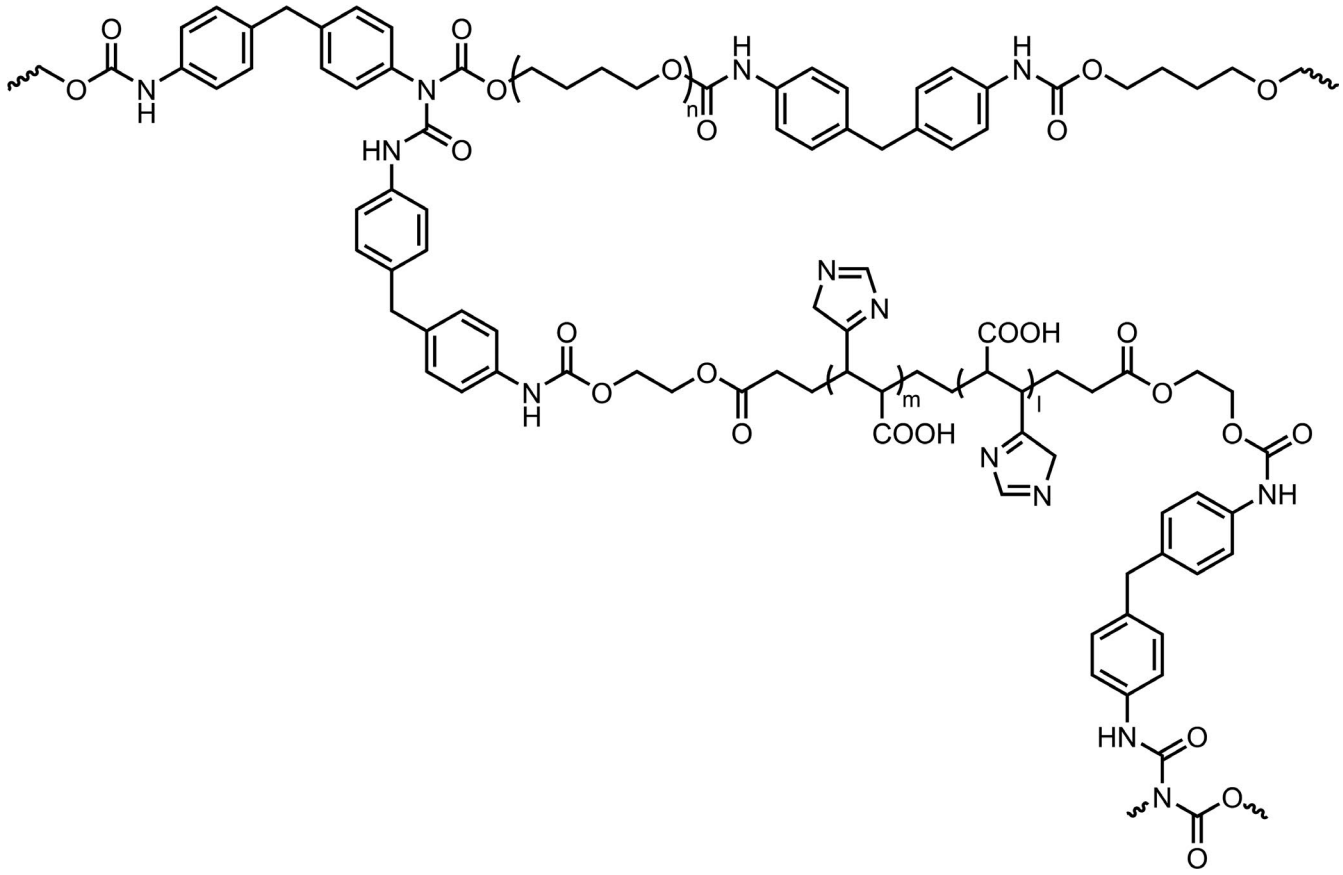

FIGURE 8 Imidazole-containing polyurethanes synthesized by Chung, et al. (2018)

cyclopium and *Trichoderma* spp. fungi. Although this work was originally envisioned as an anticorrosive additive to pipes, polymeric materials such as LDPE are very common on medical devices, and thus, the application of multinitrogen rings onto polymers may be a viable solution for antifungal polymers in the future (Tsarenko et al., 1998).

3 | FUNGICIDE ADDITION TO POLYMERS

In contrast to intrinsic antifungal polymers or macromolecules, some polymers used in medical devices have been doped or modified by the addition of well-known antimicrobial agents, including antibacterial, antifungal and biocidal compounds. The addition of this kind of compounds into polymers has been employed mainly with the aim of avoiding bacterial adhesion, and thus preventing the contamination of medical devices such as catheters and valves. There are several studies on the synthesis of drugs to prevent fungal biofilm formation, since it causes health hazards (Costa-Orlandi et al., 2017; Desai et al., 2014).

There are at least three ways to provide antifungal properties to polymers by adding organic or inorganic fungicides: first, formation of fungicide/polymer composites or blends, second, covalent attachment of fungicide moieties in the polymeric structure and third, use

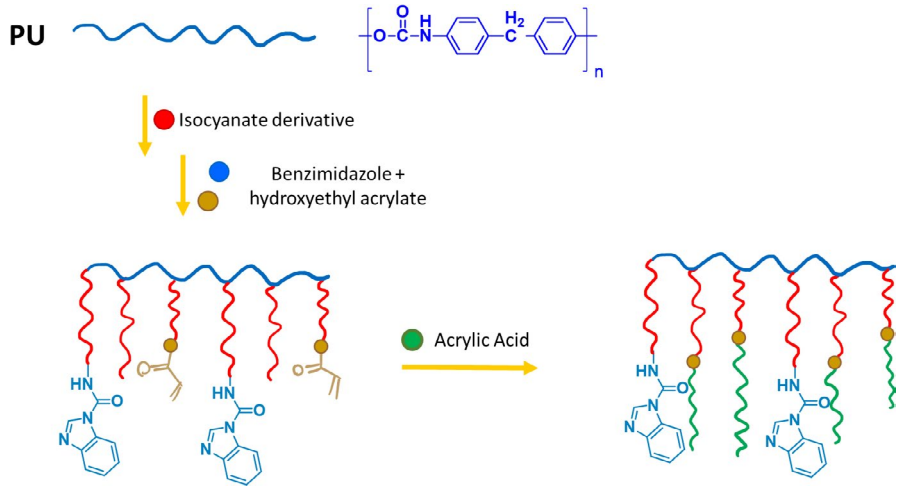

FIGURE 9 Benzimidazole-AAc grafts onto polyurethane surface (Chung, Park, et al., 2018)

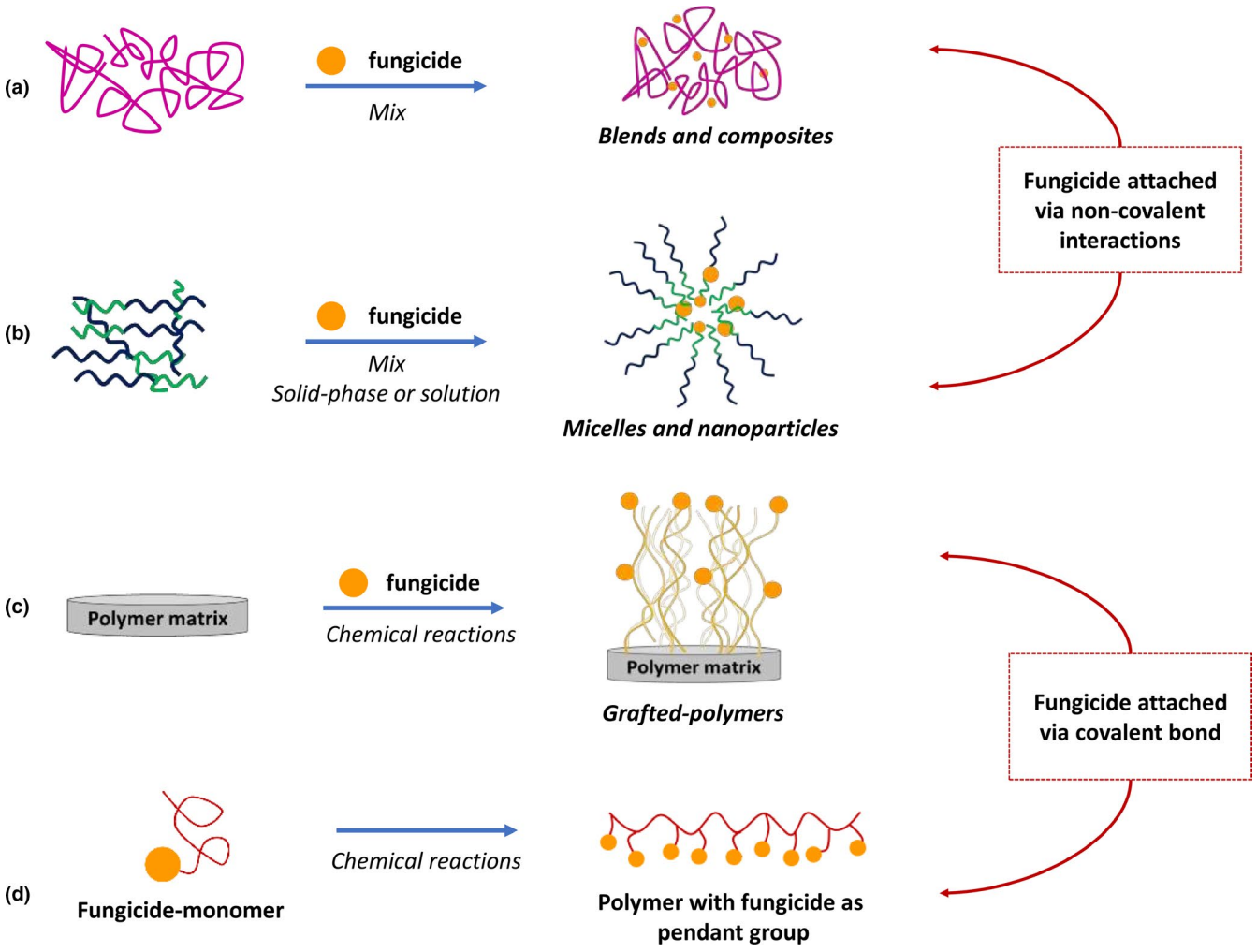

FIGURE 10 Incorporation of fungicides into polymers for biomedical applications. (a) Blends and composites, (b) Micelles and nanoparticles and (c) Grafts onto polymer surface and (d) Polymers with fungicide as pendant group

of polymeric micelles and nanoparticles for fungicide retention and release.

The most common of the three methods is mixing both components to obtain a polymer/fungicide composite or a simple mixture or blend (Figure 10a). This approach has allowed the formation of controlled-release systems such as micelles or polymer nanoparticles (Figure 10b). In these two methods, the fungicide is attached, loaded or immobilized by non-covalent interactions with the polymeric structure. In another method, the active compound can be attached via covalent bond by conventional chemical reactions, such as nucleophilic substitution or condensation reactions. The resulting material usually shows antifungal activity due to the active compound. The modification can be performed onto the surface of a polymer (Figure 10c) or in other polymers and hydrogels (Figure 10d).

Although this kind of modifications is less effective than the use of intrinsic antifungal polymers (especially cationic polymers), this approach is extensively used in the development of antifouling polymeric surfaces and for the synthesis of fungicide delivery systems. These fungicides can be metallic nanoparticles, metal cations, organic compounds such as polyenes, azole rings and lipopeptides, among others. Firstly, in this section, we will review the metal-loaded polymers and composites.

3.1 | Metal-loaded polymers and composites

Metal-nanocomposites with nanoparticles (NP) embedded into polymeric matrices have been developed during the last two decades due to their good antimicrobial properties in medical devices, food-packing and other applications in which sterile coatings are needed (Hanemann & Szabó, 2010; Jaramillo et al., 2019; Muñoz-Escobar & Reyes-López, 2020). The most common metals studied as NP embedded into polymeric matrices are Ag, Cu and Zn. Their antimicrobial properties are function of cation identity, cation controlled-releasing properties as well as selectivity to the target cells (Tamayo et al., 2018). Regarding the pathways of metal toxicity, the main mechanisms described in the literature for silver NPs are Ag^{+} binding to proteins which produces changes in the cell wall and their metabolism as well as the binding to nitrogenous bases of DNA and RNA. Additionally, CuNPs and AgNPs can produce oxidative stress by the formation of ROS species (Akter et al., 2018; Vazquez-Muñoz et al., 2017). Furthermore, it is generally accepted that although most of the research has been developed for their effects on bacterial growth, the mechanisms are similar for the inhibition of fungi species (Vincent et al., 2018).

Antifungal coatings against *Saccharomyces cerevisiae* yeast have been reported using CuNPs loaded into water-insoluble polymeric matrices of polyvinylmethylketone (PVMK), polyvinylchloride (PVC) and polyvinylidenefluoride (PVDF). With a surface metal loading of 1%–2% and NP diameter of 4.6 nm ± 1.8 nm, the composite CuNP-PVMK displayed the strongest antifungal activity since no CFU/ml was observed. In an additional experiment, the antifungal activity of CuNP-PVMK was correlated as a function of seven different CuNPs loadings, thus indicating interesting controlled-release properties for spinnable bioactive coatings (Cioffi et al., 2004). The same authors made improvements of the CuNP-PVMK composite by CuNPs electrochemical stabilization into the polymeric matrix to minimize the damage for untargeted cells, improving controlled-releasing properties thorough formation of Cu-NPs clusters of about 500 particles (Cioffi et al., 2005).

Polycaprolactone (PCL) is one of the most used polymers in biomedical applications due to its biodegradability and biocompatibility (De Paula et al., 2018). Recent studies have explored PCL fibres as loading matrices for CuONPs (average size 35 nm) against fungi components of oral candidiasis: *C. albicans*, *C. glabratea* and *C. tropicalis*. The CuONPs showed increased diameter (90%) in the composite nanofibres (PCL- CuONPs). The CuONPs were loaded from solutions with 1 to 100 nM initial concentrations, and the evaluation of their antifungal activity was carried out with EUCAST protocol, showing a marked antifungal activity against all tested *Candida* species at initial concentration of 25 nM of CuONPs. Apoptotic cell death was the main pathway observed, caused by the rupture of the cell wall and was attributed to the Cu^{2+} leaching in the biological environment. This study remarkably underlined the effect of pH, ionic strength and dissolved organic matter in the displayed toxicity by the leaching of CuONPs (Muñoz-Escobar & Reyes-López, 2020).

Oral diseases (e.g. denture stomatitis) caused by *C. albicans* in denture prosthetics have shown resistance against conventional antifungal agents and thus have become an issue in the dental area. To mitigate this, the development of a new antifungal polymeric agent consisting of AgBr-NPs loaded into quaternary ammonium salt polymer 4-vinylpyridinium (NPVP) and then mixed with polymethylmethacrylate (PMMA) denture resin has shown an inhibitory effect on the growth of *C. albicans*. The composite AgBr-NPVP was mixed at 1% concentration with PMMA to get (after dilutions) concentrations ranging from 0.1% to 0.5% of the metal agent mixed within the resin. With this procedure, the AgBr-NPs (average size 30 nm) were embedded into the cationic NPVP. The MIC reported was 250 μg/ml and was obtained in a culture medium using artificial saliva. A correlation between loaded Ag-NPs and the antifungal activity was found, showing controlled-release properties for this system (Zhang et al., 2017).

AgNPs in binary nanocomposites Ag@F_3O_4 and Fe_2O_3@Ag in which non-cytotoxic polyacrylate (relative mass = 8,000 g/mol) was used as a spacer between AgNPs and the oxide particles showed both antifungal and magnetic properties. These features are promising for drug delivery applications where an antimicrobial agent could be targeted and removed by an applied external magnetic field (Prucek et al., 2011). Interestingly, the polyacrylate spacer suppresses most of the interparticle interactions. The composite Ag@F_3O_4 (AgNPs average size 70 nm) showed lesser antifungal activity compared with the nanocomposite Fe_2O_3@Ag (AgNPs average size 5 nm), this is in line with the known correlation between antimicrobial properties of AgNPs and the NP size (Baker et al., 2005). The reported MIC values against four *Candida* species were from 1.9 mg/L to 31.3 mg/L.

Composites of AgNPs with chitosan (from crustacean waste) have been synthesized to avoid agglomeration of nanoparticles (Kalaivani et al., 2018). Amino groups in chitosan were proposed to be actuating as ligands for stabilizing the spherical NPs with size ranging from 10 to 60 nm. The chitosan-AgNPs showed antifungal activity towards *A. niger* (inhibition zone 15 mm), *A. fumigatus* (13 mm), *A. flavus* (13 mm) and *C. albicans* (11 mm). The results observed in the characterization of the NPs by FTIR showed that the primary amino groups of chitosan were involved in the interaction with AgNPs' surface; thus, chitosan is acting as a capping site within the AgNPs composite, as indicated by the increasing AgNPs size with a decrease in chitosan initial concentrations. In this work, the authors concluded that crustacean waste (chitosan) represents a cheaper source to produce small AgNPs for medical applications.

Graphene oxide (GO) has also been used to get Ag nanoparticle-stabilized systems. The composite (PVA/GO–AgNPs) in which GO surface has been decorated with AgNPs (average size 3.1 nm) and then incorporated as a reinforcing filler into poly(vinyl alcohol) (PVA) matrix. PVA has been used for its biocompatibility, biodegradability, low toxicity and its mechanical properties. The composite showed antimicrobial properties and promising use in wound healing as well as infection prevention (Cobos et al., 2020).

Bandage material cotton fibres (cellulose) have also been the target of several works on nanocomposites. Cotton fibres have been covered with bimetallic NPs of composition Ag/Cu 1:1, forming composites with high antimycotic properties. The composite fibre with Ag/Cu NPs 0.06%–0.25% w/w showed high antifungal activity against *C. albicans*. Interestingly, the AgNPs coated cotton fibres did not show antifungal properties but only antibacterial proliferation. The antimycotic properties did not change after washing, and the preparation method is highlighted because cotton fibres are just immersed in water solutions of $AgNO_3$ and $CuSO_4$ by 30 min and subsequently ironed. The antifungal activity remains after 6 months (Mathew & Kuriakose, 2013).

Nowadays, zinc oxide nanoparticles (ZnONPs) are also considered viable as antimicrobial substrate due to their potential antifungal properties, are registered as 'Generally Recognized as Safe' (GRAS) by the FDA and have several promising applications (e.g. drug delivery and antiseptic properties). The pathways of actions for antimicrobial and antifungal properties are currently not completely understood, but it is generally accepted that they displayed multimodal activity (ROS mediated and zinc direct effects) (Cierech et al., 2016; Roy Choudhury et al., 2017). As an example of this, a composite of ZnONPs (30 nm diameter) coated with chitosan-linoleic acid has been reported to show antifungal properties against *C. albicans* comparable to that of fluconazole. The MIC shown by the composite is 32 mg/ml vs 8 mg/ml for fluconazole. The chitosan-coated with ZnONPs has a higher inhibitory activity than the chitosan itself in antifungal biofilm formation; thus, the composite is proposed as a novel agent for decreasing the adhesion capacity of *C. albicans* (Barad et al., 2017).

Packaging films using agar as polymer matrix are used due to their flexibility and transparent properties both in the food industry and in biomedical devices. It has been demonstrated that ZnO-agar composite at 2%–4% (w/w) enhances the antifungal properties of fruits wraps showing promising features in biomedical applications (Kumar et al., 2019).

Aflatoxins produced by moulds such as *Aspergillus flavus* are mutagens with important clinical implications that grow in soils and grains. Appropriated films to inhibit their growth have been reported by using poly lactic acid (PLA) as a matrix and layered with ZnONPs from 1% to 5%. The composite films were tested for antifungal activity against *Aspergillus flavus* and *Aspergillus parasticus* showing an inhibitory effect as the percentage of ZnONPs increases (Nasab et al., 2019).

The development of novel materials for metallic prosthesis in orthopaedic surgeries presents challenging problems concerning the antifungal properties of the materials. Titanium surfaces are prone to the formation *C. albicans* films (Dhir, 2013), and biocompatible materials such as hydroxyapatite (HAp) are not the exception (Ciuca et al., 2016). Interestingly, composite materials based on titanium as the substrate and coated with poly(dimethyl siloxane) (PDMS) have been reported as matrices for layering with doped hydroxyapatite. The composite AgHAp-PDMS displayed the strongest antifungal activity, and the observations showed a strong decrease of the biofilm (*C. albicans*) and almost total disappearance after 48 and 72 hr. On the other hand, ZnHAp-PDMS composite showed just a slight decrease of the fungal cells' biofilm (Groza et al., 2016).

3.2 | Addition of organic-fungicide compounds to polymers

As it was mentioned previously, another approach to provide antifungal activity to a polymer is attaching the organic compound via covalent bond to the polymer chains. Commonly, the active compound can be added in two ways: first, the compound is grafted to the polymer by conventional chemical reactions, or second by the synthesis of the fungicide monomer, sometimes a vinyl moiety is added to the compound structure and then polymerized. The approach of covalent binding of the active compound to the surface may achieve prolonged action against fungal adhesion to the biomedical device (Costa et al., 2011; Yu et al., 2019).

The covalent immobilization of lipopeptides onto polymers has been tested to avoid the formation or to defeat existing biofilms; this procedure has been achieved by several chemical treatments of polymers with the antifungal drugs (Alves & Olívia Pereira, 2014; Coad et al., 2015; Griesser et al., 2015; Kucharíková et al., 2016). The fungicide caspofungin was coupled using a conventional bimolecular nucleophilic substitution benefiting from the primary amines in its structure. A promissory polymer for antifungal coatings made of allyl glycidyl ether polymerized by plasma treatment was functionalized via the spontaneous reaction between amine and epoxide groups on the surface, as can be seen in Figure 11. Caspofungin-grafted polymers were very efficient against the two fungal pathogens *C. albicans* and *C. glabrata*; additionally, the materials showed

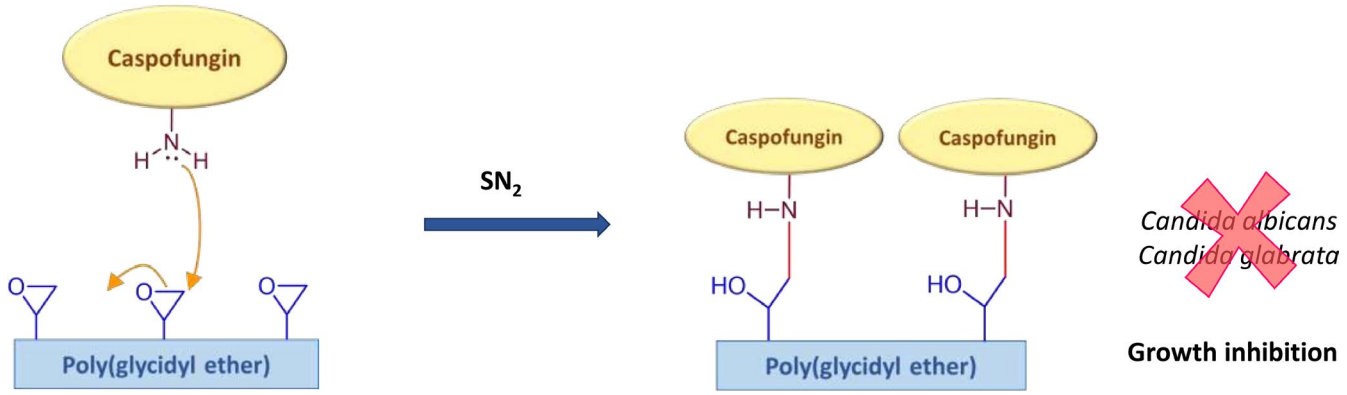

FIGURE 11 Covalent immobilization of caspofungin by amine nucleophilic attack to epoxy groups onto polymeric surface (Michl, Giles, Cross, et al., 2017)

biocompatibility (Michl, Giles, Cross, et al., 2017). More recently, caspofungin has been grafted onto polymethacrylates (Alex et al., 2020) such as poly(2-hydroxyethylmethacrylate) (PHEMA) (Michl, Giles, Mocny, et al., 2017) for antifungal activity against *Candida* and *Aspergillus* species.

According to mixtures or composites, there are reports of polymeric surfaces coated with fluorocarbon (CF_4) films and deposited by ion plasma technology. In these reports, polyethylene terephthalate (PET) was treated with CF_4 via plasma, and when the fluorine-containing got over 60%, the fungi stopped growing, showing high efficacy (Elinson et al., 2018).

Other polymer/fungicide-clay nanocomposite was prepared for their antifungal activity. First, a mixture of montmorillonite and terbinafine hydrochloride (OMMT) was obtained by solution intercalation; subsequently, the OMMT was mixed with poly(dimethyl siloxane) (PDMS) to get a composite with the fungicide. These nanocomposites were tested for antifungal activity against *Candida albicans* which strongly inhibited the fungus growth in a plate (Meng et al., 2009).

Other fungicides, such as carbendazim (a benzimidazole derivative), have been supported on poly(ethylene-co-vinyl alcohol) and epoxy resin to provide antifungal capacity to the polymer surface, and the resulting polymers demonstrated to be effective against *Aspergillus fumigatus* and *Penicillium pinophilum* (Park et al., 2001).

Finally, antifungal hydrogels have been investigated (AbouSamra et al., 2019; Liu et al., 2019; Zumbuehl et al., 2008). For example, a thermo-responsive hydrogel was loaded with an antifungal living bacterium. In 2018, Lufton et al. made a formulation of poly(ethylene oxide)-poly(propylene oxide)-poly(ethylene oxide) and *Bacillus subtilis*, since this bacterium efficiently produces and secretes potent antifungal compounds. The authors used this formulation against *C. albicans* and demonstrated similar antifungal activity as that of ketoconazole. The use of a hydrogel with a lower critical solution temperature (LCST) around body temperature allows its administration through skin, which is useful for fungi skin infections (Lufton et al., 2018).

4 | DRUG DELIVERY SYSTEMS

Nowadays, there are several investigations about new fungicide delivery systems made out of polymers and the modification of polymers to avoid the problem of hospital-associated infections and contamination of the medical materials (Howard et al., 2020).

The use of micelles for drug distribution and releasing has been employed since they favour the administration of water-insoluble drugs. Polymeric micelles with an amphiphilic structure allow the complexation of some drugs in the hydrophobic core. The hydrophilic section of the structure can interact with the human cells decreasing cytotoxicity and therefore improves the biodistribution through the body. The mechanism of action (release) of any micelle system depends directly on the compatibility between the drug and the core, which is closely related to the chemical nature of the polymer used, molecular weight and particle size (Kulthe et al., 2012).

Studies report polymeric micelle systems or nanoparticles for fungicide retention and controlled release. Additionally, some of them tried to decrease the side effects and toxicity of the orally drug administration, enhance their pharmacokinetic profile and improve the frequency of doses (Souza & Amaral, 2017). One of the most used is the amphotericin B (AmB) due to its broad-spectrum antifungal activity and its biphasic behaviour, which allows the complexation via non-covalent interactions with almost any polymer when controlling the chemical structure. This versatility has allowed the synthesis of new polymeric systems for AmB releasing, decreasing its cytotoxicity (as it will be referred in the section dealing with polyenes and echinochandins).

Polymer nanoparticles, micelles and nanocarriers have been employed for AmB encapsulation and have been tested as controlled delivery systems driven by diffusion for systemic or localized fungal infections, systematic or through the skin. For example, AmB has been loaded into polycarbonate micelles functionalized with donor–acceptor hydrogen bond groups. In 2016, Wang *et al.* added phenylboronic acids (B) and urea (U) as pendant groups in PEGylated-polycarbonate chains to form micelles and to keep AmB

molecules inside attached by hydrogen bond and other non-covalent interactions. The chemical nature of the pendant groups allows micelle formation, as represented in Figure 12.

The above-mentioned micelles were formed using either urea- and boronic acid-modified polycarbonate or both. The best performance was shown by two micelles, the B-modified and the mixed (U + B). The release of AmB in sink conditions after 24 hr reached almost 50% and 60%, respectively. In addition, the *in vitro* essays showed similar inhibition to free AmB (Fungizone®) against *C. albicans*. Moreover, these AmB-release systems showed low nephrotoxicity and low haemolytic degree (Wang et al., 2016).

This kind of micelle-type drug delivery systems has been developed with many different polymers and fungicides. For instance, *block* copolymers of poly(ethylene oxide) (PEO) and poly(amino acids) have demonstrated to be effective against some fungi, such as *C. albicans*. Additionally, they showed low haemolysis compared with conventional antifungal drugs and the antifungal activity was four to eight times higher than Fungizone® in terms of minimal inhibitory concentrations (MICs) (Yu, Okano, Kataoka, & Kwon, 1998; Yu, Okano, Kataoka, Sardari, et al., 1998).

In 2003, Kwon's group developed polymeric micelles for AmB retention, and Adams *et al.* used aspartic acid derivatives to form micelles with encapsulation of the fungicide. Conveniently, the controlled release decreased the toxicity of AmB and the loaded micelles inhibited fungal growth (Adams et al., 2003; Adams & Kwon, 2003; Lavasanifar et al., 2002).

In another example, PEO and polyethylene glycol (PEG) were combined with several polymers such as polystyrene (PS) as *block* copolymers to form micelles and retain AmB (Kun Han et al., 2007) and poly(ε-caprolactone)/retinol. Both systems showed good efficacy against common Candida species; moreover, the second one demonstrated improved antifungal efficiency against *C. albicans* and *C. auris* strains compared with Fungizone® rather than the PS copolymer (Rodriguez et al., 2020).

Additionally, polysaccharides have been used with the same purpose, as it was mentioned in the section dealing with cationic polymers, chitosan is widely used for antimicrobial and biocompatibility applications. Cross-linked chitosan/porphyrin (CS/POR) polymer nanoparticles were useful for AmB encapsulation, and different ratios of the components were tested. The particle size varied between 100 and 360 nm, and all of them proved to inhibit the growth of *C. albicans* and three *Aspergillus* spp. The most effective system was the CS/POR-AmB without a crosslinking agent, showing the lowest half-maximal inhibitory concentration (IC_{50}) against four fungi species (*A. fumigatus*, *A. niger*, *A. flavus* and *C. albicans*). They even resulted more effective than the conventional fungicides with AmB as active substance (Bhatia et al., 2014). Also, CS-dextran sulphate nanoparticles have been used for AmB loading (Tiyaboonchai & Limpeanchob, 2007). Another study used polycyclodextrins and dextran to keep AmB in the microscale with antifungal activity against the common yeast *Saccharomyces cerevisiae* (Haley et al., 2019).

AmB has also been loaded in D-α-tocopheryl polyethylene glycol 1,000 succinate and poly(ε-caprolactone-*ran*-glycolide) nanoparticles with activity against *C. albicans*; PDMAEMA-*b*-PCL-*b*-PDMAEMA nanocarriers with reduced haemotoxicity and antifungal activity against three *Candida* species, *C. albicans*, *C. krusei* and *C. glabrata* and, finally in poly(α-glutamic acid) and polyrotaxanes (Diaz et al., 2015; Mohamed-Ahmed et al., 2013; Tang et al., 2014; Zhang, Ke, et al., 2009).

Natamycin, an antifungal polyene, has been loaded in self-assembled poly(ethylene glycol)-*block*-poly(glycidyl methacrylate) (PEG-*b*-PGMA) micelles, the delivery process is more prolonged than the pure natamycin, and thus, it can be used as a controlled delivery system with better pharmacokinetic profile and low cytotoxicity when being tested in corneal epithelial cells. Additionally, the natamycin-loaded micelles required lower doses for the same activity compared to pure natamycin and a decrease in the dose frequency due to the prolonged release profile (Guo et al., 2020).

Recently, stimuli-responsive polymers have been employed to immobilize azole fungicides and avoid *C. albicans* biofilms formation with a reduction of the biomass (>50%). For example, in 2020, Albayaty and collaborators developed pH-responsive micellar systems based on poly(ethylene glycol) ethyl ether methacrylate (PEGMA) and poly(2-diethylamino) ethyl methacrylate (PDEAEMA) leading to *block* copolymers P(PEGMA-*b*-DEAEMA) loaded with itraconazole. PDEAEMA has a tertiary amine which is sensitive to pH changes, and the fungi biofilms tend to acidify the zone, thus

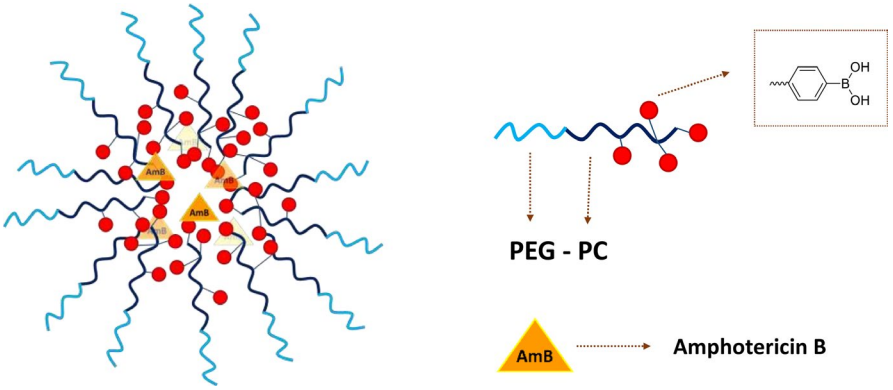

FIGURE 12 PEG/PC-B micelles with AmB encapsulation (Wang et al., 2016)

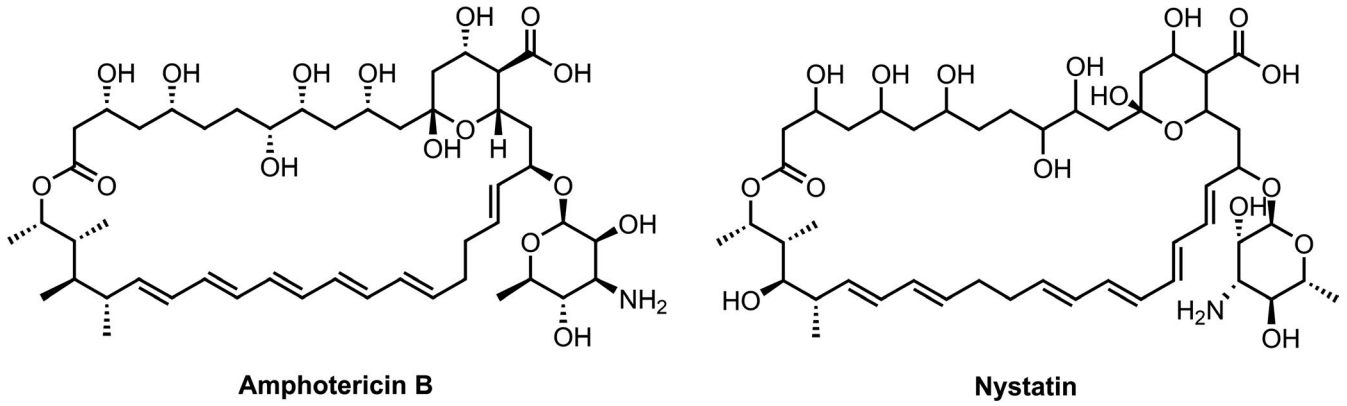

FIGURE 13 Amphotericin B and Nystatin, the two most common polyene macrolide drugs for treatment of fungal infections

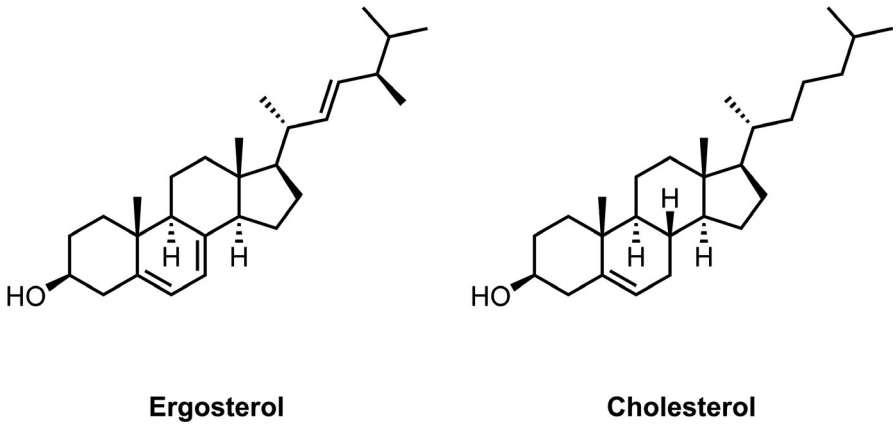

FIGURE 14 Ergosterol and cholesterol molecular structures. Note the structural similarity of both sterol molecules

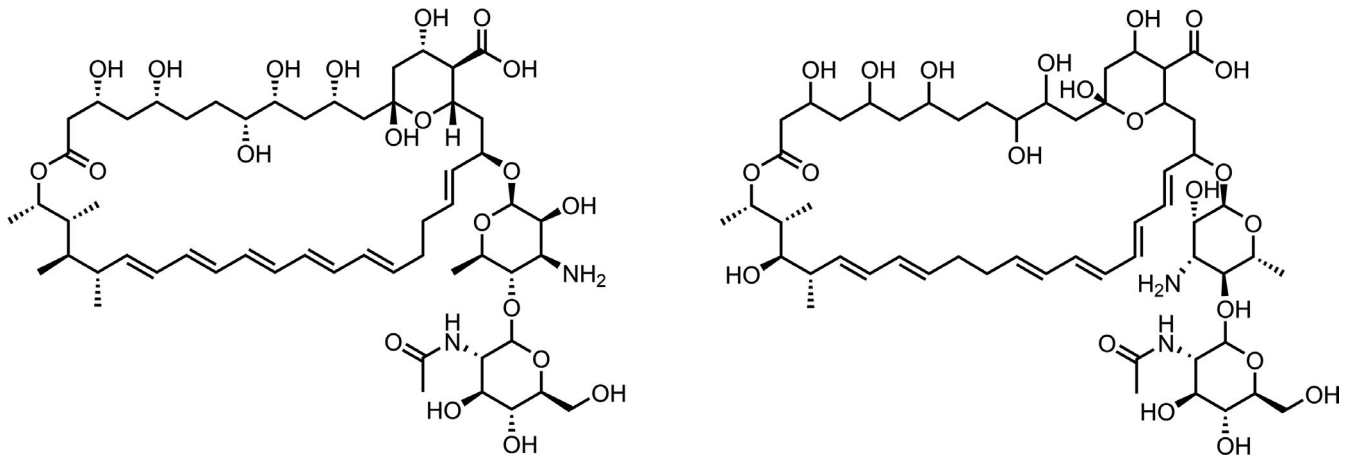

FIGURE 15 Derivatives of AMB and Nystatin A1 obtained by Kim et al. (2018)

triggering the drug release as a consequence of the repulsive charges of the protonated amines (Albayaty et al., 2020).

5 | POLYENE MACROLIDES AND ECHINOCANDINS

Polyene macrolides are a series of very powerful broad-spectrum antifungals which are often used to treat moderate to serious fungal infections. The structures of the two most important examples of this kind of macrocyclic/polymeric antifungals are shown in Figure 13, Amphotericin B (AmB) and Nystatin which are both obtained from biosynthetic pathway (Tevyashova et al., 2013).

The main structural feature of these drugs is that the macrocycles contain various conjugated dienes. These molecules are often the preferred agents when dealing with serious fungal infections and are often administered to immunocompromised patients to stop infections after organ transplant or severe radiation treatment.

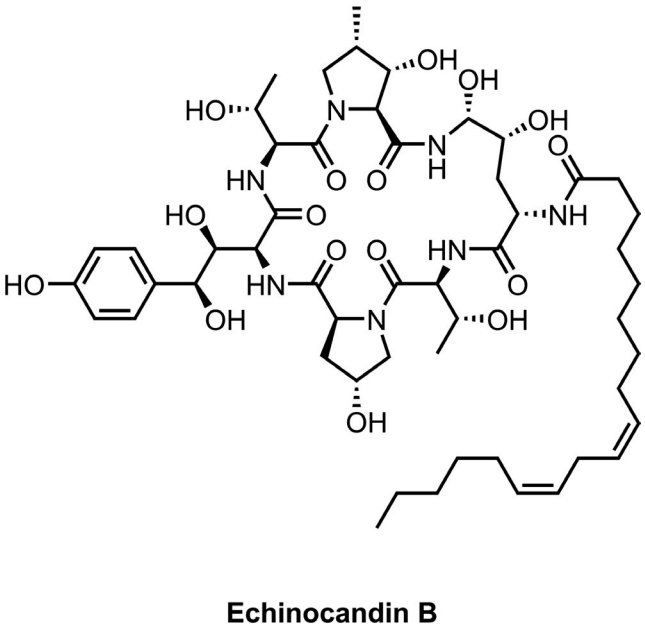

FIGURE 16 Chemical structure of broad-spectrum antifungal echinocandin B

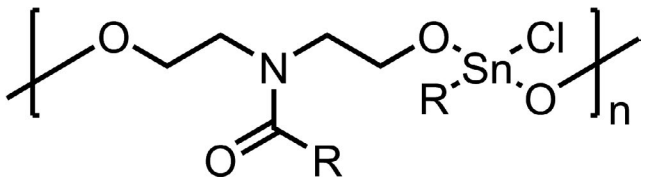

FIGURE 17 Organotin polymer with good antifungal activity against *C. albicans*

Although these drugs are highly effective, they have the disadvantage of not being selective to fungi cells and are often toxic to mammal cells. The mechanism of action of AmB starts with binding of the drug with ergosterol on fungi cell walls, following leakage of ions due to pore formation on the cell walls and finally killing the pathogen. AmB is often toxic to mammal cells since the structure of cholesterol is similar to ergosterol, which causes binding of AmB to mammal cells (see Figure 14). Therefore, these drugs also tend to affect the kidneys, liver and central nervous system of patients; this is an important concern for AmB (Borowski, 2000; Tevyashova et al., 2013).

Since these drugs have been prescribed since the 1950s, incremental doses are often needed to combat resistant fungi, increasing the concern for ineffectiveness and aggressive side effects. However, these drugs are still very useful since they are antifungals which are the least prone to increase fungi resistance (although as mentioned before, they are not exempt of generating this undesired effect). Due to the advantages and the effectiveness of these antifungals, new derivatives of AmB and Nystatin have been developed during the last decades. These modifications have been performed by direct chemical modification of the polyene macrolides or by bioengineering the organisms that produce them naturally. Since this comprise only modifications of existing macrocyclic compounds mostly through biochemical means, and not the synthesis of new polymers, this review will only cover two recent representative examples of these modifications due to the importance of these compounds. However, if the reader is interested in a more thorough analysis of this kind of antifungals, we encourage to look on the following references which include current research and existing reviews on the topic (Caffrey et al., 2008; Jarzebski et al., 1982; Kim et al., 2017; Ojika et al., 2003; Qi et al., 2015; Solovieva et al., 2011; Tevyashova et al., 2013).

A chemical modification of AmB is presented as the first example. It is important to mention that this route is not usually the preferred one to modify polyene macrolides because since compounds are usually sensitive to both acidic and alkaline conditions and have poor solubility (Solovieva et al., 2011). In this particular work, a modification of the amine group of the mycosamine portion of AmB was performed by reductive amination of aldehydes of pure and esterified AmB (carbon C-16) with yields between 20% and 76%. MICs were obtained as low as 0.020 mg/L for some of the modified compounds (AmB MIC: 0.3 mg/L), while attaining higher

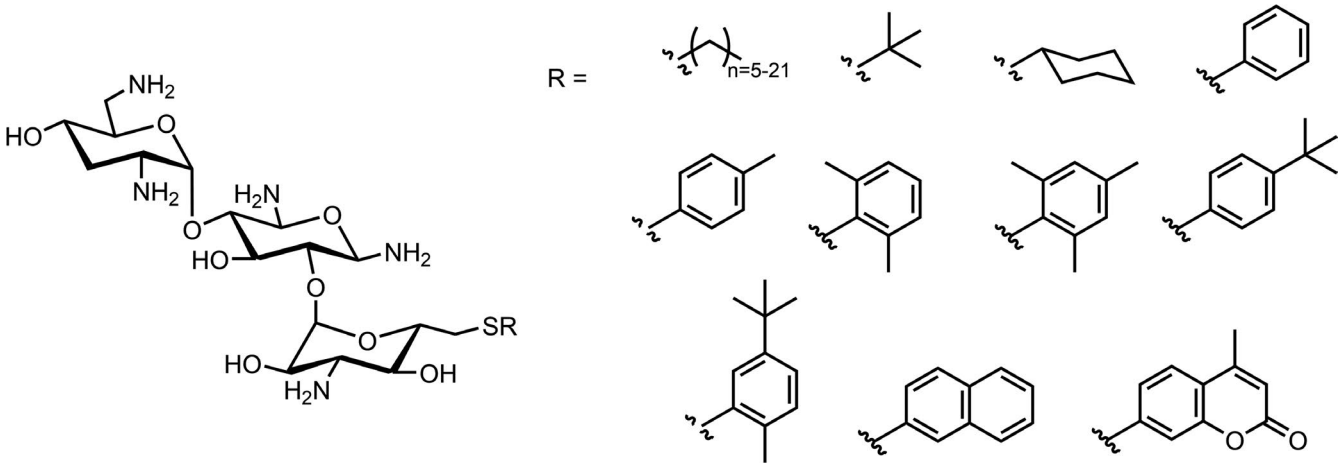

FIGURE 18 Effective tobramycin antibacterials and antifungals derivatives (Shrestha, Fosso, Green, et al., 2015; Shrestha, Fosso, Garneau-Tsodikova, et al., 2015)

TABLE 3 Compilation of recent advances in antifungal polymers

Antifungal polymer	References
Chitosan modifications	Jia et al. (2016) Tabriz et al. (2019) Tan et al. (2017) Wei et al. (2018) Tan et al. (2018) Zhang et al. (2020)
Nylon-3 derivatives	Liu et al. (2014) Rank et al. (2017) Rank et al. (2018)
Guanidine derivatives	Choi et al. (2017) Buxbaum et al., (2006); Jana et al. (2005); Manetti et al. (2009)
Azoles covalently embedded onto polymers	WO 2019/088917 A1 (2019) Wei et al. (2019) Chung, Kim, et al. (2018) Chung, Park, et al. (2018) Tsarenko et al. (1998)
Metal-loaded polymers and composites	Cioffi et al. (2005) Muñoz-Escobar and Reyes-López (2020) Zhang et al. (2017) Baker et al. (2005) Cobos et al. (2020) Mathew and Kuriakose (2013) Barad et al. (2017) Kumar et al. (2019) Nasab et al. (2019) Dhir (2013) Ciuca et al. (2016) Groza et al. (2016)
Addition of organic-fungicide compounds to polymers	Costa et al. (2011); Yu et al. (2019) Alves and Olívia Pereira (2014); Coad et al. (2015); Griesser et al. (2015); Kucharíková et al. (2016) Michl, Giles, Cross, et al. (2017) Alex et al. (2020) Michl, Giles, Mocny, et al. (2017) Elinson et al. (2018) Meng et al. (2009) Park et al. (2001) AbouSamra et al. (2019); Liu et al. (2019); Zumbuehl et al. (2008) Lufton et al. (2018)
Antifungal drug delivery systems	Wang et al. (2016) Yu, Okano, Kataoka, and Kwon (1998); Yu, Okano, Kataoka, Sardari, et al. (1998). Adams et al. (2003); Adams and Kwon (2003); Lavasanifar et al. (2002) Rodriguez et al. (2020) Haley et al. (2019) Diaz et al. (2015); Mohamed-Ahmed et al. (2013); Tang et al. (2014); Zhang, Ke, et al. (2009) Guo et al. (2020) Albayaty et al. (2020)
Polyene macrolides and echinocandins	Caffrey et al. (2008); Jarzebski et al. (1982); Kim et al. (2017); Ojika et al. (2003); Qi et al. (2015); Solovieva et al. (2011); Tevyashova et al. (2013) Kim et al. (2018) Aguilar-Zapata et al. (2015); Debono et al. (1989); Debono et al. (1995); Hashimoto (2009); James et al. (2017)
Other antifungal polymers	Ahmad et al., (2011) Herzog et al., (2012) Shrestha, Fosso, Green, et al. (2015) Shrestha et al. (2015)

biocompatibility than pure AmB (Paquet & Carreira, 2006). In a more recent work, the bioengineering pathway "as followed by the production of new derivatives of AmB and Nystatin A1 containing an extra lactone moiety. These derivatives were produced by *Pseudonocardia autotrophica* with a further enzymatic modification to form an analogue of AmB. These two derivatives had MICs comparable to AmB and Nystatin A1 while having lower haemolytic activity to human cells. The structures of both derivatives are depicted in Figure 15 (Kim et al., 2018).

Another promising set of molecules are echinocandins, which are also called 'penicillis for fungi' since they act in a similar manner as penicillin with bacteria (inhibition of glucan synthesis on cell walls) (Rubin, 2009). Echinocandin B (Figure 16) is the most common echinocandin used as a broad-spectrum antifungal. To the best of our knowledge, most of the developments on echinocandin based structures include new biosynthetic or semisynthetic derivatives to avoid antifungal resistance and to apply versatility to echinocandin formulations. As with polyene macrolides, we include a set of non-extensive references that may be helpful for the reader who wants a deeper analysis of developments in these areas (Aguilar-Zapata et al., 2015; Debono et al., 1989, 1995; Hashimoto, 2009; James et al., 2017).

6 | OTHER ANTIFUNGAL POLYMERS

The previous sections have focused on antifungal polymers classes which share a certain number of characteristics. Nonetheless, some other polymeric antifungal substrates have been found to be individually interesting. In this last brief section, we comment two isolated examples of two systems.

In the first example, we discuss the development of organometallic polymer containing tin and produced by the use of hydroxyethyl castor fatty amide oil, a sustainable natural resource. In this work, the formed organometallic polymer (Figure 17) demonstrated inhibition of different strains of *C. albicans* and even good performance against fluconazole resistant strains. Additional to the antifungal test, ergosterol biosynthesis inhibition was determined for this system, demonstrating that this polymer attacks fungi cells by inhibiting the production of this component of the fungi cell wall (Ahmad et al., 2011).

Another example is a series of studies performed between 2012 and 2015 about amphiphilic tobramycin derivatives as oligomers for polymeric substrates which may act as antibacterial and antifungal agents. Tobramycin is a well-known antibiotic that although is effective against regular bacteria, has started to be ineffective against resistant bacteria. Originally in 2012, this work focused on modifying tobramycin through the formation of amphiphilic long chain structures containing pendant aromatic rings and thioether groups (Figure 18). These compounds were confirmed to be antibacterial against several resistant strains (Herzog et al., 2012). On a follow-up study of this kind of compounds, their antifungal activity was tested against several fungi strains (resistant and nonresistant) of species *C. albicans*, *C. neoformans* with MICs as low as 2 mg/L and very low cytotoxicity (Shrestha, Fosso, Green, et al., 2015). In the final study of this series, the use of these new antifungals combined with fluconazole, itraconazole, posaconazole or variconazole was tested with good results showing synergistic effects between the antifungals (Shrestha, Fosso, Garneau-Tsodikova, et al., 2015).

7 | CONCLUSIONS

Even though antifungal polymers research is a pioneer area compared with the research in antibacterial polymers, the importance of these systems cannot be underestimated since fungi growth is a public health problem; therefore, it is important to find alternatives and new materials with such properties.

In general, new formulations of novel polymeric antifungals such as cationic polymers, azole-containing polymers, polymeric/fungicide mixtures, blends and composites, and modified macrocyclic antifungals have demonstrated to be effective against the most common fungi species including resistant fungi. They have been used not only in medical applications but also as paint additives and as packages in the alimentary industry (Higazy et al., 2010; Hoque et al., 2015; Shemesh et al., 2015). At the same time, the drug delivery systems that have been envisioned for novel and existing antifungals have enhanced the bioavailability and prolonged the fungicide release, driving to decreasing drug ingestion, localized therapy and more convenient administration. At the moment, the research is very active for the production, characterization, testing and future applications of these materials. With further advances on this area, new materials with clinical effectiveness or versatile applications will be produced. As a final reference for the reader, a compilation of current advances is summarized in Table 3.

ACKNOWLEDGEMENTS

The authors are thankful to Dirección General de Asuntos del Personal Académico, Universidad Nacional Autónoma de México under Grant IN202320. Thanks to CONACyT for the master's degree scholarship for Luis Alberto Camacho Cruz (916557), the doctoral scholarship provided for Marlene Alejandra Velazco Medel (696062/583700).

CONFLICT OF INTEREST

The authors declare no conflict of interest.

ORCID

Marlene Alejandra Velazco-Medel https://orcid.org/0000-0002-3691-6884
Luis Alberto Camacho-Cruz https://orcid.org/0000-0003-1902-8938
José Carlos Lugo-González https://orcid.org/0000-0002-3580-0900
Emilio Bucio https://orcid.org/0000-0003-4853-125X

ENDNOTES

[1]Zone of inhibition test: Another way to quantify the antimicrobial effect is to measure the circular zone of inhibition when the material is placed on a petri dish culture containing ~10^6 CFU/ml of a given pathogen.

[2]HC_{10}: Concentration of a substance needed for lysis of 10% of human red blood cells.

[3]IC_{10}: Concentration of a substance needed for the death of 10% of NIH 3 T3 fibroblasts.

[4]Ionene: Polymer which contain ionic groups on the main chain.

REFERENCES

AbouSamra, M. M., Basha, M., Awad, G. E. A., & Mansy, S. S. (2019). A promising nystatin nanocapsular hydrogel as an antifungal polymeric carrier for the treatment of topical candidiasis. *Journal of Drug Delivery Science and Technology*, *49*, 365–374. https://doi.org/10.1016/j.jddst.2018.12.014

Adams, M. L., Andes, D. R., & Kwon, G. S. (2003). Amphotericin B encapsulated in micelles based on poly(ethylene oxide)-block-poly(L-amino acid) derivatives exerts reduced in vitro hemolysis but maintains potent in vivo antifungal activity. *Biomacromolecules*, *4*(3), 750–757. https://doi.org/10.1021/bm0257614

Adams, M. L., & Kwon, G. S. (2003). Relative aggregation state and hemolytic activity of amphotericin B encapsulated by poly(ethylene oxide)-block–poly(N-hexyl-L-aspartamide)-acyl conjugate micelles: Effects of acyl chain length. *Journal of Controlled Release*, *87*(1–3), 23–32. https://doi.org/10.1016/S0168-3659(02)00347-4

Aguilar-Zapata, D., Petraitiene, R., & Petraitis, V. (2015). Echinocandins: The expanding antifungal armamentarium. *Clinical Infectious Diseases*, *61*(Suppl 6), S604–S611. https://doi.org/10.1093/cid/civ814

Ahmad, A., Khan, A., Bharathi, N. P., Hashmi, A. A., Khan, L. A., & Manzoor, N. (2011). Impaired ergosterol biosynthesis mediated fungicidal activity of oil based tin polymer. *Medicinal Chemistry Research*, *20*(8), 1141–1146. https://doi.org/10.1007/s00044-010-9449-4

Akter, M., Sikder, M. T., Rahman, M. M., Ullah, A. K. M. A., Hossain, K. F. B., Banik, S., Hosokawa, T., Saito, T., & Kurasaki, M. (2018). A systematic review on silver nanoparticles-induced cytotoxicity: Physicochemical properties and perspectives. *Journal of Advanced Research*, *9*(6), 1–16. https://doi.org/10.1016/j.jare.2017.10.008

Albayaty, Y. N., Thomas, N., Ramírez-García, P. D., Davis, T. P., Quinn, J. F., Whittaker, M. R., & Prestidge, C. A. (2020). pH-Responsive copolymer micelles to enhance itraconazole efficacy against *Candida albicans* biofilms. *Journal of Materials Chemistry B*, *8*(8), 1672–1681. https://doi.org/10.1039/C9TB02586C

Alex, J., González, K., Kindel, T., Bellstedt, P., Weber, C., Heinekamp, T., Orasch, T., Guerrero-Sanchez, C., Schubert, U. S., & Brakhage, A. A. (2020). Caspofungin functionalized polymethacrylates with antifungal properties. *Biomacromolecules*, *21*(6), 2104–2115. https://doi.org/10.1021/acs.biomac.0c00096

Ali, S., & Wilson, A. P. R. (2017). Effect of poly-hexamethylene biguanide hydrochloride (PHMB) treated non-sterile medical gloves upon the transmission of Streptococcus pyogenes, carbapenem-resistant *E. coli*, MRSA and *Klebsiella pneumoniae* from contact surfaces. *BMC Infectious Diseases*, *17*(1), 1–8. https://doi.org/10.1186/s12879-017-2661-9

Allen, D., Wilson, D., Drew, R., & Perfect, J. (2015). Azole antifungals: 35 years of invasive fungal infection management. *Expert Review of Anti-Infective Therapy*, *13*(6), 787–798. https://doi.org/10.1586/14787210.2015.1032939

Alves, D., & Olívia Pereira, M. (2014). Mini-review: Antimicrobial peptides and enzymes as promising candidates to functionalize biomaterial surfaces. *Biofouling*, *30*(4), 483–499. https://doi.org/10.1080/08927014.2014.889120

Anderson, E. B., & Long, T. E. (2010). Imidazole- and imidazolium-containing polymers for biology and material science applications. *Polymer*, *51*(12), 2447–2454. https://doi.org/10.1016/j.polymer.2010.02.006

Andersson Trojer, M., Movahedi, A., Blanck, H., & Nydén, M. (2013). Imidazole and Triazole coordination chemistry for antifouling coatings. *Journal of Chemistry*, *2013*, 1–23. https://doi.org/10.1155/2013/946739

Arora, A., & Mishra, A. (2018). Antibacterial polymers - A mini review. *Materials Today: Proceedings*, *5*(9), 17156–17161. https://doi.org/10.1016/j.matpr.2018.04.124

Arslan, M., Saraydin, D., Öztop, A. Y., & Şahiner, N. (2017). Radiation-induced acrylamide/4-vinyl pyridine biocidal hydrogels: Synthesis, characterization, and antimicrobial activities. *Polymer - Plastics Technology and Engineering*, *56*(12), 1295–1306. https://doi.org/10.1080/03602559.2016.1275683

Baker, C., Pradhan, A., Pakstis, L., Pochan, D. J., & Shah, S. I. (2005). Synthesis and antibacterial properties of silver nanoparticles. *Journal of Nanoscience and Nanotechnology*, *5*(2), 244–249. https://doi.org/10.1166/jnn.2005.034

Barad, S., Roudbary, M., Nasrollahi Omran, A., & Porgham Daryasari, M. (2017). Preparation and characterization of ZnO nanoparticles coated by chitosan-linoleic acid; fungal growth and biofilm assay. *Bratislava Medical Journal*, *118*(3), 169–174. https://doi.org/10.4149/BLL_2017_034

Bhatia, S., Kumar, V., Sharma, K., Nagpal, K., & Bera, T. (2014). Significance of algal polymer in designing amphotericin B nanoparticles. *Scientific World Journal*, *2014*, 1–21. https://doi.org/10.1155/2014/564573

Bongomin, F., Gago, S., Oladele, R., & Denning, D. (2017). Global and multi-national prevalence of fungal diseases—Estimate precision. *Journal of Fungi*, *3*(4), 57. https://doi.org/10.3390/jof3040057

Borowski, E. (2000). Novel approaches in the rational design of antifungal agents of low toxicity. *Farmaco*, *55*(3), 206–208. https://doi.org/10.1016/S0014-827X(00)00024-0

Buxbaum, A., Kratzer, C., Graninger, W., & Georgopoulos, A. (2006). Antimicrobial and toxicological profile of the new biocide Akacid plus®. *Journal of Antimicrobial Chemotherapy*, *58*(1), 193–197. https://doi.org/10.1093/jac/dkl206

Caffrey, P., Aparicio, J., Malpartida, F., & Zotchev, S. (2008). Biosynthetic engineering of polyene macrolides towards generation of improved antifungal and antiparasitic agents. *Current Topics in Medicinal Chemistry*, *8*(8), 639–653. https://doi.org/10.2174/156802608784221479

Choi, F. D., Juhasz, M. L. W., & Atanaskova Mesinkovska, N. (2019). Topical ketoconazole: A systematic review of current dermatological applications and future developments. *Journal of Dermatological Treatment*, *30*(8), 760–771. https://doi.org/10.1080/09546634.2019.1573309

Choi, H., Kim, K. J., & Lee, D. G. (2017). Antifungal activity of the cationic antimicrobial polymer-polyhexamethylene guanidine hydrochloride and its mode of action. *Fungal Biology*, *121*(1), 53–60. https://doi.org/10.1016/j.funbio.2016.09.001

Chung, Y. C., Kim, H. Y., Choi, J. W., & Chun, B. C. (2018). Graft polymerization of 4-imidazole acrylic acid onto polyurethane for the improvement of water compatibility and antifungal activity. *Polymer Engineering and Science*, *58*(11), 2088–2097. https://doi.org/10.1002/pen.24820

Chung, Y. C., Park, J. E., Choi, J. W., & Chun, B. C. (2018). Synthesis and characterizations of antifungal polyurethanes with enhanced tensile and shape recovery performances. *Advances in Polymer Technology*, *37*(8), 3392–3400. https://doi.org/10.1002/adv.22123

Cierech, M., Kolenda, A., Grudniak, A. M., Wojnarowicz, J., Woźniak, B., Gołaś, M., Swoboda-Kopeć, E., Łojkowski, W., &

Mierzwińska-Nastalska, E. (2016). Significance of polymethylmethacrylate (PMMA) modification by zinc oxide nanoparticles for fungal biofilm formation. *International Journal of Pharmaceutics*, *510*(1), 323–335. https://doi.org/10.1016/j.ijpharm.2016.06.052

Cioffi, N., Torsi, L., Ditaranto, N., Sabbatini, L., Zambonin, P. G., Tantillo, G., Ghibelli, L., D'Alessio, M., Bleve-Zacheo, T., & Traversa, E. (2004). Antifungal activity of polymer-based copper nanocomposite coatings. *Applied Physics Letters*, *85*(12), 2417–2419. https://doi.org/10.1063/1.1794381

Cioffi, N., Torsi, L., Ditaranto, N., Tantillo, G., Ghibelli, L., Sabbatini, L., Bleve-Zacheo, T., D'Alessio, M., Zambonin, P. G., & Traversa, E. (2005). Copper nanoparticle/polymer composites with antifungal and bacteriostatic properties. *Chemistry of Materials*, *17*(21), 5255–5262. https://doi.org/10.1021/cm0505244

Ciuca, S., Badea, M., Pozna, E., Pana, I., Kiss, A., Floroian, L., Semenescu, A., Cotrut, C. M., Moga, M., & Vladescu, A. (2016). Evaluation of Ag containing hydroxyapatite coatings to the *Candida albicans* infection. *Journal of Microbiological Methods*, *125*, 12–18. https://doi.org/10.1016/j.mimet.2016.03.016

Coad, B. R., Lamont-Friedrich, S. J., Gwynne, L., Jasieniak, M., Griesser, S. S., Traven, A., Peleg, A. Y., & Griesser, H. J. (2015). Surface coatings with covalently attached caspofungin are effective in eliminating fungal pathogens. *Journal of Materials Chemistry B*, *3*(43), 8469–8476. https://doi.org/10.1039/C5TB00961H

Cobos, M., De-La-Pinta, I., Quindós, G., Fernández, M. J., & Fernández, M. D. (2020). Synthesis, physical, mechanical and antibacterial properties of nanocomposites based on poly(vinyl alcohol)/graphene oxide-silver nanoparticles. *Polymers*, *12*(3), 723. https://doi.org/10.3390/polym12030723

Cohen, M. E., Salmasian, H., Li, J., Liu, J., Zachariah, P., Wright, J. D., & Freedberg, D. E. (2017). Surgical antibiotic prophylaxis and risk for postoperative antibiotic-resistant infections. *Journal of the American College of Surgeons*, *225*(5), 631–638.e3. https://doi.org/10.1016/j.jamcollsurg.2017.08.010

Costa, F., Carvalho, I. F., Montelaro, R. C., Gomes, P., & Martins, M. C. L. (2011). Covalent immobilization of antimicrobial peptides (AMPs) onto biomaterial surfaces. *Acta Biomaterialia*, *7*(4), 1431–1440. https://doi.org/10.1016/j.actbio.2010.11.005

Costa-Orlandi, C., Sardi, J., Pitangui, N., de Oliveira, H., Scorzoni, L., Galeane, M., Medina-Alarcón, K., Melo, W., Marcelino, M., Braz, J., Fusco-Almeida, A., & Mendes-Giannini, M. (2017). Fungal biofilms and polymicrobial diseases. *Journal of Fungi*, *3*(2), 22. https://doi.org/10.3390/jof3020022

De Paula, M. M. M., Bassous, N. J., Afewerki, S., Harb, S. V., Ghannadian, P., Marciano, F. R., Viana, B. C., Tim, C. R., Webster, T. J., & Lobo, A. O. (2018). Understanding the impact of crosslinked PCL/PEG/GelMA electrospun nanofibers on bactericidal activity. *PLoS One*, *13*(12), e0209386. https://doi.org/10.1371/journal.pone.0209386

De Pauw, B. E. (2011). What are fungal infections? *Mediterranean Journal of Hematology and Infectious Diseases*, *3*(1), e2011001. https://doi.org/10.4084/mjhid.2011.001

Debono, M., Abbott, B. J., Fukuda, D. S., Barnhart, M., Willard, K. E., Molloy, R. M., Michel, K. H., Turner, J. R., Butler, T. F., & Hunt, A. H. (1989). Synthesis of new analogs of echinocandin B by enzymatic deacylation and chemical reacylation of the echinocandin B peptide: Synthesis of the antifungal agent cilofungin (LY121019). *The Journal of Antibiotics*, *42*(3), 389–397. https://doi.org/10.7164/antibiotics.42.389

Debono, M., Turner, W. W., Lagrandeur, L., Burkhardt, F. J., Nissen, J. S., Nichols, K. K., & Eli, L. (1995). Semisynthetic chemical modification of the antifungal lipopeptide echinocandin B (ECB). *Journal of Medicinal Chemistry*, *38*(17), 3271–3281.

De-la-Pinta, I., Cobos, M., Ibarretxe, J., Montoya, E., Eraso, E., Guraya, T., & Quindós, G. (2019). Effect of biomaterials hydrophobicity and roughness on biofilm development. *Journal of Materials Science: Materials in Medicine*, *30*(7), 77. https://doi.org/10.1007/s10856-019-6281-3

Desai, J. V., Mitchell, A. P., & Andes, D. R. (2014). Fungal biofilms, drug resistance, and recurrent infection. *Cold Spring Harbor Perspectives in Medicine*, *4*(10), a019729. https://doi.org/10.1101/cshperspect.a019729

Dhir, S. (2013). Biofilm and dental implant: The microbial link. *Journal of Indian Society of Periodontology*, *17*(1), 5. https://doi.org/10.4103/0972-124X.107466

Diaz, I. L., Parra, C., Linarez, M., & Perez, L. D. (2015). Design of micelle nanocontainers based on PDMAEMA-b-PCL-b-PDMAEMA triblock copolymers for the encapsulation of amphotericin B. *An Official Journal of the American Association of Pharmaceutical Scientists*, *16*(5), 1069–1078. https://doi.org/10.1208/s12249-015-0298-9

Elinson, V. M., Shchur, P. A., & Silnitskaya, O. A. (2018). Multifunctional polymer materials with antifungal activity, modified by fluorocarbon films by methods of ion-plasma technology. *Journal of Physics: Conference Series*, *1121*(1), 71–74. https://doi.org/10.1088/1742-6596/1121/1/012012

Ergene, C., Yasuhara, K., & Palermo, E. F. (2018). Biomimetic antimicrobial polymers: Recent advances in molecular design. *Polymer Chemistry*, *9*(18), 2407–2427. https://doi.org/10.1039/c8py00012c

Fisher, M. C., Henk, D. A., Briggs, C. J., Brownstein, J. S., Madoff, L. C., McCraw, S. L., & Gurr, S. J. (2012). Emerging fungal threats to animal, plant and ecosystem health. *Nature*, *484*(7393), 186–194. https://doi.org/10.1038/nature10947

Gamaletsou, M. N., Walsh, T. J., & Sipsas, N. V. (2018). Invasive fungal infections in patients with hematological malignancies: Emergence of resistant pathogens and new antifungal therapies. *Turkish Journal of Hematology*, *35*(1), 1–11. https://doi.org/10.4274/tjh.2018.0007

Garber, G. (2001). An overview of fungal infections. *Drugs*, *61*(Supplement 1), 1–12. https://doi.org/10.2165/00003495-200161001-00001

Griesser, S. S., Jasieniak, M., Coad, B. R., & Griesser, H. J. (2015). Antifungal coatings by caspofungin immobilization onto biomaterials surfaces via a plasma polymer interlayer. *Biointerphases*, *10*(4), 04A307. https://doi.org/10.1116/1.4933108

Groza, A., Ciobanu, C., Popa, C., Iconaru, S., Chapon, P., Luculescu, C., Ganciu, M., & Predoi, D. (2016). Structural properties and antifungal activity against *Candida albicans* biofilm of different composite layers based on Ag/Zn doped hydroxyapatite-polydimethylsiloxanes. *Polymers*, *8*(4), 131. https://doi.org/10.3390/polym8040131

Guo, Y., Karimi, F., Fu, Q., Qiao, G., & Zhang, H. (2020). Reduced administration frequency for the treatment of fungal keratitis: A sustained natamycin release from a micellar solution. *Expert Opinion on Drug Delivery*, *17*(3), 407–421. https://doi.org/10.1080/17425247.2020.1719995

Haley, R. M., Zuckerman, S. T., Gormley, C. A., Korley, J. N., & Von Recum, H. A. (2019). Local delivery polymer provides sustained antifungal activity of amphotericin B with reduced cytotoxicity. *Experimental Biology and Medicine*, *244*(6), 526–533. https://doi.org/10.1177/1535370219837905

Hanemann, T., & Szabó, D. V. (2010). Polymer-nanoparticle composites: From synthesis to modern applications. *Materials. Multidisciplinary Digital Publishing Institute (MDPI)*, *3*(6), 3468–3517. https://doi.org/10.3390/ma3063468

Hashimoto, S. (2009). Micafungin: A sulfated echinocandin. *Journal of Antibiotics*, *62*(1), 27–35. https://doi.org/10.1038/ja.2008.3

Hassan, M. M. (2015). Binding of a quaternary ammonium polymer-grafted-chitosan onto a chemically modified wool fabric surface: Assessment of mechanical, antibacterial and antifungal properties. *RSC Advances*, *5*(45), 35497–35505. https://doi.org/10.1039/c5ra03073k

Herzog, I. M., Green, K. D., Berkov-Zrihen, Y., Feldman, M., Vidavski, R. R., Eldar-Boock, A., Satchi-Fainaro, R., Eldar, A., Garneau-Tsodikova, S.,

& Fridman, M. (2012). 6″-thioether tobramycin analogues: Towards selective targeting of bacterial membranes. *Angewandte Chemie - International Edition*, *51*(23), 5652–5656. https://doi.org/10.1002/anie.201200761

Higazy, A., Hashem, M., ElShafei, A., Shaker, N., & Hady, M. A. (2010). Development of antimicrobial jute packaging using chitosan and chitosan–metal complex. *Carbohydrate Polymers*, *79*(4), 867–874. https://doi.org/10.1016/j.carbpol.2009.10.011

Hoque, J., Akkapeddi, P., Yadav, V., Manjunath, G. B., Uppu, D. S. S. M., Konai, M. M., Yarlagadda, V., Sanyal, K., & Haldar, J. (2015). Broad spectrum antibacterial and antifungal polymeric paint materials: Synthesis, structure-activity relationship, and membrane-active mode of action. *ACS Applied Materials and Interfaces*, *7*(3), 1804–1815. https://doi.org/10.1021/am507482y

Howard, K. C., Dennis, E. K., Watt, D. S., & Garneau-Tsodikova, S. (2020). A comprehensive overview of the medicinal chemistry of antifungal drugs: Perspectives and promise. *Chemical Society Reviews*, *49*(8), 2426–2480. https://doi.org/10.1039/C9CS00556K

James, K. D., Laudeman, C. P., Malkar, N. B., Krishnan, R., & Polowy, K. (2017). Structure-activity relationships of a series of echinocandins and the discovery of CD101, a highly stable and soluble echinocandin with distinctive pharmacokinetic properties. *Antimicrobial Agents and Chemotherapy*, *61*(2), 1–8. https://doi.org/10.1128/AAC.01541-16

Jana, G. H., Jain, S., Arora, S. K., & Sinha, N. (2005). Synthesis of some diguanidino 1-methyl-2,5-diaryl-1H-pyrroles as antifungal agents. *Bioorganic and Medicinal Chemistry Letters*, *15*(15), 3592–3595. https://doi.org/10.1016/j.bmcl.2005.05.080

Jaramillo, A. F., Riquelme, S. A., Sánchez-Sanhueza, G., Medina, C., Solís-Pomar, F., Rojas, D., Montalba, C., Melendrez, M. F., & Pérez-Tijerina, E. (2019). Comparative study of the antimicrobial effect of nanocomposites and composite based on poly(butylene adipate-co-terephthalate) using Cu and Cu/Cu2O nanoparticles and CuSO4. *Nanoscale Research Letters*, *14*(1), 1–17. https://doi.org/10.1186/s11671-019-2987-x

Jarzebski, A., Falkowski, L., & Borowski, E. (1982). Synthesis and structure-activity relationships of amides of amphotericin b. *The Journal of Antibiotics*, *35*(2), 220–229. https://doi.org/10.7164/antibiotics.35.220

Jia, R., Duan, Y., Fang, Q., Wang, X., & Huang, J. (2016). Pyridine-grafted chitosan derivative as an antifungal agent. *Food Chemistry*, *196*, 381–387. https://doi.org/10.1016/j.foodchem.2015.09.053

Jiao, Y., Niu, L.-N., Ma, S., Li, J., Tay, F. R., & Chen, J.-H. (2017). Quaternary ammonium-based biomedical materials: State-of-the-art, toxicological aspects and antimicrobial resistance. *Progress in Polymer Science*, *71*, 53–90. https://doi.org/10.1016/j.progpolymsci.2017.03.001

Kalaivani, R., Maruthupandy, M., Muneeswaran, T., Hameedha Beevi, A., Anand, M., Ramakritinan, C. M., & Kumaraguru, A. K. (2018). Synthesis of chitosan mediated silver nanoparticles (Ag NPs) for potential antimicrobial applications. *Frontiers in Laboratory Medicine*, *2*(1), 30–35. https://doi.org/10.1016/j.flm.2018.04.002

Kariduraganavar, M. Y., Kittur, A. A., & Kamble, R. R. (2014). *Polymer synthesis and processing. Natural and synthetic biomedical polymers* (1st ed.). Elsevier Inc. https://doi.org/10.1016/B978-0-12-396983-5.00001-6

Kenawy, E.-R., Worley, S. D., & Broughton, R. (2007). The chemistry and applications of antimicrobial polymers: A state-of-the-art review. *Biomacromolecules*, *8*(5), 1359–1384. https://doi.org/10.1021/bm061150q

Kim, H.-J., Han, C.-Y., Park, J.-S., Oh, S.-H., Kang, S.-H., Choi, S.-S., Kim, J.-M., Kwak, J.-H., & Kim, E.-S. (2018). Nystatin-like Pseudonocardia polyene B1, a novel disaccharide-containing antifungal heptaene antibiotic. *Scientific Reports*, *8*(1), 1–8. https://doi.org/10.1038/s41598-018-31801-y

Kim, H. J., Kang, S. H., Choi, S. S., & Kim, E. S. (2017). Redesign of antifungal polyene glycosylation: Engineered biosynthesis of disaccharide-modified NPP. *Applied Microbiology and Biotechnology*, *101*(12), 5131–5137. https://doi.org/10.1007/s00253-017-8303-8

Kucharíková, S., Gerits, E., De Brucker, K., Braem, A., Ceh, K., Majdič, G., & Thevissen, K. (2016). Covalent immobilization of antimicrobial agents on titanium prevents *Staphylococcus aureus* and *Candida albicans* colonization and biofilm formation. *Journal of Antimicrobial Chemotherapy*, *71*(4), 936–945. https://doi.org/10.1093/jac/dkv437

Kulthe, S. S., Choudhari, Y. M., Inamdar, N. N., & Mourya, V. (2012). Polymeric micelles: Authoritative aspects for drug delivery. *Designed Monomers and Polymers*, *15*(5), 465–521. https://doi.org/10.1080/1385772X.2012.688328

Kumar, S., Boro, J. C., Ray, D., Mukherjee, A., & Dutta, J. (2019). Bionanocomposite films of agar incorporated with ZnO nanoparticles as an active packaging material for shelf life extension of green grape. *Heliyon*, *5*(6), e01867. https://doi.org/10.1016/j.heliyon.2019.e01867

Kun Han, M. A., Miah, J., Shanmugam, S., Yong, C. S., Choi, H.-G., Kim, J. A., & Yoo, B. K. (2007). Mixed micellar nanoparticle of amphotericin b and poly styrene-block-poly ethylene oxide reduces nephrotoxicity but retains antifungal activity. *Archives of Pharmacal Research*, *30*(10), 1344–1349. https://doi.org/10.1007/BF02980276

Lavasanifar, A., Samuel, J., Sattar, S., & Kwon, G. S. (2002). Block copolymer micelles for the encapsulation and delivery of amphotericin B. *Pharmaceutical Research*, *19*, 418–422.

Lee, W. R., Tobias, K. M., Bemis, D. A., & Rohrbach, B. W. (2004). In vitro efficacy of a polyhexamethylene biguanide-impregnated gauze dressing against bacteria found in veterinary patients. *Veterinary Surgery*, *33*(4), 404–411. https://doi.org/10.1111/j.1532-950X.2004.04059.x

Lim, N., Goh, D., Bunce, C., Xing, W., Fraenkel, G., Poole, T. R. G., & Ficker, L. (2008). Comparison of polyhexamethylene biguanide and chlorhexidine as monotherapy agents in the treatment of acanthamoeba keratitis. *American Journal of Ophthalmology*, *145*(1), 130–135. https://doi.org/10.1016/j.ajo.2007.08.040

Liu, R., Chen, X., Falk, S. P., Mowery, B. P., Karlsson, A. J., Weisblum, B., & Gellman, S. H. (2014). Structure-activity relationships among antifungal nylon-3 polymers: Identification of materials active against drug-resistant strains of *Candida albicans*. *Journal of the American Chemical Society*, *136*(11), 4333–4342. https://doi.org/10.1021/ja500036r

Liu, R., Chen, X., Hayouka, Z., Chakraborty, S., Falk, S. P., Weisblum, B., Masters, K. S., & Gellman, S. H. (2013). Nylon-3 polymers with selective antifungal activity. *Journal of the American Chemical Society*, *135*(14), 5270–5273. https://doi.org/10.1021/ja4006404

Liu, Z., Zheng, Y., Dang, J., Zhang, J., Dong, F., Wang, K., & Zhang, J. (2019). A novel antifungal plasma-activated hydrogel. *ACS Applied Materials & Interfaces*, *11*(26), 22941–22949. https://doi.org/10.1021/acsami.9b04700

Long, S. S., Prober, C. G., & Fischer, M. (2017). Principles and practice of pediatric infectious diseases. *Clinical Infectious Diseases*, *25*(5), 1277. https://doi.org/10.1086/516117

López-Saucedo, F., Flores-Rojas, G. G., Bucio, E., Alvarez-Lorenzo, C., Concheiro, A., & González-Antonio, O. (2017). Achieving antimicrobial activity through poly(N-methylvinylimidazolium) iodide brushes on binary-grafted polypropylene suture threads. *MRS Communications*, *7*(4), 938–946. https://doi.org/10.1557/mrc.2017.121

López-Saucedo, F., Flores-Rojas, G. G., López-Saucedo, J., Magariños, B., Alvarez-Lorenzo, C., Concheiro, A., & Bucio, E. (2018). Antimicrobial silver-loaded polypropylene sutures modified by radiation-grafting. *European Polymer Journal*, *100*, 290–297. https://doi.org/10.1016/j.eurpolymj.2018.02.005

Lufton, M., Bustan, O. R., Eylon, B.-H., Shtifman-Segal, E., Croitoru-Sadger, T., Shagan, A., Shabtay-Orbach, A., Corem-Salkmon, E., Berman, J., Nyska, A., & Mizrahi, B. (2018). Living bacteria in thermoresponsive gel for treating fungal infections. *Advanced Functional Materials*, *28*(40), 1–7. https://doi.org/10.1002/adfm.201801581

Manetti, F., Castagnolo, D., Raffi, F., Zizzari, A. T., Rajamaki, S., D'Arezzo, S., & Botta, M. (2009). Synthesis of new linear guanidines and macrocyclic amidinourea derivatives endowed with high antifungal activity against *Candida* spp. and *Aspergillus* spp. *Journal of Medicinal Chemistry*, *52*(23), 7376–7379. https://doi.org/10.1021/jm900760k

Mathew, T. V., & Kuriakose, S. (2013). Photochemical and antimicrobial properties of silver nanoparticle- encapsulated chitosan functionalized with photoactive groups. *Materials Science and Engineering C*, *33*(7), 4409–4415. https://doi.org/10.1016/j.msec.2013.06.037

Meléndez-Ortiz, H. I., Alvarez-Lorenzo, C., Burillo, G., Magariños, B., Concheiro, A., & Bucio, E. (2015). Radiation-grafting of N-vinylimidazole onto silicone rubber for antimicrobial properties. *Radiation Physics and Chemistry*, *110*, 59–66. https://doi.org/10.1016/j.radphyschem.2015.01.025

Meléndez-Ortiz, H. I., Alvarez-Lorenzo, C., Concheiro, A., Jiménez-Páez, V. M., & Bucio, E. (2016). Modification of medical grade PVC with N-vinylimidazole to obtain bactericidal surface. *Radiation Physics and Chemistry*, *119*, 37–43. https://doi.org/10.1016/j.radphyschem.2015.09.014

Meng, N., Zhou, N. L., Zhang, S. Q., & Shen, J. (2009). Synthesis and antifungal activities of polymer/montmorillonite-terbinafine hydrochloride nanocomposite films. *Applied Clay Science*, *46*(2), 136–140. https://doi.org/10.1016/j.clay.2009.07.003

Michl, T. D., Giles, C., Cross, A. T., Griesser, H. J., & Coad, B. R. (2017). Facile single-step bioconjugation of the antifungal agent caspofungin onto material surfaces: Via an epoxide plasma polymer interlayer. *RSC Advances*, *7*(44), 27678–27681. https://doi.org/10.1039/c7ra03897f

Michl, T. D., Giles, C., Mocny, P., Futrega, K., Doran, M. R., Klok, H.-A., & Coad, B. R. (2017). Caspofungin on ARGET-ATRP grafted PHEMA polymers: Enhancement and selectivity of prevention of attachment of *Candida albicans*. *Biointerphases*, *12*(5), 05G602. https://doi.org/10.1116/1.4986054

Mohamed-Ahmed, A. H. A., Les, K. A., Seifert, K., Croft, S. L., & Brocchini, S. (2013). Noncovalent complexation of amphotericin-B with poly(α-glutamic acid). *Molecular Pharmaceutics*, *10*(3), 940–950. https://doi.org/10.1021/mp300339p

Muñoz-Bonilla, A., & Fernández-García, M. (2012). Polymeric materials with antimicrobial activity. *Progress in Polymer Science (Oxford)*, *37*(2), 281–339. https://doi.org/10.1016/j.progpolymsci.2011.08.005

Muñoz-Escobar, A., & Reyes-López, S. Y. (2020). Antifungal susceptibility of Candida species to copper oxide nanoparticles on polycaprolactone fibers (PCL-CuONPs). *PLoS One*, *15*(2), e0228864. https://doi.org/10.1371/journal.pone.0228864

Narayana, S. V. V. S., & Pichika, S. V. V. S. (2019). A review on surface modifications and coatings on implants to prevent biofilm. *Regenerative Engineering and Translational Medicine*, *6*(3), 330–346. https://doi.org/10.1007/s40883-019-00116-3

Nasab, M. S., Tabari, M., & Bidarigh, S. (2019). Antifungal activity of nano-composite films-based poly lactic acid. *Nanomedicine Research Journal*, *4*(3), 186–192. https://doi.org/10.22034/NMRJ.2019.03.007

Niu, B., Huai, W., Deng, Z., & Chen, Q. (2017). Fungicidal, corrosive, and mutational effects of polyhexamethylene biguanide combined with 1-bromo-3-chloro-5,5-dimethylimidazolidine-2,4-dione. *BioMed Research International*, *2017*, 1–6. https://doi.org/10.1155/2017/4357031

Ojika, M., Itou, Y., & Sakagami, Y. (2003). Structural studies and antifungal activity of unique polyene amides, clathrynamide a and three new derivatives, from a marine sponge, psammoclemma sp. *Bioscience, Biotechnology and Biochemistry*, *67*(7), 1568–1573. https://doi.org/10.1271/bbb.67.1568

Paquet, V., & Carreira, E. M. (2006). Significant improvement of antifungal activity of polyene macrolides by bisalkylation of the mycosamine. *Organic Letters*, *8*(9), 1807–1809. https://doi.org/10.1021/ol060353o

Park, E.-S., Lee, H.-J., Park, H. Y., Kim, M.-N., Chung, K.-H., & Yoon, J.-S. (2001). Antifungal effect of carbendazim supported on poly(ethylene-co-vinyl alcohol) and epoxy resin. *Journal of Applied Polymer Science*, *80*(5), 728–736. https://doi.org/10.1002/1097-4628(20010502)80:5<728:AID-APP1149>3.0.CO;2-7

Patton, L. L., Bonito, A. J., & Shugars, D. A. (2001). A systematic review of the effectiveness of antifungal drugs for the prevention and treatment of oropharyngeal candidiasis in HIV-positive patients. *Oral Surgery, Oral Medicine, Oral Pathology, Oral Radiology, and Endodontology*, *92*(2), 170–179. https://doi.org/10.1067/moe.2001.116600

Pérez-Calixto, M. P., Ortega, A., Garcia-Uriostegui, L., & Burillo, G. (2016). Synthesis and characterization of N-vinylcaprolactam/N, N-dimethylacrylamide grafted onto chitosan networks by gamma radiation. *Radiation Physics and Chemistry*, *119*, 228–235. https://doi.org/10.1016/j.radphyschem.2015.10.030

Pfaller, M. A., Pappas, P. G., & Wingard, J. R. (2006). Invasive fungal pathogens: Current epidemiological trends. *Clinical Infectious Diseases*, *43*(Supplement_1), S3–S14. https://doi.org/10.1086/504490

Prucek, R., Tuček, J., Kilianová, M., Panáček, A., Kvítek, L., Filip, J., Kolář, M., Tománková, K., & Zbořil, R. (2011). The targeted antibacterial and antifungal properties of magnetic nanocomposite of iron oxide and silver nanoparticles. *Biomaterials*, *32*(21), 4704–4713. https://doi.org/10.1016/j.biomaterials.2011.03.039

Qi, Z., Kang, Q., Jiang, C., Han, M., & Bai, L. (2015). Engineered biosynthesis of pimaricin derivatives with improved antifungal activity and reduced cytotoxicity. *Applied Microbiology and Biotechnology*, *99*(16), 6745–6752. https://doi.org/10.1007/s00253-015-6635-9

Rank, L. A., Walsh, N. M., Lim, F. Y., Gellman, S. H., Keller, N. P., & Hull, C. M. (2018). Peptide-like nylon-3 polymers with activity against phylogenetically diverse, intrinsically drug-resistant pathogenic fungi. *mSphere*, *3*(3), 1–15. https://doi.org/10.1128/mSphere.00223-18

Rank, L. A., Walsh, N. M., Liu, R., Lim, F. Y., Bok, J. W., Huang, M., Keller, N. P., Gellman, S. H., & Hull, C. M. (2017). A cationic polymer that shows high antifungal activity against diverse human pathogens. *Antimicrobial Agents and Chemotherapy*, *61*(10), 1–15. https://doi.org/10.1128/AAC.00204-17

Rodriguez, Y. J., Quejada, L. F., Villamil, J. C., Baena, Y., Parra-Giraldo, C. M., & Perez, L. D. (2020). Development of amphotericin B micellar formulations based on copolymers of poly(ethylene glycol) and poly(ε-caprolactone) conjugated with retinol. *Pharmaceutics*, *12*(3), 196. https://doi.org/10.3390/pharmaceutics12030196

Roy Choudhury, S., Ordaz, J., Lo, C.-L., Damayanti, N. P., Zhou, F., & Irudayaraj, J. (2017). ZnO nanoparticles induced reactive oxygen species promotes multimodal cyto- and epigenetic toxicity. *Toxicological Sciences*, *kfw252*, https://doi.org/10.1093/toxsci/kfw252

Rubin, R. H. (2009). Fungal infection in the organ transplant recipient. In *Clinical mycology* (pp. 473–480). Elsevier. https://doi.org/10.1016/B978-1-4160-5680-5.00021-9

Sawyer, P. R., Brogden, R. N., Pinder, R. M., Speight, T. M., & Avery, G. S. (1975). Clotrimazole: A review of its antifungal activity and therapeutic efficacy. *Drugs*, *9*(6), 424–447. https://doi.org/10.2165/00003495-197509060-00003

Shemesh, R., Krepker, M., Goldman, D., Danin-Poleg, Y., Kashi, Y., Nitzan, N., Vaxman, A., & Segal, E. (2015). Antibacterial and antifungal LDPE films for active packaging. *Polymers for Advanced Technologies*, *26*(1), 110–116. https://doi.org/10.1002/pat.3434

Shih, P.-Y., Liao, Y.-T., Tseng, Y.-K., Deng, F.-S., & Lin, C.-H. (2019). A potential antifungal effect of chitosan against *Candida albicans*

is mediated via the inhibition of SAGA complex component expression and the subsequent alteration of cell surface integrity. *Frontiers in Microbiology*, *10*, 602–616. https://doi.org/10.3389/fmicb.2019.00602

Shrestha, S. K., Fosso, M. Y., & Garneau-Tsodikova, S. (2015). A combination approach to treating fungal infections. *Scientific Reports*, *5*, 1–11. https://doi.org/10.1038/srep17070

Shrestha, S. K., Fosso, M. Y., Green, K. D., & Garneau-Tsodikova, S. (2015). Amphiphilic tobramycin analogues as antibacterial and antifungal agents. *Antimicrobial Agents and Chemotherapy*, *59*(8), 4861–4869. https://doi.org/10.1128/AAC.00229-15

Solovieva, S. E., Olsufyeva, E. N., & Preobrazhenskaya, M. N. (2011). Chemical modification of antifungal polyene macrolide antibiotics. *Russian Chemical Reviews*, *80*(2), 103–126. https://doi.org/10.1070/rc2011v080n02abeh004145

Souza, A. C. O., & Amaral, A. C. (2017). Antifungal therapy for systemic mycosis and the nanobiotechnology era: Improving efficacy, biodistribution and toxicity. *Frontiers in Microbiology*, *8*, 336–349. https://doi.org/10.3389/fmicb.2017.00336

Tabriz, A., Ur Rehman Alvi, M. A., Khan Niazi, M. B., Batool, M., Bhatti, M. F., Khan, A. L., Khan, A. U., Jamil, T., & Ahmad, N. M. (2019). Quaternized trimethyl functionalized chitosan based antifungal membranes for drinking water treatment. *Carbohydrate Polymers*, *207*, 17–25. https://doi.org/10.1016/j.carbpol.2018.11.066

Tamayo, L., Palza, H., Bejarano, J., & Zapata, P. A. (2018). *Polymer composites with metal nanoparticles: Synthesis, properties, and applications* (pp. 249–286). Elsevier. https://doi.org/10.1016/B978-0-12-814064-2.00008-1

Tan, W., Li, Q., Dong, F., Chen, Q., & Guo, Z. (2017). Preparation and characterization of novel cationic chitosan derivatives bearing quaternary ammonium and phosphonium salts and assessment of their antifungal properties. *Molecules*, *22*(9), 1438. https://doi.org/10.3390/molecules22091438

Tan, W., Zhang, J., Mi, Y., Dong, F., Li, Q., & Guo, Z. (2018). Synthesis, characterization, and evaluation of antifungal and antioxidant properties of cationic chitosan derivative via azide-alkyne click reaction. *International Journal of Biological Macromolecules*, *120*, 318–324. https://doi.org/10.1016/j.ijbiomac.2018.08.111

Tang, X., Zhu, H., Sun, L., Hou, W., Cai, S., Zhang, R., & Liu, F. (2014). Enhanced antifungal effects of amphotericin B-TPGS-b-(PCL-ran-PGA) nanoparticles in vitro and in vivo. *International Journal of Nanomedicine*, *9*(1), 5403–5413. https://doi.org/10.2147/IJN.S71623

Tevyashova, A. N., Olsufyeva, E. N., Solovieva, S. E., Printsevskaya, S. S., Reznikova, M. I., Trenin, A. S., Galatenko, O. A., Treshalin, I. D., Pereverzeva, E. R., Mirchink, E. P., Isakova, E. B., Zotchev, S. B., & Preobrazhenskaya, M. N. (2013). Structure-antifungal activity relationships of polyene antibiotics of the amphotericin B group. *Antimicrobial Agents and Chemotherapy*, *57*(8), 3815–3822. https://doi.org/10.1128/AAC.00270-13

Tiyaboonchai, W., & Limpeanchob, N. (2007). Formulation and characterization of amphotericin B-chitosan-dextran sulfate nanoparticles. *International Journal of Pharmaceutics*, *329*(1–2), 142–149. https://doi.org/10.1016/j.ijpharm.2006.08.013

Tsarenko, I. V., Makarevich, A. V., & Orekhov, D. A. (1998). Microbicidal properties of polymer films modified by five-membered polynitrogen heterocycles. *Bioprocess Engineering*, *19*(6), 469. https://doi.org/10.1007/s004490050549

Vazquez-Muñoz, R., Borrego, B., Juárez-Moreno, K., García-García, M., Mota Morales, J. D., Bogdanchikova, N., & Huerta-Saquero, A. (2017). Toxicity of silver nanoparticles in biological systems: Does the complexity of biological systems matter? *Toxicology Letters*, *276*, 11–20. https://doi.org/10.1016/j.toxlet.2017.05.007

Vincent, M., Duval, R. E., Hartemann, P., & Engels-Deutsch, M. (2018). Contact killing and antimicrobial properties of copper. *Journal of Applied Microbiology*, *124*(5), 1032–1046. https://doi.org/10.1111/jam.13681

Wang, Y., Ke, X., Voo, Z. X., Yap, S. S. L., Yang, C., Gao, S., Liu, S., Venkataraman, S., Obuobi, S. A. O., Khara, J. S., Yang, Y. Y., & Ee, P. L. R. (2016). Biodegradable functional polycarbonate micelles for controlled release of amphotericin B. *Acta Biomaterialia*, *46*, 211–220. https://doi.org/10.1016/j.actbio.2016.09.036

Wei, L., Chen, Y., Tan, W., Li, Q., Gu, G., Dong, F., & Guo, Z. (2018). Synthesis, characterization, and antifungal activity of pyridine-based triple quaternized chitosan derivatives. *Molecules*, *23*(10), 2604. https://doi.org/10.3390/molecules23102604

Wei, L., Li, Q., Chen, Y., Zhang, J., Mi, Y., Dong, F., Lei, C., & Guo, Z. (2019). Enhanced antioxidant and antifungal activity of chitosan derivatives bearing 6-O-imidazole-based quaternary ammonium salts. *Carbohydrate Polymers*, *206*, 493–503. https://doi.org/10.1016/j.carbpol.2018.11.022

Wiederhold, N. P. (2017). Antifungal resistance: Current trends and future strategies to combat. *Infection and Drug Resistance*, *10*, 249–259. https://doi.org/10.2147/IDR.S124918

World Health Organization (n.d.). *Antimicrobial resistance*.

Xue, Y., Pan, Y., Xiao, H., & Zhao, Y. (2014). Novel quaternary phosphonium-type cationic polyacrylamide and elucidation of dual-functional antibacterial/antiviral activity. *RSC Advances*, *4*(87), 46887–46895. https://doi.org/10.1039/c4ra08634a

Yang, Y., Cai, Z., Huang, Z., Tang, X., & Zhang, X. (2018). Antimicrobial cationic polymers: From structural design to functional control. *Polymer Journal*, *50*(1), 33–44. https://doi.org/10.1038/pj.2017.72

Yu, B., Okano, T., Kataoka, K., & Kwon, G. (1998). Polymeric micelles for drug delivery: Solubilization and haemolytic activity of amphotericin B. *Journal of Controlled Release*, *53*(1–3), 131–136. https://doi.org/10.1016/S0168-3659(97)00245-9

Yu, B., Okano, T., Kataoka, K., Sardari, S., & Kwon, G. (1998). In vitro dissociation of antifungal efficacy and toxicity for amphotericin B-loaded poly(ethylene oxide)-block-poly(β-benzyl-l-aspartate) micelles. *Journal of Controlled Release*, *56*(1–3), 285–291. https://doi.org/10.1016/S0168-3659(98)00095-9

Yu, M., Ding, X., Zhu, Y., Wu, S., Ding, X., Li, Y., Yu, B., & Xu, F.-J. (2019). Facile surface multi-functionalization of biomedical catheters with dual-microcrystalline broad-spectrum antibacterial drugs and antifouling poly(ethylene glycol) for effective inhibition of bacterial infections. *ACS Applied Bio Materials*, *2*(3), 1348–1356. https://doi.org/10.1021/acsabm.9b00049

Zegers, S. H. J., Dieleman, J., van der Bruggen, T., Kimpen, J., Kimpen, J., & de Jong-de Vos van Steenwijk, C. (2017). The influence of antibiotic prophylaxis on bacterial resistance in urinary tract infections in children with spina bifida. *BMC Infectious Diseases*, *17*(1), 1–9. https://doi.org/10.1186/s12879-016-2166-y

Zhang, J., Kissounko, D. A., Lee, S. E., Gellman, S. H., & Stahl, S. S. (2009). Access to poly-β-peptides with functionalized side chains and end groups via controlled ring-opening polymerization of β-lactams. *Journal of the American Chemical Society*, *131*(4), 1589–1597. https://doi.org/10.1021/ja8069192

Zhang, J., Mi, Y., Sun, X., Chen, Y., Miao, Q., Tan, W., Li, Q., Dong, F., & Guo, Z. (2020). Improved antioxidant and antifungal activity of chitosan derivatives bearing urea groups. *Starch/Staerke*, *72*(5-6), 5–6. https://doi.org/10.1002/star.201900205

Zhang, X., Ke, F., Han, J., Ye, L., Liang, D., Zhang, A., & Feng, Z. (2009). The self-aggregation behaviour of amphotericin B-loaded polyrotaxane-based triblock copolymers and their hemolytic evaluation. *Soft Matter*, *5*(23), 4797. https://doi.org/10.1039/b914664d

Zhang, Y. U., Chen, Y., Huang, L., Chai, Z., Shen, L., & Xiao, Y. (2017). The antifungal effects and mechanical properties of silver bromide/cationic polymer nano-composite-modified poly-methyl

methacrylate-based dental resin. *Scientific Reports*, *7*(1), 1547. https://doi.org/10.1038/s41598-017-01686-4

Zhang, Y., & Yuan, Y. (2019). *WO 2019/088917 A1*. World Intellectual Property Organization.

Zumbuehl, A., Ferreira, L., Kuhn, D., Astashkina, A., Long, L., Yeo, Y., Kohane, D. S. (2008). Antifungal hydrogels. *8th World Biomaterials Congress*, *1*(32), 245.

How to cite this article: Velazco-Medel MA, Camacho-Cruz LA, Lugo-González JC, Bucio E. Antifungal polymers for medical applications. *Med Devices Sens*. 2020;00:e10134. https://doi.org/10.1002/mds3.10134